

**Synthesis and Solution Properties of Water-soluble
Fullerene Polymeric Systems**

by

Zhaoling Yao

A thesis
presented to the University of Waterloo
in fulfillment of the
thesis requirement for the degree of
Doctor of Philosophy
in
Chemical Engineering

Waterloo, Ontario, Canada, 2011

©Zhaoling Yao 2011

AUTHOR'S DECLARATION

I hereby declare that I am the sole author of this thesis. This is a true copy of the thesis, including any required final revisions, as accepted by my examiners. I understand that my thesis may be made electronically available to the public.

Abstract

Water-soluble fullerene containing polymers comprising of poly(2-(dimethylamino) ethyl methacrylate)-fullerene (PDMAEMA-C₆₀) with targeting moieties, poly(oligo(ethylene glycol) methyl ether methacrylate)-C₆₀ (POEGMA-C₆₀), nanocrystalline cellulose-fullerene (NCC-C₆₀) and NCC-C₆₀-POEGMA were synthesized and their solution properties were investigated.

PDMAEMA-C₆₀ with galactose targeting moiety was prepared by atom transfer radical polymerization (ATRP) and atom transfer radical addition (ATRA) processes. The self-assembly of galactose functionalized PDMAEMA-C₆₀ structure in aqueous solutions was investigated using dynamic light scattering (DLS) at different pHs. A smaller hydrodynamic radius (R_h) was observed at pH 10 than at pH 3 due to electrostatic repulsion at low pH values. In addition, free PDMAEMA chains induced the demicellization of self-assembled nanostructures caused by the formation of charge transfer complex between PDMAEMA and C₆₀.

A well-defined poly(di(ethylene glycol) methyl ether methacrylate-stat-oligo(ethylene glycol) methyl ether methacrylate)-block-poly(di(ethylene glycol) methyl ether methacrylate ((PMEO₂MA-*stat*-POEGMA₃₀₀)-*b*-PMEO₂)) was successfully synthesized at room temperature via a two-step ATRP process. The block copolymer exhibited two thermal transitions at ~ 30 and 45 °C, which was believed to be associated with the formation of micelles and larger aggregates. The R_h of the aggregates increased from 47 to 90 nm, the aggregation number increased from 76 to ~9800 and R_g/R_h increased from 0.75 to 1.2 within the temperature range of 34 to 45°C. Well-defined statistical (PMEO₂MA-*stat*-POEGMA₃₀₀)-C₆₀ was synthesized via ATRP and ATRA. The lower critical solution temperature (LCST) of (PMEO₂MA-*stat*-POEGMA₃₀₀)-C₆₀ increased with methanol content in water, exhibiting lower LCSTs than PMEO₂MA-*stat*-POEGMA₃₀₀ for all methanol/water compositions. Higher critical micelle concentration (CMC) and larger spherical micelles were observed for (PMEO₂MA-*stat*-POEGMA₃₀₀)-C₆₀ with increasing

methanol content. The R_h of the micelles remained constant at temperature below the LCST and increased dramatically at temperature greater than the LCST, and (R_g/R_h) increased from ~ 0.75 to ~ 1.0 . Nanocrystalline cellulose (NCC) was modified with water-soluble C_{60} -(β -cyclodextrin) and (PMEO₂MA-*stat*-POEGMA₃₀₀)- C_{60}) through a radical coupling reaction. NCC- C_{60} -(PMEO₂MA-*stat*-POEGMA₃₀₀) possessed thermal responsive behavior in water and ~ 3.5 °C hysteresis associated with the heating/cooling cycles. No observable damage to NCC occurred during the radical coupling reaction as determined by TEM. NCC- C_{60} -(β -cyclodextrin) possessed a similar thermal degradation behavior as NCC except it possessed a broader temperature range. Both NCC-fullerene systems demonstrated a radical scavenging activity when screened with the 2,2-diphenyl-1-picrylhydrazyl (DPPH).

In addition, the drug loading and delivery using PDMAEMA- C_{60} with targeting moieties was explored. Two model drugs, namely fluorescein and pyrene were employed to evaluate the location of drug in the self-assembled structure of PDMAEMA- C_{60} . It was found that the hydrophobic drugs were partitioned between the PDMAEMA shells and the hydrophobic fullerene cores. The drug delivery profiles indicated that PDMAEMA- C_{60} is an efficient drug carrier, however, it was cytotoxic to cells. The gene transfection efficacy of PDMAEMA- C_{60} to different cell lines was investigated and the results demonstrated that PDMAEMA- C_{60} exhibited good gene transfection performance. However, the targeting selectivity to liver cells cannot be determined in both cases.

This study demonstrates that nanostructures of stimuli-responsive fullerene polymers can be controlled and manipulated by changing the external environments. Several potential applications, such as in drug and gene delivery, and free radical scavenging can be further explored.

Acknowledgements

Along the journey of my Ph.D. program, I am very fortunate to have interacted with many people, such as teachers, friends and colleagues, to support me through all the ups and downs periods of the PhD research. My thanks to all of them, as their partnership made this thesis possible.

Firstly, I would like to express my sincere gratitude to my supervisor Dr. Michael Tam for his encouragement, time, support, patience, knowledge during my research program.

My thanks and appreciation goes to my Ph.D. committee members: Drs. Duhamel, McManus and Gu for their valuable discussion, suggestions and comments during my study.

I would also like to thank Dr. Duhamel and Dr. Gauthier for allowing me to use their laboratory facilities. At the same time, my special thanks go to Michael Fowler for his guidance with the UV and fluorescence measurements, Toufic Aridi for GPC measurement and Ho Yoon Khei (National University of Singapore) for drug delivery data.

I would like to thank the Natural Sciences and Engineering Research Council (NSERC) of Canada and the University of Waterloo for granting me the NSERC scholarship and President Scholarship for my Ph.D. studies.

Special thanks go to my friends and labmates for their friendship and assistance during my Ph.D. studies.

I am indebted to my parents for their continued love and support in every stage of my life. My heartfelt gratitude goes to my children Daniel and Erin for bringing us heavenly joy to my family. Finally, I owe my deepest gratitude to my husband, Dr. H. Pan, for his love, encouragement and support.

Table of Contents

| | |
|---|-------|
| AUTHOR'S DECLARATION | II |
| ABSTRACT..... | III |
| ACKNOWLEDGEMENTS..... | V |
| LIST OF FIGURES..... | X |
| LIST OF TABLES..... | XVII |
| LIST OF SCHEMES | XVIII |
| CHAPTER 1 INTRODUCTION..... | 1 |
| 1.1 Background..... | 1 |
| 1.2 Research objectives..... | 2 |
| 1.2.1 Synthesis of water soluble C ₆₀ containing polymer with targeting ligands..... | 3 |
| 1.2.2 Biocompatible responsive fullerene containing polymers..... | 3 |
| 1.2.3 Water soluble fullerene containing derivatives as building blocks..... | 4 |
| 1.3 Outline of the Thesis | 4 |
| CHAPTER 2 LITERATURE REVIEW | 6 |
| 2.1 Introduction | 6 |
| 2.2 Synthetic approaches for producing C ₆₀ containing polymers..... | 14 |
| 2.2.1 Grafting polymers to C ₆₀ through carbanion..... | 16 |
| 2.2.2 Grafting polymers to C ₆₀ through macro-radicals..... | 17 |
| 2.2.3 Grafting polymers to C ₆₀ through azide group | 22 |
| 2.3 Stimuli-responsive C ₆₀ containing polymers | 24 |
| 2.3.1 pH-responsive C ₆₀ containing polymers..... | 25 |
| 2.3.2 Temperature responsive C ₆₀ containing polymers..... | 29 |
| 2.3.3 Multi-responsive C ₆₀ containing polymers..... | 38 |
| 2.4 Fullerene containing polymer with targeting moieties..... | 46 |
| 2.4.1 Polymeric micelles used as drug carriers..... | 46 |
| 2.4.2 Targeted drug delivery using polymeric micelles | 47 |
| 2.5 Poly (oligo(ethylene glycol)methyl ether methacrylate) (POEGMA) and its copolymers | 52 |
| 2.6 NCC and its polymer modification derivatives | 53 |
| 2.6.1 Chemical modifications of NCC..... | 53 |
| 2.7 Current and Future Applications of Stimuli-Responsive Fullerene Polymers | 55 |

| | |
|-----------------------|----|
| 2.8 Conclusions | 57 |
|-----------------------|----|

| | |
|---|-----------|
| CHAPTER 3 SYNTHESIS AND SELF-ASSEMBLY OF STIMULI-RESPONSIVE POLY (2-(DIMETHYLAMINO) ETHYL METHACRYLATE)-FULLERENE (PDMAEMA-C₆₀) AND THE SELF-ASSEMBLY UNDER DIFFERENT CONDITIONS..... | 59 |
|---|-----------|

| | |
|------------------------|----|
| 3.1 Introduction | 59 |
|------------------------|----|

| | |
|-----------------------|----|
| 3.2 Experimental..... | 61 |
|-----------------------|----|

| | |
|----------------------|----|
| 3.2.1 Materials..... | 61 |
|----------------------|----|

| | |
|---|----|
| 3.2.2 Synthesis of 6-Isobromobutyryl-1,2:3,4-di- <i>O</i> -isopropylidene-D-galactopyranose (I) | 62 |
|---|----|

| | |
|--|----|
| 3.2.3 Synthesis of PDMAEMA-Cl (II) | 62 |
|--|----|

| | |
|--|----|
| 3.2.4 Preparation of PDMAEMA-C ₆₀ (III) | 63 |
|--|----|

| | |
|---|----|
| 3.2.5 Preparation of PDMAEMA-C ₆₀ with galactose moieties (IV) | 63 |
|---|----|

| | |
|-------------------------------|----|
| 3.2.6 Sample preparation..... | 64 |
|-------------------------------|----|

| | |
|-----------------------------|----|
| 3.2.7 Characterization..... | 64 |
|-----------------------------|----|

| | |
|---------------------------------|----|
| 3.3 Results and Discussion..... | 65 |
|---------------------------------|----|

| | |
|--|----|
| 3.3.1 Synthesis of PDMAEMA-C ₆₀ with galactose moieties | 65 |
|--|----|

| | |
|---|----|
| 3.3.2 Self –assembly of PDMAEMA-C ₆₀ with galactose moieties | 71 |
|---|----|

| | |
|---|----|
| 3.3.3 Free PDMAEMA chains induced demicellization | 74 |
|---|----|

| | |
|-----------------------|----|
| 3.4 Conclusions | 81 |
|-----------------------|----|

| | |
|---|-----------|
| CHAPTER 4 DRUG DELIVERY USING PDMAEMA-C₆₀ | 82 |
|---|-----------|

| | |
|------------------------|----|
| 4.1 Introduction | 82 |
|------------------------|----|

| | |
|-----------------------|----|
| 4.2 Experimental..... | 83 |
|-----------------------|----|

| | |
|----------------------|----|
| 4.2.1 Materials..... | 83 |
|----------------------|----|

| | |
|---------------------------------------|----|
| 4.2.2 Fluorescence measurements | 84 |
|---------------------------------------|----|

| | |
|------------------------------|----|
| 4.2.3 ITC measurements | 84 |
|------------------------------|----|

| | |
|---|----|
| 4.3 Drug and polymer interaction using fluorescent techniques | 85 |
|---|----|

| | |
|--|----|
| 4.5 ITC study of PDMAEMA-C ₆₀ with pyrene and fluorescein | 95 |
|--|----|

| | |
|---|------------|
| CHAPTER 5 TEMPERATURE INDUCED MICELLIZATION AND AGGREGATION OF BIOCOMPATIBLE POLY(OLIGO(ETHYLENE GLYCOL)METHYL ETHER METHACRYLATE) BLOCK COPOLYMER ANALOGUES IN AQUEOUS SOLUTIONS..... | 100 |
|---|------------|

| | |
|------------------------|-----|
| 5.1 INTRODUCTION | 100 |
|------------------------|-----|

| | |
|-----------------------|-----|
| 5.2 Experimental..... | 103 |
|-----------------------|-----|

| | |
|----------------------|-----|
| 5.2.1 Materials..... | 103 |
|----------------------|-----|

| | |
|---|-----|
| 5.2.2 Synthesis of random copolymer of PMEO ₂ MA- <i>stat</i> -POEGMA ₃₀₀ | 103 |
|---|-----|

| | |
|---|-----|
| 5.2.3 Preparation of block copolymer of (PMEO ₂ MA- <i>stat</i> -POEGMA ₃₀₀)- <i>b</i> -PMEO ₂ MA | 104 |
|---|-----|

| | |
|-------------------------------|-----|
| 5.2.4 Sample preparation..... | 104 |
|-------------------------------|-----|

| | |
|-----------------------------|-----|
| 5.2.5 Characterization..... | 105 |
|-----------------------------|-----|

| | |
|---------------------------------|-----|
| 5.3 Results and Discussion..... | 106 |
|---------------------------------|-----|

| | |
|--|-----|
| 5.3.1 Synthesis of (PMEO ₂ MA- <i>stat</i> -POEGMA ₃₀₀)- <i>b</i> -PMEO ₂ MA by ATRP | 106 |
|--|-----|

| | |
|--|------------|
| 5.3.2 Thermal responsive properties of (PMEO ₂ MA- <i>stat</i> -POEGMA ₃₀₀)- <i>b</i> -PMEO ₂ MA in aqueous solutions | 108 |
| 5.3.3 Light scattering to investigate the self-assembly behavior of (PMEO ₂ MA- <i>stat</i> -POEGMA ₃₀₀)- <i>b</i> -PMEO ₂ MA..... | 112 |
| 5.3.4 TEM visualization of the micelles formed by (PMEO ₂ MA- <i>stat</i> -POEGMA ₃₀₀)- <i>b</i> -PMEO ₂ MA | 119 |
| 5.3.5 Proposed mechanism for the self-assembly of (PMEO ₂ MA- <i>stat</i> -POEGMA ₃₀₀)- <i>b</i> -PMEO ₂ MA in aqueous solution at different temperatures..... | 120 |
| | |
| CHAPTER 6 SELF-ASSEMBLY OF THERMO-RESPONSIVE POLY(OLIGO(ETHYLENE GLYCOL) METHYL ETHER METHACRYLATE)-C₆₀ IN WATER-METHANOL MIXTURES | 123 |
| 6. 1. Introduction | 123 |
| 6.2 Experimental..... | 124 |
| 6.2.1 Materials..... | 124 |
| 6.2.2 Synthesis of PME ₂ O ₂ MA- <i>stat</i> -POEGMA ₃₀₀ | 124 |
| 6.2.3 Preparation of amphiphilic copolymer of (PME ₂ O ₂ MA- <i>stat</i> -POEGMA ₃₀₀)-C ₆₀ | 125 |
| 6.2.4 Sample Preparation..... | 125 |
| 6.2.5 Characterization..... | 126 |
| 6.3 Results and Discussion..... | 126 |
| 6.3.1 Synthesis of (PME ₂ O ₂ MA- <i>stat</i> -POEGMA ₃₀₀)-C ₆₀ by ATRP and ATRA..... | 126 |
| 6.3.2 Effect of methanol composition on the LCST of PME ₂ O ₂ MA- <i>stat</i> -POEGMA ₃₀₀ and (PME ₂ O ₂ MA- <i>stat</i> -POEGMA ₃₀₀)-C ₆₀ | 131 |
| 6.3.3 Self-assembly behavior of (PME ₂ O ₂ MA- <i>stat</i> -POEGMA ₃₀₀)-C ₆₀ in water/methanol at different temperatures..... | 133 |
| 6.4 Conclusions | 139 |
| | |
| CHAPTER 7 FUNCTIONALIZATION OF NANOCRYSTAL CELLULOSE WITH FULLERENE DERIVATIVES VIA RADICAL COUPLING REACTION..... | 140 |
| 7.1 Introduction | 140 |
| 7.2.1 Materials..... | 142 |
| 7.2.2 Preparation of NCC-C ₆₀ | 143 |
| 7.2.3 Preparation of NCC-C ₆₀ -POEGMA..... | 143 |
| 7.2.4 Characterization..... | 145 |
| 7.3 Results and Discussion..... | 145 |
| 7.3.1 Synthesis and characterization of NCC-C ₆₀ -(β-cyclodextrin)..... | 145 |
| 7.3.2 Synthesis and characterization of NCC-C ₆₀ -(PME ₂ O ₂ MA- <i>stat</i> -POEGMA ₃₀₀) | 150 |
| 7.3.3 Radical scavenging of DPPH..... | 156 |
| 7.4 Conclusions | 156 |
| | |
| CHAPTER 8 CONCLUSIONS AND RECOMMENDATIONS | 158 |
| 8.1 General Contributions | 158 |
| 8.1.1 PDMAEMA-C ₆₀ with targeting moieties..... | 158 |
| 8.1.2 Block copolymer of POEGMA analogues | 159 |
| 8.1.3 Synthesis of thermal responsive POEGMA-C ₆₀ and its self-assembly in solvent mixtures | 159 |
| 8.1.4 Synthesis of NCC-C ₆₀ -(β-cyclodextrin) and NCC-C ₆₀ -POEGMA and their physical properties..... | 160 |
| 8.2 Recommendations for future work..... | 160 |

| | |
|--|------------|
| 8.2.1 Improving the targeting efficacy of fullerene containing polymer for drug delivery applications | 161 |
| 8.2.2 Block copolymers of POEGMA analogues with different LCSTs | 162 |
| 8.2.3 Other methods to modify NCC using fullerene derivatives | 163 |
| APPENDIX DRUG DELIVERY AND GENE TRANSFECTION USING PDMAEMA-C₆₀ | 164 |
| A.1 MATERIALS | 164 |
| A.2 EXPERIMENTAL | 164 |
| A.2.1 Drug delivery..... | 164 |
| A.2.2 Gene transfection | 164 |
| A.3 Results AND Discussion | 165 |
| A.3.1 In vitro drug delivery study | 165 |
| A.3.2 Gene transfection using PDMAEMA-C₆₀ | 168 |
| A.4 Conclusions | 169 |
| REFERENCES | 170 |

List of Figures

| | |
|---|----|
| Figure 2. 1 Structures of C ₆₀ containing polymers | 8 |
| Figure 2. 2 A. Dependence of R _h on α for 0.1 wt % PAA-C ₆₀ (○) and C ₆₀ -PAA-C ₆₀ (●) in 0.1 M NaCl solution; (B). Dependence of R _h (○), R _g (●), and R _g /R _h (▲) on pH for 0.1 wt % C ₆₀ -PAA-C ₆₀ in 0.1 M NaCl. | 26 |
| Figure 2. 3 (a). Effect of salt concentration on R _h for 0.2 wt% PMAA-C ₆₀ at $\alpha = 1$; (b). Dependence of Rh on degree of neutralization α for 0.2 wt% PMAA-C ₆₀ in aqueous solution...28 | 28 |
| Figure 2. 4 (A) TEM images of PAA-C ₆₀ film cast from water solution; (B) Cartoon of molecular packing of PAA-C ₆₀ in film. | 29 |
| Figure 2. 5 Fluorescence emission spectra of (A) pyrene-poly(<i>N</i> -isopropylacrylamide)-fullerene (4); (B) pyrene-poly(<i>N</i> -isopropylacrylamide- <i>co</i> -fullerenylethyl methacrylate) (8) at various temperatures irradiated at 340 nm. | 31 |
| Figure 2. 6 Temperature dependence of optical transmittance at 700 nm obtained for 2.0 g/L aqueous solutions of N ₃ -PNIPAM ₉₈ , C ₆₀ -PNIPAM ₉₈ , (N ₃) ₂ -PNIPAM ₁₀₀ , and (C ₆₀) ₂ -PNIPAM ₁₀₀ | 34 |
| Figure 2. 7 Hydrodynamic radius distributions, $f(R_h)$, obtained for 0.5 g/L aqueous solutions of C ₆₀ -PNIPAM ₉₈ and (C ₆₀) ₂ -PNIPAM ₁₀₀ at 25 °C. | 35 |
| Figure 2. 8 Temperature dependence of optical transmittance at 600 nm of PNIPAM (▲) and PNIPAM-C ₆₀ (●) and the cumulative diameter of PNIPAM-C ₆₀ (○) in water as a function of temperature. | 37 |
| Figure 2. 9 ¹ H NMR spectra of Bet-PDMAEMA-C ₆₀ in D ₂ O measured at different temperatures. | 41 |

| | |
|--|----|
| Figure 2. 10 Schematic representation of <i>Bet</i> -PDMAEMA- <i>b</i> -C ₆₀ in the presence of different concentrations of NaCl. | 42 |
| Figure 2.11 Schematic representation of the possible microstructures of P(MAA ₁₀₂ - <i>b</i> -DMAEMA ₆₇)- <i>b</i> -C ₆₀ in aqueous solutions at different pH and temperatures. | 45 |
| Figure 2. 12 Passive targeting delivery via EPR effect..... | 48 |
| Figure 2. 13 Active targeting delivery via drug carrier with targeting moieties | 49 |
| Figure 2. 14 Chemical structures used to modify NCC | 55 |
| Figure 3. 1 ¹ H NMR spectrum of 6-Isobromobutyryl-1,2:3,4-di- <i>O</i> -isopropylidene-D-galactopyranose..... | 67 |
| Figure 3. 2 GPC traces of (a) PDMAEMA; (b) PDMAEMA-C ₆₀ and (c) PDMAEMA-C ₆₀ with galactose moieties. | 68 |
| Figure 3. 3 ¹ H NMR spectra of (i). PDMAEMA-C ₆₀ and (ii). PDMAEMA-C ₆₀ with galactose moieties. | 69 |
| Figure 3. 4 UV-vis spectrum of PDMAEMA-C ₆₀ with galactose moieties (IV) in water. | 70 |
| Figure 3. 5 ¹³ C NMR spectrum of PDMAEMA-C ₆₀ (IV)..... | 70 |
| Figure 3. 6 Decay time distribution functions at pH 3 and 10 for PDMAEMA-C ₆₀ with galactose moieties. | 73 |
| Figure 3. 7 (a) TEM and (b) SEM images of PDMAEMA-C ₆₀ with galactose moieties. | 73 |
| Figure 3. 8 Decay time distribution of PDMAEMA-C ₆₀ : (a) 18k and (b) 8k | 75 |
| Figure 3. 9 Dynamic light scattering to measure the CMC of PDMAEMA-C ₆₀ | 76 |
| Figure 3. 10 Effect of PDMAEMA on the hydrodynamic radii of PDMAEMA-C ₆₀ at pH 3 and 10..... | 78 |

| | |
|--|----|
| Figure 3. 11 Decay time distribution functions of (a) PDMAEMA-C ₆₀ and mixtures of PDMAEMA and PDMAEMA-C ₆₀ at mole ratio of (b) 1; (c) 2 and (d) 4 at pH 3. | 78 |
| Figure 3. 12 Decay time distribution functions of (a) PDMAEMA-C ₆₀ and mixtures of PDMAEMA and PDMAEMA-C ₆₀ at mole ratio of (b) 1; (c) 2 and (d) 4 at pH 10 | 79 |
| Figure 3. 13 Schematic diagram describing the self-assembly behaviors of PDMAEMA-C ₆₀ with and without addition of free PDMAEMA at pH 3 and 10). | 80 |
| Figure 4. 1 Pictures of (a). aqueous solution of fluorescein; (b). aqueous solution of fluorescein and PDMAEMA-C ₆₀ | 86 |
| Figure 4. 2 UV-Vis spectra of (a) fluorescein and (b) fluorescein/PDMAEMA-C ₆₀ | 87 |
| Figure 4. 3 Steady state fluorescence of different concentrations of fluorescein (a). 400; (b). 600; (c). 800; (d).1000 and (e) 1200 nM..... | 88 |
| Figure 4. 4 Steady state fluorescence of mixture of fluorescein/PDMAEMA (0.2 mg/ml) at fluorescein concentrations of (a). 400; (b). 600; (c). 800; (d).1000 and (e) 1200 nM..... | 89 |
| Figure 4. 5 Steady state fluorescence of mixture of fluorescein/PDMAEMA-C ₆₀ (0.2 mg/ml) at fluorescein concentrations of (a). 400; (b). 600; (c). 800; (d).1000 and (e) 1200 nM..... | 89 |
| Figure 4. 6 Steady state fluorescence of (a). fluorescein; (b). fluorescein with PDMAEMA and (c). fluorescein with PDMAEMA-C ₆₀ | 90 |
| Figure 4. 7 Steady state fluorescence of (a). pyrene; (b). pyrene/PDMAEMA, and (c).pyrene/PDMAEMA-C ₆₀ | 91 |
| Figure 4. 8 Steady state fluorescence of (a). pyrene; (b). pyrene/PAA and (c). pyrene/PAA-C ₆₀ | 92 |
| Figure 4. 9 Pyrene fluorescence quenching at (a). pH 3 and (b). pH 10 with different concentrations of PDMAEMA-C ₆₀ | 93 |

| | |
|---|-----|
| Figure 4. 10 Decay time distribution of drug loaded PDMAEMA-C ₆₀ at pH 7.2. | 94 |
| Figure 4. 11 Angular dependence of the decay rate of q^2 for drug loaded PDMAEMA-C ₆₀ at pH 7.2..... | 94 |
| Figure 4. 12 Schematic structures of PDMAEMA-C ₆₀ without and with drug loadings. | 95 |
| Figure 4. 13 Raw ITC data for titrating fluorescein (0.06 mM) into (a). 0.04 wt% PDMAEMA; (b). 0.04 wt% PDMAEMA-C ₆₀ | 97 |
| Figure 4. 14 Differential enthalpy curves for titrating fluorescein (0.06 mM) into 0.04 wt% (a). PDMAEMA-C ₆₀ and (b). PDMAEMA..... | 98 |
| Figure 4. 15 Differential enthalpy curves for titrating pyrene (10 mM) into 0.04 wt% (a). PDMAEMA-C ₆₀ and (b). PDMAEMA..... | 99 |
| Figure 5. 1 ¹ H NMR spectrum recorded in CDCl ₃ for (PMEO ₂ MA- <i>stat</i> -POEGMA ₃₀₀)- <i>b</i> -PMEO ₂ MA | 107 |
| Figure 5. 2 GPC traces of (a) PMEO ₂ MA- <i>stat</i> -POEGMA ₃₀₀ ; (b) (PMEO ₂ MA- <i>stat</i> -POEGMA ₃₀₀)- <i>b</i> -PMEO ₂ MA | 108 |
| Figure 5. 3 UV–Vis experiment at 500 nm versus temperature to measure the phase transitions: (a). PMEO ₂ MA- <i>stat</i> -POEGMA ₃₀₀ ; (b). (PMEO ₂ MA- <i>stat</i> -POEGMA ₃₀₀)- <i>b</i> -PMEO ₂ MA in aqueous solution at 4 mg/mL..... | 111 |
| Figure 5. 4 Differential data of Figure 5.3. (a). PMEO ₂ MA- <i>stat</i> -POEGMA ₃₀₀ ; (b). (PMEO ₂ MA- <i>stat</i> -POEGMA ₃₀₀)- <i>b</i> -PMEO ₂ MA in aqueous solution at 4 mg/mL..... | 111 |
| Figure 5. 5 DSC curves of (a). PMEO ₂ MA- <i>stat</i> -POEGMA ₃₀₀ ; (b). (PMEO ₂ MA- <i>stat</i> -POEGMA ₃₀₀)- <i>b</i> -PMEO ₂ MA in aqueous solution at 4 mg/mL..... | 112 |
| Figure 5. 6 Dependence of decay rate on q^2 for (PMEO ₂ MA- <i>stat</i> -POEGMA ₃₀₀)- <i>b</i> -PMEO ₂ MA in aqueous solution at 38 °C | 113 |

| | |
|--|-----|
| Figure 5. 7 Effect of temperature on the hydrodynamic radius (R_h) and radius of gyration (R_g) of the aggregates of 0.2 mg/ml (PMEO ₂ MA- <i>stat</i> -POEGMA ₃₀₀)- <i>b</i> -PMEO ₂ MA aqueous solution . | 114 |
| Figure 5. 8 Decay time distribution recorded at different temperatures of 0.2 mg/ml (PMEO ₂ MA- <i>stat</i> -POEGMA ₃₀₀)- <i>b</i> -PMEO ₂ MA aqueous solution..... | 114 |
| Figure 5. 9 Dependence of scattering light intensity on time at different temperatures measured at 90° for 0.2 mg/ml (PMEO ₂ MA- <i>stat</i> -POEGMA ₃₀₀)- <i>b</i> -PMEO ₂ MA in aqueous solution..... | 115 |
| Figure 5. 10 Berry plot of (PMEO ₂ MA- <i>stat</i> -POEGMA ₃₀₀)- <i>b</i> -PMEO ₂ MA in aqueous solution with concentration of 0.2 mg/ml at 36 and 45°C | 117 |
| Figure 5. 11 KC/R(q) vs. the scattering vector (q^2) for 0.6 mg/ml (PMEO ₂ MA- <i>stat</i> -POEGMA ₃₀₀)- <i>b</i> -PMEO ₂ MA aqueous solution at different temperatures | 119 |
| Figure 5. 12 TEM images of micelles formed by (PMEO ₂ MA- <i>stat</i> -POEGMA ₃₀₀)- <i>b</i> -PMEO ₂ MA at different temperatures: (a). 38°C and (b). 45°C | 120 |
| Figure 5. 13 Schematic diagram to describe the self-assembly behaviors of (PMEO ₂ MA- <i>stat</i> -POEGMA ₃₀₀)- <i>b</i> -PMEO ₂ MA at different temperatures..... | 121 |
| Figure 6. 1 GPC profiles of copolymer PMEO ₂ MA- <i>stat</i> -POEGMA ₃₀₀ | 128 |
| Figure 6. 2 (A). ¹ H NMR spectrum recorded in CDCl ₃ for (PMEO ₂ MA- <i>stat</i> -POEGMA ₃₀₀)-C ₆₀ and (B). ¹³ C NMR spectrum recorded in C ₆ D ₆ for (PMEO ₂ MA- <i>stat</i> -POEGMA ₃₀₀)-C ₆₀ | 130 |
| Figure 6. 3 UV-Vis spectra of PMEO ₂ MA- <i>stat</i> -POEGMA ₃₀₀ and (PMEO ₂ MA- <i>stat</i> -POEGMA ₃₀₀)-C ₆₀ in water solution. | 130 |
| Figure 6. 4 Effects of methanol composition (from left to right: 0, 5, 10, 15, 20, 25 and 30%) on the LCST of (a). PMEO ₂ MA- <i>stat</i> -POEGMA ₃₀₀ and (b). (PMEO ₂ MA- <i>stat</i> -POEGMA ₃₀₀)-C ₆₀ . . | 132 |
| Figure 6. 5 LCSTs of PMEO ₂ MA- <i>stat</i> -POEGMA ₃₀₀ and PMEO ₂ MA- <i>stat</i> -POEGMA ₃₀₀)- <i>b</i> -C ₆₀ at various methanol contents. | 132 |

| | |
|--|-----|
| Figure 6. 6 CMC of (PMEO ₂ MA- <i>stat</i> -POEGMA ₃₀₀)-C ₆₀ in (a). water and (b). 25% methanol/water at 25°C measured by DLS. | 134 |
| Figure 6. 7 Effect of methanol content on CMC of (PMEO ₂ MA- <i>stat</i> -POEGMA ₃₀₀)-C ₆₀ in water/methanol mixtures. | 135 |
| Figure 6. 8 Effect of temperature on the hydrodynamic radius (R _h) of the micelles of (PMEO ₂ MA- <i>stat</i> -POEGMA ₃₀₀)-C ₆₀ in methanol/water solution measured at 0.2 mg/ml. | 135 |
| Figure 6. 9 Hydrodynamic radius (R _h) of micelles of (PMEO ₂ MA- <i>stat</i> -POEGMA ₃₀₀)- <i>b</i> -C ₆₀ in various methanol/water compositions measured at 0.2 mg/ml below the LCST. | 136 |
| Figure 6. 10 TEM images of micelles formed by (PMEO ₂ MA- <i>stat</i> -POEGMA ₃₀₀)-C ₆₀ in: (a) water ; (b) 10% methanol/water at 25°C, (c). water at 45 °C and (d). 10 vol% methanol/water at 50 °C. | 138 |
| Figure 7. 1 Aqueous solutions of (a). NCC-C ₆₀ -(β-cyclodextrin) and (b). NCC. | 148 |
| Figure 7. 2 UV-Vis spectrum of (a). NCC and (b). NCC-C ₆₀ -(β-cyclodextrin) and (c). NCC-C ₆₀ -(PMEO ₂ MA- <i>stat</i> -POEGMA ₃₀₀) in water solution. | 149 |
| Figure 7. 3 TGA curves of (a). NCC; (b) NCC-C ₆₀ -(β-cyclodextrin); (c) (PMEO ₂ MA- <i>stat</i> -POEGMA ₃₀₀)-C ₆₀ and d. NCC-C ₆₀ - (PMEO ₂ MA- <i>stat</i> -POEGMA ₃₀₀). | 149 |
| Figure 7. 4 TEM images of (a) NCC-C ₆₀ -(β-cyclodextrin) and (b) NCC-C ₆₀ - (PMEO ₂ MA- <i>stat</i> -POEGMA ₃₀₀). | 150 |
| Figure 7. 5 ¹ H NMR spectra for (i). (PMEO ₂ MA- <i>stat</i> -POEGMA ₃₀₀)- <i>b</i> -C ₆₀ (in CDCl ₃) and (ii).NCC-C ₆₀ -(PMEO ₂ MA- <i>stat</i> -POEGMA ₃₀₀) (in D ₂ O). | 153 |
| Figure 7. 6(a) UV–Vis experiment to measure the phase transitions upon heating and cooling the aqueous solution of NCC-C ₆₀ -(PMEO ₂ MA- <i>stat</i> -POEGMA ₃₀₀) (4 mg/mL) and (b) Differential curves of Figure 7.6(a). | 155 |

| | |
|--|-----|
| Figure 7. 7 UV-Vis to measure the DPPH radical scavenging activity: (a). DPPH in DMSO solution, (b). DPPH solution mixed with NCC-C ₆₀ -(β-cyclodextrin) ; (c). DPPH solution mixed with NCC-C ₆₀ -(PMEO ₂ MA- <i>stat</i> -POEGMA ₃₀₀) | 156 |
| Figure A-1 Micrographs of cells (a). HepG2; (b). N2a; (c). HepG2 with fluorescein; (d). N2a with fluorescein; (e). HepG2 with fluorescein loaded PDMAEMA-C ₆₀ ; (f). N2a with fluorescein loaded PDMAEMA-C ₆₀ | 167 |
| Figure A-2 Addition of trypan blue to (a). HepG2 cells; (b). HepG2 cells treated flourescein loaded PDMAEMA-C ₆₀ | 167 |
| Figure A-3 Fluorescence micrographs (×10) of the gene expression using PDMAEMA-C ₆₀ at N/P 20 to different cells (a). HepG2; (b). N2a and (c). NG108..... | 169 |
| Figure A-4 Fluorescence micrographs (×10) of the gene expression using a positive control with LPEI at N/P 20 to different cells (a). HepG2; (b). N2a and (c). NG108..... | 169 |

List of Tables

| | |
|---|-----|
| Table 2. 1 Modification of C ₆₀ with various polymeric systems | 9 |
| Table 2. 2 Polymeric micelles with targeting moieties | 50 |
| Table 5. 1 Effect of temperature on the ratio of R _g /R _h and the aggregation number (N _{agg}) | 116 |
| Table 6. 1 Micelle properties of (PMEO ₂ MA- <i>stat</i> -POEGMA ₃₀₀)-C ₆₀ in water/methanol mixtures of various compositions at different temperatures | 137 |

List of Schemes

| | |
|---|-----|
| Scheme 2. 1 Synthesis of polystyrene-C ₆₀ using C ₆₀ based ATRP initiator | 16 |
| Scheme 2. 2 Synthesis of isotactic PMMA-C ₆₀ using carbanion | 17 |
| Scheme 2. 3 Synthesis of C ₆₀ -(polystyrene) ₂ using TEMPO macro-radicals | 18 |
| Scheme 2. 4 Synthesis of PNIPAM-C ₆₀ using macro-radicals generated by RAFT | 19 |
| Scheme 2. 5 Synthesis of PPV-b-PS-(C ₆₀) _m using ATRA method | 21 |
| Scheme 2. 6 Synthesis of Pst-C ₆₀ and PMMA-C ₆₀ using combination of ATRP and ATRA. | 21 |
| Scheme 2. 7 Synthesis of C ₆₀ -PEO-C ₆₀ using azido coupling reaction. | 22 |
| Scheme 2. 8 Synthesis of PAA-C ₆₀ via ATRP and azido coupling. | 24 |
| Scheme 2. 9 (A). Synthesis of pyrene-poly(<i>N</i> -isopropylacrylamide)-fullerene (4), and (B). pyrene-poly(<i>N</i> -isopropylacrylamide- <i>co</i> -fullerenylethyl methacrylate) (8). | 31 |
| Scheme 2. 10 Synthesis of C ₆₀ -PNIPAM, (C ₆₀) ₂ -PNIPAM and PEG-C ₆₀ -b-PNIPAM. | 33 |
| Scheme 2. 11 Synthesis of <i>Bet</i> -PDMAEMA-C ₆₀ | 40 |
| Scheme 3. 1 Synthetic scheme of PDMAEMA-C ₆₀ with targeting moiety | 66 |
| Scheme 4. 1 Chemical structures of (a). Fluorescein; (b). Pyrene..... | 86 |
| Scheme 5. 1 Synthetic scheme of block copolymer of (PMEO ₂ MA- <i>stat</i> -POEGMA ₃₀₀)- <i>b</i> - PMEO ₂ MA | 106 |
| Scheme 6. 1 Synthetic scheme of (PMEO ₂ MA- <i>stat</i> -POEGMA ₃₀₀)-C ₆₀ | 127 |
| Scheme 7. 1 Synthetic scheme for NCC-C ₆₀ | 147 |
| Scheme 7. 2 Synthetic scheme for NCC-C ₆₀ -(PMEO ₂ MA- <i>stat</i> -POEGMA ₃₀₀)..... | 152 |
| Scheme 8. 1 Synthesis of PDMAEMA-C ₆₀ with different galactose contents..... | 162 |

Chapter 1 Introduction

1.1 Background

Since its discovery in 1985, fullerene (C_{60}) has been drawing increasing research attention, especially its water-soluble polymer modified derivatives due to their attractive properties. Modification of C_{60} using hydrophilic molecules is necessary to improve the solubility of C_{60} in aqueous solution resulting in the broadening of its applications. In general, this modification can be divided into two categories: (1) modification of C_{60} with small molecules including carboxylic acids, [Cerar et al. 2003] hydroxyls, [Chiang et al. 1996] or amines [Richardson et al. 2000], cyclodextrins, etc. (2) modification of C_{60} with hydrophilic polymer chains, such as poly(acrylic acid) (PAA), polyethylene oxide (PEO), poly (methacrylic acid) PMAA etc.

Compared to the modification of C_{60} with small molecules, modification of C_{60} with hydrophilic polymers is more prevalent because a lower degree of substitution is needed to achieve solubility, hence the pristine nature of C_{60} is maintained.

A number of functional groups, such as amine, carbanion, macro-radical, and azide can directly react with the [6,6] bonds of C_{60} and they were used in the synthesis of a wide range of fullerene derivatives. Polymer C_{60} derivatives produced via these functional groups are well-documented, where well-defined polymers with proper functional groups, prepared from anionic polymerization, controlled radical polymerizations including atom transfer radical polymerization (ATRP), stable free radical polymerization (SFRP), reversible addition reversible addition fragmentation chain transfer (RAFT), ring opening polymerization (ROP) were used to modify C_{60} .

Stimuli-responsive polymers are important and popular classes of systems since these types of functionalization of C_{60} can undergo conformational changes upon the application of external stimuli, such as temperature or pH. A series of stimuli-responsive water-soluble fullerene systems have been reported, such as PMAA- C_{60} , [Ravi et al. 2005a] PDMAEMA- C_{60} [Dai et al. 2004, Yao et al. 2011] and its betainization derivative [Ravi et al. 2005b], P(MAA-DMAEMA)- C_{60} , [Teoh et al. 2005] PAA- C_{60} [Yang et al. 2003, Ravi et al. 2006, Wang et al. 2007] and PNIPAM- C_{60} systems [Li et al. 2009, Tamura et al. 2006, Hong et al. 2009, Liu et al. 2008]. The variation of pH, temperature, salt or solvent composition can lead to the formation of different morphologies of aggregates for the stimuli-responsive water-soluble C_{60} containing polymers. These interesting solution behaviors extend the applications of the fullerene containing polymers to the fields of material chemistry and biotechnology. Some potential applications, such as photoconductivity and temperature sensor have been investigated.

Research on water-soluble C_{60} polymer derivatives is becoming more challenging, especially when it is being explored for actual applications. In addition, many new applications could be explored if new materials are used to modify C_{60} . In this thesis, we seek to address some of these issues and extend the list of polymers that can be used to modify C_{60} .

1.2 Research objectives

Based on the understanding of the background and the research trend of fullerene containing polymer derivatives, we formulated the following goals for this thesis.

1.2.1 Synthesis of water soluble C₆₀ containing polymer with targeting ligands

It is known that polymeric micelles can be used as drug carriers because of their unique sizes and architectures. [Zhang, et al. 1997, Shin et al. 1998, Yu et al. 1998, Jeong et al. 1999, Han et al. 2000]. Owing to the findings that some of the water-soluble fullerene polymers, such as PDMAEMA-C₆₀, were found to form micelles in aqueous solution, we anticipated that these micelles with a fullerene core and hydrophilic polymer shells could be used as drug vehicles since they could act as reservoirs for hydrophobic drugs through π - π hydrophobic interaction. In order to achieve targeted delivery to the specific sites, active targeting has been developed by attaching certain kinds of targeting moieties to the drug carriers. Polymeric micelles as drug carriers have been extensively studied and they showed promising results for targeted drug delivery. Therefore, one of our goals was to synthesize well-defined fullerene containing stimuli responsive water-soluble polymers with targeting moieties and explore their self-assembly and drug delivery behaviors.

1.2.2 Biocompatible responsive fullerene containing polymers

Although various kinds of polymers have been used to fabricate C₆₀ containing systems, however, only a limited number of them are biocompatible. Recent studies [Lutz et al. 2006a, 2006b, 2007, 2009, 2011] reported that copolymers of OEGMA analogues exhibited a tunable thermal responsive behavior and in-vitro cell tests of several POEGMA analogues showed excellent biocompatibility [Lutz et al. 2008, Lutz et al. 2007b]. Therefore, biocompatible thermal responsive polymers composed of oligo(ethylene glycol) methacrylate (POEGMA) [Han et al 2003, Mertoglu et al. 2005, Kitano et al 2004, Lutz et al. 2006a, Lutz et al. 2007a] have attracted increasing attention. In addition, modification of C₆₀ with POEGMA will produce a

biocompatible thermo-responsive water-soluble C_{60} polymer which is critical for biological applications.

1.2.3 Water soluble fullerene containing derivatives as building blocks

A wide variety of water-soluble C_{60} derivatives have been produced and some applications have been investigated. However, there has been no further exploration in using them as building blocks. We believe that it will benefit the research community if we can develop a method by modifying some materials using water-soluble C_{60} derivatives since this will impart attractive properties to the new materials. Nanocrystalline cellulose (NCC), a renewable and biodegradable nano-material, is attracting increasing attention because it possesses high tensile strength, low density, and large surface area. The utility of NCC can be explored in diverse fields including electronics, [Mangilal et al. 2009] materials science [Sturcova et al. 2005] and biomedical science [Wojciech et al. 2007] As a result of the attractive features of NCC, we seek to develop a facile method for modifying NCC with fullerene derivatives to yield functional materials that could potentially be used in free-radical scavenging applications.

1.3 Outline of the Thesis

The work in this thesis can be divided into three parts: (1) Active drug delivery exploration of stimuli-responsive water-soluble C_{60} polymer with targeting moieties; (2) Modify C_{60} with a biocompatible responsive polymer, i.e. POEGMA analogues to make C_{60} containing polymer more versatile in terms of biomedical applications; (3) Functionalizing nanocrystalline cellulose (NCC) with C_{60} and responsive C_{60} containing polymers to construct more interesting structures.

Chapter 1 presents a brief overview of the current research status of water-soluble C₆₀ polymers where the objectives of this thesis are clearly described. Chapter 2 reviews the literature on the synthesis and solution behaviors of stimuli-responsive water-soluble fullerene containing polymers, POEGMA copolymers and chemical modification of NCC. The synthesis and self-assembly study PDMAEMA-C₆₀ with targeting moieties will be described and discussed in Chapter 3. Chapter 4 attempts to investigate the drug loading, drug delivery and gene transfection using the PDMAEMA-C₆₀ systems.

The synthesis and self-assembly of block copolymer of POEGMA composed of two segments with different LCSTs will be reported in Chapter 5.

Chapter 6 presents the synthesis of POEGMA-C₆₀ using ATRP and ATRA techniques, and the self-assembly behavior was examined at various temperatures. The synthesis of NCC-C₆₀-(β-CD) and NCC-C₆₀-POEGMA using the radical coupling reaction and the physical properties was investigated and discussed in Chapter 7. Chapter 8 summarizes the original contributions of the thesis and presents several recommendations for future study.

Chapter 2 Literature review

2.1 Introduction

Fullerene (C_{60}), which was discovered in 1985 by Kroto, Curl and Smalley [Kroto et al. 1985] possess a diverse range of attractive properties, such as electronic, conducting, antioxidant and magnetic properties due to its unusual symmetry and electron conjugate characteristic. [Rosseinsky et al. 1995, Stephens et al. 1992] However, its strong cohesive nature and poor solubility in common aqueous and organic solvents [Ruoff et al. 1993] hampered its applications in the fields of biomedical [Sariciftci et al. 1993, Shih et al. 2001, Bosi et al. 2004 and 2003] and material chemistry.[Dardel et al. 2001, Koppe et al. 2007] Therefore, various types of functionalization strategies have been explored to broaden and expand its end-use applications. [Kraulova et al. 1999, Ravi et al. 2007] In particular, water-soluble fullerene systems are undoubtedly of great interest, particularly for biomedical applications. [Kasermann et al. 1997, Ueng et al. 1997, Ros et al. 1999, Friedman et al. 1993, Thakral et al. 2006, Tegos et al. 2005] In general, water-soluble C_{60} derivatives could be obtained by modifying C_{60} with polar functional groups either through covalent or non-covalent route. Small molecules including carboxylic acid, [Cerar et al. 2003] hydroxyl, [Chiang et al. 1996,] or amine [Richardson et al. 2000] were used to covalently modify C_{60} . The non-covalent complexes of C_{60} with cyclodextrins, [Filippone et al. 2002, Samal et al. 2000, Anderson et al. 1992, Liu et al. 2005, Chen et al. 2006] calixerenes, [Atwood et al. 1994] phospholipids, [Hwang et al. 1992 and 1993] liposomes [Bensasson et al. 1994] and organic compounds bearing electron donating groups to form complexes. [Zgonnik et al. 1998, Ungurenasu et al. 2000] Grafting hydrophilic polymer chains onto the surface of C_{60} is another desirable approach to modify C_{60} because it not only increases the solubility of C_{60} , but it offers other attractive properties to the system. Compared to the covalent modification of C_{60}

with small molecules, where the functionalization involves multiple functional groups that may damage the π - π conjugation and thus partially disrupting the physical properties of C_{60} . Thus, a lower degree of substitution is needed, which can be achieved by polymer grafting to C_{60} , which helps retain the unique property of C_{60} . Hydrophilic polymers with stimuli-responsive properties are of great interest since these types of functionalization of C_{60} can yield potentially new systems with responsive characteristics. Stimuli-responsive polymers are capable of conformational and chemical changes when subjected to external stimuli, such as temperature, pH, or solvent composition. C_{60} modified with these kinds of polymers combines the unique properties of C_{60} with the stimuli characteristics of the polymers that may extend their end-use applications in the fields of biotechnology and biomedicine. In the recent years, a variety of stimuli-responsive water-soluble fullerene systems have been reported, such as PMAA- C_{60} , [Ravi et al. 2005a] PDMAEMA- C_{60} [Dai et al. 2004, Yao et al. 2011] and its betainization derivative [Ravi et al. 2005b] and P(MAA-DMAEMA)- C_{60} , [Teoh et al. 2005] PAA- C_{60} [Yang et al. 2003, Ravi et al. 2006, Wang et al. 2007] and PNIPAM- C_{60} systems. [Li et al. 2009, Tamura et al. 2006, Hong et al. 2009, Liu et al. 2008]

Over the last two decades, various C_{60} containing polymers, including hydrophobic and hydrophilic polymers have been prepared and their structures are shown schematically in Figure 2.1. An overview and summary of the major systems including preparation methods, physical properties and characterization on the modification of C_{60} with different polymers are documented in Table 2.1. In this chapter, we will discuss the synthetic approaches of producing C_{60} containing polymers, evaluate their physical properties in aqueous solution, and outline the current and potential applications of these systems in various fields. In addition, we will discuss targeted drug delivery and some new materials including poly(oligo(ethylene glycol)methyl ether

methacrylate) (POEGMA) and nanocrystalline cellulose (NCC), which were used to modify C_{60} in our research.

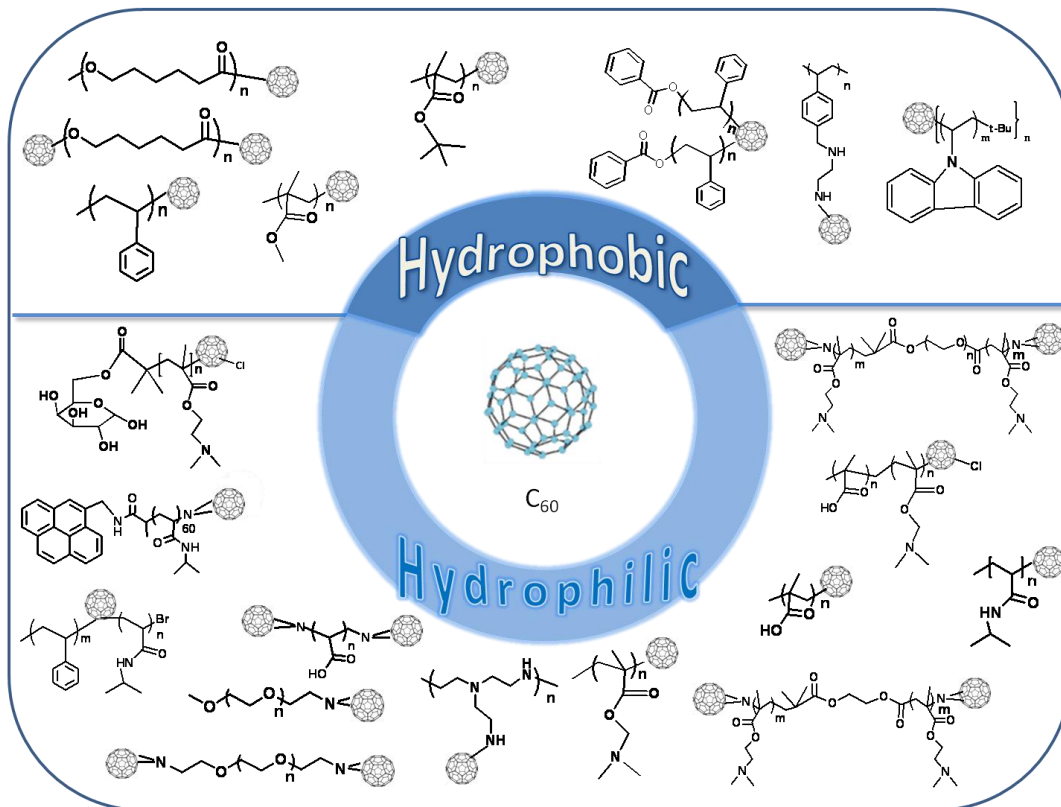
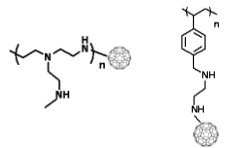
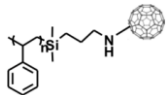
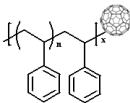
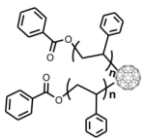
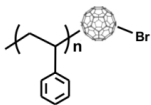
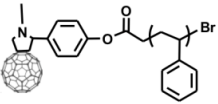
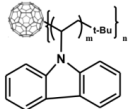
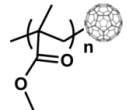
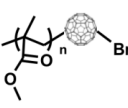
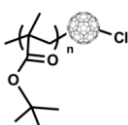
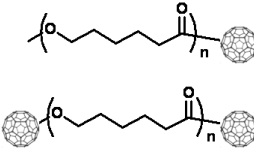
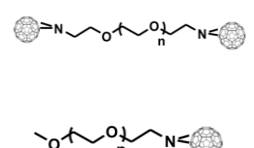
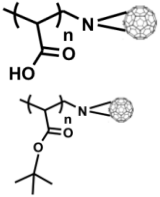
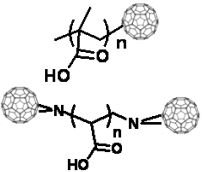
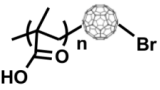
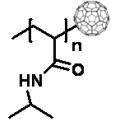
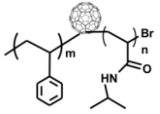


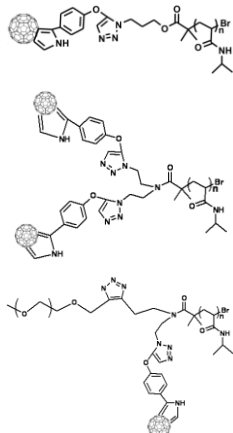
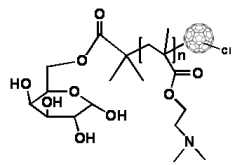
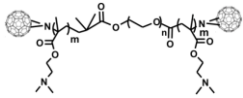
Figure 2. 1 Structures of C_{60} containing polymers (Refer to Table 2.1 for description of structures)

Table 2. 1 Modification of C₆₀ with various polymeric systems

| Polymers | Synthetic methods/Reagents | Physical properties/note | Structures | Characterizations | References |
|---|--|--|---|---|----------------------|
| poly(ethylene imine), poly[4-[(2-aminoethyl)imino]methyl]styrene | Amine addition to fullerene | Solubility of C ₆₀ was increased |  | C ₆₀ confirmed using solid-state ¹³ C MAS NMR at 147.2 ppm. | Geckeler et al. 1993 |
| Polystyrene (PSt) | Amine addition to fullerene | homogeneous films formed |  | SEC confirmed the product was mono-substituted | Weis et al. 1995 |
| | Carbanion addition/Iodomethane, C ₆₀ toluene solution, 25°C | Nanophase separation was observed within the casted film |  | M _n of PSt = 1,990 Dag/mol, M _w /M _n = 1.07 | Samulski et al. 1992 |
| | Macro-radical generated by TEMPO reaction | di-substituted derivatives were produced |  | M _w /M _n is less than 1.18 for all PSt samples. GPC showed bis-adduct was formed. | Okamura et al. 1997 |
| | ATRP and ATRA CuBr/ 2,2'-Bipyridine | Mono-substituent is dominant. PSt-C ₆₀ showed fluorescence property |  | M _w /M _n is less than 1.39 | Zhou et al. 2000b |
| | ATRP/C ₆₀ based initiator /CuBr/ 2,2'-Bipyridine | Grafting from method |  | M _w /M _n is less than 1.37 | Zhou et al. 2000a |

| Polymers | Synthetic methods/Reagents | Physical properties/note | Structures | Characterizations | References |
|--|---|---|---|---|--|
| poly(<i>N</i> -vinylcarbazole) | Carbanion addition | Photoconductive, potential application in photovoltaic cells |  | | Chen et al. 1996 and Huang et al. 1996 |
| PMMA | Carbanion addition, hydrolysis and methylation with CH ₃ I | Highly isotactic PMMA-C ₆₀ produced |  | AFM visualized PMMA-C ₆₀ | Kawauchi et al. 2005 |
| | ATRP and ATRA/ CuBr / 2,2'-Bipyridine | Monosubstituent is dominant. possessed fluorescence property |  | M _w /M _n is less than 1.39 | Zhou et al. 2000b |
| poly(<i>tert</i> -butyl methacrylate) (PtBMA) | ATRP and ATRA/HMTETA/Cu Cl | Large compound vesicles formed in mixed chlorobenzene /ethyl acetate solvents |  | TEM and light scattering were used to study the self-assembly behavior. | Tan et al. 2004 |
| Polycaprolactone (PCL) | Ring opening polymerization/azido addition | C ₆₀ affects the crystallization of PCL. Potential in biomedical applications. |  | M _w /M _n for all samples are less than 1.4 | Hua et al. 2008 |
| PEO | Azido Addition/SOCl ₂ /NaN ₃ | Increase the miscibility with PEO, PAA, and poly(<i>p</i> -vinylphenol) |  | | Huang et al. 2000 and Song et al. 2002 |

| Polymers | Synthetic methods/Reagents | Physical properties/note | Structures | Characterizations | References |
|--|---|---|---|---|-------------------|
| poly(<i>tert</i> -butyl acrylate) (PtBuA) poly(acrylic acid) (PAA) | ATRP and azido coupling/ <i>N,N',N'',N'''</i> -tetramethylethylenediamine (PMDETA)/CuBr, NaN ₃ | Photoconductivity of PtBA-C ₆₀ was increased, whereas it was decreased for PAA-C ₆₀ |  | M _n ranges from 10,000 to 45,000 Da, and M _w /M _n is less than 1.5 | Yang et al. 2003 |
| PAA | ATRP and azido addition/ PMDETA/CuBr, NaN ₃ | PAA-C ₆₀ and C ₆₀ -PAA-C ₆₀ show pH-responsive and water-soluble properties at high pH |  | M _n =11,000 Da, M _w /M _n is less than 1.15 | Ravi et al. 2006 |
| PMAA | ATRP and ATRA catalyzed by CuCl:HMTET followed by hydrolysis using HCl. | Size of the micelle and large compound micelles depended on pH and salt concentration |  | M _n = 16,000 Da, M _w /M _n = 1.13. | Ravi et al. 2005a |
| PNIPAM | RAFT/ benzyl dithiobenzoate and AIBN were used | Thermal responsive |  | M _n =12,400 Da, M _w /M _n = 1.22 | Zhou et al. 2007 |
| PS-PNIPAM | ATRP | Self-assembled into toroidal structure in chloroform and in dried state |  | M _n = 22 200 Da. M _w /M _n is 1.66. | Liu et al. 2008 |

| Polymers | Synthetic methods/Reagents | Physical properties/note | Structures | Characterizations | References |
|--|--|--|---|---|-----------------|
| PNIPAM | ATRP/click chemistry/ ME ₆ TREN/CuCl,alkyl-C ₆₀ | Spherical nanoparticles were formed in aqueous solution and they exhibited thermo-induced collapsed/aggregation behavior. |  | M _n = 10,300, 10,100 and 12,700 Da with M _w /M _n of less than 1.15 | Li et al. 2009 |
| PDMAEMA with targeting moieties | ATRP and ATRA catalyzed by CuCl/HMTETA | Micelles with different sizes formed at various pHs, micelles disrupted in the presence of free PDMAEMA chains in basic solution |  | M _n =8,300 Da and M _w /M _n of 1.20 | Yao et al. 2011 |
| DMAEMA- <i>b</i> -EO- <i>b</i> -DMAEMA | ATRP and azido coupling/HMTETA/ CuCl, NaN ₃ | Micelles formed in aqueous solution. LCST increased due to the EO block and formation of micelles |  | M _n =23,000 Da, M _w /M _n =1.19 | Yu et al. 2005 |

| Polymers | Synthetic methods/Reagents | Physical properties/note | Structures | Characterizations | References |
|------------------------------------|---|---|------------|---|-------------------|
| betainized PDMAEMA-C ₆₀ | ATRP and ATRA and used 1,3-Propane sultone to betainize PDMAEMA | UCST (Upper critical Solution Temperature) varied with salt concentration. Above UCST, micelles formed | | $M_n=13,000$ Da and $M_w/M_n=1.18$ | Ravi et al. 2005b |
| P(MAA- <i>b</i> -DMAEMA) | ATRP and ATRA/ hydrolysis to remove T-butyl group | Solubility and self assembly of P(MAA- <i>b</i> -DMAEMA)-C ₆₀ varies with pH and Temperature | | M_n of 25 200 Da and M_w/M_n of 1.18 for P(<i>t</i> BMA- <i>b</i> -DMAEMA)-C ₆₀ | Teoh et al. 2005 |

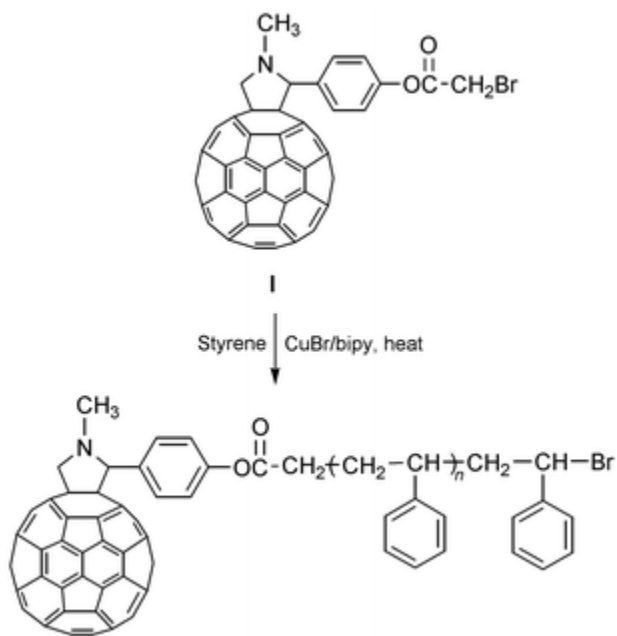
2.2 Synthetic approaches for producing C₆₀ containing polymers

Chemically speaking, a fullerene is any carbon-based compound composed of hexagonal, or sometimes pentagonal or heptagonal rings. In this review, we will focus on fullerene (C₆₀), which is more extensively studied than other types of fullerenes, such as C₇₀, C₈₀ and others. C₆₀ consists of 20 hexagonal and 12 pentagonal rings and it has two bond lengths including the [6,6] and [6,5] ring bonds. The [6,6] bonds can be considered as "double bonds", therefore, C₆₀ can participate in various organic reactions, [Kroto et al. 1993] which opens up opportunities for the synthesis of a wide range of fullerene derivatives. Soon after the discovery of fullerenes, the first fullerene containing polymer was synthesized by Prakash et al. using AlCl₃ catalyst, where mono-dispersed polystyrene was grafted to fullerenes. [Olah et al. 1991] Since then, a wide variety of polymer-C₆₀ systems have been prepared and some of these systems have been documented in various monographs. [Ravi et al. 2005a, Dai et al. 2004, Yao et al. 2011, Ravi et al. 2005b, Teoh et al. 2005, Yang et al. 2003, Ravi et al. 2006, Wang et al. 2007, Li et al. 2009, Tamura et al. 2006, Hong et al. 2009, Liu et al. 2008, Wrobel et al. 2006, Prato et al. 1997, Chen et al. 1998, Dai et al. 1999a and 1999b, Geckeler et al. 1999 and 2000, Dai et al. 2001, Wang et al. 2004, Ravi et al. 2007]

In general, C₆₀ containing polymers could be prepared via three synthetic approaches, namely; (1) 'graft through' method via copolymerization of various monomers with C₆₀, (2) 'grafting to' method via substitution or end-capping of C₆₀ with functionalized precursor polymers, and (3) 'grafting from' method via polymerization using C₆₀ functionalized initiators. Depending on the synthetic methodologies used, different structures could be produced, such as C₆₀ on the main polymeric chain, C₆₀ on the side chain of the polymers, hyperbranched C₆₀ containing polymers, star-like polymers, mono or dual end-capped well-defined polymers, etc.

Using the ‘grafting through’ method, C₆₀ can be polymerized as a co-monomer with various vinyl based monomers, such as styrene or methyl methacrylate, through the addition polymerization reaction.[Ford et al. 1997 and 2000] However, the structure prepared by this approach is not well-controlled. To address this issue, ‘grafting from’ and ‘grafting to’ methods were developed, in which well-defined polymers were grafted to fullerenes. In the ‘grafting from’ method, a C₆₀ based initiator was produced by attaching an initiator to C₆₀, then polymerization of a monomer of interest was conducted to produce well-defined C₆₀ containing polymers. For instance, Zhou et al. [Zhou et al. 2000a] synthesized uniform hammer-like polystyrene-C₆₀ with designed molecular weight and narrow molecular weight distribution using C₆₀ based ATRP initiator (Scheme 2.1). Because multiple synthetic steps must be performed on C₆₀ prior to polymerization, the grafting from method has not been widely used. The “grafting to” method allows for the preparation of a wide range of well-defined polymers with different reactive groups, which can be grafted directly to C₆₀. Therefore it has been utilized in most studies. The requirement for this method is that the polymer precursor must possess reactive groups that can react with C₆₀. A wide selection of functional groups, such as amine, carbanion, macro-radical, azide and malonate ester can directly react with C₆₀. Therefore, polymers with these groups have to be prepared first prior to grafting to C₆₀. Reaction of polymer containing primary amine groups with C₆₀ has been used to prepare well-defined water-soluble mono-substituted polymeric C₆₀ derivative. [Geckeler et al. 1993, Manolova et al. 1994, Weis et al. 1995] Water-soluble poly(azomethine) was end-capped with C₆₀ by reacting amine terminated poly(azomethine) with C₆₀ in DMF/toluene solvent mixture, [Nepal et al. 2003] where C₆₀ was used as end-capping agent with polyrotaxane as the self-dopant. Chu. et al. used the Bingel cyclopropanation between malonate ester group and C₆₀ to synthesize C₆₀-anchored two-armed

poly(*tert*-butyl acrylate) (PtBA). [Chu et al. 2005] Multi-steps synthetic strategy was adopted, where dibromo-functionalized initiator bearing a malonate ester core was synthesized and used for the polymerization of *t*BA. Finally, C₆₀ was functionalized with the polymer via a Bingel cyclo-propanation on the C₆₀ to produce C₆₀ containing two arms of PtBA. The PtBA was further transformed to poly(acrylic acid) by an acidic treatment. In the following section, grafting polymers onto C₆₀ through carbanion, macro-radical, and azide functionalities will be discussed in more details because they are the most extensively studied methods.

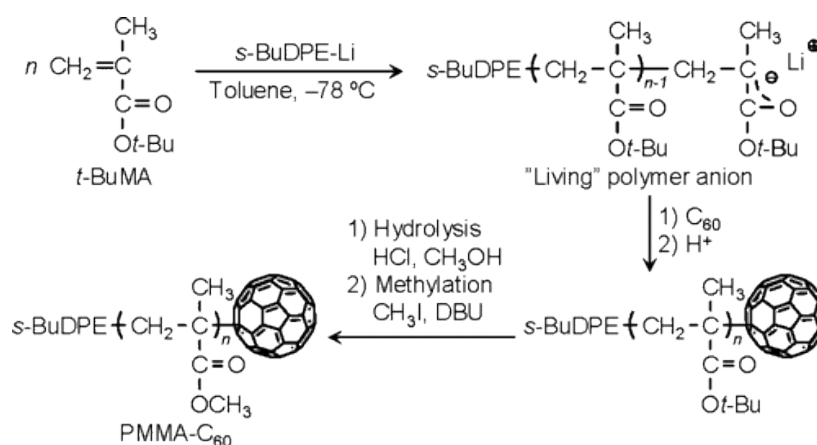


Scheme 2. 1 Synthesis of polystyrene-C₆₀ using C₆₀ based ATRP initiator [Zhou et al. 2000a]

2.2.1 Grafting polymers to C₆₀ through carbanion

Anionic polymerization leads to products with very narrow polydispersity [Szwarc et al. 1968] and the living chain ended with carbanion can be added to the double bonds on the C₆₀. The first study on the addition of living polystyrene-Li onto C₆₀ was reported by Samulski et al.[Samulski et al. 1992] The living polymeric active carbanion intermediates generated by

anionic polymerization react with C₆₀ to produce C₆₀ end-capped polymers. [Wignall et al. 1995, Chen et al. 1997, Vinogradova et al. 2008, Ederle et al. 1997] Polymeric photoconductor of poly(*N*-vinylcarbazole)-C₆₀ [Chen et al. 1996, Huang et al. 1996] was synthesized using anionic polymerization by introducing C₆₀ to the active carbanion moiety and the resulting C₆₀ derivative exhibited remarkable photoconducting properties. Recently, Kawauchi et al. synthesized highly isotactic PMMA-C₆₀ [Kawauchi et al. 2005] with a narrow molecular weight distribution by the stereo-specific anionic living polymerization of tert-butyl methacrylate followed by end-capping with C₆₀, hydrolysis of the pendant esters, and methylation with CH₃I as shown in Scheme 2.2.



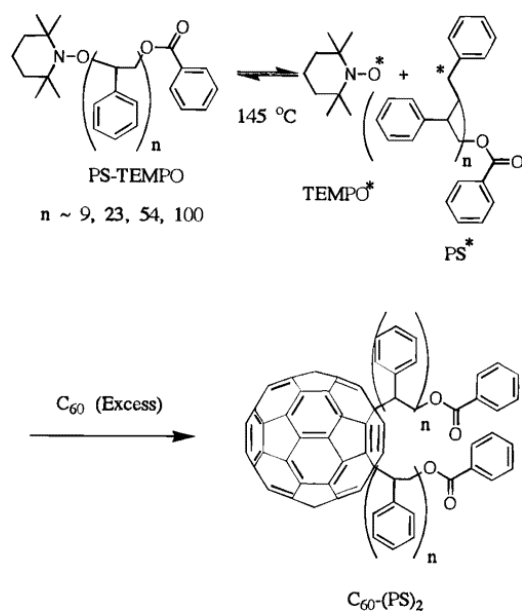
Scheme 2. 2 Synthesis of isotactic PMMA-C₆₀ using carbanion [Kawauchi et al. 2005]

2.2.2 Grafting polymers to C₆₀ through macro-radicals

Although the anionic polymerization has a better control of on the polydispersity of the prepared polymer, the requirements for stringent reaction conditions and specific monomers limits its utility. Controlled/“living” radical polymerizations including stable free radical polymerization (SFRP) [Benoit et al. 2000, Robin et al. 2002] atom transfer radical polymerization (ATRP) [Wang et al. 1995, Tsarevsky et al. 2007] and reversible addition-fragmentation chain-transfer (RAFT) [Chiefari et al. 1998] offer more attractive routes to

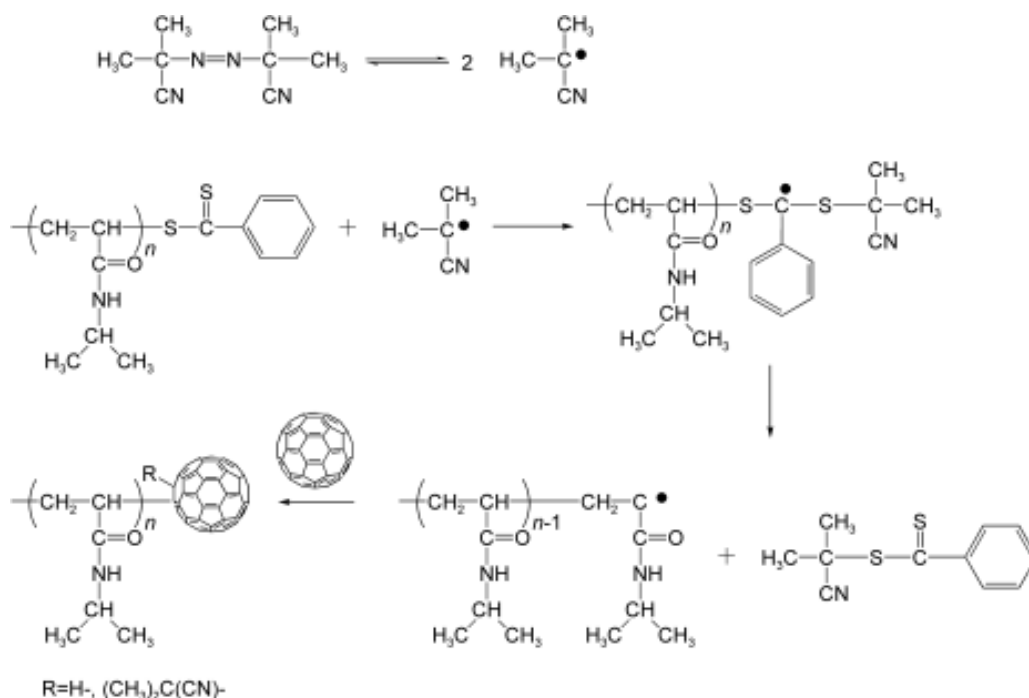
synthesize polymers with predictable molecular weights and low polydispersity. A polymer synthesized by these controlled radical polymerizations possesses a living end-group which can be further initiated to form macro-radicals. Such macro-radicals can react with the double bond on C_{60} to form a given polymeric architecture end-capped with C_{60} .

Okamura et al. first reported the synthesis of well-defined di-substituted polymer derivatives of C_{60} using thermally induced radicals from polymer chains prepared by SFRP mediated with TEMPO (2,2,6,6-tetramethylpiperidinyl-1-oxy). Using this method, they grafted well-defined polystyrene (PS) [Okamura et al. 1997] (Scheme 2.3), poly(vinylphenol) (PVP) and diblock copolymer of PS-*b*-PVP [Okamura et al. 1998] onto C_{60} molecules. Ford et al. succeeded in producing well-defined mono- and di- substituted polystyrene with C_{60} using TEMPO mediated polymerization. [Ford et al. 2001]



Scheme 2. 3 Synthesis of C_{60} -(polystyrene)₂ using TEMPO macro-radicals [Okamura et al. 1997]

Zhou et al. synthesized PNIPAM using benzyl dithiobenzoate as the chain-transfer agent and azobisisobutyronitrile (AIBN) as the initiator via RAFT polymerization (Scheme 2.4). Then they attached the PNIPAM chain bearing an active functional group (-S-C(S)-Ph) at one end of the chain to C₆₀ through the reaction of macro-radicals and C₆₀. The resulting PNIPAM-C₆₀ retained the thermosensitive property of PNIPAM. [Zhou et al. 2007]

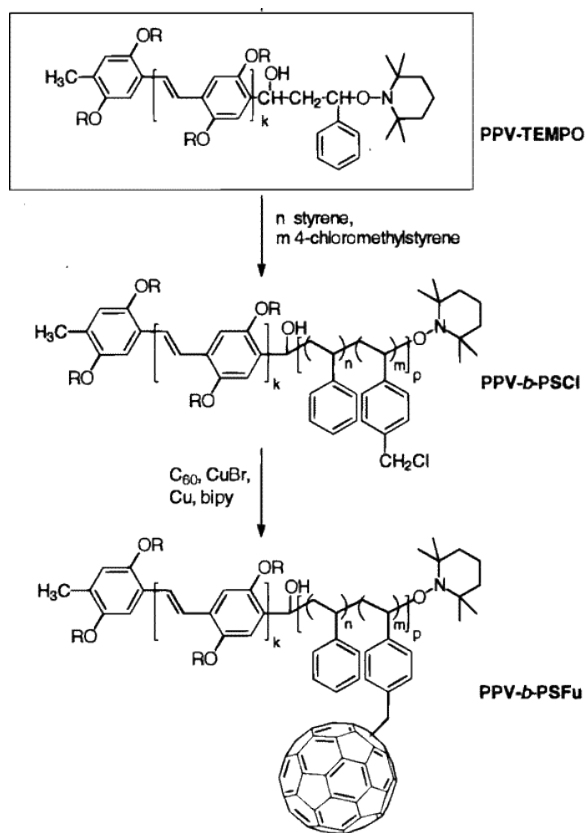


Scheme 2. 4 Synthesis of PNIPAM-C₆₀ using macro-radicals generated by RAFT [Zhou et al. 2007]

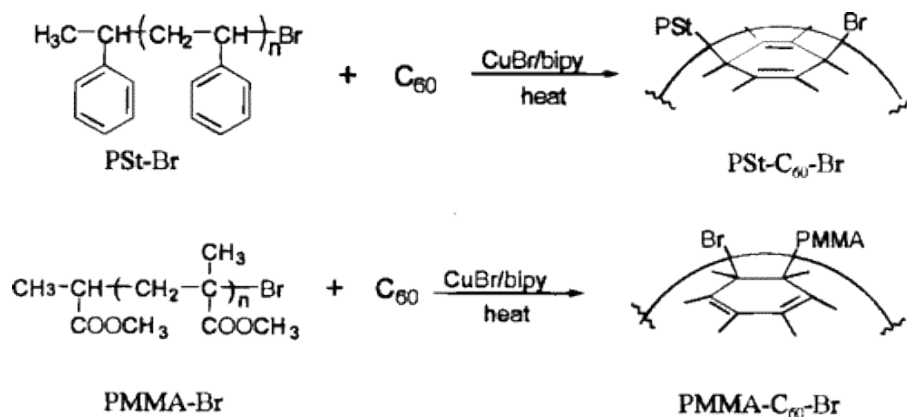
The development and advancement of ATRP processes have provided an attractive and efficient method to prepare well-defined C₆₀-polymer derivatives, since the chlorine or bromine terminated polymer chains can be added to C₆₀ through the atom transfer radical addition (ATRA) reaction. [Zhou et al. 2000b, Peng et al. 2011, Wu et al. 2007, Tan et al. 2004] Utilization of ATRA to synthesize polymer C₆₀ derivatives was first developed by Stalmach et al. [Stalmach et al. 2000] In their study, well-defined rod-coil block copolymers containing a

poly(*p*-phenylenevinylene) (PPV) block as the rigid part and statistical block of PS-*stat*-poly(4-chloromethylstyrene) (PCMS) as a flexible coil was first prepared by nitroxide-mediated “living” radical polymerization, and then C₆₀ was subsequently incorporated to this block copolymer at the chloromethyl group on PCMS segment via ATRA (Scheme 2.5). Zhou et al. used ATRP technique to synthesize well-defined polystyrene and poly(methyl methacrylate) (PMMA) end-capped with C₆₀ (Scheme 2.6). [Zhou et al. 2000b] First, well-defined –Br terminated PS and PMMA macroinitiators were synthesized by ATRP of styrene and MMA using *l*-phenylethyl bromide and methyl-2-bromopropionate as initiators respectively, and CuBr/bipyridine (CuBr/bipy) as the catalyst system. Subsequently, ATRA of PSt and PMMA macro-radicals onto C₆₀ was performed in the presence of an excess of C₆₀ using CuBr/bipy catalyst system in *l*,2-dichlorobenzene to produce well-defined mono end-capped PS-*b*-C₆₀ and PMMA-*b*-C₆₀ with narrow polydispersity. However, Mathis et al. demonstrated that di- and tetra-PS chains were attached to C₆₀ by direct addition of PS macro-radicals prepared by ATRP onto C₆₀ in the presence of CuBr/bipy at 100 °C regardless of the stereochemistry of PSBr/C₆₀, [Audouin et al. 2004] which contradicted to the findings of Zhou et al. [Zhou et al. 2000b] They explained these results and proposed that a C₆₀–Br bond was easier to break than the terminal C–Br bond of PS–Br. Therefore even numbers of PS arms were attached to C₆₀ core. ATRP was also used to synthesize mono end-capped C₆₀ with rod-coil block copolymers of terfluorene-*b*-PS segments in the presence of the CuBr/bipy catalyst system in *o*-dichlorobenzene at 110 °C. [Chochos et al. 2005] The resulting C₆₀ end-capped polymer exhibited the emission of stable blue light. Four arm well-defined star-like polymer with C₆₀ end-capped PS and PMMA polymers were attempted by Zhao et al. by synthesizing –Br terminated four arm polymers using *l*,2,4,5-tetrakis(bromomethyl) benzene as an initiator by ATRP, followed by ATRA reaction to attach

the polymer onto C₆₀. [Zhao et al. 2007] The synthesized C₆₀ end-capped PS and PMMA showed an optical limiting response.



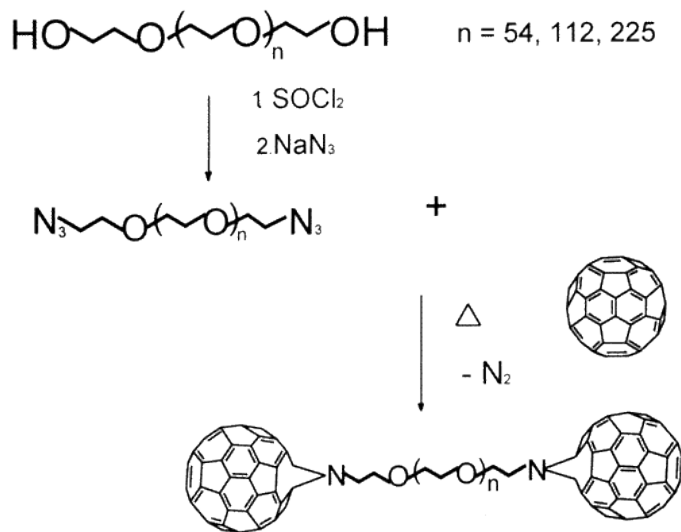
Scheme 2. 5 Synthesis of PPV-b-PS-(C₆₀)_m using ATRA method [Stalmach et al. 2000]



Scheme 2. 6 Synthesis of Pst-C₆₀ and PMMA-C₆₀ using combination of ATRP and ATRA. [Zhou et al. 2000b]

2.2.3 Grafting polymers to C₆₀ through azide group

Besides the addition of polymer through carbanion or micro-radicals to C₆₀, another extensively studied method is the azido coupling reaction, which resulted in the mono-substitution of the polymer with C₆₀. [Yang et al. 2004, Wang et al. 2006, Yu et al. 2007 and 2005] Well-defined water-soluble fullerene with mono or double end-capped polyethylene oxide (PEO) chains were synthesized by azido coupling reaction between azide terminated PEO and C₆₀. [Huang et al. 2000, Song et al. 2002, 2003a and 2003b] For instance, Song et al. [Song et al. 2002] synthesized C₆₀-end-capped PEOs via the azido coupling reaction (Scheme 2.7). The hydroxyl groups of PEO were first converted to chlorine groups through reaction with thionyl chloride. Then the chloro-terminated PEO was reacted with sodium azide to form azido-terminated PEO, which subsequently underwent the azido cycloaddition reaction with C₆₀ to produce C₆₀-PEO-C₆₀.

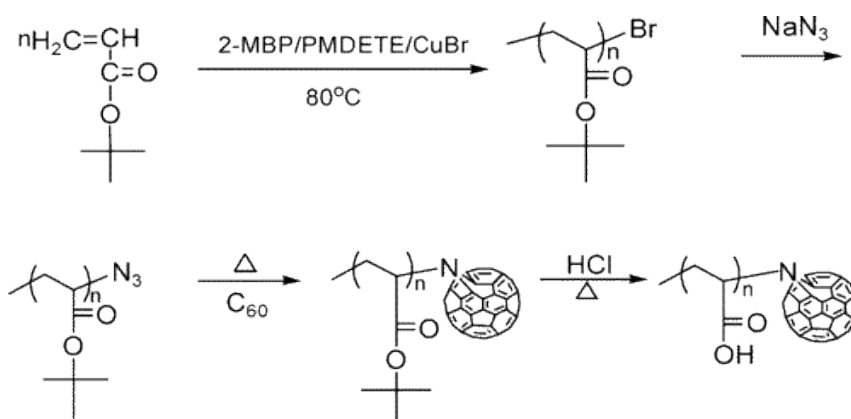


Scheme 2. 7 Synthesis of C₆₀-PEO-C₆₀ using azido coupling reaction. [Song et al. 2002]

Wang et al. used ATRP combined with azido coupling to synthesize poly(*tert*-butyl acrylate)-C₆₀ (PtBA-C₆₀) and poly(acrylic acid)-C₆₀ (PAA-C₆₀) polymers with narrow

polydispersity as shown in Scheme 2.8. [Yang et al. 2003] Well-defined poly(*tert*-butylacrylate) (PtBA) with narrow polydispersity was first synthesized via ATRP followed by azide substitution of –Br end groups to yield PtBA-N₃. PtBA-N₃ was added to C₆₀ using azido coupling to yield PtBA-C₆₀, which was further hydrolyzed with HCl to produce PAA-C₆₀. The photoconductivities of PtBA-C₆₀ and PAA-C₆₀ were dramatically enhanced by combining the polymer chains with C₆₀. The same group synthesized well-defined amphiphilic block copolymer of PAA-*b*-PS-*b*-C₆₀ using a similar technique [Yang et al. 2004] and the resulting product represents a class of well-defined water-soluble amphiphilic block copolymer that possesses good photoconducting properties. Tam and coworkers synthesized pH-responsive well-defined telechelic C₆₀ containing polymers by the combination of ATRP technique and azido coupling [Ravi et al 2005]. Well-defined Br-PtBA-Br was first synthesized using bifunctional initiator of diethyl-*meso*-2,5-dibromo adipate (DEDBA) in anisole at 60 °C. The bromine end-groups were converted to the corresponding azide terminated PtBA and subsequently PtBA end-capped with C₆₀ was obtained by refluxing the azide terminated N₃-PtBA-N₃ with excess C₆₀ in 1,2-dichlorobenzene for 24 hrs. The di-substituted C₆₀-*b*-PtBA-*b*-C₆₀ was soluble in most organic solvents. Finally, the *tert*-butyl protecting groups were removed by hydrolysis in the presence of trifluoroacetic acid in dichloromethane at room temperature to yield a well-defined C₆₀-*b*-PAA-*b*-C₆₀. Tri-block copolymer of dual C₆₀ end-capped ABA type can also be prepared using a similar approach. The synthesis of amphiphilic ABA type double hydrophilic triblock copolymer of C₆₀-PDMAEMA₆₀-*b*-PEO₁₀₅-*b*-PDMAEMA₆₀-C₆₀ using the combination of ATRP followed by azido coupling has also been reported [Yu et al. 2005]. To synthesize this polymer, a Br-PEO-Br macroinitiator was synthesized and used for the polymerization of DMAEMA in aqueous medium in the presence of CuCl/HMTETA catalyst.

Subsequently, azide substitution of the triblock copolymer followed by the azido coupling addition with C_{60} afforded the well-defined polymer end-capped with C_{60} . The same technique was used to synthesize the dual end capped C_{60} -PDMAEMA- C_{60} starting from a dual ATRP initiator. [Yu et al. 2007] Recently, biodegradable poly(ϵ -caprolactone) (PCL) synthesized by ring opening polymerization (ROP) was end-capped with C_{60} through azido coupling reaction and the fullerene-capped PCLs are expected to have application in biomedical engineering. [Hua et al. 2008]



Scheme 2. 8 Synthesis of PAA- C_{60} via ATRP and azido coupling. [Yang et al. 2003]

2.3 Stimuli-responsive C_{60} containing polymers

Stimuli-responsive polymers are attracting increasing attention because they undergo structural changes when exposed to external triggers, such as pH, heat or light. These polymers are found useful in a wide range of biological applications, such as drug delivery, diagnostics, tissue engineering and biosensors. [Stuart et al. 2010]. pH-responsive polymeric systems are polymers whose solubility, volume and conformation can be reversibly manipulated by changes in external pH. [Park et al. 1997, Roy et al. 2003] The polymeric components are usually weak polyacid and polybase with a pK_a value of between 3 and 10. The most common pH-responsive polymers include poly(acrylic acid) (PAA), poly(methacrylic acid) (PMAA), poly(ethylene

imine) (PEI), poly(N,N-dimethylaminoethyl methacrylate) (PDMAEMA). Thermo-responsive polymers show lower critical solution temperature (LCST) or upper critical solution temperature (UCST). The most well known thermo-responsive polymers include poly(N-isopropylacrylamide) (PNIPAM), [Heskins et al. 1968, Schild et al. 1992] poly(N-acryloylpiperidine), [Gan et al. 2000,] poly(N-acryloylpyrrolidine), [Kuramoto et al. 1994,] PDMAEMA, [Plamper et al. 2007] poly(oligo(ethylene glycol) methyl ether methacrylate) (POEGMA) analogues. [Lutz et al. 2006a, 2006b and 2007] When the temperature is raised above the LCST, the respective polymer undergoes coil-to-globule transitions as it becomes hydrophobic in nature. One of the most common and widely studied thermo-responsive polymers is PNIPAM as it displays a LCST at 32°C, which is just below the human body temperature of 37°C. Most stimuli-responsive polymers are water-soluble and the attachment of C₆₀ to these kinds of polymers will result in an amphiphilic polymeric system containing a hydrophobic C₆₀ and a hydrophilic polymer. In aqueous solution, these C₆₀ containing polymers form core-shell micelle comprising a C₆₀ core and a hydrophilic polyelectrolyte shell.

2.3.1 pH-responsive C₆₀ containing polymers

Tam and coworkers synthesized mono- and dual-substituted C₆₀-PAA systems by reacting C₆₀ with well-defined mono and dual azide end-functionalized poly(*tert*-butyl acrylate)s prepared by ATRP, followed by hydrolysis using trifluoroacetic acid. Both PAA-C₆₀ and C₆₀-PAA-C₆₀ formed different types of morphologies in aqueous solution and showed pH-responsive behaviors. [Ravi et al. 2006] The dependence of hydrodynamic radius (R_h) on the degree of neutralization (α) of carboxylic groups is shown in Figure 2.2A. The hydrodynamic radii for PAA-C₆₀ and C₆₀-PAA-C₆₀ increased with increasing α and reached their maxima of 102 and 128 nm, respectively at $\alpha \approx 0.5$ due to the electrostatic repulsion arising from ionized carboxylic

groups. Figure 2.2 B shows the z-average radius of gyration (R_g), R_h , and R_g/R_h at various pH conditions for C_{60} -PAA- C_{60} . R_h increased from ~ 80 to ~ 128 nm, whereas R_g remained almost constant at approximately 70 nm and R_g/R_h decreased from 0.76 to 0.56 when the pH was increased from 3 to 12. These results indicated the morphologies of the aggregates changed from hard spheres to large compound micelles (LCM) with R_h of ~ 128 nm. The formation of LCM was further confirmed by TEM. The M_w of the LCM and core-shell micelle determined from Berry-plot was $\sim 3.50 \times 10^7$ and 3.42×10^6 respectively. The aggregation number (N_{agg}) for C_{60} -PAA- C_{60} was much higher (~ 4670) than for PAA- C_{60} (~ 456) corresponding to a LCM and core-shell micelle respectively.

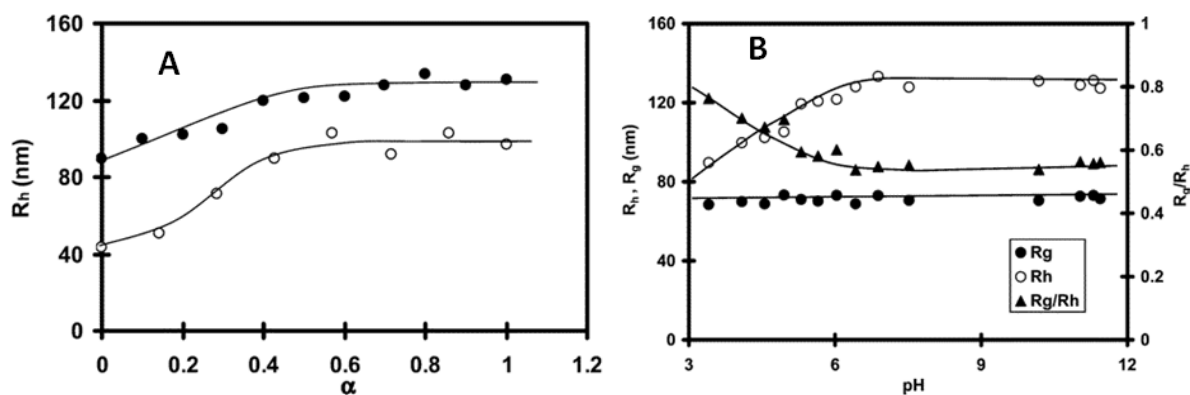


Figure 2. 2 (A). Dependence of R_h on α for 0.1 wt % PAA- C_{60} (O) and C_{60} -PAA- C_{60} (●) in 0.1 M NaCl solution; (B). Dependence of R_h (O), R_g (●), and R_g/R_h (▲) on pH for 0.1 wt % C_{60} -PAA- C_{60} in 0.1 M NaCl. [Ravi et al. 2006]

Well-defined mono end-capped C_{60} containing alkali-soluble PMAA (PMAA- C_{60}) was synthesized using the combination of ATRP and ATRA method. [Ravi et al. 2005a] First, well-Well-defined mono end-capped C_{60} containing alkali-soluble PMAA (PMAA- C_{60}) was synthesized using the combination of ATRP and ATRA method. [Ravi et al. 2005a] First, well-

defined stable $-Cl$ -terminated P t BMA with PDI of 1.13 was synthesized by ATRP, then ATRA was utilized to attach C_{60} to the end of P t BMA with an excess amount of C_{60} in order to avoid multiple substitutions of polymer chains onto C_{60} . Finally, the t -butyl protecting group was removed by hydrolysis. The resulting PMAA- C_{60} was found to be soluble at high pH and exhibited pH-responsive properties. In dilute solution, the micelles coexisted with large secondary aggregates. These secondary aggregates comprise of individual micelles that possess a microstructure similar to LCM. The R_h of micelles increased from 6 to 10 nm with increasing degree of neutralization (α) and remained constant at 10 nm in the presence of salt. Addition of NaCl shields the electrostatic interaction between charged polyelectrolyte segments, enhancing the chain flexibility of the PMAA segments. The increase in the aggregation number and the reduction in hydrodynamic size of fully neutralized PMAA segments maintained a small micellar size with increasing NaCl concentrations (Figure 2.3a). Both R_h and R_g of the LCM increased from 91 to 153 nm and 210 to 335 nm respectively with increasing α and maintaining the M_w of the LCM ($\sim 4.0 \times 10^7$ g/mol) and R_g/R_h values (~ 2.30) unchanged. However, both R_h and R_g of the LCM decreased from 153 to 105 nm and 335 to 168 nm respectively with increasing NaCl concentration (Figure 2.3b). The LCMs were stabilized by electrostatic interactions from charged polyelectrolyte backbones and counterions. At high salt concentrations, the carboxylate groups are shielded by oppositely charged counterions, and the PMAA chains shrink, causing a reduction in the particle size of the LCM. TEM studies revealed the formation of LCM microstructures comprised of individual micelles.

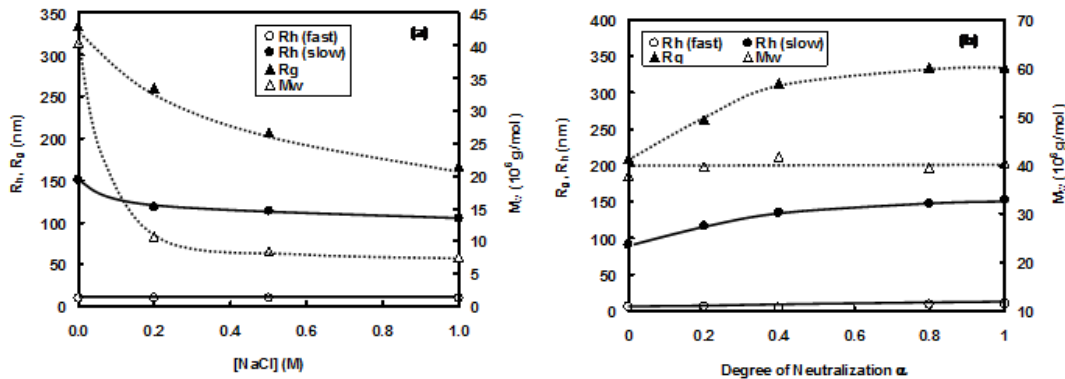


Figure 2. 3 (a) Effect of salt concentration on Rh for 0.2 wt% PMAA-C₆₀ at $\alpha = 1$; (b) Dependence of Rh on degree of neutralization α for 0.2 wt% PMAA-C₆₀ in aqueous solution. [Ravi et al. 2005a]

Yang et al. used ATRP combined with azido coupling to synthesize water-soluble poly(acrylic acid)-*b*-C₆₀ (PAA-C₆₀) polymer with narrow polydispersity (Scheme 2.8). [Yang et al. 2003] They found that PAA-C₆₀ formed micelles in aqueous solution and the hydrodynamic diameter was about 191 nm with polydispersity of 0.42 determined from DLS measurement. The micellar structure still remained after casting into film as confirmed by TEM (Figure 2.4a). As a result, the photoconductivity of the PAA-C₆₀ film was reduced because the charge transportation could overcome the hindrance of the PAA layer and hop to another C₆₀ micro-domain (Figure 2.4b). On the other hand, the photoconductivity of PtBA-C₆₀ was dramatically enhanced by C₆₀. In their study, they did not examine the pH-responsive property of PAA-C₆₀.

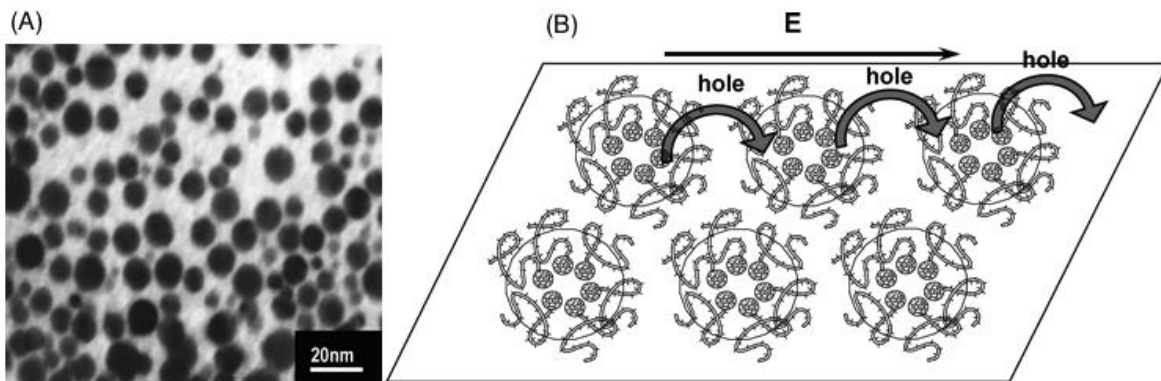


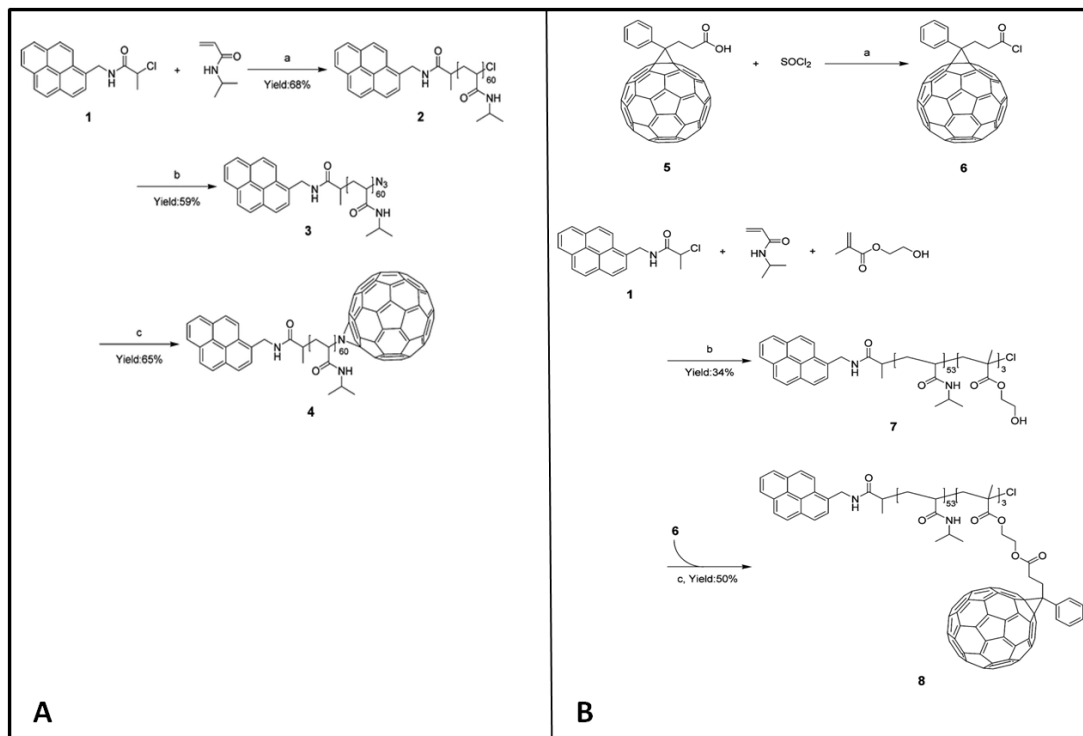
Figure 2. 4 (A) TEM images of PAA-C₆₀ film cast from water solution; (B) Cartoon of molecular packing of PAA-C₆₀ in film [Yang et al. 2003]

2.3.2 Temperature responsive C₆₀ containing polymers

Poly(*N*-isopropylacrylamide) (PNIPAM) is the most widely studied thermo-responsive polymer because it possesses a LCST close to body temperature together with a sharp coil-to-globule transition for possible applications in controlled drug delivery. [Yan et al. 2005] The covalent attachment C₆₀ to PNIPAM imparted some interesting properties in addition to the thermo-responsive property of PNIPAM.

Recently, pyrene labeled thermo-responsive PNIPAM end-capped with one or three C₆₀ molecules were prepared using pyrene-based ATRP initiator, [Hong et al. 2009] and their photophysical behaviors were examined as a function of temperature. Two types of C₆₀ attached PNIPAM labeled with pyrene were synthesized and their thermal responsive properties were evaluated by examining the fluorescence quenching efficiency of C₆₀. The two structures are pyrene-poly(*N*-isopropylacrylamide)-fullerene (Pyr-PNIPAM-C₆₀), and pyrene-poly(*N*-isopropylacrylamide-*co*-fullerenylethyl methacrylate) Pyr-P(NIPAM-*co*-C₆₀). The first structure was prepared using ATRP and azide coupling reaction (Scheme 2.9A). The preparation of the second structure is shown in Scheme 2.9B, where pyrene-poly(*N*-isopropylacrylamide-*co*-

2-hydroxyethyl methacrylate was prepared by ATRP. Subsequently C_{60} -COOH was attached to the polymer via an esterification reaction between C_{60} -COOH and the hydroxyl groups of the 2-hydroxyethyl methacrylate (HEMA) segments. Figure 2.5 shows the fluorescence quenching ability of the prepared structures, which showed a strong dependence on temperature. Below the LCST, C_{60} did not have an effect on the fluorescence emission from pyrene because the extended conformation of PNIPAM kept the pyrene and C_{60} apart. However, when the temperature exceeded the LCST of PNIPAM, the PNIPAM chain collapsed, reducing the distance between pyrene and C_{60} , such that C_{60} can effectively quench the fluorescent emission of pyrene. In addition, the quenching efficiency of Pyr-P(NIPAM-*co*- C_{60}) was larger than Pyr-PNIPAM- C_{60} , since Pyr-P(NIPAN-*co*- C_{60}) had more C_{60} located closer to Pyr than Pyr-PNIPAM- C_{60} . Two reasons are responsible for this phenomenon; firstly C_{60} is mainly responsible for quenching the fluorescence of pyrene, thus more C_{60} translates into stronger quenching capacity; secondly, the smaller MW of PNIPAM in Pyr-P(NIPAN-*co*- C_{60}) reduces the distance between C_{60} and pyrene, hence the quenching efficiency is enhanced compared to Pyr-PNIPAM- C_{60} . The authors claimed that the sharp transition in a narrow temperature region for this type of fullerene containing polymers suggested that they can be used as alarm-type probes or sensors for detecting a specific temperature, thereby providing a platform for designing a new temperature sensor.



Scheme 2. 9 (A). Synthesis of pyrene-poly(*N*-isopropylacrylamide)-fullerene (4), and (B). pyrene-poly(*N*-isopropylacrylamide-*co*-fullerenylethyl methacrylate) (8). [Hong et al. 2009]

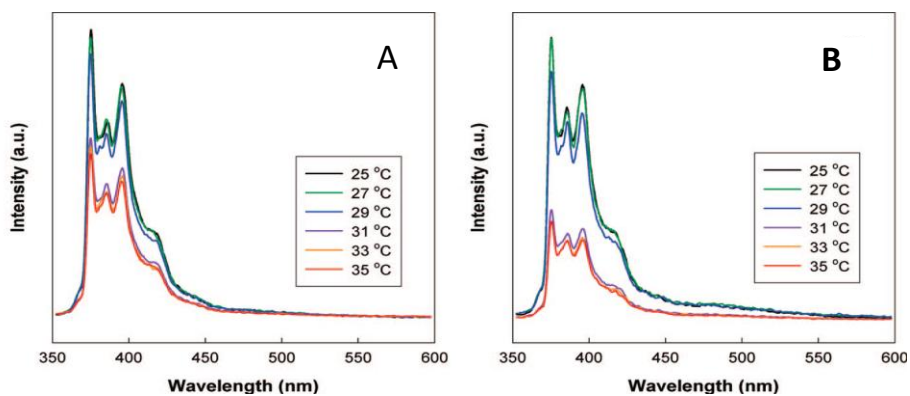
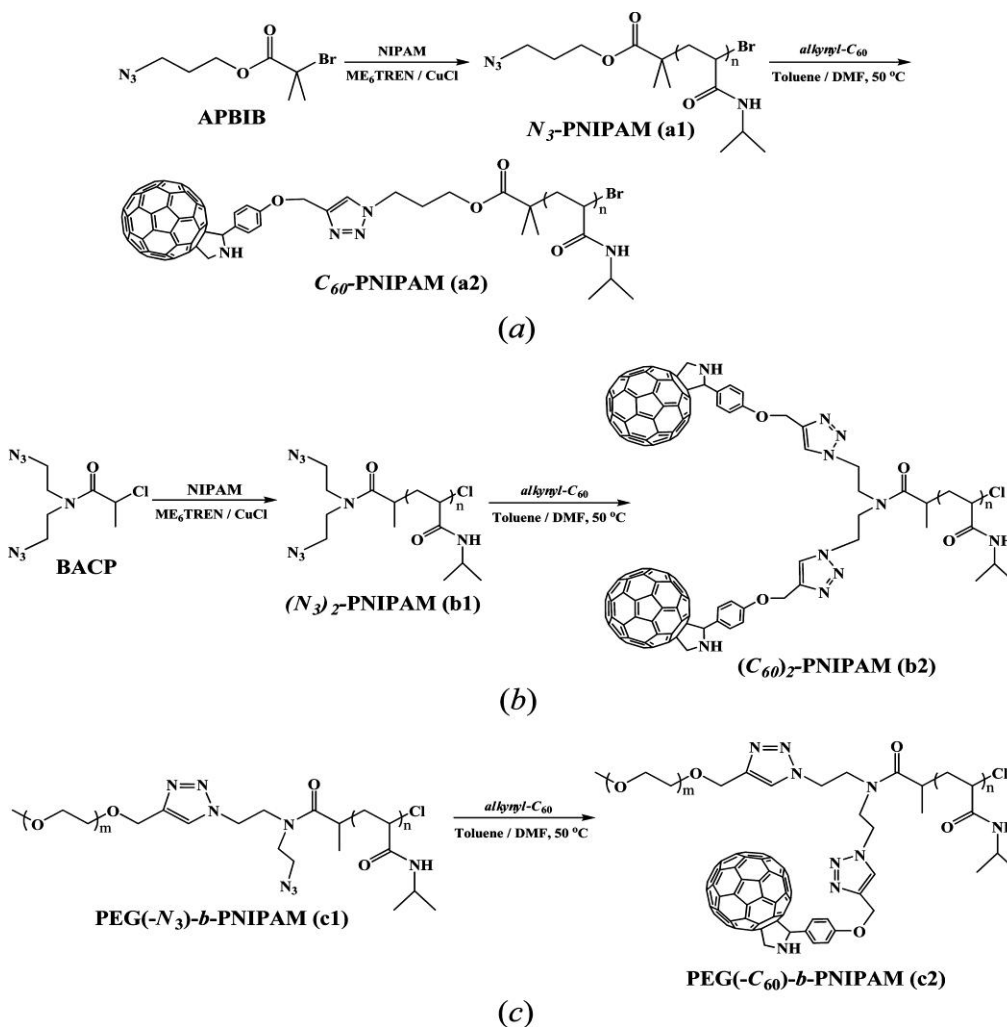


Figure 2.5 Fluorescence emission spectra of (A) pyrene-poly(*N*-isopropylacrylamide)-fullerene (4); (B) pyrene-poly(*N*-isopropylacrylamide-*co*-fullerenylethyl methacrylate) (8) at various temperatures irradiated at 340 nm. [Hong et al. 2009]

Li et al. reported on the synthesis of well-defined thermo-responsive water-soluble diblock copolymer and homopolymers functionalized with controlled numbers of C_{60} moieties at predetermined positions via the combination of atom transfer radical polymerization (ATRP) and azide coupling reaction (Scheme 2.10). [Li et al. 2009] Azide-containing polymer precursors including N_3 -PNIPAM and $(N_3)_2$ -PNIPAM, as well as poly(ethylene glycol)-b-PNIPAM with one azide moiety at the diblock junction (e.g. PEG(- N_3)-b-PNIPAM) were synthesized via ATRP using specific azide-functionalized small molecule and polymeric initiators. On the other hand, alkynyl- C_{60} was prepared by reacting 4-prop-2-ynoxybenzaldehyde with pristine C_{60} in the presence of glycine. Subsequently, the click reaction of N_3 -PNIPAM, $(N_3)_2$ -PNIPAM, or PEG(- N_3)-b-PNIPAM and alkynyl- C_{60} produced water-soluble thermoresponsive C_{60} containing polymer including C_{60} -PNIPAM, $(C_{60})_2$ -PNIPAM and PEG(- C_{60})-b-PNIPAM. The supramolecular self-assembly in aqueous solution of the resulting C_{60} -containing polymeric hybrid were characterized by dynamic and static light scattering and transmission electron microscopy (TEM). It was found that these fullerenated polymers retained the thermo-responsiveness of PNIPAM and the self-assembled hybrid nanoparticles exhibited thermo-induced aggregation behavior due to the LCST phase transition of PNIPAM chains.



Scheme 2. 10 Synthesis of C_{60} -PNIPAM, $(C_{60})_2$ -PNIPAM and PEG- C_{60} -*b*-PNIPAM. [Li et al. 2009]

Thermo-responsive behaviors of a1, a2, b1 and b2 [shown in Scheme 2.10] in aqueous solutions were evaluated using optical transmittance as shown in Figure 2.6. It was found that a1 and b1 were transparent at room temperature, and the optical transmittance decreased dramatically above the LCST ($\sim 32^\circ\text{C}$) due to the coil to globule transformation. On the other hand, aqueous solutions of a2 and b2 exhibited optical transmittances of $\sim 50\text{--}70\%$ at room temperature at a wavelength of 700 nm, which might be associated with the presence of self-assembled aggregates due to the hydrophobicity of C_{60} . However, lower aggregation

temperature (~ 30 °C) of a2 and b2 in aqueous solutions was observed, which might be ascribed to the presence of the hydrophobic C_{60} moieties. [Wang et al. 2007, Tamura et al. 2006, Xia et al. 2006]

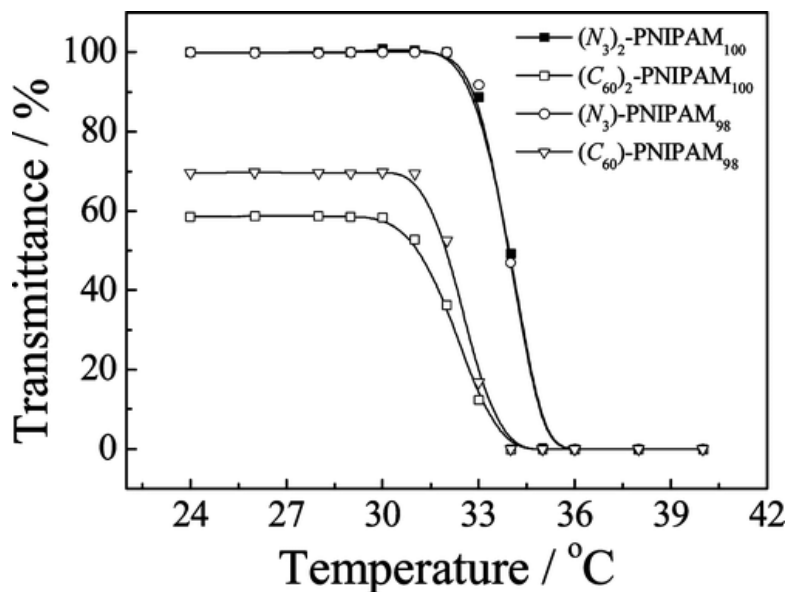


Figure 2. 6 Temperature dependence of optical transmittance at 700 nm obtained for 2.0 g/L aqueous solutions of N_3 -PNIPAM₉₈, C_{60} -PNIPAM₉₈, $(N_3)_2$ -PNIPAM₁₀₀, and $(C_{60})_2$ -PNIPAM₁₀₀. [Li et al. 2009]

Dynamic and static light scattering were used to characterize the aggregates formed by C_{60} -PNIPAM, $(C_{60})_2$ -PNIPAM, PEG($-C_{60}$)-*b*-PNIPAM and PEG₁₁₃($-C_{60}$)-*b*-PNIPAM₇₀. It was found that nanoparticles with average R_h of 42 nm were formed for C_{60} -PNIPAM, whereas larger nanoparticles with average R_h of 118 nm were formed for $(C_{60})_2$ -PNIPAM as shown in Figure 2.7. The apparent molar mass ($M_{w,app}$) determined from static light scattering for $(C_{60})_2$ -PNIPAM (6.93×10^6 g/mol) was ca. 4 times larger than that of C_{60} -PNIPAM. Accordingly, the average aggregation numbers, N_{agg} , of the aggregates were 110 and ~ 460 for C_{60} -PNIPAM and $(C_{60})_2$ -PNIPAM respectively.

PEG₁₁₃(-C₆₀)-*b*-PNIPAM₇₀ is the first example of C₆₀ being located at the junction of a double hydrophilic block copolymer. Two micellar states were observed in aqueous solution due to the presence of thermo-responsive PNIPAM and hydrophilic PEG segments. At 25 °C, micelles consisting of hydrophobic cores of C₆₀ stabilized by PEG/PNIPAM coronas with a R_h of 54 nm were formed. Upon heating to 50 °C, aggregates with smaller R_h of 19 nm were observed, which was believed to consist of mixed C₆₀/PNIPAM cores and hydrated PEG shells. The decrease of aggregate sizes at elevated temperatures was ascribed to the collapse and aggregation of PNIPAM segments. Below 35 °C, R_h remained almost constant at ca. 54 nm and R_h began to decrease above 35 °C, and stabilized at ~20 nm above 45 °C. This clearly indicated the re-arrangement of the initially formed loose aggregates upon heating.

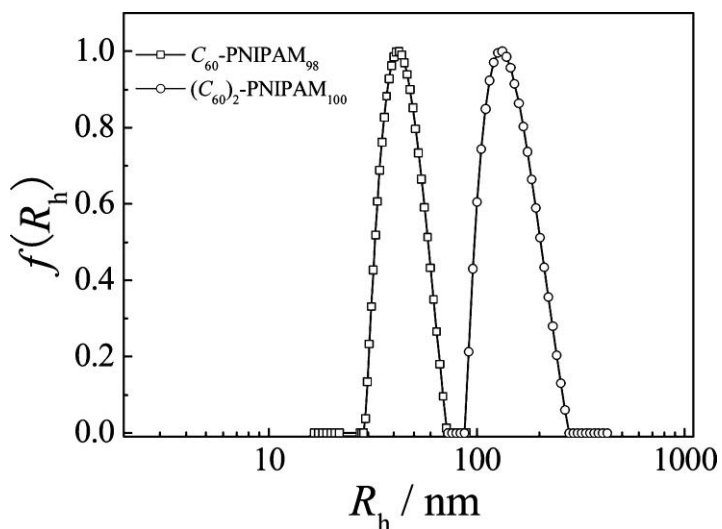


Figure 2. 7 Hydrodynamic radius distributions, $f(R_h)$, obtained for 0.5 g/L aqueous solutions of C₆₀-PNIPAM₉₈ and (C₆₀)₂-PNIPAM₁₀₀ at 25 °C. [Li et al. 2009]

Yajima et al. synthesized PNIPAM-C₆₀ via an azide coupling reaction. [Tamura et al. 2006] In this study, PNIPAM terminated with a terminal hydroxyl group (PNIPAM-OH) was

synthesized by telomerization using 2-mercaptoethanol as a chain-transfer agent. Then the hydroxyl on PNIPAM was converted to an azide using p-toluenesulfonyl chloride and sodium azide in a two-step reaction. They observed that PNIPAM-C₆₀ possessed a unique property of reversible dispersion–aggregation transition of the conjugates micelle in water in heating/cooling thermal cycles below and above the LCST (Figure 2.8). The optical transmittance (at 600 nm) of PNIPAM–C₆₀ and PNIPAM-OH in water (2.0 mg/mL) was measured upon heating. Above the LCST of around 33 °C, the transmittance of PNIPAM-C₆₀ was reduced dramatically, which indicated that the PNIPAM-C₆₀ became aggregated. The LCST values of PNIPAM-OH and PNIPAM–C₆₀ were estimated to be approximately 31 and 32 °C, respectively. They explained that the slight increase in the LCST value of PNIPAM with the C₆₀ moiety was induced by a restricted conformation [Yakushiji et al.] of PNIPAM chains interacting with C₆₀ molecules.

The cumulative diameters of the self-assembled particles from PNIPAM-C₆₀ in aqueous solution were measured by DLS (Figure 2.8). Below the LCST, the diameters remained at 100 nm, which indicated that PNIPAM–C₆₀ formed a core–shell micelle structure composed of inner core of C₆₀ molecules and outer shell layer of PNIPAM chains. They also found that the CMC of PNIPAM-C₆₀ was about 1.0 mg/L, which was much lower than the alkyl-terminated PNIPAM (PNIPAM-C₁₈H₃₅) (80 mg/L), [Chung et al. 1997] indicating that more stable micelles were formed, which was induced by the strong hydrophobic interaction of C₆₀. Above the LCST, the PNIPAM chain collapsed, due to the hydrophobic interaction of the PNIPAM chains resulting in the formation of larger aggregations.

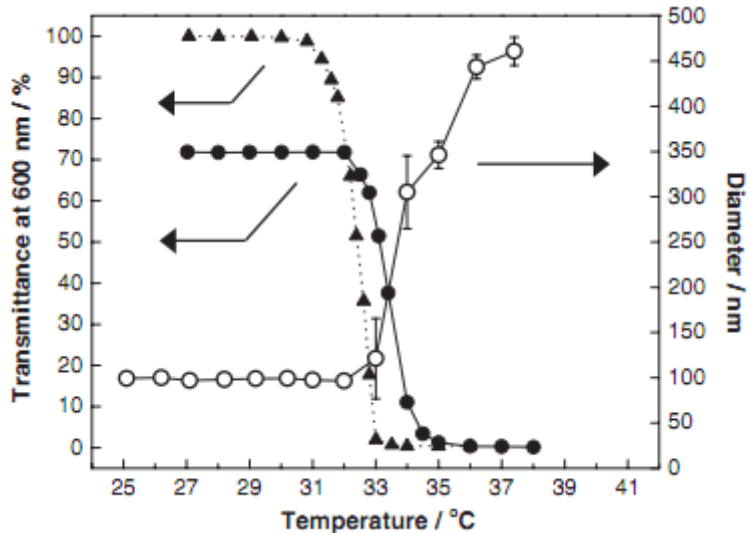


Figure 2. 8 Temperature dependence of optical transmittance at 600 nm of PNIPAM (▲) and PNIPAM-C₆₀ (●) and the cumulative diameter of PNIPAM-C₆₀ (○) in water as a function of temperature. The optical transmittance of both PNIPAM and PNIPAM-C₆₀ were measured at a concentration of 2.0 mg/mL. The cumulative diameter of PNIPAM-C₆₀ was measured by DLS, at a concentration of 0.5 mg/mL [Tamura et al. 2006]

Zhou et al. synthesized PNIPAM using benzyl dithiobenzoate as the chain-transfer agent and azobisisobutyronitrile (AIBN) as the initiator by means of RAFT polymerization. They then attached PNIPAM chains bearing active functional groups (-S-C(S)-Ph) at one end of the chain to C₆₀ through the reaction of macro-radicals and C₆₀. The resulting PNIPAM-C₆₀ retained the thermosensitivity of PNIPAM. [Zhou et al. 2007] At the same time, they also demonstrated that PNIPAM-C₆₀ could have potential biomedical applications. Different cells are known to produce radicals, such as NO⁻ and O₂⁻, which harm biomolecules and affect the functions of cells. Since fullerenes and their derivatives are known to possess radical scavenging capability, [Xiao et al. 2005, Geckeler et al. 2001] they studied the effect of radicals on cells in the presence of PNIPAM-C₆₀. They found that the addition of PNIPAM-C₆₀ improved the NO⁻ effects and

significantly increased the cell viability and metabolic activity. Also, the addition of PNIPAM- C_{60} did not reduce the cell viability or metabolic activity.

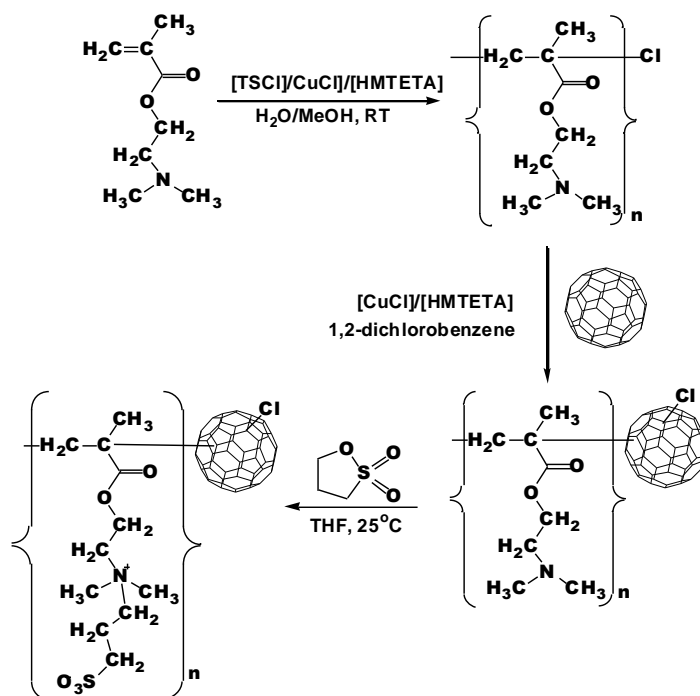
2.3.3 Multi-responsive C_{60} containing polymers

It is known that polydimethylaminoethyl methacrylate (PDMAEMA) exhibits both pH and thermo-responsive properties. At low pH, the protonated PDMAEMA chains yield a water-soluble polyelectrolyte, while at high pH, the PDMAEMA chains are deprotonated and become water-insoluble when the temperature exceeds the lower critical solution temperature (LCST). [Lowe et al. 1997] The LCST of PDMAEMA varies significantly depending on the chain length, pH and solution concentration. [Lee et al. 2003] Tam and co-workers synthesized a well-defined pH responsive poly(2-(dimethyl amino)ethyl methacrylate) (PDMAEMA) coupled with C_{60} via ATRA by reacting PDMAEMA-Cl prepared by ATRP in the presence of CuCl/HMTETA catalyst. [Dai et al. 2004] The pH dependence of the aqueous PDMAEMA- C_{60} solution was studied by laser light scattering techniques. At low pH, micelle-like aggregates were produced comprising of C_{60} hydrophobic cores and protonated PDMAEMA shells. At high pH and at temperature below LCST, only unimeric PDMAEMA- C_{60} were observed due to the formation of a charge-transfer complex between PDMAEMA and C_{60} molecule. The LCST of PDMAEMA- C_{60} determined from light transmittance (UV-vis) was ~ 45 °C. At 55 °C, the PDMAEMA- C_{60} became insoluble at pH > 7.8. Laser light scattering studies of PDMAEMA- C_{60} in aqueous solutions at different pHs indicated that the hydrodynamic radius R_h decreased with pH. At low pH, the electrostatic repulsion between protonated PDMAEMA chains was responsible for the increase in R_h . At pH 3, core-shell micelles with $R_h \sim 55$ nm coexisted with substantial proportion of unimers ($R_h = 5.5$ nm) at 25 and 55 °C, and the micellar formation was driven by the amphiphilic properties of PDMAEMA-*b*- C_{60} . Interestingly, only unimers with R_h of ~ 4 nm

were present at pH 10 and 25 °C in aqueous solution. At high pH (> 9) and low temperature, the deprotonated PDMAEMA chains (electron donor) formed charge-transfer complex (CT) with the C₆₀ (electron acceptor).

A polyzwitterion, betainised-PDMAEMA modified C₆₀ (*Bet*-PDMAEMA-*b*-C₆₀), prepared by Ravi et al. [Ravi et al. 2005b] showed thermal and salt responsive characteristics in aqueous solutions. Poly-zwitterions possess both cationic and anionic species on the same monomer residue [Lowe et al. 2002] and they respond to external stimuli, such as temperature or ionic strength. [Kudaibergenov et al. 1999] Another interesting characteristic of these polymers is their lack of solubility in water at low temperature due to the formation of a cross-linked network structure induced by strong intra- or inter molecular electrostatic attraction. Addition of small electrolytes, such as NaCl, destroys the electrostatic interaction, which enhances its solubility and induces an “anti-polyelectrolyte effect” resulting in the chain expansion. The synthetic Scheme of *Bet*-PDMAEMA-C₆₀ is shown in Scheme 2.11. First, PDMAEMA-C₆₀ was prepared using a combination of ATRP and ATRA techniques, then the betainization of tertiary amine residues on the PDMAEMA was accomplished quantitatively using 1,3-sulfobetain in THF in mild reaction condition (room temperature). The ¹H NMR studies indicated that the quantitative betainization (> 95%) of PDMAEMA-C₆₀ was achieved. *Bet*-PDMAEMA-C₆₀ showed responsiveness to both temperature and electrolyte. At room temperature, *Bet*-PDMAEMA-C₆₀ was water-insoluble due to strong electrostatic attractive force from oppositely charged ion pairs along the polymer chains. When the temperature was increased to a critical value, such that the thermal energy exceeded the electrostatic attractive force, *Bet*-PDMAEMA-*b*-C₆₀ became water-soluble when temperature exceeds its UCST. The *Bet*-PDMAEMA-C₆₀ exhibited an UCST of ~ 32 °C, which was higher compared to *Bet*-PDMAEMA (< 20 °C).

[Weaver et al. 2002] The temperature dependent solubility of *Bet*-PDMAEMA- C_{60} was further confirmed by $^1\text{H-NMR}$ spectroscopy (Figure 2.9), where the chemical shift peaks corresponding to *Bet*-PDMAEMA segments became less pronounced at low temperature and the peaks shifted to lower fields with more pronounced peaks at temperature greater than the UCST.



Scheme 2. 11 Synthesis of *Bet*-PDMAEMA- C_{60} . [Ravi et al. 2005b]

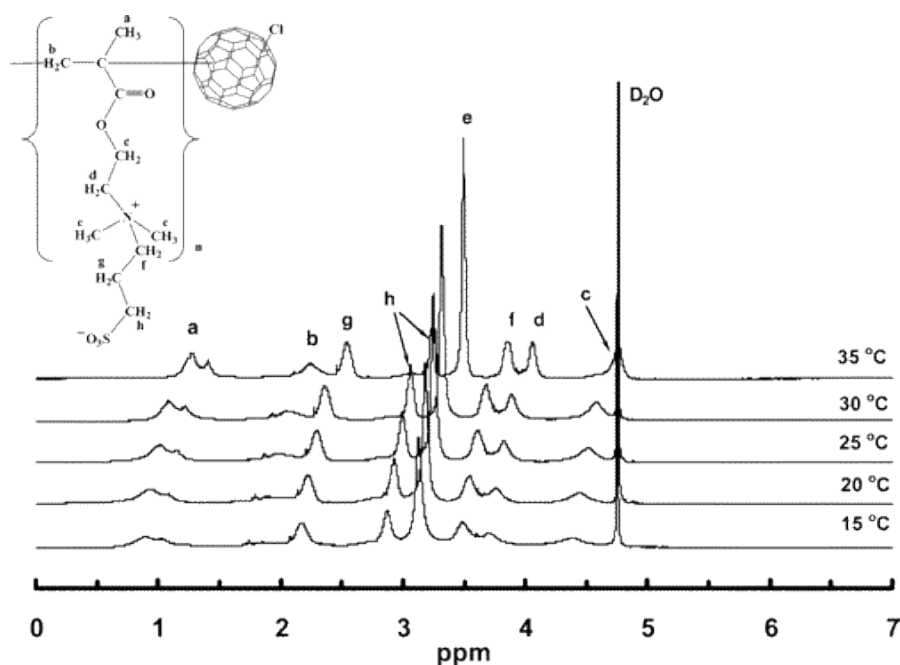


Figure 2. ^1H NMR spectra of *Bet*-PDMAEMA- C_{60} in D_2O measured at different temperatures. [Ravi et al. 2005b]

An interesting behavior corresponding to the “polyelectrolyte effect” and “anti-polyelectrolyte effect” was observed for the first time for *Bet*-PDMAEMA-*b*- C_{60} as a function of NaCl concentrations. Addition of small amounts of salt led to an initial increase in the UCST of *Bet*-PDMAEMA-*b*- C_{60} in low salt concentration regime and after attaining a maximum of 49 °C at 0.35 wt% (NaCl), the UCST decreased at higher salt regime, which was also supported by both viscometric and light transmittance studies. Below the UCST, the strong inherent energy due to intermolecular electrostatic attraction produced a compact chain conformation, which causes the polymer to phase separate. However, there are small amounts of ion pairs that are exposed in bulk water due to its zwitterionic property. At low salt concentration, the small electrolyte ions bind to these exposed ion pairs resulting in the shrinkage of the polymeric chains. Such behavior is similar to the addition of salt to the polyelectrolyte solution, which not only enhances the inter-molecular electrostatic interaction but also decreases the solubility of the

zwitterionic polymers in water. When the salt concentration was saturated with exposed ions, a maximum UCST was observed. Further increase in the salt concentration (> 0.35 wt% NaCl) resulted in the shielding of intermolecular electrostatic attraction, which facilitates the dissolution of polymer chains (“anti-polyelectrolyte”). *Bet*-PDMAEMA-*b*-C₆₀ also tends to form micelle in 0.5 M NaCl aqueous solution at room temperature. These micelles with an R_h of ~ 47 nm are in dynamic equilibrium with unimers having a R_h of ~ 5 nm. However, *Bet*-PDMAEMA existed as unimers with R_h of ~ 5 nm. The hydrophobic C₆₀ induces the formation of uniform micelles with a more compact structure. The averaged apparent M_w calculated from Berry plot was found to be $\sim 1.60 \times 10^5$ g/mol with a R_g of ~ 42 nm and an apparent aggregation number of ~ 25 . The mechanism describing the salt dependence of *Bet*-PDMAEMA-C₆₀ and the “anti-polyelectrolyte” effect were illustrated in Figure 2.10.

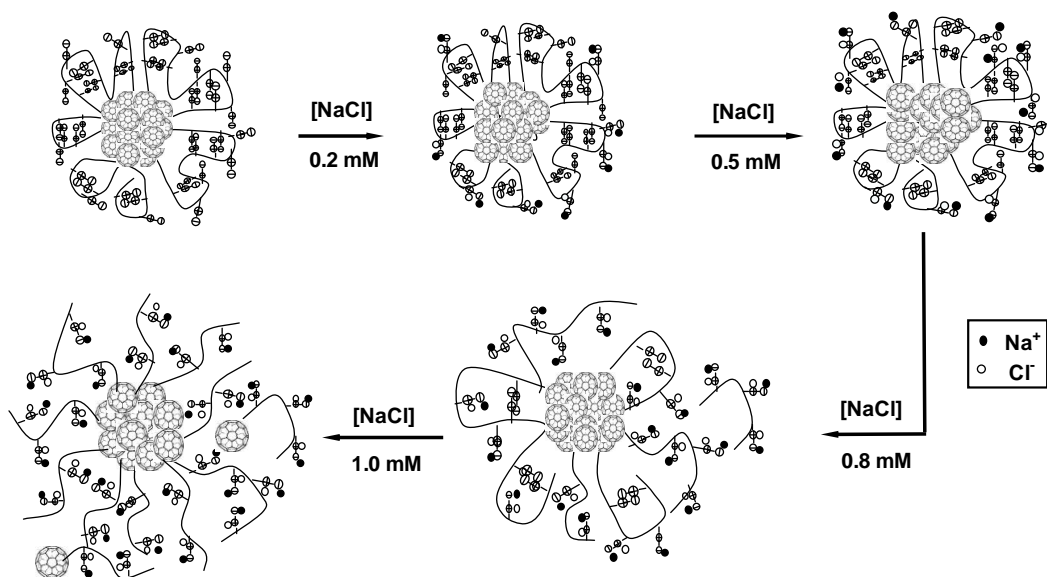


Figure 2. 10 Schematic representation of *Bet*-PDMAEMA-*b*-C₆₀ in the presence of different concentrations of NaCl. [Ravi et al. 2005b]

Tam and coworkers conducted a systematic study on the self-assembly behavior of a well-defined C₆₀ containing polyampholyte block copolymer, namely, P(MAA-*b*-DMAEMA)-C₆₀, as functions of pH and temperature. [Teoh et al. 2005] It is known that the self-assembly behavior of polyampholytic block copolymers depends on the type of monomers and pK_a of two blocks. [Gohy et al. 2001] Therefore, attachment of well-defined polyampholyte to C₆₀ offers more appealing properties to the polyampholytic copolymers. Poly(MAA-*b*-DMAEMA)-C₆₀ was synthesized via the ATRP and ATRA techniques. First block copolymer of P(*t*BMA-*b*-DMAEMA)-Cl was synthesized using ATRP, followed by the grafting of C₆₀ via ATRA process. Finally P(MAA-*b*-DMAEMA)-C₆₀ was prepared using the acid hydrolysis to remove the *t*-butyl group from P(*t*BMA) segments. It was found that the copolymer became insoluble at pH ranging from 5.4 to 8.8 due the overall charge neutralization near its isoelectric point (IEP), [Lowe et al. 1998, Gohy et al. 2000] and the water-soluble P(MAA-*b*-DMAEMA)-*b*-C₆₀ retained its polyampholyte behavior of P(MAA-*b*-DMAEMA). At both high and low pH at 25 °C, the unimers and large aggregates of R_h ~ 120 nm coexisted and the size of the aggregate was largely unaffected by variations in pH due to the difference in the pK_a values of MAA (~ 4.7-5.5) and PDMAEMA (~ 7.5-8.5) monomers. Thus, the self-assembled microstructure was stable below and above the insoluble pH range (pH 5.4 to 8.8). The temperature and pH dependence of P(MAA-*b*-DMAEMA)-*b*-C₆₀ are illustrated in Figure 2.11. At pH 3 and 25 °C, the balance of hydrophobic attraction and electrostatic repulsion arising from -NH⁺(CH₃)₂ accounts for the association of P(MAA-*b*-DMAEMA)-*b*-C₆₀, giving rise to the formation of aggregates. Instead of forming simple core-shell micelles, the aggregates possessed a microgel-like structure with two hydrophobic domains composed of C₆₀ and PMAA segments interconnected by charged hydrophilic PDMAEMA segments. At 55 °C, the R_h distribution was nearly identical to the one

produced at 25 °C with R_h of ~ 120 nm (large aggregates) and ~ 5 nm (unimers) coexisting in solution.

At pH 11 and 25 °C, both unimers and aggregates are in equilibrium, with R_h of ~ 5 and ~ 120 nm respectively. Both the ionized COO^- and deprotonated PDMAEMA segments are hydrophilic at this temperature, while the C_{60} is hydrophobic. Some of the C_{60} molecules self-aggregated through hydrophobic interaction, while the others formed charge transfer (CT) complex with PDMAEMA segments, and they acted as physical cross-linkers. At pH 11 and between 25 and 45 °C, unimers and aggregates coexisted without changes in their sizes. Beyond 50 °C, R_h corresponding to small particle sizes disappeared and an intermediate particle size with R_h of ~ 13 nm appeared, while the size of large aggregates decreased to about 90 nm. The appearance of the intermediate particle size, disappearance of unimers, and the reduction in the aggregate R_h all occurred between 45 and 50 °C. As the temperature was increased, C_{60} and PDMAEMA (LCST ~ 45 °C) formed a continuous hydrophobic domain at higher temperatures with ionized PMAA as the hydrophilic shell. The intermediate size resulted in the tendency for micelle formation (R_h ~13 nm), with C_{60} and PDMAEMA comprising the hydrophobic core and ionized PMAA the hydrophilic shell.

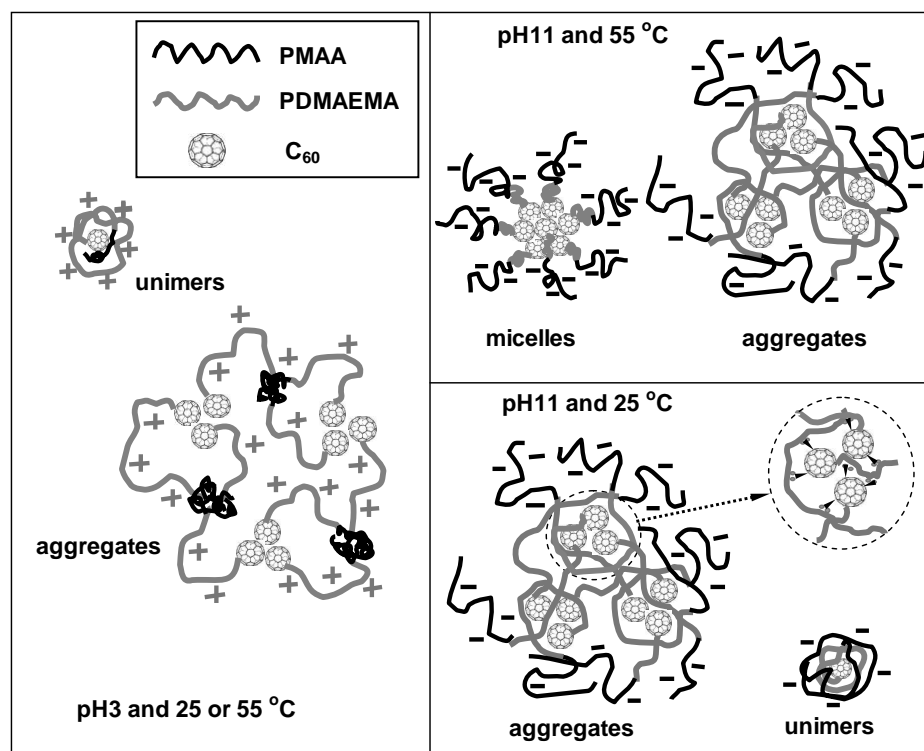


Figure 2.11 Schematic representation of the possible microstructures of P(MAA₁₀₂-*b*-DMAEMA₆₇)-*b*-C₆₀ in aqueous solutions at different pH and temperatures. The inset is the enlargement of the charge-transfer complex section. [Teoh et al. 2005]

Yu et al. synthesized the dual C₆₀ end-capped PDMAEMA using ethylene oxide based dual initiator. [Yu et al. 2007] In this study, C₆₀-PDMAEMA-*b*-EO-*b*-PDMAEMA-C₆₀ was synthesized using a combination of ATRP followed by azido coupling reaction. A Br-PEO-Br macroinitiator was used for the polymerization of DMAEMA in aqueous medium in the presence of CuCl/HMTETA catalyst. Subsequently, azide substitution of the triblock copolymer followed by the azido coupling addition with C₆₀ afforded the well-defined polymer end-capped with C₆₀. They investigated the aggregation behavior of C₆₀-PDMAEMA-*b*-PEO-*b*-PDMAEMA-C₆₀ in unbuffered distilled water and in acidic solution at pH 3 by laser light scattering and found micelles formed with aggregation number (N_{agg}) of ~242 and 81 in pH 7 (unbuffered distilled

water) and pH 3 solutions, respectively. But the micelle size at pH 3 was much bigger due to the highly stretched corona resulting from the positive charge repulsion among the protonated amino groups. They also found that the critical micelle concentration (CMC) of PDMAEMA-*b*-EO-*b*-PDMAEMA-C₆₀ was lower in unbuffered distilled water (28.6 mg/mL) than in solution at pH 3 (176.8 mg/mL).

2.4 Fullerene containing polymer with targeting moieties

2.4.1 Polymeric micelles used as drug carriers

Polymeric micelles were first proposed as drug carriers by Ringsdorf in 1984 [Bader et al. 1984] because of their unique sizes and architectures. The core of the micelles can be utilized as a reservoir for hydrophobic drugs through hydrophobic interaction as well as other interactions, such as metal-ligand coordination bonding [Yokoyama, et al. 1996; Nishiyama et al. 2001]. The formulation of hydrophobic drugs in polymeric micelles has been shown to increase the water solubility of hydrophobic drugs by up to 30,000 folds [Liu et al. 2006]. On the other hand, the shell ensures the stability of the micelles through steric stabilization. Extensive studies on amphiphilic block copolymer micelles have been reviewed by Lavasanifar and co-workers [Mahmud et al. 2007; Aliabadi et. al.2006]. Overall, studies on polymeric micelles in drug delivery have shown that polymeric micelles are highly effective drug delivery vehicles [Zhang, et al. 1997; Shin et al. 1998; Yu et al. 1998; Jeong et al. 1999; Han et al. 2000].

Most polymeric micelles used as drug delivery carriers often consist of poly(ethylene oxide) (PEO), a non-toxic water-soluble polymer and a hydrophobic block, such as poly(propylene oxide) (PPO), poly(L-amino acid) (PLAA), or a poly(ester), e.g., poly(lactic acid) (PLA), a well-known biodegradable and biocompatible polymer. While the list of polymeric micelles available for drug delivery is extensive, the fulfillment of requirements of

biocompatibility limits the numbers available for use in clinical applications. Rapoport and co-workers explored polymeric micelles produced from a variety of acrylamide derivatives, such as acrylic, and methacrylic acid [Rapoport, et al. 2003, 2005] for the encapsulation of antitumor drugs (e.g. paclitaxel and doxorubicin). Kwon et al. have developed a vast platform of thermo-responsive amphiphiles for drug solubilization, stabilization and delivery [Kwon, et al. 2004 and 2005]. The association or dissociation depend on the pH of the medium [Sant et al. 2006]. The results with using polymeric micelles as drug carriers have proved to be quite promising.

Polymeric micelles can also be used as targeted drug delivery systems. The targeting can be achieved via the enhanced permeability and retention effect (EPR) or by attaching specific targeting ligand molecules to the micellar surface. The following section will focus on different polymeric micelles functionalized with different targeting ligands.

2.4.2 Targeted drug delivery using polymeric micelles

Drug delivery carriers using polymeric micelles can enter tumor cells via passive or active targeting approaches. The passive targeting is achieved by the enhanced permeability and retention effect (EPR). Nanoparticles with the desired surface properties and size ranges can escape from capture by the reticuloendothelial system. These particles can selectively accumulate in tumor tissues through the numerous disorganized and dilated pores caused by the fast growing tumor cells. These features are referred to as the EPR effect as schematically shown in Figure 2.12 [Cho et al. 2008].

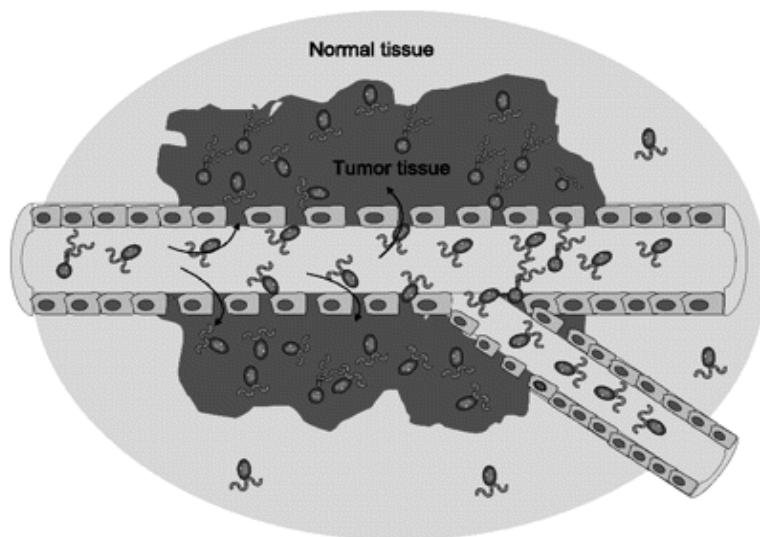


Figure 2. 12 Passive targeting delivery via EPR effect [Cho et al. 2008]

It is evident that the passive targeting is mainly dominated by physiochemical properties of drug carriers and the anatomical characteristics of tumor cells, therefore it is hard to control the delivery of drugs to the target site using this method. To address this issue, active targeting was developed by attaching certain kinds of targeting moieties to the drug carriers. These targeting molecules can recognize the receptors on the cell membrane surfaces by utilizing biologically specific interactions including antigen-antibody and ligand-receptor bindings. Figure 2.13 shows the process of active targeting drug delivery [Cho et al. 2008].

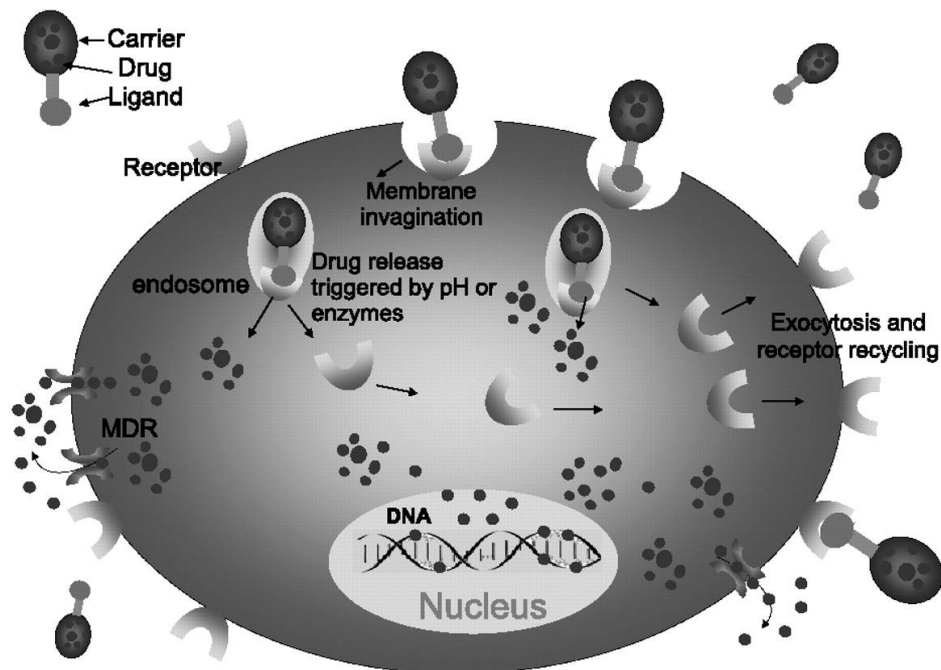


Figure 2. 13 Active targeting delivery via drug carrier with targeting moieties [Cho et al. 2008]

The most commonly studied targeting ligands can be classified into the categories of small organic molecules (folic acid, galactose and lactose, etc), and antibodies. Studies using sugars [Yasugi et al. 1999; 2001; Nagasaki et al. 2001; Jeong et al. 2005; Jule et al. 2003; David et al. 2004; Sinha et al. 2001; Yamazaki et al. 2000], folates [Yoo et al. 2004; Park et al. 2005a; 2005b], and antibodies [Lukyanov et al. 2004; Mao et al. 2004] are listed in Table 2.2. Since this research is focused on the application of sugar targeting ligands, the functionalization of polymeric micelles using sugars will be reviewed.

Table 2. 2 Polymeric micelles with targeting moieties

| Ligands | Micelle compositions | Drugs | References |
|--------------------|-----------------------------|--------------|-----------------------------|
| Folic acid | PEG-PLGA | Dox | Yoo et al. 2004 |
| Folic acid | PEG-PCL | Paclitaxel | Park et al. 2005a and 2005b |
| Galactose, lactose | PEG-PLA | | Yasugi et al. 1999 |
| Galactose | PEG-PLA | | Nagasaki et al. 2001 |
| Galactose | Poly(L-benzyl l-glutamate) | Paclitaxel | Jeong et al. 2005 |
| lactose | PEG-PLA | | Jule et al. 2003 |
| Anti GFA Ab | Pluronic | Haloperidol | Kabanov et al. 1989 |
| mAb 2C5 mAb 2G4 | PEG-PE | Paclitaxel | Torchilin et al. 2003 |
| Anti-PSMA | PEG-PLA | Docetaxel | Farokhzad et al. 2004 |

The receptor-mediated delivery using sugar is also called glycol-targeting. In particular, the asialoglycoprotein receptor (ASGPR) commonly found in liver cells [Ashwelland et al, 1982] is a particularly attractive target because of its very high density on liver cell surfaces (50,000 to 500,000 per cell) [Eisenberg et al. 1991]. Sugar molecules, such as galactose and mannose are known to be specific ligands for ASGPR, thereby ASGPR-based strategies have been used to target drugs for the treatment of liver diseases [Kopacek et al. 1987]. In addition to being present in normal liver cells, ASGPR is also over-expressed in hepatocellular carcinoma [Wands et al. 1991], which makes it a useful target for liver-specific chemotherapy.

The first example of targeting of sugar-macromolecule conjugate carriers in humans was reported in 1999 [Julyan et al. 1999; Ferry et al. 1999]. A phase I clinical study of a poly[*N*-(2-hydroxypropyl)methacrylamide] (HMPA) copolymer bearing doxorubicin and galactosamine was

monitored using I-based imaging, which demonstrated 30% delivery of polymer prodrug to the liver. Jeong and co-workers [Jeong et al. 2005] prepared polymeric micelles comprising of galactose-conjugated poly(ethylene glycol)-copoly-(benzyl L-glutamate) block copolymer (gal-PEG-b-PBLG) with paclitaxel loaded inside the micelles. In-vitro cytotoxicity studies showed that an ASGPR-expressing cancer cell line exhibited greater uptake of these micelles with a 30% increase in cytotoxicity compared to an analogous non-ASGPR expressing cell line. Yasugi et al. [Yasugi et al. 1999] developed carbohydrate-conjugated PEG-b-PLA micelles and evaluated their binding affinity to a representative cell surface receptor. Lectin binding studies of resulting micelles demonstrated multivalent advantage of micelles over ligand-conjugated small molecules. As an example, 80% functionalized lactose-encoded micelles were found to bind in a trivalent manner with a fast association but a very slow dissociation rate. This multivalent effect increased the association constant by over two-fold, while decreasing the main dissociation constant by 145-folds compared to 20% functionalized micelles, which behaved like monovalent systems. This was attributed to the additional ligands being able to bind to additional surface receptors after the initial binding. This additional binding enhances the attachment of the micelles to the receptor covered surfaces, which prevents detachment. Overall, the results using sugars as targeting moieties in polymeric drug carriers showed higher targeting efficacy, especially polymeric micelles bearing sugar ligands demonstrated stronger binding effect to the receptors.

Polymeric micelles as drug carriers have been extensively studied and they showed promising results for targeted drug delivery. However, there is no report for well-defined fullerene containing stimuli responsive water-soluble polymers with targeting moieties. We postulate that the fullerene core formed in polymeric micelles will yield a hydrophobic interior

domain that can encapsulate hydrophobic drugs via the π - π hydrophobic interactions. The targeting ligands located at the outer shells of the polymeric micelles will lead the drug loaded carriers to the specific sites.

2.5 Poly (oligo(ethylene glycol)methyl ether methacrylate) (POEGMA) and its copolymers

Various kinds of polymers have been used to fabricate C_{60} containing systems, however, only a few of them including PEO and PDMAEMA [Verónica et al. 2008] are biocompatible polymers. PNIPAM has been extensively studied as thermal responsive polymers because its LCST is close to the body physiological temperature and is not affected by salt concentrations or ionic strengths. However, there are limited commercial applications using PNIPAM on human body because NIPAM monomer is suspected to be carcinogenic. [Harsh et al. 1991] Recent studies [Lutz et al. 2006a, 2006b, 2007, 2009, 2011] suggest that copolymers of OEGMA analogues prepared via atom transfer radical polymerization (ATRP) exhibited a thermal responsive behavior and the LCST of the copolymers can be precisely tuned by varying the feed ratio of the monomers. Therefore, biocompatible thermal responsive polymers composed of oligo(ethylene glycol) methacrylate (POEGMA) [Han et al. 2003, Mertoglu et al. 2005, Kitano et al. 2004, Lutz et al. 2006a, Lutz et al. 2007a] have attracted increasing attention.

Polymeric micelles have potential applications for drug delivery and other biological applications, [Kataoka et al. 2001] and amphiphilic diblock copolymers containing POEGMA analogues are of great research interest because they are biocompatible and possess tunable thermal properties. To the best of our knowledge, linear block copolymers composed of POEGMA segments with different LCSTs and fullerene containing POEGMA systems have not yet been explored. It is expected that the thermal behavior of this copolymer will be similar to PNIPMAM-b-POEGMA [Jochum et al. 2010] block copolymer, i.e. they will form micelles

when the temperature exceeds the LCST of one block and precipitate from the solution above the LCST of both blocks. POEGMA block copolymers possess two significant advantages over other responsive block copolymers; firstly, they are biocompatible since they possess only POEGMA analogues, and secondly, the LCST of each block can be tuned by varying the ratio of different OEGMA monomers. Thus, the polymeric micelles formed by these copolymers may have potential applications as drug delivery carriers.

In addition, we anticipated that amphiphilic copolymer POEGMA- C_{60} will possess interesting solution behaviors due to the thermal responsive POEGMA segments and unique properties of C_{60} .

2.6 NCC and its polymer modification derivatives

Nanocrystalline cellulose (NCC), as a renewable and biocompatible nano-material, is prepared from cellulose by removing the amorphous regions from the cellulose microfibrils through an acid treatment. Its low density, high tensile strength and biocompatibility make NCC attractive in the applications in the fields of materials science and biomedical science. In most applications, modification becomes necessary to minimize the agglomeration and impart more versatile functions.

2.6.1 Chemical modifications of NCC

Similar to the chemical nature of cellulose, the numerous hydroxyl groups on the nanocrystal surface can be used to modify NCC with small chemical molecules or polymers. For instance, NCC was labeled by fluorescent markers for bioimaging applications [Dong et al. 2007] through epoxide ring opening reaction; dual fluorescent labeled NCC was prepared for pH sensing through the thiol-ene click reaction; [Lise et al. 2010] cationic epoxypropyl trimethyl ammonium chloride (EPTMAC) [Merima et al. 2008] was attached to NCC through the epoxide

ring opening reaction; nanoplatelet gel composed of NCC [Filpponen et al. 2010] and imidazolium salt functionalized NCC [Samuel et al. 2011] were prepared through the reaction between azide and alkyne group. Polymer functionalized NCC can be prepared by “grafting from” or “grafting to” approaches. In the “grafting from” method, the polymer chains were produced by in-situ surface initiated polymerization from immobilized initiators on the NCC surface, thus a higher grafting density is possible. However, it is very difficult to characterize the polymer without cleaving the grafted chains from the NCC surface. Conversely, the “grafting to” method suffers from low theoretical polymer graftings due to steric repulsion between the grafted and reacting polymeric chains. This method allows for the characterization of polymer chains prior to grafting, thus offering the possibility of controlling the properties of the resulting material. Using grafting from approach, researchers modified NCC with poly(ϵ -caprolactone) via ring-opening polymerization [Habibi et al. 2008a] and the mechanical performance of PCL was improved significantly when mixed with PCL-grafted NCC; polystyrene modified NCC was prepared by surface initiated atom transfer radical polymerization (ATRP) [Morandi et al. 2009] and this composite demonstrated the capacity to absorb 1,2,4-trichlorobenzene and hold promise for pollutant removal applications; temperature responsive polymers, such as poly(N-isopropylacrylamide) (PNIPAM) [Zoppe et al. 2010] and poly(N,N-dimethylaminoethyl methacrylate) (PDMAEMA) [Yi et al. 2009] were grafted to NCC through ATRP and the resulting composites may have potential for use in stimuli responsive applications. Researchers used the ‘grafting to’ approach to modify NCC with isothiocyanate decorated polycaprolactone [Habibi et al. 2008b] and epoxide terminated poly(ethylene oxide). [Elisabeth et al. 2010] Figure 2.14 lists the structures of small molecules and polymers that have been used to modify NCC.

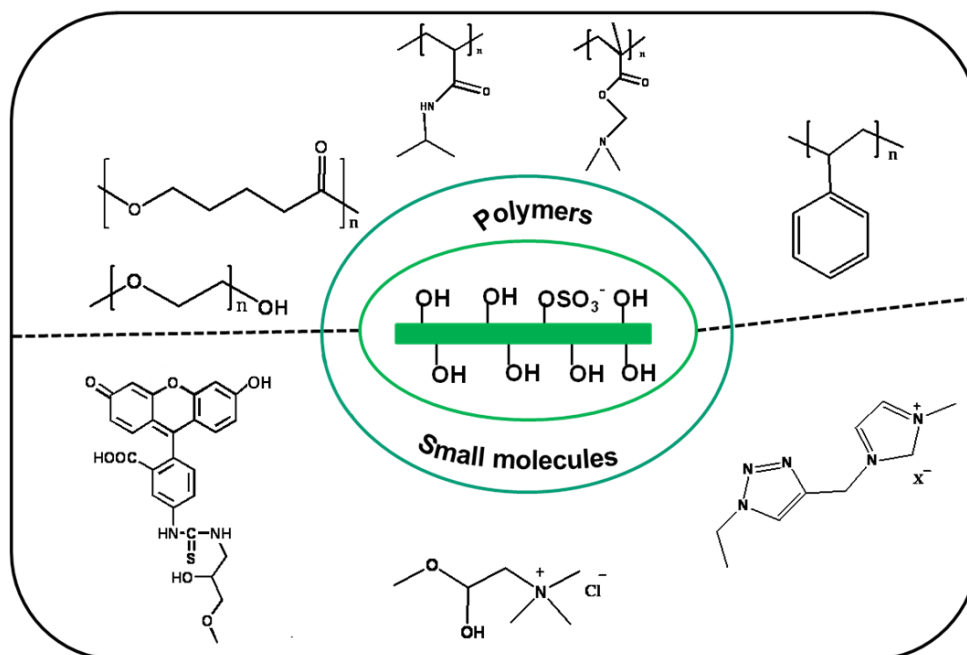


Figure 2. 14 Chemical structures used to modify NCC

We can see that all the modifications of NCC are focused on using polymers and small organic molecules. Modification of NCC using C_{60} and C_{60} containing polymers has not been explored yet. If these structures could be synthesized, a new class of materials will be added to the family of water-soluble fullerene containing polymers.

2.7 Current and Future Applications of Stimuli-Responsive Fullerene Polymers

The problem with the water solubility of fullerene (C_{60}) has been addressed synthetically by grafting water-soluble polymeric chains onto C_{60} . Many attractive properties of C_{60} -polymer systems have been identified and elucidated, which pave the way for their applications in a wide range of fields, such as diagnostics, pharmaceuticals, environmental and energy. The low toxicity of fullerenes [Gharbi et al. 2005] and their unique properties have stimulated researchers to investigate the physicochemical properties of these fascinating molecules. The biological applications of water-soluble fullerenes are broad and rapidly evolving in the field of

immunotherapy, [Ashcroft et al. 2006] enzyme inhibition, [Innocenti et al. 2010] gene transfection, [Isobe et al. 2005] and antibiotic. [Tegos et al. 2005] A commercial product (called Radical Sponge) was recently registered for cosmetic application by Vitamin C₆₀ BioResearch Corp. It comprises of a water-soluble C₆₀ encapsulated within PVP that can slow down the aging of skin. [<http://www.vc60.com>] This application was developed due to the fact that C₆₀ exhibits free radical scavenging activity. [Krusic et al. 1991]

Although there are no commercial applications for stimuli-responsive fullerene polymers yet, they are projected to have increasing impact in terms of their potential applications because their physical properties can be controlled by the manipulation of external environment. For example, pyrene labeled thermo-responsive PNIPAM [Hong et al. 2009] is expected to be used as alarm-type probes or sensors for detecting a specific temperature. Another potential application is in the delivery of hydrophobic drugs, where the hydrophobic fullerene cores provide an ideal environment for encapsulating hydrophobic drug molecules via π - π and hydrophobic interactions. Polymeric micelles have been proven to be effective drug delivery vehicles. By proper design, the stimuli-responsive fullerene polymers can be used as drug carriers, where the drugs can be released in a controlled manner by manipulating the external environment.

Besides biological applications, water-soluble fullerenes have also found application in the field of organic photovoltaics (OPVs), where a layer-by-layer technique was used to fabricate multilayer films for photovoltaic cells. [Mwaura et al. 2005] Although there has not been any report on using stimuli-responsive fullerene polymer in OPVs yet, the self-organization characteristics of these systems may be advantageous for the control of morphologies beneficial

for application in solar cells. As new systems are being developed and their beneficial properties identified, new applications will emerge in the future.

2.8 Conclusions

Fullerene containing polymers, especially stimuli-responsive water-soluble C_{60} derivatives, continue to attract the attention of researchers due to their special physicochemical properties and potential applications in various fields. C_{60} containing polymers can be produced through various methods, such as direct copolymerization in the presence of C_{60} using conventional radical polymerization, polymerization of monomers using C_{60} based initiators, substitution or end-capping of C_{60} with precursor polymers bearing reactive groups including amino group, carbanion, azide, macro-radicals. Depending on the synthetic methodologies used, different architectures could be produced, such as C_{60} on the main polymer chain, C_{60} on the side chain of the polymers, hyper-branched C_{60} containing polymers, star-like polymers, mono or dual end-capped polymers. The development of controlled/living radical polymerization, particularly ATRP, SFRP and RAFT makes the development of well-defined polymeric grafted C_{60} with different polymer composition and architecture possible. Various interesting C_{60} containing systems were synthesized using this controlled radical polymerization technique.

The variation of pH, temperature or salt can lead to the formation of different morphologies of aggregates for the stimuli-responsive water-soluble C_{60} containing polymers. The development in the synthetic methodologies of C_{60} containing polymers and the understanding of the solution properties could provide the basis for the future applications of these water-soluble fullerene materials. The future research in this field can be envisioned in several areas: (1) drug delivery exploration of the existing or emerging stimuli-responsive water-soluble C_{60} polymer with different targeting moieties; (2) attachment of stimuli-responsive

biocompatible polymers, such as POEGMA analogues to make C_{60} containing polymers more versatile in terms of biomedical applications; (3) utilization of stimuli-responsive water-soluble C_{60} polymers as building blocks to construct more interesting structures. Important breakthrough in the near future can be foreseen because the fundamental studies in this field have been established and any new idea on top of the existing systems will benefit this research community significantly.

Chapter 3 Synthesis and self-assembly of stimuli-responsive poly (2-(dimethylamino) ethyl methacrylate)-fullerene (PDMAEMA-C₆₀) and the self-assembly under different conditions

3.1 Introduction

Polymeric micelles are self-assembled structures formed by amphiphilic block copolymers in aqueous media and they have attracted increasing research interests for drug delivery applications because they facilitate solubilization of hydrophobic drugs. [Kwon et al. 1996, Rosler et al. 2001, Aliabadi et al. 2007, Torchilin et al. 2004] The formulation of hydrophobic drugs in polymeric micelles has been shown to increase the drug solubility by up to 30,000 times. [Liu et al. 2006] In addition to commonly used hydrophobic polymers, such as poly (propylene oxide) (PPO), poly(L-amino acid) (PLAA) and poly(ester), fullerene has also been used as a hydrophobic segment for preparing amphiphilic copolymers. The fullerene core in polymeric micelles provides a hydrophobic domain that can encapsulate hydrophobic drugs via π - π and hydrophobic interactions. A series of well-defined stimuli-responsive water-soluble fullerene containing polymers, such as poly (acrylic acid)-C₆₀ (PAA-C₆₀), [Ravi et al. 2006, Yang et al. 2003] poly(methacrylic acid)-C₆₀ (PMAA-C₆₀), [Ravi et al. 2005] poly(N-isopropylacrylamide)-C₆₀ (PNIPAM-C₆₀), [Tamura et al. 2006] and poly(methacrylic acid)-poly (2-(dimethylamino) ethyl methacrylate)-C₆₀ (PMAA-PDMAEMA-C₆₀) [Teoh et al. 2005] have been prepared and the self assembly behaviors in aqueous solution at different conditions were investigated. It was found that these structures formed micelles under certain conditions and such observations are critical in exploring the applications of polymer-C₆₀ systems as drug delivery vehicles. Among these copolymers, stimuli-responsive polymeric micelles are attractive systems

since the drug release process can be controlled by external stimuli, such as temperature or pH. PDMAEMA- C_{60} systems were reported by Dai and co-workers [Dai et al. 2004] and they demonstrated that the aggregation behavior of PDMAEMA- C_{60} depended on pH and temperature. It was found that micelles were formed in acidic solution, but only unimers existed in basic solution at 25 °C.

Polymeric micelles with cellular-specific targeting functionalities have been developed in order to achieve the delivery of drug to target cells. [Jule et al. 2003, Jule et al. 2002, Yasugi et al. 1999, David et al. 2004] In this study, we describe the development of stimuli-responsive polymeric micelles decorated with galactose targeting moieties. The block copolymer composed of three components, namely PDMAEMA, galactose targeting moiety and C_{60} . It is believed that this structure will form micellar aggregates comprising of C_{60} hydrophobic core with targeting ligands on the surface of PDMAEMA coronas. It is anticipated that these micelles have potential applications as drug carriers to deliver hydrophobic drugs to liver cells due to two features; (1) PDMAEMA copolymer systems [Yuan et al. 2007] were shown to be useful drug release vehicles and the release rate of an anticancer drug was effectively controlled by manipulating the pH of the medium; (2) galactose is known as an efficient targeting ligand for binding to asialoglycoprotein receptor (ASGPR) expressed on the membrane of liver cells. [Eisenberg et al. 1991, Jeong et al. 2005]

The self-assembly behavior of PDMAEMA- C_{60} with targeting moieties at different pH conditions was investigated and they are of critical importance for their applications as drug carriers. We were expecting that the prepared polymer with targeting moiety would possess a similar behavior as PDMAEMA- C_{60} previously prepared by Dai and coworkers. [Dai et al. 2004] However, to our surprise, we observed that PDMAEMA- C_{60} with targeting moieties also formed

micelles in aqueous solution at pH 10, and the size of the micelles is smaller than at pH 3. This finding is different from the results reported earlier by Dai and coworkers, where only unimers were observed in basic solutions. To explain this, several hypotheses were formulated, such as differences in the end groups of the block copolymers, and the presence of free PDMAEMA chains. The DLS data presented by Dai and coworkers showed that the intensity for unimers was significantly strong compared to micelles at pH 3, which led us to wonder if there were unreacted PDMAEMA chains in their system. Based on the preliminary results, it became apparent that free PDMAEMA chains could play an important role in disrupting the micellar structure at high pH. Dai and coworker explained that the formation of charge transfer (CT) complex between PDMAEMA and C₆₀ was the reason why there was no micelles formed at pH 10. They did not realize that there was unreacted PDMAEMA polymer in their samples, thus their conclusion did not take into account the presence of free PDMAEMA chains present in their polymeric system. For solution containing predominantly PDMAEMA-C₆₀ chains, one PDMAEMA chain was not adequate to prevent the formation of micelles at basic condition. This unexpected result may offer a possible approach to alter the micellar structure, allowing the control of drug release induced by the demicellization process caused by free PDMAEMA chains. In this chapter, we report on the synthesis and self-assembly of PDMAEMA-C₆₀ with galactose targeting moiety at different conditions, such as different pH and amounts of free PDMAEMA chains. This work was published by Yao et al. [Yao et al. 2011a]

3.2 Experimental

3.2.1 Materials

C₆₀ (>99.5%) was purchased from MTR, Ltd. (Cleveland, OH), 2- (dimethylamino) ethyl methacrylate (DMAEMA), 1,2:3,4-di-o-isopropylidene-d-galacto,2-bromoisobutyryl bromide,

copper (I) chloride (99.5%), trifluoroacetic acid (TFA), 1,1,4,7,10,10-hexamethyl triethylene tetramine (HMTETA, 97%), anhydrous 1,2-dichlorobenzene and triethylamine were purchased from Sigma-Aldrich. HPLC grade tetrahydrofuran was purchased from VWR. DMAEMA was purified by distillation under reduced pressure prior to use.

3.2.2 Synthesis of 6-Isobromobutyryl-1,2:3,4-di-*O*-isopropylidene-*D*-galactopyranose (I)

A solution of 2-bromoisobutyryl bromide (1 mL, 8.06 mmol) was added dropwise to a 25 mL round-bottomed flask containing CH₂Cl₂ (50 mL), 1,2:3,4-di-*O*-isopropylidene-*D*-galactopyranose (1.20 g, 4.6 mmol), and triethylamine (2.0 mL, 13.8 mmol), which was maintained in an ice-bath. The reaction mixture was stirred at room temperature for 24 h, and 100 mL of distilled water was then added. The mixture was then transferred to a 250 mL separatory funnel. The CH₂Cl₂ phase was washed three times using distilled water, dried over Na₂SO₄ and then filtered. The filtrate was concentrated using a rotary evaporator. The residue was re-crystallized with methanol and the off-white solid was collected after filtration.

3.2.3 Synthesis of PDMAEMA-Cl (II)

The polymerization of DMAEMA using the initiator (I) was performed in ethanol via the ATRP process based on the procedure described by Yu et al. [Yu et al. 2007] In a typical experiment, DMAEMA (4.0 mL, 23.7 mmol), initiator (I) (142.7 mg, 0.348 mmol) and ethanol (4.0 mL) were added to a 25 mL flask and the mixture was bubbled with argon for 30 mins. Then the mixture was transferred using a double tipped needle into a flask charged with CuCl (69.04 mg, 0.697 mmol) and HMTETA (189.7 μ L, 0.697 mmol) equipped with a magnetic stirring bar under argon atmosphere. After stirring at room temperature overnight, the reaction mixture was terminated by adding THF (10 mL), which was then passed through a neutral alumina column to remove the catalyst. After evaporating the THF solution to about 2 mL, PDMAEMA was

precipitated using a 20-fold excess of hexane, and the white solid was isolated after drying in a vacuum oven at 25 °C, giving a yield of 84%. The chemical structures and M_w of the polymers were characterized by ^1H NMR and GPC. PDMAEMA with molecular weight of 8300 g/mol (M_n) was synthesized and the polydispersity index (PDI) was 1.2, which means that the ATRP reaction was well-controlled.

3.2.4 Preparation of PDMAEMA- C_{60} (III)

PDMAEMA-Cl (II) and anhydrous dichlorobenzene were charged into a flask filled with argon. In a separate flask, excess amount of C_{60} , CuCl and HMTETA (1:2 molar ratio of macroinitiator) were dissolved in 20 mL of 1, 2-dichlorobenzene. The two flasks were bubbled with argon for 30 minutes and finally, under an argon atmosphere, the macroinitiator was transferred into the catalyst system via a double-tipped needle. The reaction mixture was stirred for 24 h at 90 °C. After 24 h, the reaction mixture was diluted with THF and the catalyst was removed by passing the THF solution through a basic alumina column. The unreacted C_{60} was removed by dissolving the copolymer in THF, filtered, and passed through the basic alumina column. The filtrate was concentrated and precipitated in excess of hexane to yield a brown solid. The procedure was repeated three times to ensure the complete removal of unreacted C_{60} . The polymer was then dried under vacuum and stored in the dark.

3.2.5 Preparation of PDMAEMA- C_{60} with galactose moieties (IV)

Deprotection of the sugar residue located at the end of PDMAEMA was performed in a mixture of trifluoroacetic acid (TFA) and water at a ratio of 8:2 (v/v) for 30 mins at room temperature. The reaction was stopped by pouring the reaction mixture into a 100-fold of 2-propanol kept at -20 °C. The precipitate was collected after centrifugation at 5000 rpm for 5

mins. Then the solid was dissolved in distilled water and cleaned in a dialysis tubing (MW cut off is 3000 Da) for 24 hours, and the product was isolated after freeze drying.

3.2.6 Sample Preparation

Solutions containing 0.2 mg/mL PDMAEMA-C₆₀ were prepared by dissolving PDMAEMA-C₆₀ sample in water at pH 3 and 10. Mixture of free PDMAEMA and PDMAEMA-C₆₀ were prepared in two steps: first, solutions of different concentrations of PDMAEMA in pH 10 solution were prepared, and then PDMAEMA-C₆₀ was dissolved in PDMAEMA solutions in the desired ratio.

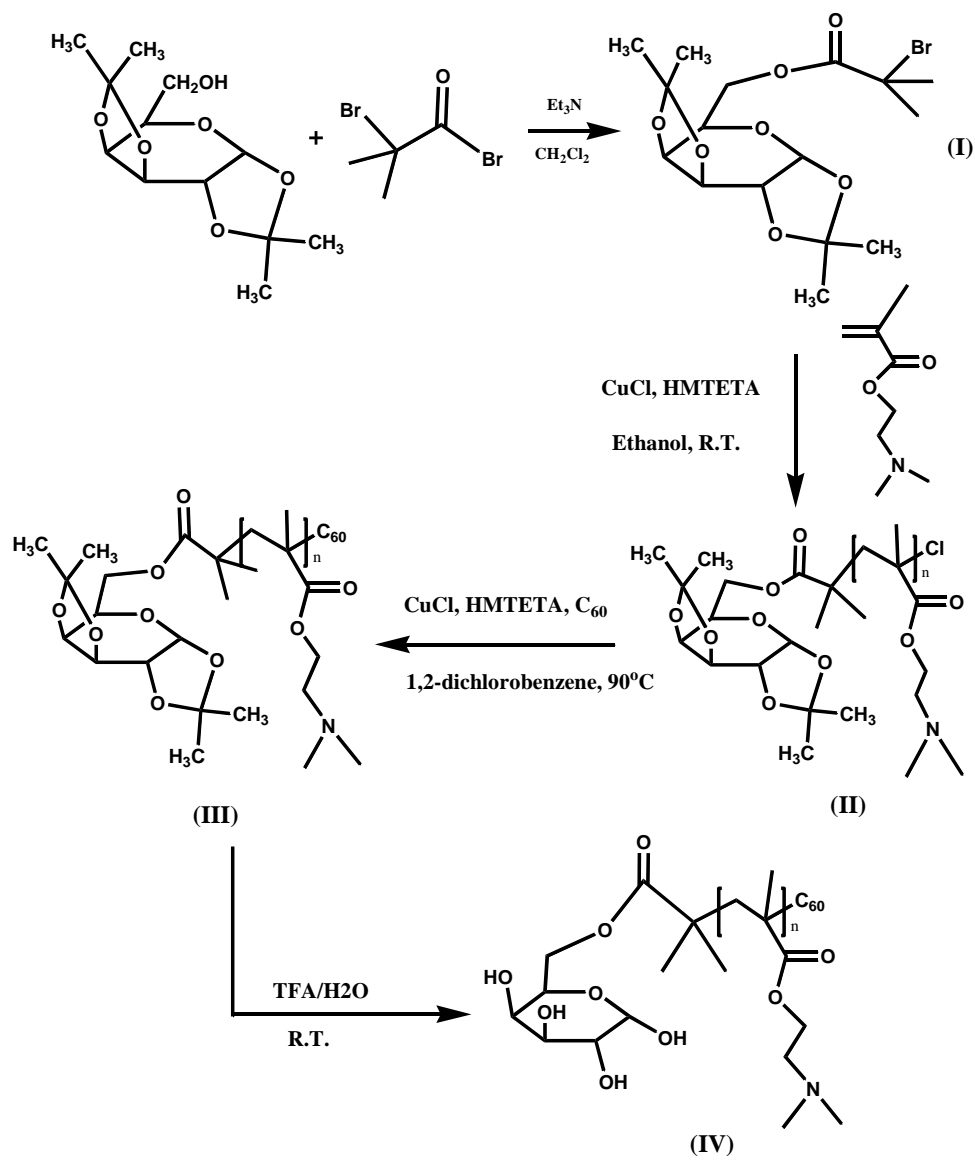
3.2.7 Characterization

An OmniSEC GPC system equipped with a ViscoGel Column, a RI detector, and a light scattering detector was used to determine the molecular weights and molecular weight distributions of the polymers. The RI detector was calibrated with narrow molecular weight polystyrene standards. HPLC-grade THF stabilized with BHT containing 0.6% triethylamine was used as the mobile phase. The flow rate was maintained at 1.0 mL/min. ¹H NMR analysis was conducted on a Bruker Avance 300 instrument. Spectroscopy (UV-Vis), UV-vis spectra were acquired using a Perkin Elmer Lambda 35 spectrophotometer. Dynamic light scattering (DLS) measurements were performed on a Brookhaven BI-200SM goniometer system. The deionized water was further purified in a Millipore purification system equipped with a 0.45 μm filter, while HCl and NaOH, were used to adjust the pH. A 0.45 μm filter was used to remove dust prior to the light scattering experiments. The inverse Laplace transform of REPES in the Gendist software package was used to analyze the time correlation functions with a probability of reject set to 0.5. The self-assembled micelles were observed by TEM (Philips CM12) and SEM.

3.3 Results and Discussion

3.3.1 Synthesis of PDMAEMA-C₆₀ with galactose moieties

Recently, mono-substituted C₆₀ derivatives of PDMAEMA were successfully prepared. [Dai et al. 2004] In this work, a similar method was used to prepare a well-defined PDMAEMA-C₆₀ with galactose moieties. The synthesis involved four steps as shown in Scheme 3.1. First, ATRP initiator with galactose residues protected with isopropylidene groups was synthesized and the NMR spectrum of the initiator is shown in Figure 3.1. Second, a well-defined PDMAEMA was prepared via ATRP reaction catalyzed by CuCl/HMTETA in ethanol. PDMAEMA with molecular weight of 8300 g/mol and PDI of 1.2 was prepared (Figure 3.2 a). Third, ATRA in dichlorobenzene was performed to synthesize PDMAEMA-C₆₀ and ¹H NMR (Figure 3.3 I) showed that the peaks corresponded well with those found in the NMR spectrum of PDMAEMA in the absence of C₆₀. Finally, the isopropylidene groups were removed by acid treatment to yield PDMAEMA-C₆₀ with galactose targeting moieties. TFA treatment is a general procedure used to remove isopropylidene protecting groups from the sugar residue. [Christen et al. 1968, Bes et al. 2003]



Scheme 3. 1 Synthetic Scheme of PDMAEMA-C₆₀ with targeting moiety.

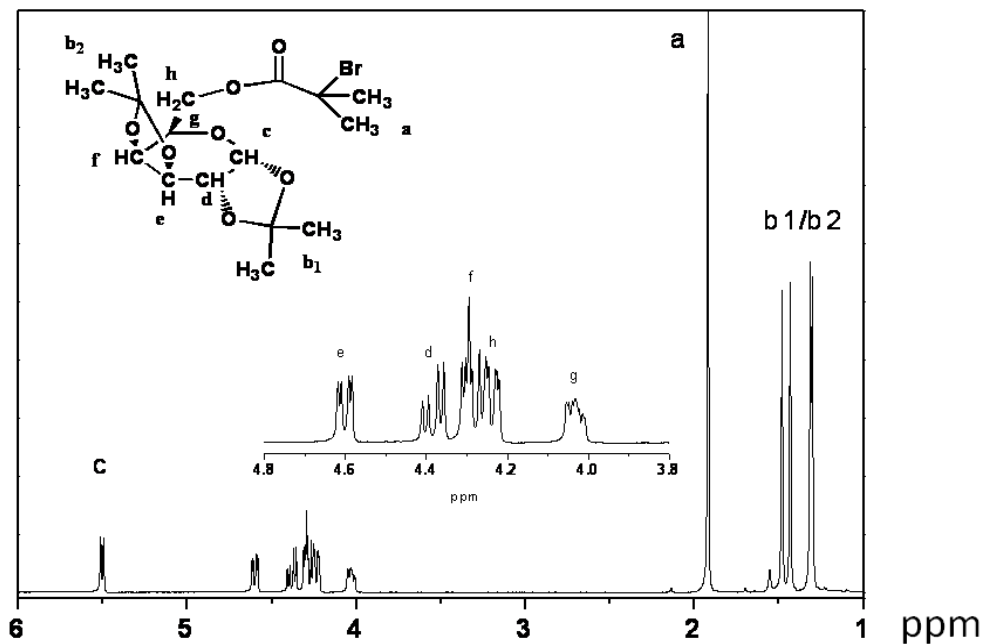


Figure 3. 1 ^1H NMR spectrum of 6-Isobromobutyryl-1,2:3,4-di-*O*-isopropylidene-D-galactopyranose.

It should be noted that the hydrolysis of ester linkages in the backbone and side groups may occur, therefore mild reaction conditions was used. Figure 3.3 describes the ^1H NMR spectrum, which showed that the isopropylidene group was successfully removed because the peak f corresponding to C-1 of the protected galactose residue at 5.5 ppm disappeared completely after the acid treatment. Meanwhile, a peak f' at 5.2 ppm appeared, which corresponded to the protons at the C-1 position of the deprotected galactose residue. In addition, the ester groups along the PDMAEMA polymer chains were left untouched because the integration ratio of peak "a" and peak "d" remained at a value of ca. 2 after acid treatment. The GPC traces (Figure 3.2) of PDMAEMA- C_{60} and PDMAEMA- C_{60} with galactose moieties showed that the PDIs were less than 1.2. The M_w of the three polymeric systems are almost identical because the reactions for the attachment of C_{60} and deprotection of isopropylidene groups did not significantly change the M_w of the polymer. PDMAEMA is

essentially transparent at wavelength greater than 250 nm, while the absorption bands of C₆₀ exhibited two clear peaks at around 257 and 330 nm. [Hare et al. 1991] Therefore, the presence of these two shoulders in the UV-vis absorption spectrum can be used to confirm the covalent attachment of C₆₀ to the polymer. As expected, the UV-Vis spectrum (Figure 3.4) showed two peaks at approximately 257 and 330 nm, which confirmed that C₆₀ was covalently attached to PDMAEMA since unreacted C₆₀ should have been removed after repeated precipitation and filtration treatment in THF. In addition, ¹³C NMR (Figure 3.5) showed a peak at 145 ppm, which corresponded to the resonance of the C₆₀ moiety. These also proved the covalent linkage between C₆₀ and PDMAEMA and not the physical trapping of C₆₀ within the PDMAEMA matrix.

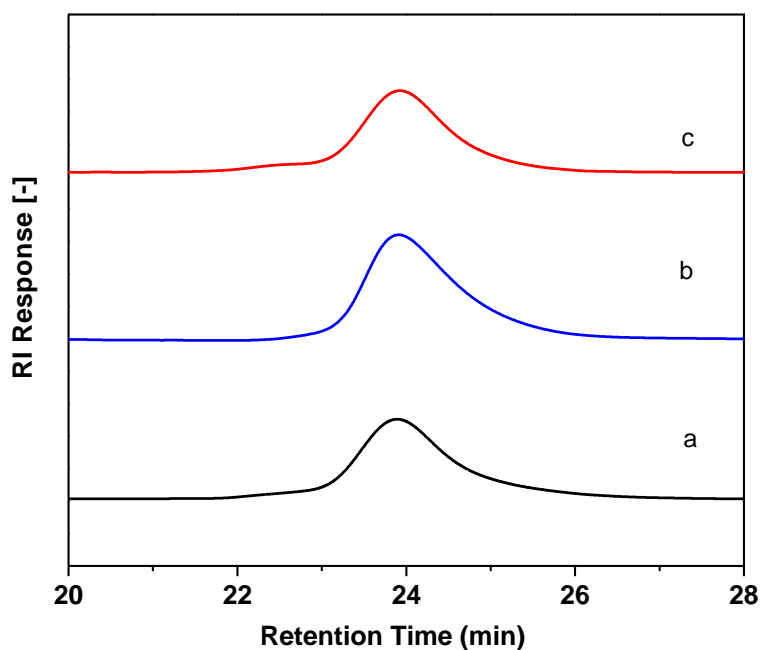


Figure 3. 2 GPC traces of (a) PDMAEMA; (b) PDMAEMA-C₆₀ and (c) PDMAEMA-C₆₀ with galactose moieties.

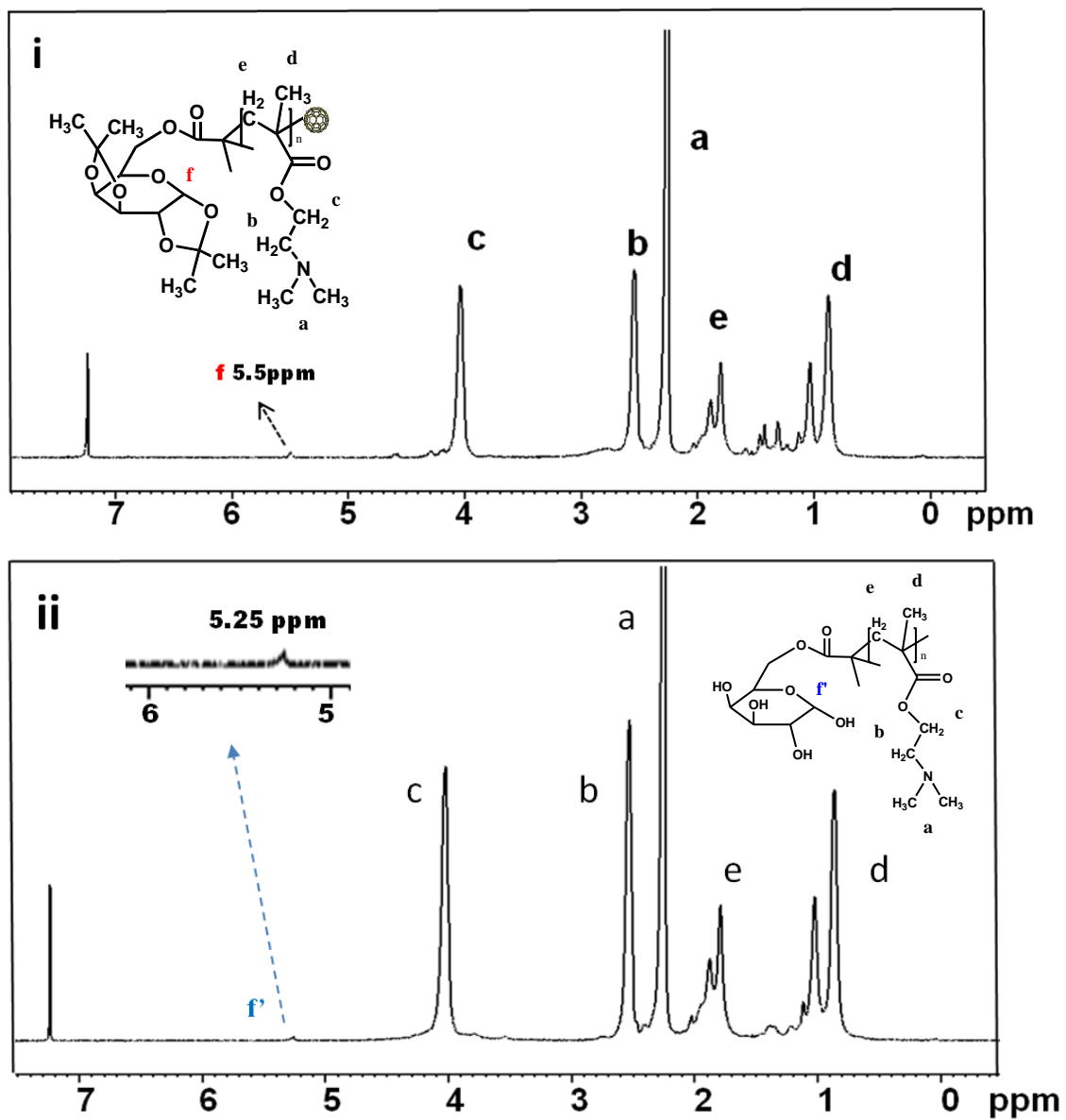


Figure 3. ^1H NMR spectra of i. PDMAEMA- C_{60} (III in Scheme 1) and ii. PDMAEMA- C_{60} with galactose moieties (IV in Scheme 3.1).

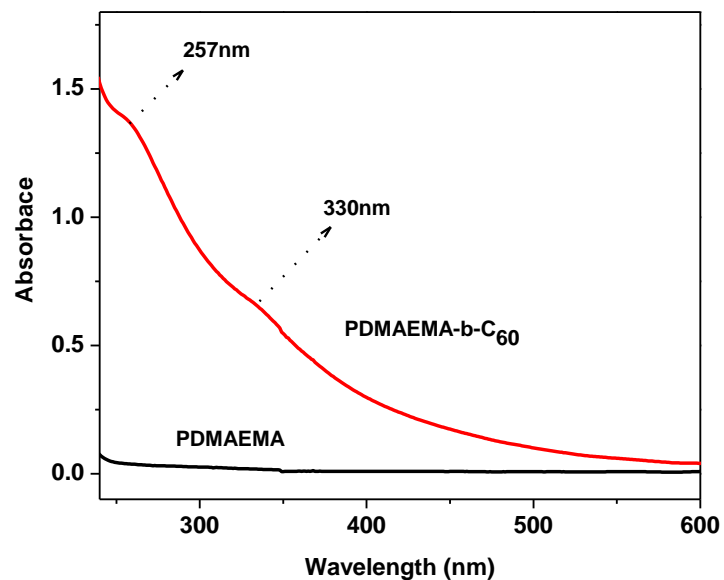


Figure 3. 4 UV-vis spectrum of PDMAEMA-C₆₀ with galactose moieties (IV) in water.

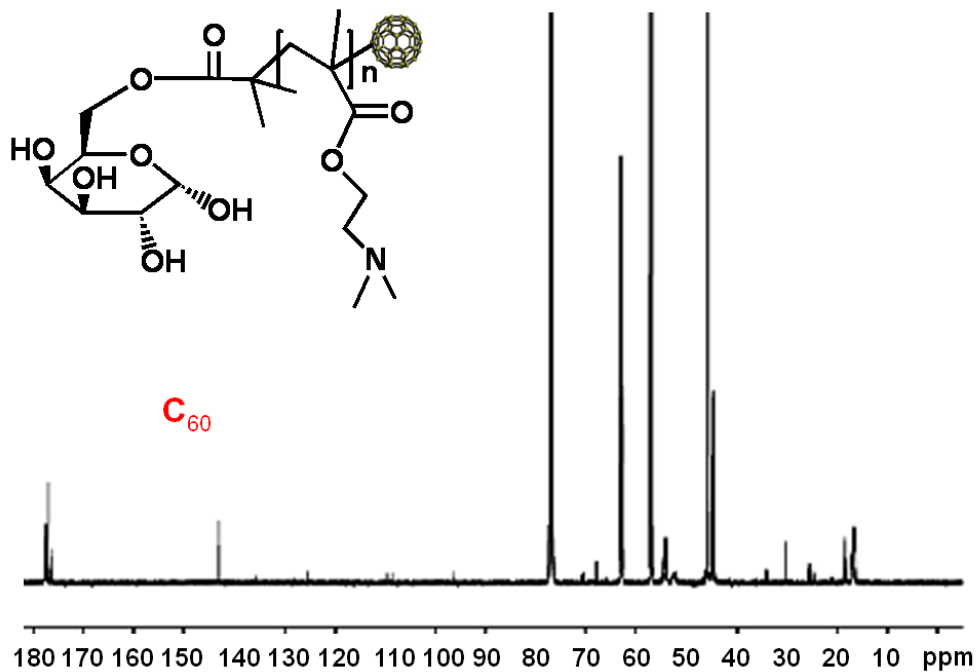


Figure 3. 5 ¹³C NMR spectrum of PDMAEMA-C₆₀ (IV)

3.3.2 Self –assembly of PDMAEMA-C₆₀ with galactose moieties

The self-assembly behaviors of PDMAEMA-C₆₀ with galactose moieties were investigated using the dynamic light scattering (DLS) technique. DLS measures the temporal fluctuations of the scattered light produced by Brownian movement of the scattering particles. This temporal variation of the scattered radiation yields the Doppler shift, and the broadening of the central Rayleigh line could be used to determine the dynamic properties of the system. The normalized field autocorrelation function is described by the expression:

$$g_1(t) = \int w(\Gamma) \exp(-\Gamma t) d\Gamma \quad (3.1)$$

where $w(\Gamma)$ is a continuous distribution function of decay rate Γ , which is the inverse of the decay time τ . If the inverse Laplace transform is used to analyze the autocorrelation function, the decay time distribution function $w(\Gamma)$ can be obtained. For the translational diffusion mode, the translational diffusion coefficient D is related to the decay rate by equation 3.2:

$$\Gamma = Dq^2 \quad (3.2)$$

The magnitude of q is determined by equation 3.3:

$$q = \frac{4\pi n_0 \sin(\theta/2)}{\lambda} \quad (3.3)$$

where n is the refractive index of the liquid, θ is the scattering angle, and λ is the wavelength of the laser in vacuum. Therefore, D can be derived from the slope of the graph of Γ versus q^2 .

As a result, the apparent hydrodynamic radius ($R_{h,a}$) can be determined from the Stokes-Einstein equation for non-interacting spheres:

$$R_{h,a} = \frac{kT}{6\pi\eta D} \quad (3.4)$$

Here, T is the absolute temperature, k is the Boltzmann constant, and η is the viscosity of the liquid. It should be pointed that the hydrodynamic radius measured from DLS is an apparent value. By definition, DLS measures the radius of a hypothetical hard sphere that diffuses with the same speed as the particle under examination. This definition is somewhat problematic since hypothetical hard spheres are non-existent. In practice, macromolecules in solution are non-spherical, dynamic and solvated. As such, the radius calculated from the diffusion properties of the particle is indicative of the apparent size of the dynamic solvated particle.

It was found that the hydrodynamic radii were 50.3 and 42.3 nm at pH 3 and 10, respectively. The decay distribution functions obtained at a scattering angle of 90° at pH 3 and 10 are shown in Figure 3.6, where we deduced that unimers and micelles coexisted. It is known that particles with smaller sizes possess faster decay times, therefore we concluded that the R_h for both unimer and micelles are smaller at pH 10 than at pH 3. This is expected since PDMAEMA chains are protonated at pH 3 and the polymeric chains tend to be more extended due to electrostatic repulsion between positively charged amino groups. TEM and SEM were used to observe the self-assembled structures of the prepared PDMAEMA- C_{60} . The diameters of the particles observed from TEM (Figure 3.7a) were smaller than those obtained from DLS measurements, suggesting that the shells of the micelles consisting PDMAEMA chains were not visible under TEM since the electron density of PDMAEMA is much lower than that of C_{60} . This phenomenon has been observed in other studies. [Yang et al. 2008, Liu, 2006] The spherical particles in the TEM images were believed to be fullerene cores. However, the particles observed in the SEM (Figure 3.7 b) images have similar sizes to those measured by DLS. It should be

noted that similar results were obtained for TEM and SEM characterization for samples prepared at pH 3 and 10, which indicated that the sizes of the micelles are similar under dry conditions.

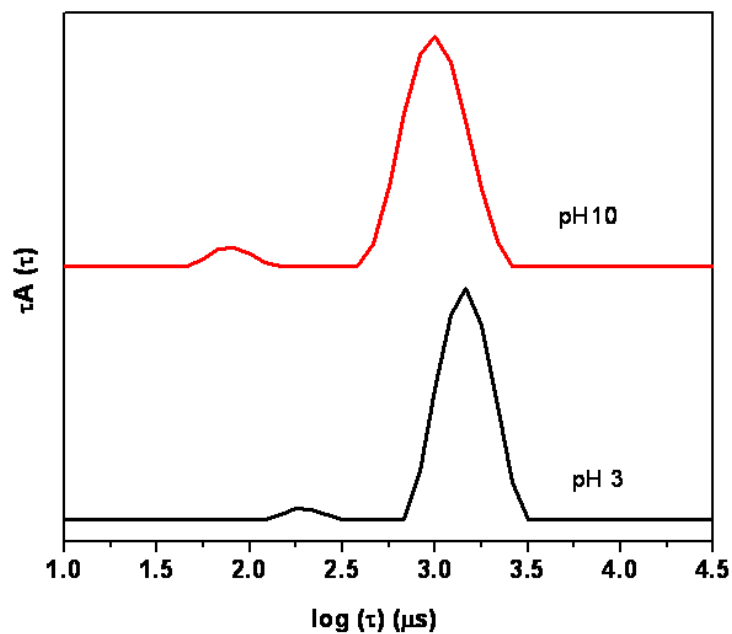


Figure 3. 6 Decay time distribution functions at pH 3 and 10 for PDMAEMA-C₆₀ with galactose moieties.

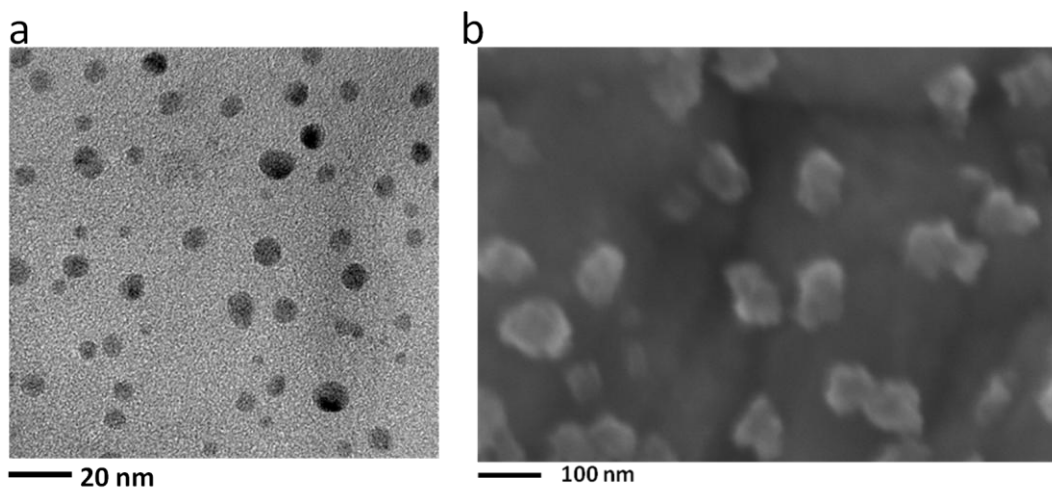


Figure 3. 7 (a) TEM and (b) SEM images of PDMAEMA-C₆₀ with galactose moieties.

3.3.3 Free PDMAEMA chains induced demicellization

Dai and coworkers found that for PDMAEMA-C₆₀ system, only unimers were present in aqueous solution at pH 10. They explained that the absence of micelles at pH 10 was due to the formation of a charge transfer (CT) complex between the PDMAEMA chains and fullerenes. However, the present study revealed the existence of both unimers and micelles. It is known that fullerene forms charge-transfer (CT) complexes with aromatic rings [Matsubara et al. 1997, Sibley et al. 1997] and tertiary amines. [Wang 1992, Sibley et al. 1995] Since the end functional group of PDMAEMA-C₆₀ in their earlier study consisted of tosyl groups, which is different from the galactose groups used in the present study, we wondered if the end groups had an influence on the formation of the CT complex. Thus, we synthesized an identical polymeric system using the same procedure described by Dai and coworkers, and we found that micelles and unimers were observed in aqueous solution at pH 10.

After careful examination of the decay distribution curves from the light scattering experiments, we found that the intensity of the peak corresponding to unimers in Dai and co-worker's published data for 18k PDMAEMA-C₆₀ was relatively larger than those of the micelles at pH 3 (Figure 3.8). It is known that the scattering intensity of polymeric micelles is much stronger than unimers since the intensity of light scattering from particles is proportional to the sixth power of its diameter based on Rayleigh's approximation. The CMC for the formation of polymeric micelles is remarkably low, in the orders of $\mu\text{g/mL}$ or lower, hence the solution should contain predominantly micelles. [Salamone et al. 1996, Adams et al. 2003] In this study, we used DLS to quantify the CMC of PDMAEMA-C₆₀ (Figure 3.9), where the intercept at the x-axis yields the CMC value of about 6 $\mu\text{g/ml}$. The low CMC indicated that the concentration of unimers in the solution is very low, therefore the intensity of light scattering in the DLS

measurement should be very weak compared to micelles. This led us to believe that there is probably significant amount of free PDMAEMA in the systems synthesized by Dai and coworkers.

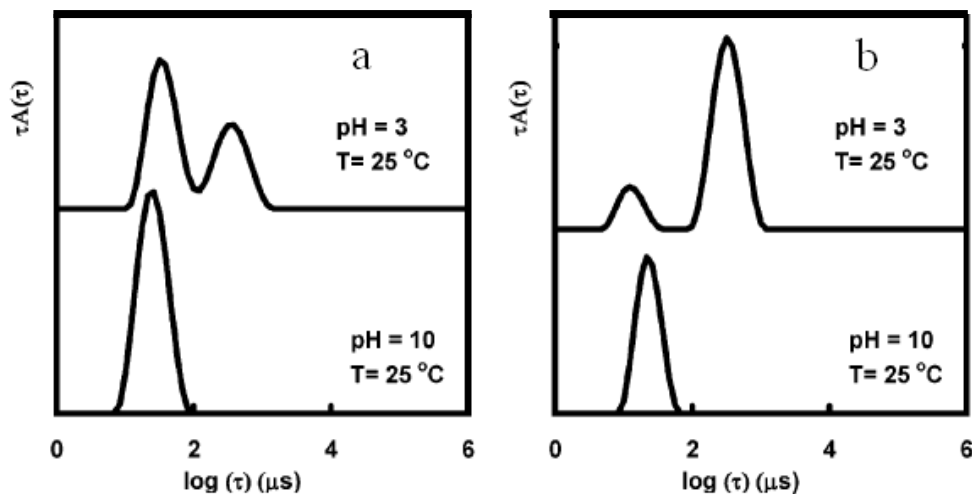


Figure 3. 8 Decay time distribution of PDMAEMA-C₆₀: (a) 18k and (b) 8k (adapted from [Dai et al. 2004])

There are three possible reasons for the presence of unreacted PDMAEMA in the polymeric system synthesized by Dai and coworkers. First, the ATRP reaction is very sensitive to oxygen and the presence of oxygen in the reaction may lead to low conversion of PDMAEMA to PDMAEMA-C₆₀. Second, it is impossible to remove unreacted PDMAEMA chains since the solubility of the PDMAEMA and PDMAMA-C₆₀ is fairly similar. Third, it is hard to detect unreacted PDMAEMA using GPC because the difference in the molecular weight between PDMAEMA and PDMAEMA-C₆₀ is about 720 g/mol, which is the molecular mass of fullerene.

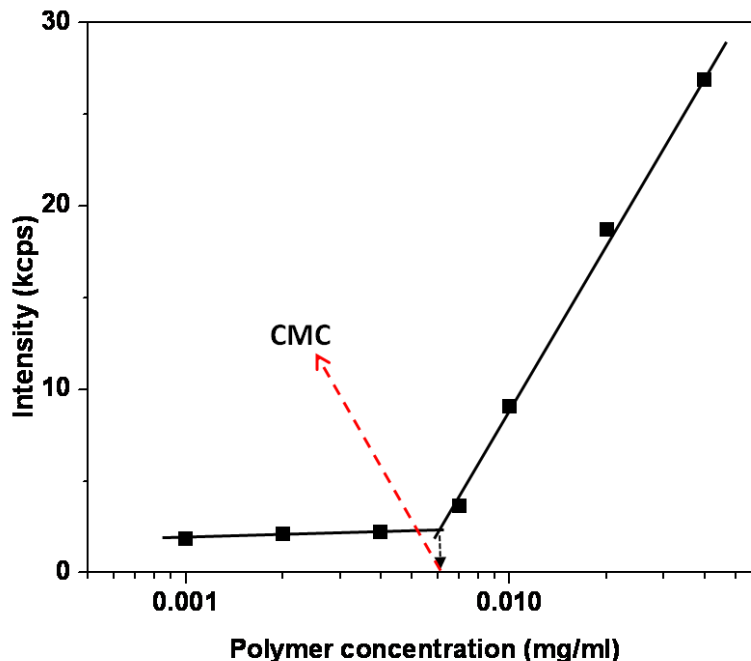


Figure 3. 9 Dynamic light scattering to measure the CMC of PDMAEMA- C_{60} .

An obvious question is, how free PDMAEMA chains present in the system leads to the destabilization of the self-assembled micellar aggregate at pH 10? The explanation proposed by Dai and coworkers corresponded to the condition when the concentration of free PDMAEMA is high. The formation of charge transfer complex between PDMAEMA and C_{60} is concentration dependant as reported by Ungurenasu et al. [Ungurenasu et al. 2000] In their study, they observed that nitrogen containing polymer, such as PVP forms a CT complex with fullerene in two different ways, depending on the concentration of the polymer. If the polymer concentration is sufficiently high, it will form contact-pairs complex, in which fullerene will be wrapped by several polymeric chains. When the concentration of the polymer is low, it forms CT-saturated complex, in which one polymer chain will form a complex with several fullerene molecules. In our case, the ratio of PDMAEMA to C_{60} is 1:1 for the copolymer PDMAEMA- C_{60} , in which the

fullerene molecule cannot be totally wrapped by PDMAEMA chains, therefore the hydrophobicity of fullerene is still sufficiently strong to facilitate the formation of micelles. Another question is how many free PDMAEMA chains are needed to break up the micelles? We prepared a series of test solutions containing different proportions of PDMAEMA and PDMAEMA-C₆₀. The hydrodynamic radii were measured by DLS at pH 3 and 10, and the results are shown in Figure 3.10. At pH 10, R_h decreased from ~ 44 to ~ 3 nm when the ratio of (PDMAEMA/ PDMAEMA-C₆₀) was increased from 0 to 4. However, at pH of 3, R_h remained constant, indicating that the micellar aggregates remained stable because PDMAEMA chains were protonated, and CT complexation did not occur. The decay time distribution curves shown in Figures 3.11 and 3.12 also reinforced the trend reported in Figure 3.10. We observed that the scattering intensity of unimers at pH 3 increased with increasing amounts of free PDMAEMA chains. When the mole ratio of (PDMAEMA/PDMAEMA-C₆₀) was about 4, the decay distribution curve was identical to that reported by Dai and co-workers, which further confirmed the presence of free PDMAEMA chains in their samples.

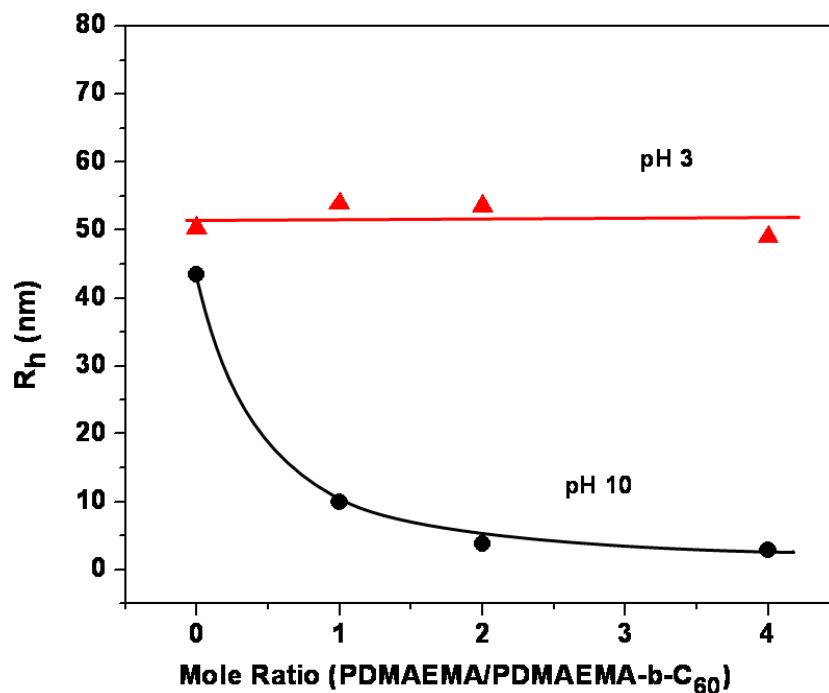


Figure 3. 10 Effect of PDMAEMA on the hydrodynamic radii of PDMAEMA-C₆₀ at pH 3 and 10.

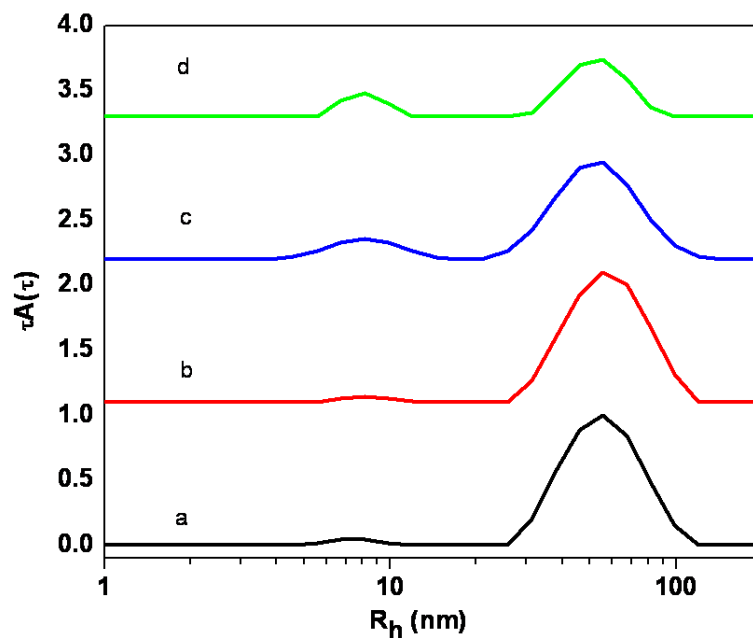


Figure 3. 11 Decay time distribution functions of (a) PDMAEMA-C₆₀ and mixtures of PDMAEMA and PDMAEMA-C₆₀ at mole ratio of (b) 1; (c) 2 and (d) 4 at pH 3.

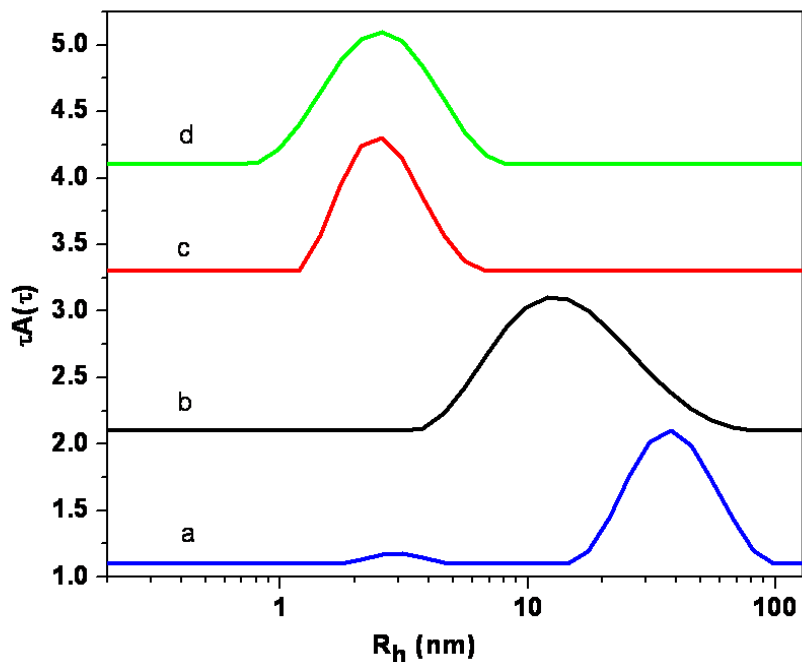


Figure 3. 12 Decay time distribution functions of (a) PDMAEMA- C_{60} and mixtures of PDMAEMA and PDMAEMA- C_{60} at mole ratio of (b) 1; (c) 2 and (d) 4 at pH 10.

Based on the above results, we propose a physical mechanism to describe the evolution of the microstructure of PDMAEMA/PDMAEMA- C_{60} mixtures in aqueous solution at the two extreme pH conditions of 3 and 10. At pH 3, the microstructure of the self-assembled aggregates remained unchanged as there is no CT complex formed between PDMAEMA chains and fullerene particles (Figure 3.13 (left panel)). Addition of excess amounts of PDMAEMA chains to the PDMAEMA- C_{60} solutions did not destabilize the self-assembled aggregates. On the other hand, at pH 10, when the mole ratio of polymer to fullerene is 1, PDMAEMA chains form CT complex with C_{60} as shown in Figure 3.13 (a), where only part of PDMAEMA chains form CT complex with fullerenes, driven by electron donor and acceptor interaction. The remaining portion of PDMAEMA chains remains in solution due to hydrogen bonding between PDMAEMA and water. As the hydrophobicity of C_{60} is dominant, the balance between the

hydrophobic C₆₀ and hydrophilic PDMAEMA chains induces the formation of micelles. When the ratio of PDMAEMA to fullerene increases to 2, the coverage of C₆₀ by CT complexation of PDMAEMA chains increases (Figure 3.13 b), the effective hydrophobicity of C₆₀ with respect to the aqueous environment decreases, yielding a condition where smaller micelles are produced. When the ratio of PDMAEMA to fullerene increases beyond 3, the hydrophobicity of C₆₀ is significantly reduced by adsorbed PDMAEMA chains on the surface of C₆₀ that destabilizes the micelles to produce unimers.

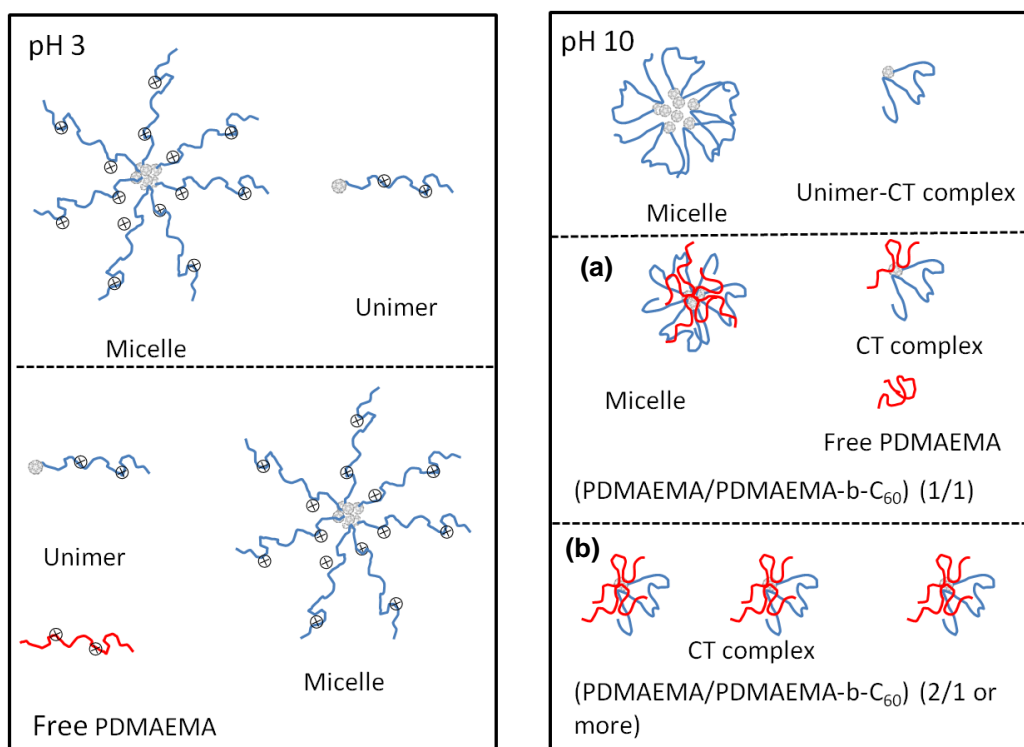


Figure 3. 13 Schematic diagram describing the self-assembly behaviors of PDMAEMA-C₆₀ with and without addition of free PDMAEMA at pH 3 (left) and 10 (right).

It is anticipated that this demicellization phenomenon can be used to trigger the release of encapsulated drug in the micelles as the drugs loaded within the micelles could be released more

rapidly in the presence of free polymer chains at higher pH. The drug delivery properties of the prepared PDMAEMA-C₆₀ with galactose targeting ligand will be examined in Chapter 4.

3.4 Conclusions

PDMAEMA-C₆₀ with galactose functionality was successfully synthesized using the ATRP process. The process was initiated by a bromine containing halide functionalized with isopropylidene protected galactose groups and catalyzed by (HMTETA)/CuCl. Isopropylidene groups were completely removed using a TFA/water mixture to produce PDMAEMA-C₆₀ systems with galactose targeting groups without hydrolyzing the appended ester groups along the PDMAEMA chains.

The self-assembly behavior of the PDMAEMA-C₆₀ with galactose moiety at different pH conditions were investigated by DLS. At pH 3 and 10, both polymeric micelles and unimers were present in aqueous solutions. However, smaller R_h was observed for PDMAEMA-C₆₀ samples at pH 10 than at pH 3. TEM images of the self-assembled micelles only showed the cores of the micelles as the PDMAEMA shells were not visible under TEM. SEM images confirmed that the spherical particles were consistent with the sizes obtained from DLS measurements. Demicellization of PDMAEMA-C₆₀ aggregates by free PDMAEMA chains was observed at pH 10, and the physical mechanism for this process was elucidated. Besides pH and temperature, free PDMAEMA chains may be added to trigger and control the release of drugs.

Chapter 4 Drug delivery using PDMAEMA-C₆₀

4.1 Introduction

Nano drug carriers including nanoparticles, micelles, dendrimers, liposomes, and polymeric microspheres are of great interest for applications in therapeutic drug delivery. Among these nano carriers, phospholipid-based liposomes have been studied extensively [Storm et al. 1998]. However, the self-assembly of phospholipids in aqueous solution produces a hydrophilic interior compartment to encapsulate hydrophilic drugs, hence they are not suitable for the encapsulation of hydrophobic molecules. Although several nanocarriers designed to entrap hydrophobic drugs have been reported, [Dhanikula et al 2005, Yang et al. 2007a and 2007b], none of them have progressed to clinical trials due to the low drug payload and restricted bioavailability of their encapsulated hydrophobic molecules [Peltier et al. 2006].

Recently, fullerene based nanocarriers have attracted increasing attention because it was envisioned that hydrophobic drugs may have strong affinity with fullerene molecules via the π - π hydrophobic interactions. Some discrepancy exists in the literature regarding the potential toxicity of fullerene in vivo. For instance, studies [Oberdorster, et al. 2004 and Zhu et al. 2006] have indicated that water solubilized C₆₀ fullerene could be slightly cytotoxic to living organisms. In contrast, another report [Gharbi et al. 2005] showed that the underivatized C₆₀ fullerenes exhibit no cytotoxicity in rodents. Moreover, the aqueous solubility and biocompatibility of fullerenes may be further increased by modifying their surfaces with various hydrophilic functional groups. Also the sizes and the morphologies vary with changes in pH and temperature. We anticipated that these micellar systems might be used as targeting hydrophobic drug carriers after modification with specific targeting moieties based on the following established facts. (1) The biocompatibility [Yu et al. 2005, Zheng et al 2003 and Du. et al. 2005]

of PDMAEMA might reduce the cytotoxicity of C₆₀. (2) PDMAEMA copolymer systems [Yuan et al. 2007] were shown to be useful as drug release vehicles, and the release rate of an anticancer drug was effectively controlled by altering the pH of the medium. (3) Galactose is known as an efficient targeting ligand specifically for binding with asialoglycoprotein receptor (*ASGPR*) expressed on the membrane of healthy and cancerous liver cells. Therefore it could be used as a targeting ligand for treating liver cancers.

In this chapter, the drug loading using the PDMAEMA-C₆₀ was investigated. First, the interaction of hydrophobic drugs with PDMAEMA-C₆₀ was examined using fluorescence and ITC techniques. The in vitro drug delivery and gene transfection studies were performed by Y.K.Ho at National University of Singapore, Singapore. The results are shown in Appendix.

4.2 Experimental

4.2.1 Materials

PDMAEMA-C₆₀ (III) and PDMAEMA-C₆₀ (IV) were used as prepared and the synthesis was described in Chapter 3. PAA was synthesized via two step reactions: ATRP catalyzed by CuCl/HMTETA to synthesize poly(*tert*-butyl acrylate) (PtBA) and then PAA was prepared by removing the *t*-butyl groups via acid hydrolysis. Fluorescein, pyrene and HEPES buffer solution and tris acetate EDTA (TAE) were purchased from Sigma-Aldrich. Fluorescein was used as received, pyrene was purified by re-crystallization in methanol prior to use. Neuroblastoma cells (N2a) obtained from the American Type Culture Collection (CCL-131, ATCC, USA) were used. The cells were incubated in Dulbecco's modification of Eagle's medium (DMEM) with 10 % fetal bovine serum (FBS, Hyclone, Logan, UT) and 1 % penicillin and streptomycin under a humidified atmosphere with 5 % carbon dioxide (CO₂) at 37 °C. The

plasmid DNA (pIRES-EGFP-EV71) used in this experiment expresses enhanced green fluorescent protein (eGFP).

4.2.2 Fluorescence measurements

The highest chromophore concentrations used in this study was 1.2×10^{-6} M and the polymer concentration was 0.2 mg/mL. These concentrations were sufficiently low to avoid inner-filter effect. [Lakowicz et al. 1999.] Steady-state fluorescence emission spectra were acquired on a PTI fluorometer equipped with an Ushio UXL-75Xe xenon arc lamp and PTI 814 photomultiplier detection system. The solutions containing fluorescein/PDMAEMA- C_{60} and pyrene/PDMAEMA- C_{60} were excited at 490 or 346 nm, respectively.

4.2.3 ITC measurements

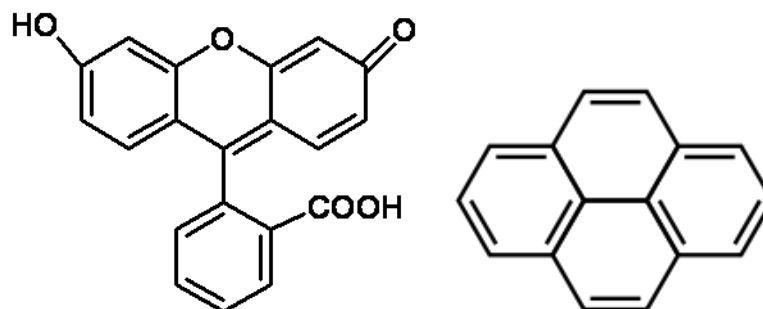
An ITC experiment measures the enthalpy changes associated with binding interactions occurring at a constant temperature. The principle of the technique is based on the temperature difference between the sample and reference cells, which is converted to units of power. This physical temperature difference is called differential power (DP) and is defined as the power required to maintain the sample and reference cells at the same temperature. Integrating the DP peaks with respect to time yields the ΔH value for the physical interactions. The enthalpy changes of the interaction between fluorescein, pyrene and PDMAEMA- C_{60} were measured by a Microcal isothermal titration calorimeter. The titrations were conducted at constant temperature of 25 °C. About 250 μ L titrant, pyrene (10 mM) or fluorescein (0.06 mM), was injected into the sample cell filled with dilute PDMAEMA or PDMAEMA- C_{60} solution (0.04 wt%). The titration was carried out by step-by-step addition at different volumes i.e. 2, 5 and 10 μ L increments.

UV-vis spectra were acquired using a Perkin Elmer Lambda 35 spectrophotometer. Dynamic light scattering (DLS) measurements were performed on a Brookhaven BI-200SM goniometer system. The deionized water was further purified in a Millipore purification system equipped with a 0.45 μm filter, while HCl and NaOH were used to adjust the pH. A 0.45 μm filter was used to remove dust prior to the light scattering experiments. The inverse Laplace transform of REPES in the Gendist software package was used to analyze the time correlation functions with a probability of reject set to 0.5.

4.3 Drug and polymer interaction using fluorescent techniques

It was demonstrated that fluorescence can be used to study the formation of micelles [Kalyanasundaram, 1988; Tummino and Gafni, 1993]. Studies also showed that C_{60} could quench the fluorescence of pyrene [Hong et al., 2009]. Therefore, two types of fluorescent probes were used to investigate the interaction of hydrophobic model drugs, namely, fluorescein (Scheme 4.1a) and pyrene (Scheme 4.1b) with PDMAEMA- C_{60} .

Fluorescein was used as a model drug because it is a hydrophobic molecule with very high fluorescence (excitation occurs at 494 nm and emission at 521 nm). Figure 4.1 showed the fluorescence of fluorescein in aqueous solution and in PDMAEMA- C_{60} solution. Since the solubility of fluorescein in water is very low, fluorescein was first dissolved in acetone, and then dried in air. The yellow powder was used to prepare aqueous solutions. It was noticed that fluorescein can readily dissolve in water in the presence of PDMAEMA- C_{60} possibly due to the formation of acid/base complexes between PDMAEMA and fluorescein and hydrophobic interaction between fullerene and fluorescein.



Scheme 4. 1 Chemical structures of (a). Fluorescein; (b). Pyrene

Interestingly, the sample of fluorescein in solution was yellowish green, while the sample of fluorescein mixed with PDMAEMA- C_{60} was reddish orange. (Figure 4.1) The UV-Vis spectrum of fluorescein possessed a λ_{max} at 490 nm. Addition of PDMAEMA and PDMAEMA- C_{60} resulted in a red shift to ca. 492 nm. (Figure 4.2) At pH 7, the dianion of fluorescein is the prevalent species. [Sjöback et al, 1995] The red shift in these UV-Vis spectra of fluorescein suggested that there was an increase in formation of acid and base complexes after mixing with PDMAEMA and PDMAEMA- C_{60} .



Figure 4. 1 Pictures of (a). aqueous solution of fluorescein; (b). aqueous solution of fluorescein and PDMAEMA- C_{60} .

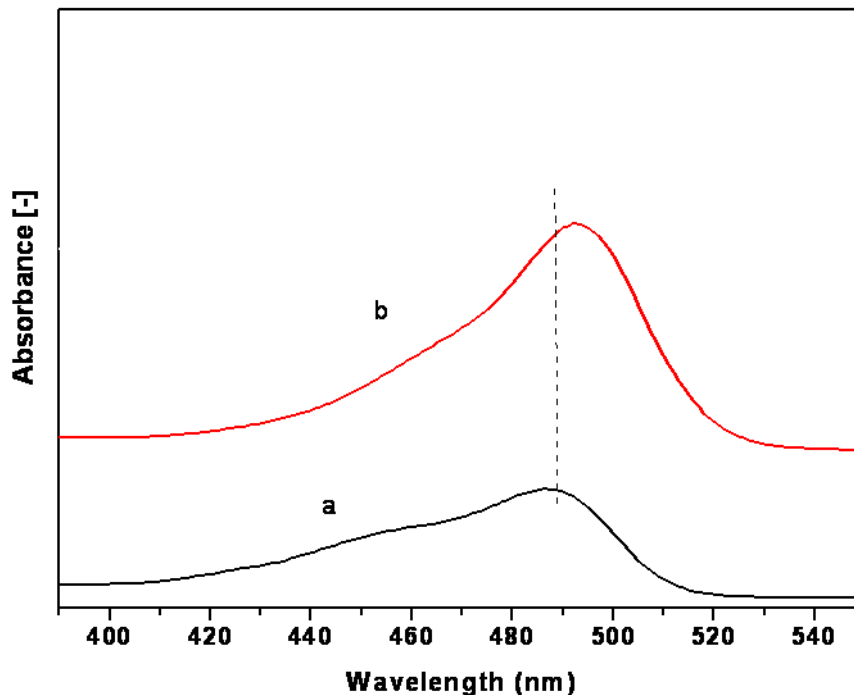


Figure 4. 2 UV-Vis spectra of (a) fluorescein and (b) fluorescein/PDMAEMA-C₆₀.

By comparing the results from the steady state fluorescence of fluorescein, (Figure 4.3), PDMAEMA and fluorescein with different concentrations (Figure 4.4) and PDMAEMA-C₆₀ and fluorescein with different concentrations (Figure 4.5), we can conclude that the fluorescence quenching of fluorescein after mixing with PDMAEMA or PDMAEMA-C₆₀ was about 20% for all concentrations. This may be due to the formation of acid-base complex between PDMAEMA and fluorescein. The acid base interactions are stronger than the hydrophobic interactions. Therefore most of fluorescein molecules are located within the shell of the micelles. These measurements were performed by mixing fluorescein with pre-formed PDMAEMA-C₆₀ micellar solutions. However, when the mixing procedure was reversed by first adding PDMAEMA-C₆₀ polymer into fluorescein solution, the quenching was much stronger for PDMAEMA-C₆₀ than PDMAEMA (Figure 4.6), exhibiting 30% quenching for PDMAEMA-C₆₀ and 20% for PDMAEMA. This indicated that the micelle

formation occurs after the interaction of fluorescein with fullerene, therefore the fluorescein can be trapped within the core of the micelles. These results suggested that the drug loading capacity depended on the preparation protocols.

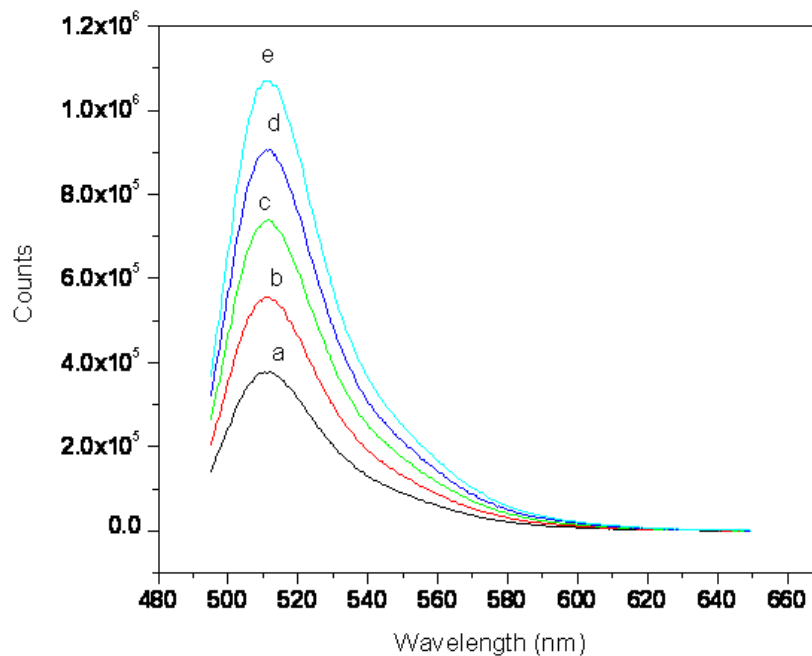


Figure 4. 3 Steady state fluorescence of different concentrations of fluorescein (a). 400; (b). 600; (c). 800; (d).1000 and (e) 1200 nM.

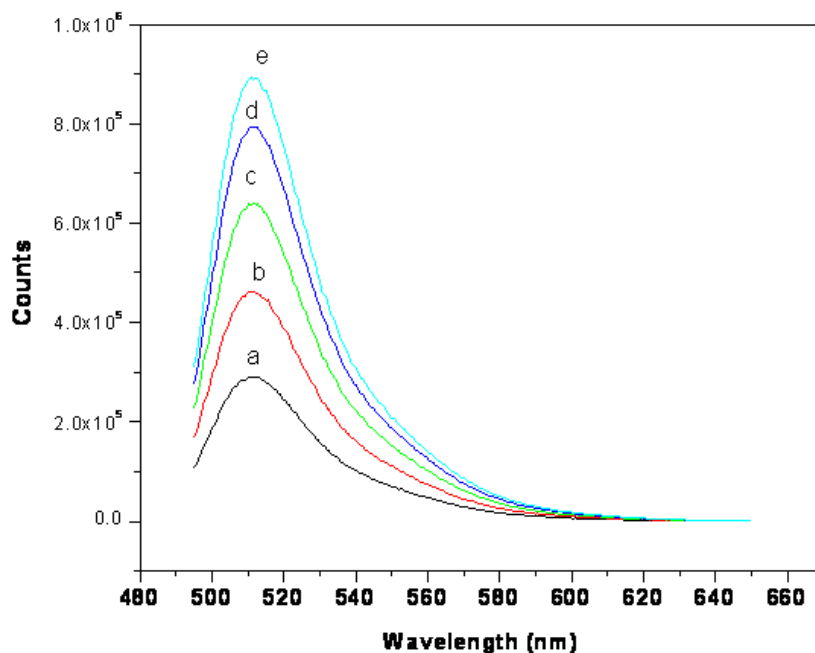


Figure 4. 4 Steady state fluorescence of mixture of fluorescein/PDMAEMA (0.2 mg/ml) at fluorescein concentrations of (a). 400; (b). 600; (c). 800; (d).1000 and (e) 1200 nM.

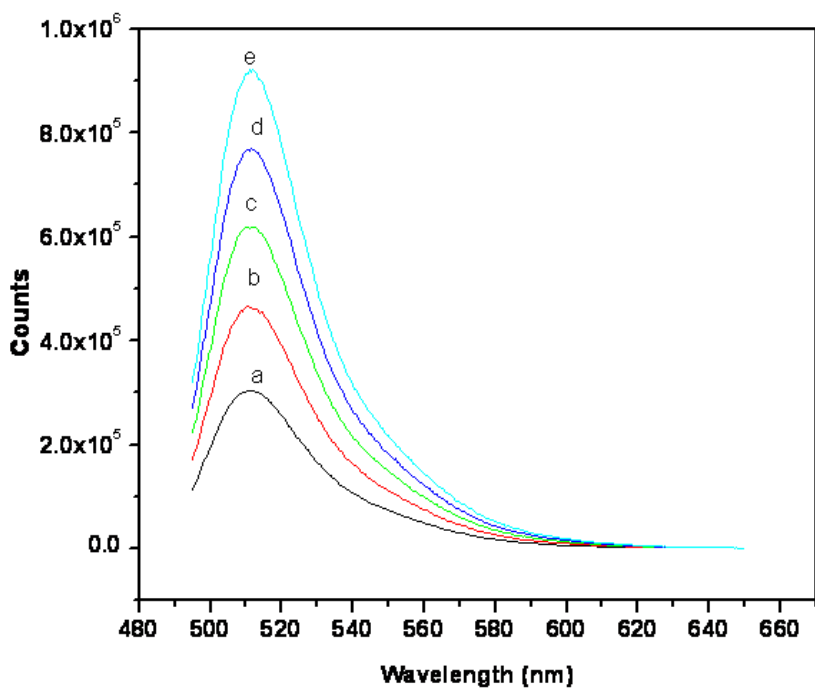


Figure 4. 5 Steady state fluorescence of mixture of fluorescein/PDMAEMA-C₆₀ (0.2 mg/ml) at fluorescein concentrations of (a). 400; (b). 600; (c). 800; (d).1000 and (e) 1200 nM.

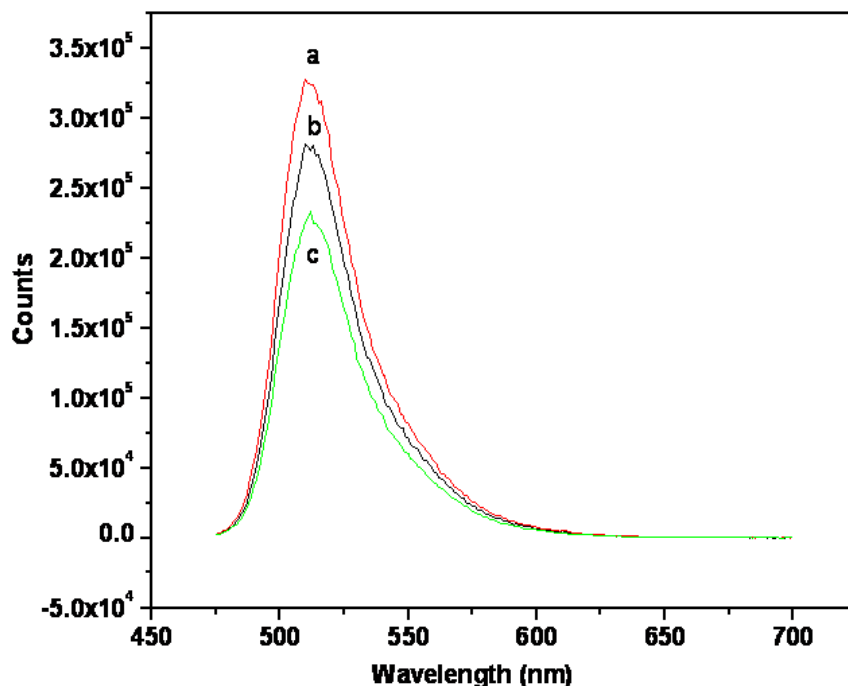


Figure 4. 6 Steady state fluorescence of (a). fluorescein; (b). fluorescein with PDMAEMA and (c). fluorescein with PDMAEMA-C₆₀.

Pyrene was also used as a model drug to investigate the interaction between hydrophobic drug and PDMAEMA-C₆₀ (Figure 4.7). The fluorescence quenching for PDMAEMA polymer is about 22%, and 48% for PDMAEMA-C₆₀. This indicated that pyrene not only located at the PDMAEMA shell but was also entrapped in the fullerene core. It should be noted that amines are excellent fluorescence quenchers [Lakowicz, 1999]. Encapsulated within the self-assembled micelles, fluorescein or pyrene molecules are tightly surrounded by amino groups PDMAEMA, therefore quenching is quite efficient. In addition, fullerene is a very good fluorescence quencher [Williams and Verhoeven, 1992; Texier et al. 2001], therefore the observation of further quenching of fluorescence of pyrene was attributed to the encapsulation of pyrene within the core of C₆₀.

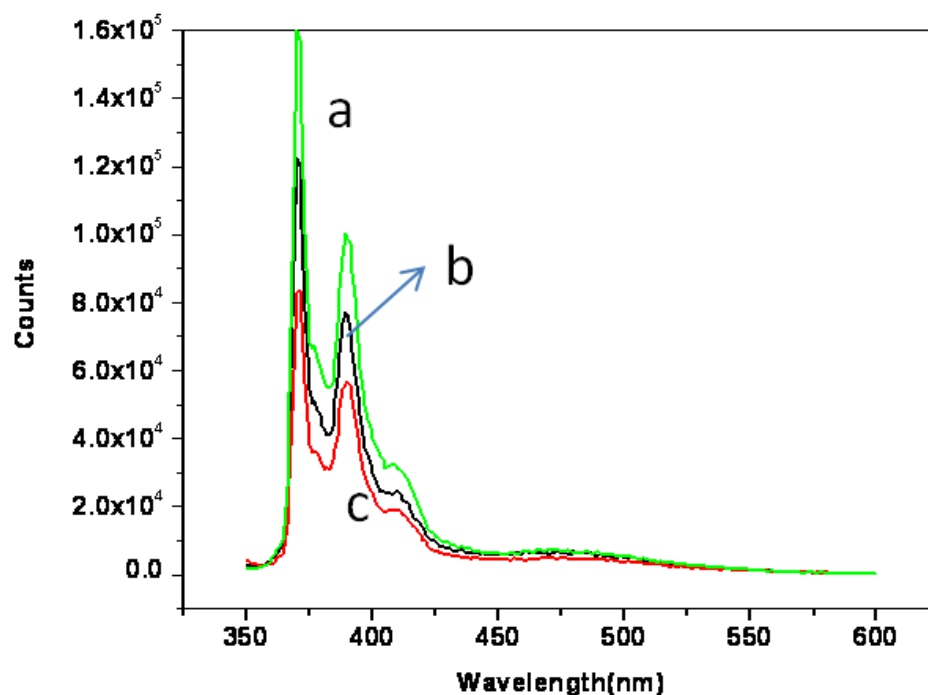


Figure 4. 7 Steady state fluorescence of (a). pyrene; (b). pyrene/PDMAEMA, and (c).pyrene/PDMAEMA-C₆₀.

In order to confirm that the encapsulation of pyrene molecules in the C₆₀ core can lead to significant fluorescence quenching, we used another fullerene containing polymer PAA-C₆₀, which formed micelles in aqueous solution. Figure 4.8 showed that about 87% quenching for PAA-C₆₀, whereas there is no quenching from PAA. This clearly indicated that C₆₀ can significantly quench the fluorescence of pyrene.

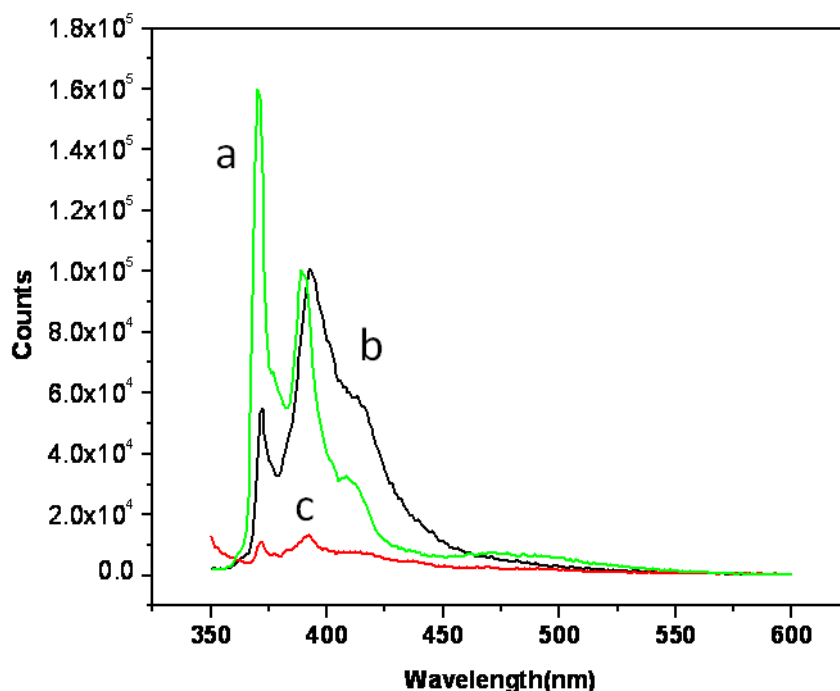


Figure 4. 8 Steady state fluorescence of (a). pyrene; (b). pyrene/PAA and (c). pyrene/PAA-C₆₀.

The effect of pH on the pyrene loading using PDMAEMA and PDMAEMA-C₆₀ was also investigated. At pH 3, the fluorescence quenching of pyrene with PDMAEMA-C₆₀ was stronger than at pH 10 (Figure 4.9). These results indicated that more pyrene was loaded into the fullerene core at pH 3 because the π - π interaction between pyrene and fullerene became dominant, whereas the interaction of pyrene and positively charged PDMAEMA are weak. In addition, stronger quenching was observed for higher concentrations of PDMAEMA-C₆₀ at both acid and base conditions. This is obvious because larger amounts of PDMAEMA-C₆₀ means higher drug loading capacity.

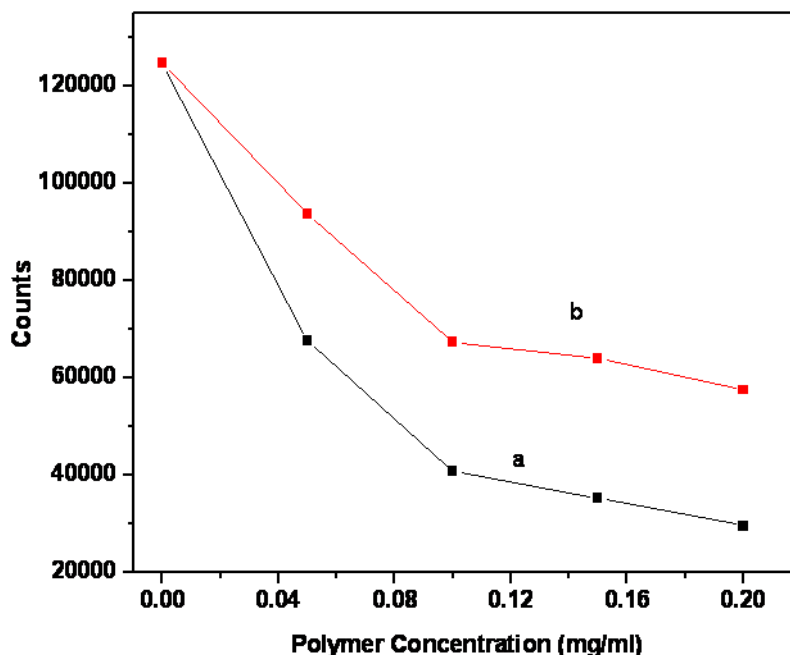


Figure 4. 9 Pyrene fluorescense quenching at (a). pH 3 and (b). pH 10 with different concentrations of PDMAEMA-C₆₀.

4.4 Changes of micellar size after drug loading

Figure 4.10 shows the decay time distribution and Figure 4.11 shows the decay rate (Γ) plotted against q^2 for the fluorescein loaded PDMAEMA-C₆₀ at pH of 7.2. It is evident that the decay rates Γ exhibited a linear dependence on q^2 , which suggested that the decay modes were caused by translational diffusion of self-assembled particles in solution. From the slope of Γ versus q^2 and utilizing the Stokes-Einstein equation, the apparent hydrodynamic radius was determined. It was found that R_h of the drug loaded PDMAEMA-C₆₀ was 49.3 nm, which is similar to the PDMAEMA-C₆₀ polymeric micelles. However, R_g for the drug loaded sample was 46.8 ± 1.0 nm, which is smaller than the R_g of 60 nm of the sample without drug loading. We attributed this to the encapsulation of hydrophobic fluorescein within the PDMAEMA shell and

C₆₀ cores, which makes the structure more dense and therefore resulting a higher R_g/R_h (Figure 4.12).

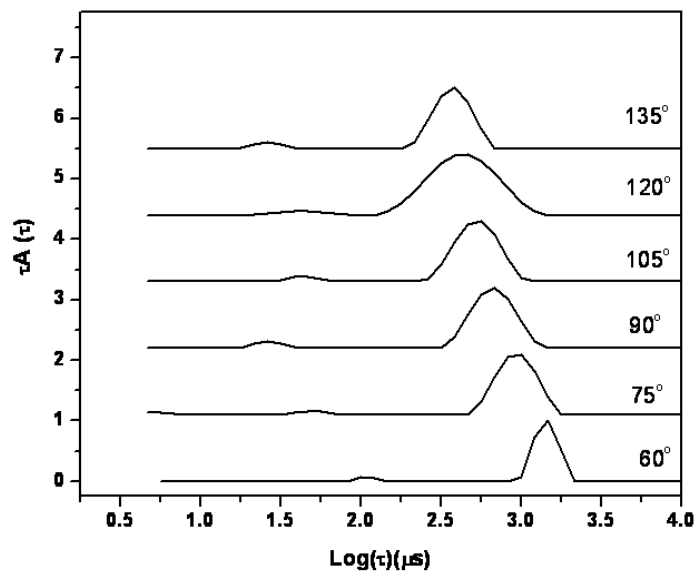


Figure 4. 10 Decay time distribution of drug loaded PDMAEMA-C₆₀ at pH 7.2.

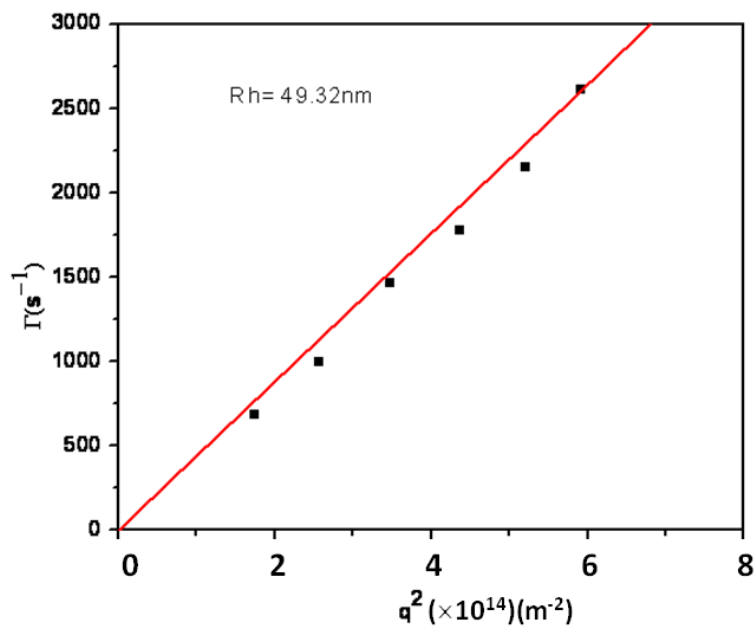


Figure 4. 11 Angular dependence of the decay rate of q^2 for drug loaded PDMAEMA-C₆₀ at pH 7.2

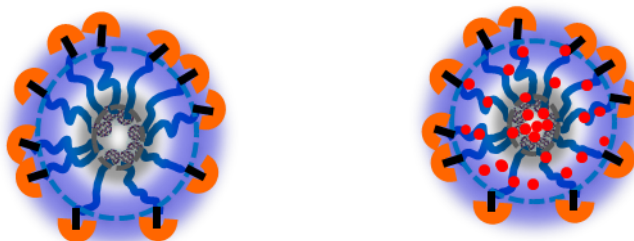


Figure 4. 12 Schematic structures of PDMAEMA-C₆₀ without and with drug loadings.

4.5 ITC study of PDMAEMA-C₆₀ with pyrene and fluorescein

The fundamental research regarding the interactions of drug molecules and PDMAEMA-b-C₆₀ systems in aqueous solution provides valuable information pertinent for drug delivery applications. It would be desirable to determine if the drug-micelle complexes are stable at different concentrations and pH conditions.

The stability of drug-micelle complexes was evaluated using the Isothermal Titration Calorimeter (ITC) [Wang et al. 2006]. The ITC can be used to study the binding interactions between the delivery systems and drug molecules. When these two species interact, heat is either generated or absorbed, and by measuring this heat, the enthalpy ΔH can be obtained.

In a typical ITC experiment, a solution of a model drug, for instance fluorescein was titrated into a solution of PDMAEMA-C₆₀. The heat released upon their interaction (ΔH) was monitored over time (Figures 4.13 a and b). Each peak represents a heat change associated with the injection of a small volume of sample into the ITC sample cell. As successive amounts of drug were titrated into the ITC cell, the quantity of heat absorbed or released represents the thermodynamics of binding interactions between drug and delivery system. The interaction between the fluorescein and PDMAEMA at pH 7 was driven by electrostatic attraction as shown

in Figure 4.13. At pH 7, the partially positively charged PDMAEMA chains and negatively charged fluorescein molecules are attracted to each other through an ion exchange process. Besides the electrostatic attraction, we were expecting to see π - π hydrophobic interaction of fluorescein and C₆₀ for the PDMAEMA-C₆₀ system. However, the binding heat of PDMAEMA-C₆₀ and fluorescein was smaller than fluorescein and PDMAEMA as evident from Figure 4.14. A binding curve was then obtained by integrating each injection against the ratio of fluorescein and the polymers (Figure 4.15). By comparing the differential enthalpy curves of fluorescein into PDMAEMA and PDMAEMA-C₆₀, we concluded that the interaction between fluorescein and PDMAEMA was stronger than PDMAEMA-C₆₀ because of the pre-formed micelles of PDMAEMA-C₆₀, which have two possible effects on drug loading. Firstly, the pre-formed micelles hindered the accessibility of fluorescein to PDMAEMA chains on the shell of micelles due to steric hindrance effect; secondly, the partitioning of fluorescein to the hydrophobic fullerene cores was hindered by PDMAEMA shells of micelles. Therefore, more fluorescein can bind onto PDMAEMA than PDMAEMA-C₆₀ chains, as reflected by the larger ΔH for PDMAEMA sample. Similar results were obtained for the pyrene and PDMAEMA-C₆₀. (Figure 4.15). This is consistent with the results from fluorescent measurements, where weaker quenching was observed when fluorescein was mixed with pre-formed PDMAEMA-C₆₀ micelles.

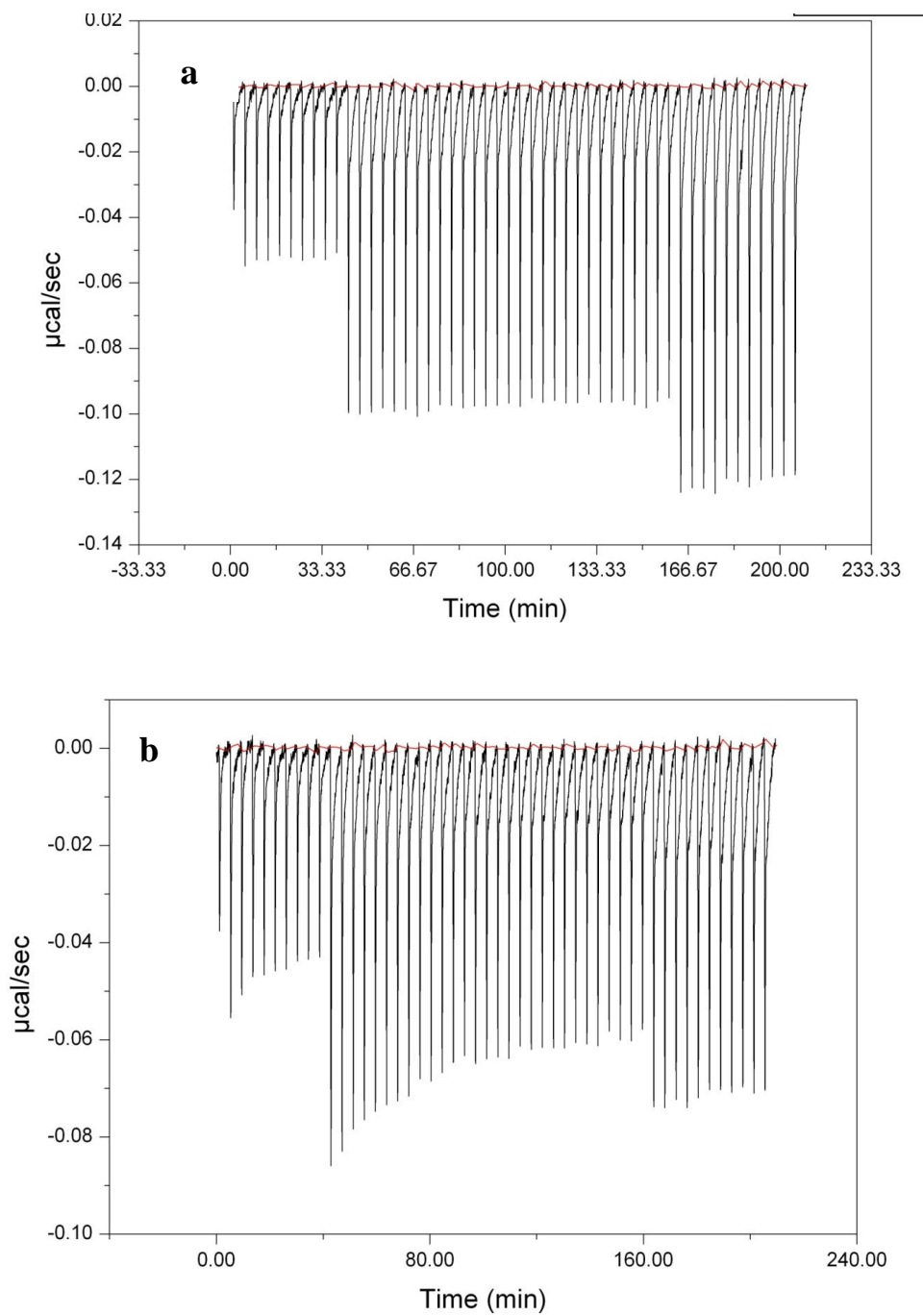


Figure 4.13 Raw ITC data for titrating fluorescein (0.06 mM) into (a). 0.04 wt% PDMAEMA; (b). 0.04 wt% PDMAEMA- C_{60}

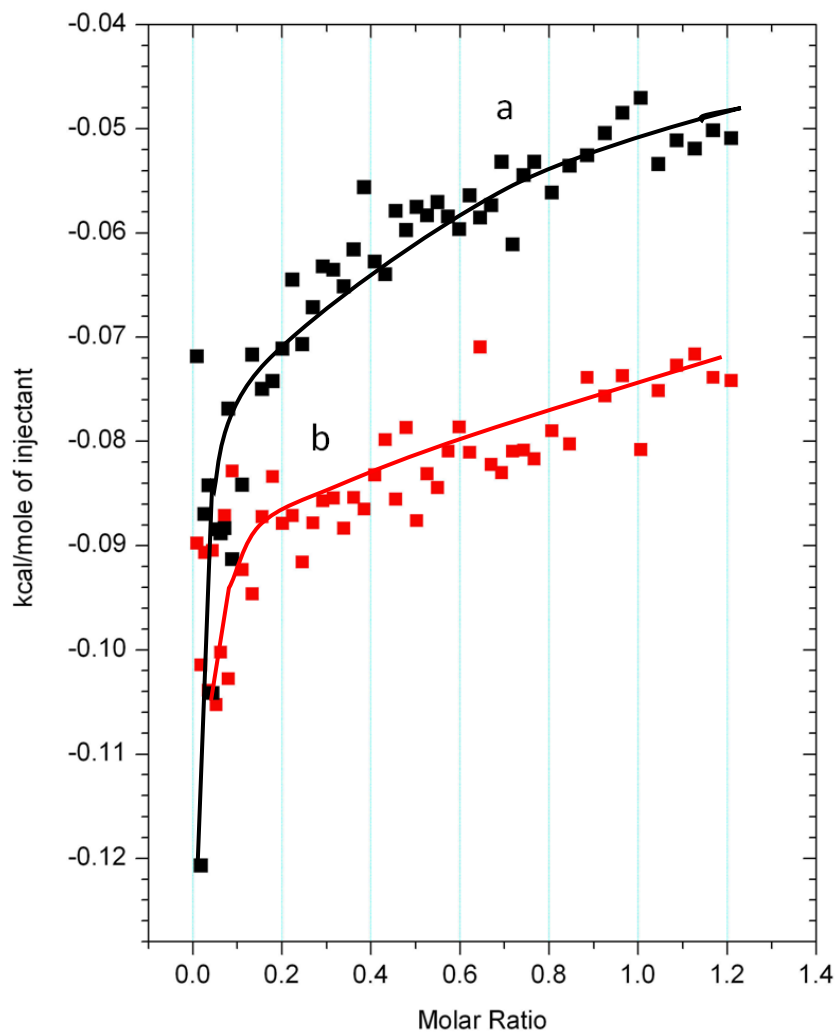


Figure 4. 14 Differential enthalpy curves for titrating fluorescein (0.06 mM) into 0.04 wt% (a). PDMAEMA-C₆₀ and (b). PDMAEMA

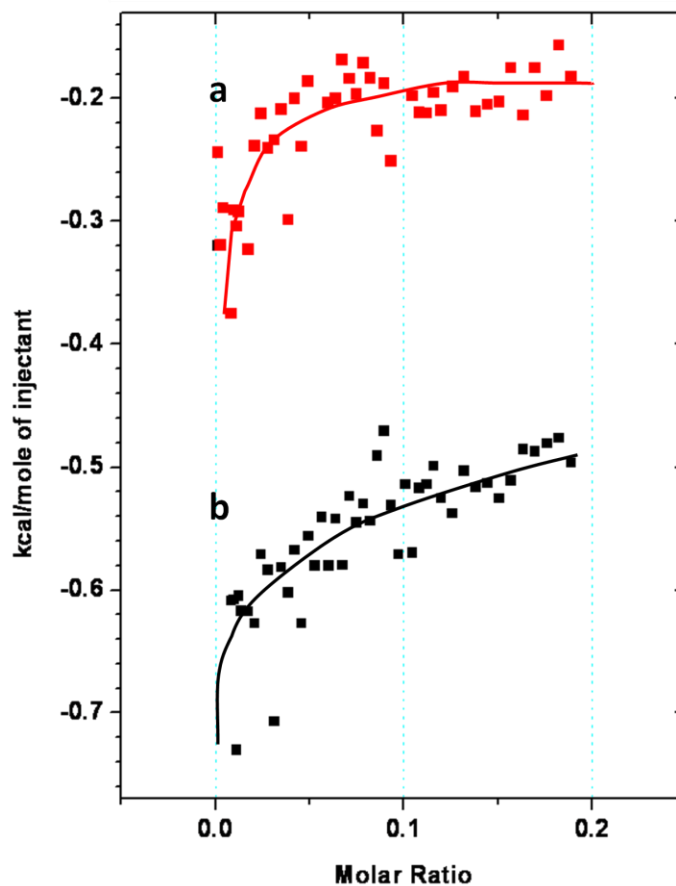


Figure 4. 15 Differential enthalpy curves for titrating pyrene (10 mM) into 0.04 wt% (a). PDMAEMA-C₆₀ and (b). PDMAEMA.

4.8 Conclusions

In this chapter, the drug loading capacity for PDMAEMA-C₆₀ system was investigated by fluorescence and ITC techniques. Two model drugs namely fluorescein and pyrene were employed to evaluate the location of drug in the self-assembled structure of PDMAEMA-C₆₀. The results showed the hydrophobic drugs were not only encapsulated in the PDMAEMA shell, but also within the hydrophobic fullerene core. The ITC results indicated that the binding energy for PDMAEMA-C₆₀ was lower than PDMAEMA for both model drugs.

Chapter 5 Temperature induced micellization and aggregation of biocompatible poly(oligo(ethylene glycol)methyl ether methacrylate) block copolymer analogues in aqueous solutions

5.1 Introduction

Recently, a great deal of interest has been focused on the synthesis of responsive block copolymers that form micelles in aqueous solution. These micelles are capable of undergoing a conformational change or phase transition upon the application of an external stimulus, such as pH, electrolyte concentration, or temperature. [Yusa et al. 2004, Virtanen et al. 2002, Arotcarena et al. 2002, Virtanen, et al. 2002, Sumerlin et al. 2003, Convertine et al. 2006, You et al. 2007, Lee et al. 2010, Topp et al. 1997, Zhang et al. 2005] Responsive block copolymers typically contain a hydrophilic block and a “smart” block whose nature can be transformed from hydrophilic to hydrophobic. Examples of such block copolymers are poly(*N,N*-dimethylacrylamide)-block-(*N*-isopropylacrylamide) (PDMA-*b*-PNIPAM), [Convertine et al. 2006] PNIPAM-block-poly(2-(dimethylamino) ethyl methacrylate) (PNIPAM-*b*-PDMAEMA) [You et al. 2007] and poly(ethylene oxide)-block-PNIPAM (PEO-*b*-PNIPAM). [Lee et al. 2010, Topp et al. 1997, Zhang et al. 2005] These block copolymers possessed thermal responsive properties in aqueous solutions. For instance, block copolymer of PEO-*b*-PNIPAM displayed temperature induced micellization above the LCST (32 °C) of PNIPAM. PNIPAM has been extensively studied as thermal responsive copolymers because its LCST is close to the body physiological temperature and is not affected by salt concentrations or ionic strengths. However, there are limited commercial applications using PNIPAM on human body because NIPAM monomer is suspected to be carcinogenic. [Harsh et al. 1991] Therefore, biocompatible thermal responsive polymers composed of oligo(ethylene glycol) methacrylate (POEGMA) [Han et al

2003, Mertoglu et al. 2005, Kitano et al. 2004, Lutz et al. 2006a, Lutz et al. 2007a] have attracted increasing attention, especially after the random copolymers of P(MEO₂MA-co-OEGMA₄₇₅) prepared via atom transfer radical polymerization (ATRP) was shown to exhibit a thermoresponsive behavior similar to PNIPAM. [Lutz et al. 2006a, Lutz et al. 2007a] It was found that the LCSTs of POEGMA based copolymers can be tuned to the body or “feverish” temperature by varying the feed ratio of the monomers. Also their LCSTs are not sensitive to salt concentration, ionic strength etc., and in-vitro cell tests of several POEGMA analogues showed excellent biocompatibility. [Lutz et al. 2008, Lutz et al. 2007 b]

Polymeric micelles have potential applications for drug delivery and other biological applications, [Kataoka et al. 2001] and amphiphilic diblock copolymers containing POEGMA analogues are of great research interest because they are biocompatible and possess tunable thermal properties. A variety of hydrophobic polymers, such as poly(benzyl methacrylate), [Bes et al. 2003] polystyrene, [Cheng et al. 2005] poly(glycidyl methacrylate), [Hu et al. 2010] poly(pentafluorostyrene) [Tan et al. 2010] and polyethylene [Wang et al. 2010] have been used to prepare amphiphilic copolymers with POEGMA analogues. By taking advantage of the hydrophilic and hydrophobic characteristics of POEGMA, a double hydrophilic block copolymer composed of poly(*N*-isopropyl methacrylamide) (PNIPMAM) and POEGMA [Jochum et al. 2010] was synthesized and they exhibited a multistage temperature-dependent self-assembly behavior. Also, a block copolymer of MEO₂MA and tri(ethylene glycol) methyl ether methacrylate (MEO₃MA) on the side chains of poly(2-(2-bromoisobutyryloxy)ethyl methacrylate (PBIEM) were synthesized by Matyjaszewski and co-workers [Yamamoto et al. 2007] and the polymer formed micelles consisting of collapsed PMEO₂MA core and soluble

PMEO₃MA corona. They also demonstrated that the size of the micelles progressively increased with heating.

Linear block copolymers composed of POEGMA segments with different LCSTs have not yet been explored. Similar to the random copolymer synthesized by Lutz and coworkers, this block copolymer can also be considered as homopolymer because the only difference is the length of the pendent ethylene glycol groups. It is expected that the thermal behavior of this copolymer will be similar to PNIPAM-b-POEGMA [Jochum et al. 2010] block copolymer, i.e. they will form micelles when the temperature exceeds the LCST of one block and precipitate from the solution above the LCST of both blocks. POEGMA block copolymers possess two significant advantages over other responsive block copolymers; firstly, they are biocompatible since they possess only POEGMA analogues, and secondly, the LCST of each block can be tuned by varying the ratio of different OEGMA monomers. Thus, the polymeric micelles formed by these copolymers may have potential applications as drug delivery carriers.

The scope of the research in this chapter is three fold. First, a random copolymer consisting of MEO₂MA and OEGMA₃₀₀ with a tunable LCST was synthesized by atom transfer radical polymerization (ATRP), and a second block will be extended from this random copolymer by polymerizing with MEO₂MA via ATRP. Secondly, the thermal phase transition was evaluated using UV-Vis and micro-DSC analyses, where a constant temperature ramp will be applied. Thirdly, the self-assembly behavior of this block copolymer over a range of temperature was investigated using light scattering techniques.

5.2 Experimental

5.2.1 Materials

2-(2-methoxyethoxy) ethyl methacrylate (188 g/mol), oligo(ethylene glycol) methyl ether methacrylate (300 g/mol) were purchased from Sigma-Aldrich and purified by passing through basic alumina column prior to use. 1,1,4,7,10,10-hexamethyl triethylene tetramine (HMTETA), copper(I) chloride, methyl 2-bromopropionate (MBP), ethanol and HPLC grade toluene were purchased from Sigma-Aldrich and used as received.

5.2.2 Synthesis of random copolymer of $\text{PMEO}_2\text{MA-}stat\text{-POEGMA}_{300}$

The polymerization of $\text{PMEO}_2\text{MA-}stat\text{-POEGMA}_{300}$ using methyl 2-bromopropionate as initiator and HMTETA/CuCl as catalyst was performed in ethanol via ATRP at room temperature. 2-(2-methoxyethoxy) ethyl methacrylate (3 g, 15.9 mmol), oligo(ethylene glycol) methyl ether methacrylate (300 g/mol) (2.05 g, 6.8 mmol), methyl 2-bromopropionate (6.43 mg, 0.38 mmol) and ethanol (4.0 mL) were added into a 25 mL flask and the mixture was bubbled with argon for 30 mins. Then the mixture was transferred using a double tipped needle into a flask charged with CuCl (38.1 mg, 0.38 mmol) and HMTETA (178.4 mg, 0.77 mmol) equipped with a magnetic stirring bar under argon atmosphere. After stirring at room temperature for 24 h, the reaction mixture was purified by dialysis for 48 hours in dialysis tubing with MW cutoff of 1000 Da. Finally, an oil-like product was isolated after freeze drying. The chemical structure and M_w of the polymers were characterized by ^1H NMR and GPC. A polymer with a molecular weight (M_n) of 11,000 g/mol was synthesized with a polydispersity index (PDI) of 1.3.

5.2.3 Preparation of block copolymer of (PMEO₂MA-*stat*-POEGMA₃₀₀)-*b*-PMEO₂MA

The solution of PMEO₂MA-*stat*-POEGMA₃₀₀ (2.5 g, 0.227 mmol) and 2-(2-methoxyethoxy)ethyl methacrylate (0.45 g, 1.51 mmol) in ethanol was charged into a flask filled with argon and oxygen dissolved in the solution was removed by purging with argon for 30 mins. Then the mixture was transferred to another argon filled flask charged with CuCl (23 mg, 0.227 mmol) and HMTETA (104 mg, 0.56 mmol) via a double tipped needle. The reaction mixture was stirred for 24 h at room temperature. After 24 h, the reaction mixture was purified by dialysis for 48 hours in dialysis tubing with MW cutoff of 1000 Da. Then, the oil-like product was isolated after freeze drying. The chemical structure and M_w of the polymers were characterized by ¹H NMR and GPC. A polymer with a molecular weight of 13,000 g/mol was synthesized with a PDI of 1.6.

5.2.4 Sample Preparation

Light scattering measurements: Solutions of (PMEO₂MA-*stat*-POEGMA₃₀₀)-*b*-PMEO₂MA block copolymer with concentration of 0.6 mg/mL were prepared by dissolving the oil-like sample in water and filtering it through a 0.45 μm membrane.

UV-Vis and micro-DSC: Solutions of PMEO₂MA-*stat*-POEGMA₃₀₀ and (PMEO₂MA-*stat*-POEGMA₃₀₀)-*b*-PMEO₂MA with concentration of 4 mg/mL were prepared by dissolving the sample in water.

TEM samples: A solution of (PMEO₂MA-*stat*-POEGMA₃₀₀)-*b*-PMEO₂MA with concentration of 0.6 mg/mL was stabilized at a desired temperature for 30 mins and one drop of the solution was added to a Formvar coated copper grid. Excess amount of solution was

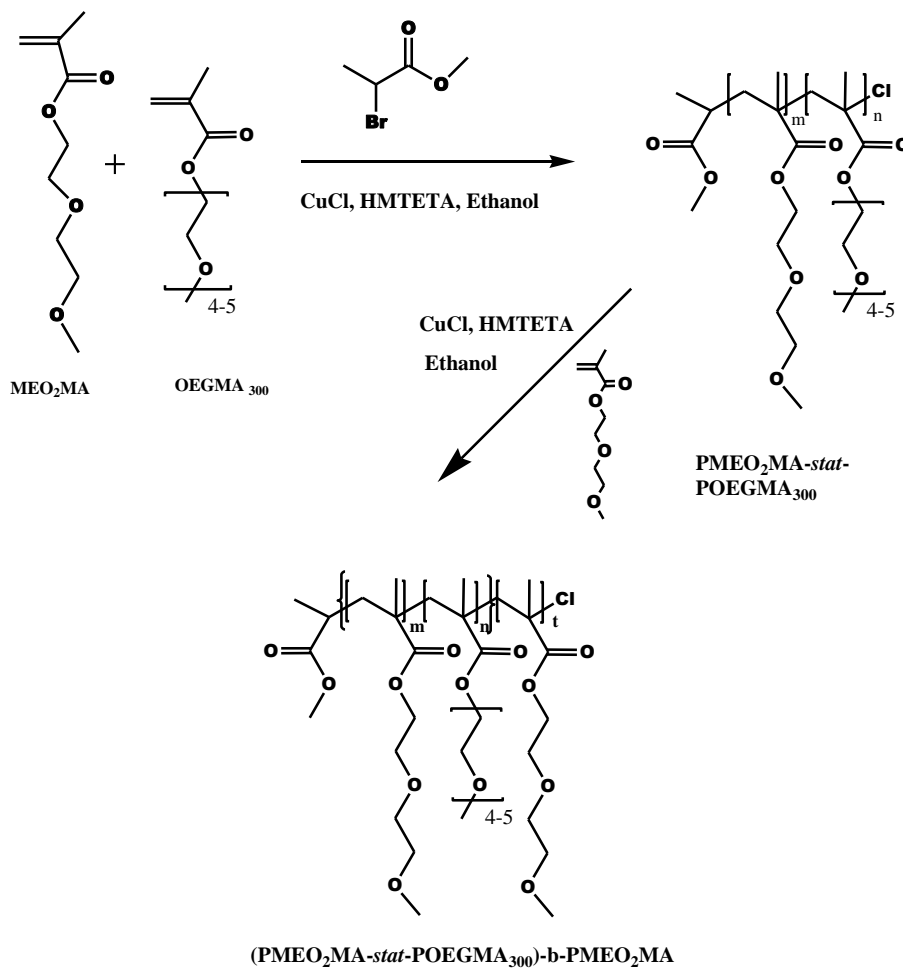
removed quickly by a filter paper to ensure that the particles will be deposited onto the grid with the morphology remaining intact.

5.2.5 Characterization

GPC and NMR are same as Chapter 3. The thermal responsive properties of the prepared copolymers were investigated using a differential scanning calorimeter (MicroCal VP-DSC) and a Varian (Carey 100 Bio) UV–Visible spectrophotometer, coupled to a temperature controller. For the DSC measurement, 4 mg/ml of polymer solution was degassed and introduced into a DSC sample cell and the reference cell was filled with deionized water. The sample was scanned from 10 to 80 °C at a heating rate of 1.5 °C min⁻¹. For the optical measurement, a 1 cm sample cell containing approximately 3 mL of polymer solution with concentration of 4 mg/mL was used against deionized water as the reference. The polymer solutions were heated from 20 to 70 °C at a heating rate 1 °C min⁻¹. All measurements were taken at a wavelength of 500 nm. Dynamic light scattering (DLS) and static light scattering (SLS) measurements were performed on a Brookhaven BI-200SM goniometer system. For DLS measurement, the inverse Laplace transform of REPES in the GENDIST software package was used to analyze the time correlation functions with a probability of reject set to 0.5. A 0.45 µm filter was used to remove dust prior to the light scattering experiments. The experimental temperature was controlled by a PolyScience water-bath. The refractive index increment used for SLS measurement was measured by a BI-DNDC differential refractometer. All measurements were performed after equilibrating the polymer samples at the required temperature to attain a stable scattering intensity. The morphologies of the aggregates were visualized by TEM (Philips CM10).

5.3 Results and Discussion

5.3.1 Synthesis of (PMEO₂MA-*stat*-POEGMA₃₀₀)-*b*-PMEO₂MA by ATRP



Scheme 5. 1 Synthetic Scheme of block copolymer of (PMEO₂MA-*stat*-POEGMA₃₀₀)-*b*-PMEO₂MA.

Chemically speaking, copolymers of POEGMA analogues can be considered as homopolymers because the chemical composition of monomers is similar. Random copolymers consisting of MEO₂MA and OEGMA₄₇₅ at various feeding ratios were synthesized via the ATRP based on the protocols proposed by Lutz and coworkers.[Lutz et al. 2006a and 2006b] They found that the LCST of the copolymer can be tuned to 26-90 °C by adjusting the feed ratio of the

two monomers. In fact, all OEGMA analogues can be used in this strategy. In the present study, a block copolymer containing only POEGMA analogues was synthesized via ATRP as shown in Scheme 5.1. First, random copolymer composed of MEO₂MA and OEGMA₃₀₀ was prepared via ATRP using HMTETA/CuCl as catalyst and ethanol as the solvent at a feeding composition of 7 to 3. Then, PMEO₂MA-*stat*-POEGMA₃₀₀ was used as the ATRP macroinitiator to synthesize the block copolymer (PMEO₂MA-*stat*-POEGMA₃₀₀)-*b*-PMEO₂MA using MEO₂MA monomer. ¹H NMR of (PMEO₂MA-*stat*-POEGMA₃₀₀)-*b*-PMEO₂MA copolymer is shown in Figure 5.1. The molecular weight of PMEO₂MA-*stat*-POEGMA₃₀₀ was about 11000 Da determined using GPC as shown in Figure 5.2a. The PDI is about 1.3. The GPC trace for the (PMEO₂MA-*stat*-POEGMA₃₀₀)-*b*-PMEO₂MA is shown in Figure 5.2b. The peak of (PMEO₂MA-*stat*-POEGMA₃₀₀)-*b*-PMEO₂MA shifted slightly to a higher molecular weight (M_n) of 13,000 Da. Both ¹H NMR and GPC confirmed that the block copolymer was successfully synthesized.

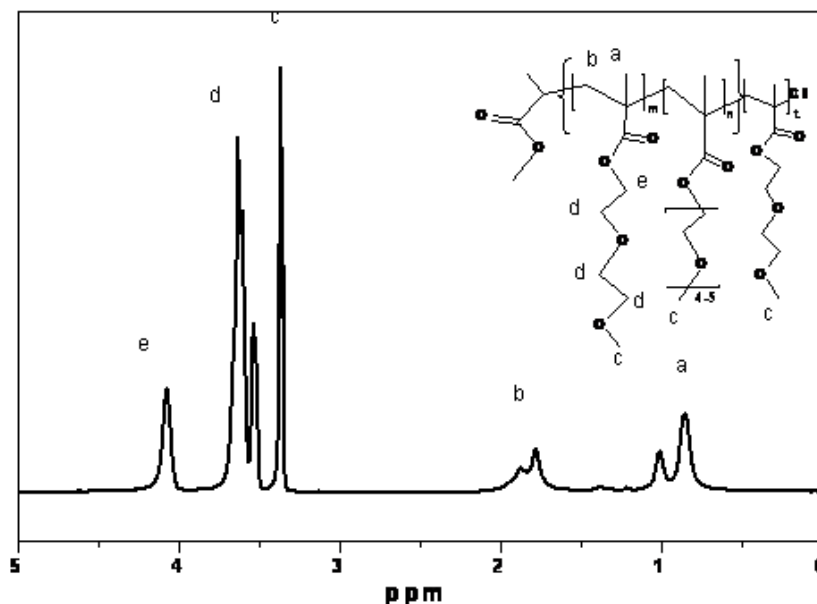


Figure 5. 1 ¹H NMR spectrum recorded in CDCl₃ for (PMEO₂MA-*stat*-POEGMA₃₀₀)-*b*-PMEO₂MA.

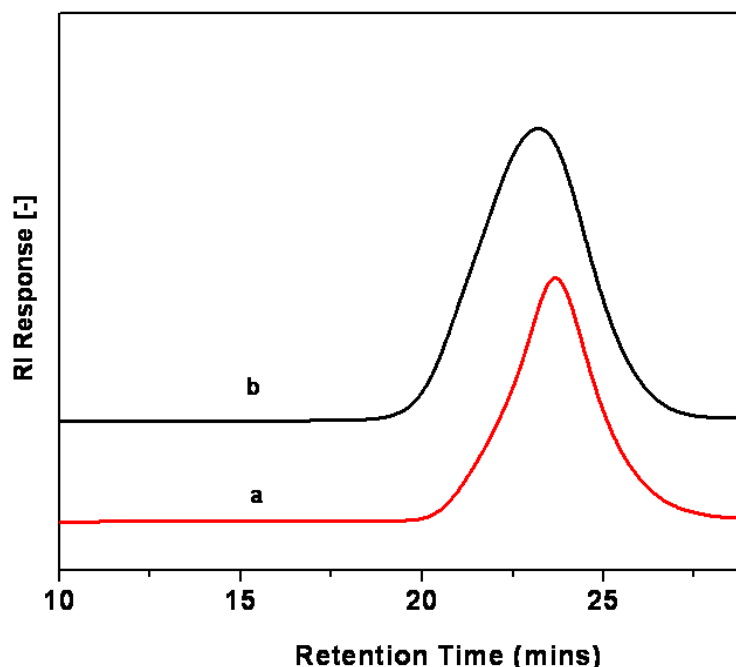


Figure 5. 2 GPC traces of (a) $\text{PMEO}_2\text{MA-}stat\text{-POEGMA}_{300}$; (b) $(\text{PMEO}_2\text{MA-}stat\text{-POEGMA}_{300})\text{-}b\text{-PMEO}_2\text{MA}$.

5.3.2 Thermal responsive properties of $(\text{PMEO}_2\text{MA-}stat\text{-POEGMA}_{300})\text{-}b\text{-PMEO}_2\text{MA}$ in aqueous solutions

Optical measurements are often used to monitor the phase transitions of thermal responsive polymers induced by temperature changes by measuring the changes in the transmittance. In this study, UV-Vis was used to investigate the transmittance variation over a range of temperature for the copolymer solutions. Figure 5.3 shows the optical transmittance of a 4 mg/mL aqueous solution of $\text{PMEO}_2\text{MA-}stat\text{-POEGMA}_{300}$ and $(\text{PMEO}_2\text{MA-}stat\text{-POEGMA}_{300})\text{-}b\text{-PMEO}_2\text{MA}$ recorded at the wavelength of 500 nm as a function of temperature at a heating rate of 1 °C/min. The solution of $\text{PMEO}_2\text{MA-}stat\text{-POEGMA}_{300}$ was clear at low temperature, which was followed by a sudden reduction in the transmittance at 45 °C (Figure 5.3a) that corresponded to the LCST of $\text{PMEO}_2\text{MA-}stat\text{-POEGMA}_{300}$ solution, and this temperature can be

adjusted by changing the feed ratio of two different monomers if necessary. In addition, the differential curve of Figure 5.3a as shown in Figure 5.4a, clearly showed a peak at 45 °C. Another commonly used technique to determine the phase transition for thermally sensitive polymers is micro differential scanning calorimetry (mDSC). In this study, mDSC measurement was performed on 4 mg/mL polymer solution at a scan rate of 1.5 °C/min over 15 to 80 °C. The result is shown in Figure 5.5. We can see that the thermal transition of $\text{PMEO}_2\text{MA-}stat\text{-POEGMA}_{300}$ occurred earlier at 40 °C compared to the optical measurement. This is because DSC can directly measure the heat changes due to the microphase separation of the polymer chains upon heating. It is known that hydrophilic OEG side chains of POEGMA copolymers form H-bonds with water below the LCST and the less polar backbones lead to a competitive hydrophobic effect. [Fechler et al. 2009] Above the LCST, POEGMA chains undergo a coil-to-globule transition, similar to that observed for PNIPAM. Therefore, DSC can capture the transition of the coil to globule transition of POEGMA chains, which occurs earlier than the cloud point (measured by UV-Vis), at which the globules of polymer chains tend to aggregate resulting in phase separation. However, the peak value from DSC curve is identical to the transmittance measurement, which is also 45 °C.

For the block copolymer, $(\text{PMEO}_2\text{MA-}stat\text{-POEGMA}_{300})\text{-}b\text{-PMEO}_2\text{MA}$, both the optical and DSC measurements displayed two transitions. The first transition occurs at the temperature of 30°C in both cases, which is associated with the LCST of PMEO_2MA block. This is as expected because copolymerization with $\text{PMEO}_2\text{MA-}stat\text{-POEGMA}_{300}$ (LCST is 45 °C) will lead to a higher LCST for the PMEO_2MA block, compared with the LCST of PMEO_2MA (26 °C). It is anticipated that $(\text{PMEO}_2\text{MA-}stat\text{-POEGMA}_{300})\text{-}b\text{-PMEO}_2\text{MA}$ form core shell micelles with $\text{PMEO}_2\text{MA-}stat\text{-POEGMA}_{300}$ as the corona and PMEO_2MA as core when the solution

temperature exceeded the LCST of the PMEO₂MA block. Above 30 °C, the hydrophobicity of the PMEO₂MA block became dominant due to the coil-to-globule transition, therefore the hydrophilic block copolymer (PMEO₂MA-*stat*-POEGMA₃₀₀)-*b*-PMEO₂MA became amphiphilic. As a result, polymeric micelles started to form at 30 °C, corresponding to a transition that is commonly referred to the critical micelle temperature (CMT). The second transition for (PMEO₂MA-*stat*-POEGMA₃₀₀)-*b*-PMEO₂MA shown in Figure 5.3b was broad when compared to that of PMEO₂MA-*stat*-POEGMA₃₀₀. Tam and coworkers [Ravi et al. 2005] also observed similar behavior for fullerene containing block copolymers. We believe this was caused by the formation of micelles. The formation of micelles is a gradual process, i.e. the size of the micelles increased at elevated temperature, therefore the transition shifted to a lower temperature range. In addition, the precipitation of the polymer chains was delayed by the micelles that were more stable, thus the transition was shifted to a higher temperature. DSC measurement shown in Figure 5.5b confirmed this trend as the first transition occurred at 30 °C and the second transition became broader. Figure 5.5b can be deconvoluted into two separated bands, which were shown in Figure 5.5c and 5d. The peaks of these two curves corresponded to the LCST of the two blocks of PMEO₂MA and PMEO₂MA-*stat*-POEGMA₃₀₀ in the block copolymer of (PMEO₂MA-*stat*-POEGMA₃₀₀)-*b*-PMEO₂MA, respectively.

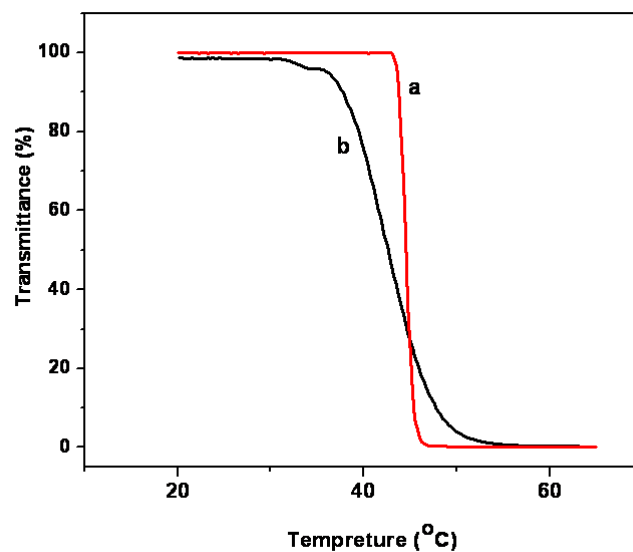


Figure 5. 3 UV–Vis experiment at 500 nm versus temperature to measure the phase transitions: (a). $\text{PMEO}_2\text{MA-}stat\text{-POEGMA}_{300}$; (b). $(\text{PMEO}_2\text{MA-}stat\text{-POEGMA}_{300})\text{-}b\text{-PMEO}_2\text{MA}$ in aqueous solution at 4 mg/mL.

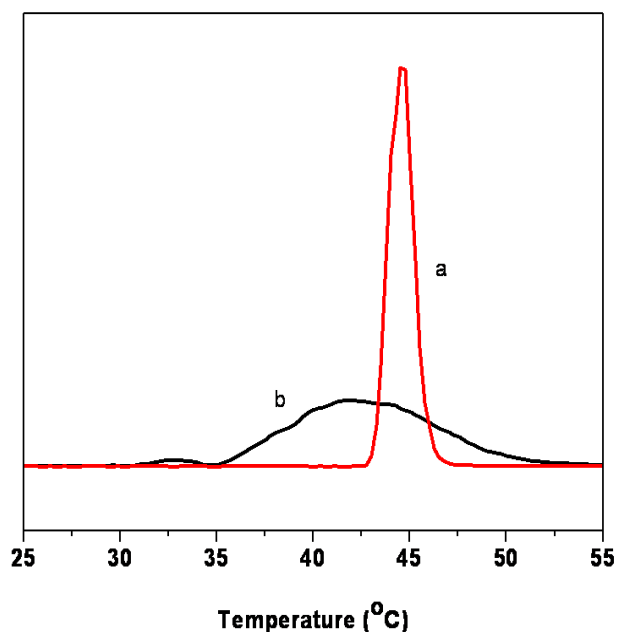


Figure 5. 4 Differential data of Figure 5.3. (a) $\text{PMEO}_2\text{MA-}stat\text{-POEGMA}_{300}$; (b) $(\text{PMEO}_2\text{MA-}stat\text{-POEGMA}_{300})\text{-}b\text{-PMEO}_2\text{MA}$ in aqueous solution at 4 mg/mL.

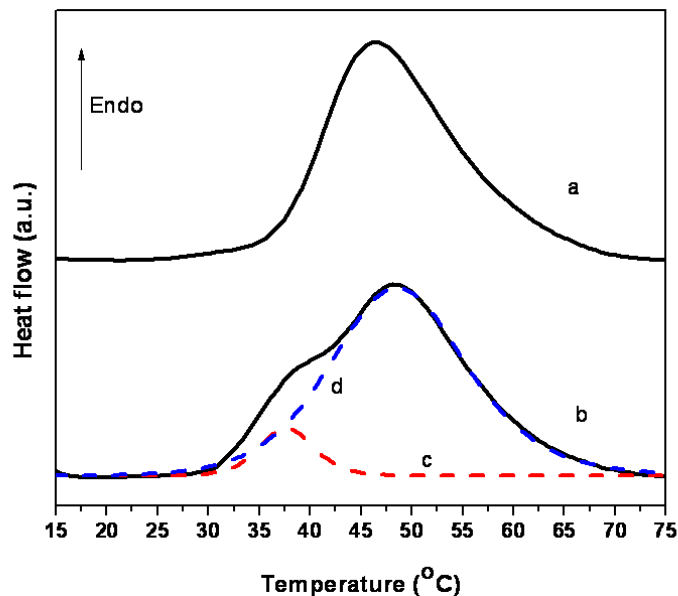


Figure 5. 5 DSC curves of (a) $\text{PMEO}_2\text{MA-}stat\text{-POEGMA}_{300}$; (b) $(\text{PMEO}_2\text{MA-}stat\text{-POEGMA}_{300})\text{-}b\text{-PMEO}_2\text{MA}$ in aqueous solution at 4 mg/mL.

5.3.3 Light scattering to investigate the self-assembly behavior of $(\text{PMEO}_2\text{MA-}stat\text{-POEGMA}_{300})\text{-}b\text{-PMEO}_2\text{MA}$

Temperature induced micellization can be followed by monitoring the changes in the hydrodynamic volume of $(\text{PMEO}_2\text{MA-}stat\text{-POEGMA}_{300})\text{-}b\text{-PMEO}_2\text{MA}$ using light scattering technique. Dynamic light scattering was applied to measure the hydrodynamic radius (R_h) using the same equations listed in Chapter 3. Figure 5.6 shows a linear dependence of the decay rate (Γ) with respect to q^2 for the measurement at 38 °C. The R_h of the micelles can be calculated from the slope and a value of 61.4 nm was obtained. The hydrodynamic radii of the micelles at different temperatures were determined, and the results are shown in Figure 5.7a. Also the decay time distributions at different temperatures are shown in Figure 5.8. At temperatures lower than the CMT, $(\text{PMEO}_2\text{MA-}stat\text{-POEGMA}_{300})\text{-}b\text{-PMEO}_2\text{MA}$ existed as unimers with R_h of about 2.5 nm and the copolymer started to form micelles with size of 24.6 nm when the temperature approached 32 °C. As the temperature was increased further from 32 to 45 °C, R_h changed from

24.6 to 95.0. In order to elucidate the kinetics of the morphological changes, the scattering light intensities at different temperatures were measured at a scattering angle of 90° for 25 minutes (Figure 5.9). Two observations can be derived from the results: 1) the size of the micelle increased with increasing temperature based on the enhanced intensity of the scattering light; 2) At a fixed temperature, the size of the micelles continued to increase and reached a stable size in about 20 minutes. It should be noted that all the DLS and SLS measurements were performed after the samples reached an equilibrium structure as indicated by a stable scattered light intensity after an equilibrating time of about 30 mins.

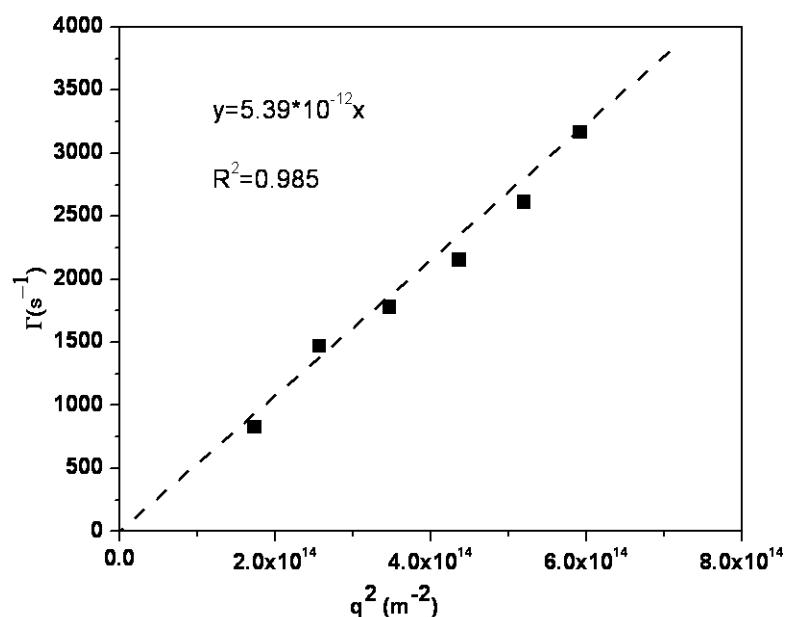


Figure 5. 6 Dependence of decay rate on q^2 for (PMEO₂MA-*stat*-POEGMA₃₀₀)-*b*-PMEO₂MA in aqueous solution at 38 °C.

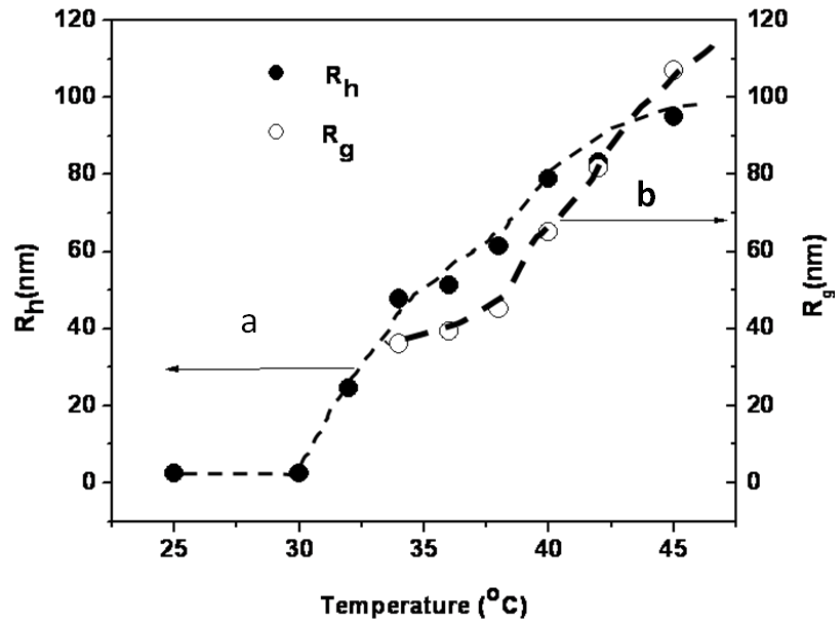


Figure 5. 7 Effect of temperature on the hydrodynamic radius (R_h) and radius of gyration (R_g) of the aggregates of 0.2 mg/ml (PMEO₂MA-*stat*-POEGMA₃₀₀)-*b*-PMEO₂MA aqueous solution.

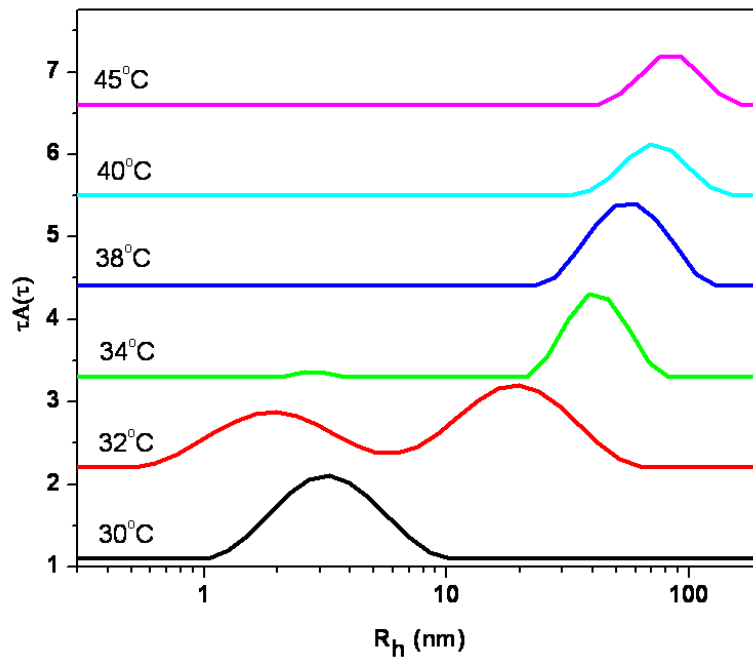


Figure 5. 8 Decay time distribution recorded at different temperatures of 0.2 mg/ml (PMEO₂MA-*stat*-POEGMA₃₀₀)-*b*-PMEO₂MA aqueous solution.

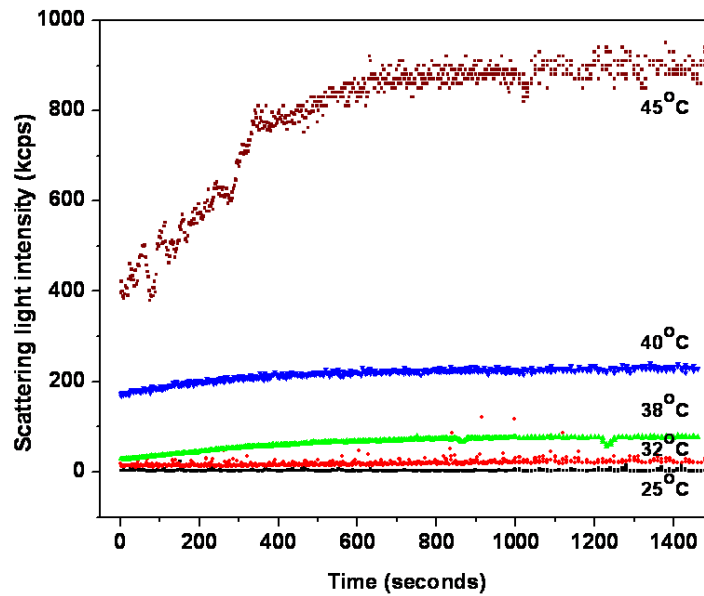


Figure 5. 9 Dependence of scattering light intensity on time at different temperatures measured at 90° for 0.2 mg/ml (PMEO₂MA-*stat*-POEGMA₃₀₀)-*b*-PMEO₂MA in aqueous solution.

The radius of gyration (R_g) was determined by performing static light scattering measurements. In the present study, a partial Berry plot shown in Equation 5.1 was used to calculate R_g , which was determined from the slope of $(\frac{1}{I_{ex(q)}})^{1/2}$ vs. q^2 , where $I_{ex(q)}$ is the excess scattering light intensity at different angles, c is the concentration of the solution and q^2 is the scattering vector. Berry plots for the measurements at 36 and 45 °C are shown in Figure 5.10, where the R_g was determined to be 39.2 and 107 nm respectively. The R_g values at other temperatures were obtained using the same method and the results are shown in Figure 5.7b. We noted that R_g increased with increasing temperature.

$$\left(\frac{1}{I_{ex(q)}}\right)^{1/2} = c \left[1 + \left(R_g^2 q^2 / 6\right)\right] \quad (5.1)$$

It is known that the value of (R_g/R_h) can provide information on the morphology of the aggregates. Theoretically, for a uniform solid sphere, a hyperbranched cluster, and a random coil, the ratios of (R_g/R_h) are about 0.774, 1.0, and 1.5, respectively.[Duan et al. 2001, Zhang et al. 2000] For a polymeric micelle, (R_g/R_h) is often less than 0.774 since the density of the core is higher than that of the shell. (R_g/R_h) ratios at different temperatures are shown in Table 1. Aggregates with R_h of 47.7 and 61.4 nm were formed at 34 and 38 °C respectively with a corresponding R_g/R_h ratio of 0.76 and 0.74, suggesting that the aggregates were core-shell micelles. As the temperature was increased to 40 and 45 °C, R_g/R_h increased correspondingly to 0.82 and 1.13, indicating that the morphologies of the micelles were transformed from a micellar structure to larger aggregates comprising of several micelles. Since the PMEO₂MA-*stat*-POEGMA₃₀₀ was not soluble when the temperature exceeded the LCST (around 40 °C), the core-shell micelles began to associate into larger aggregates.

Table 5. 1 Effect of temperature on the ratio of R_g/R_h and the aggregation number (N_{agg})

| Temperature (°C) | R_h (nm) | R_g (nm) | R_g/R_h | N_{agg} |
|------------------|------------|------------|-----------|-----------|
| 25 | 2.5 | - | - | 1 |
| 30 | 2.5 | - | - | 1 |
| 34 | 47.7 | 36.1 | 0.76 | 76 |
| 38 | 61.4 | 45.2 | 0.74 | 551 |
| 40 | 78.8 | 65 | 0.82 | 1201 |
| 45 | 95.0 | 107 | 1.13 | 9797 |

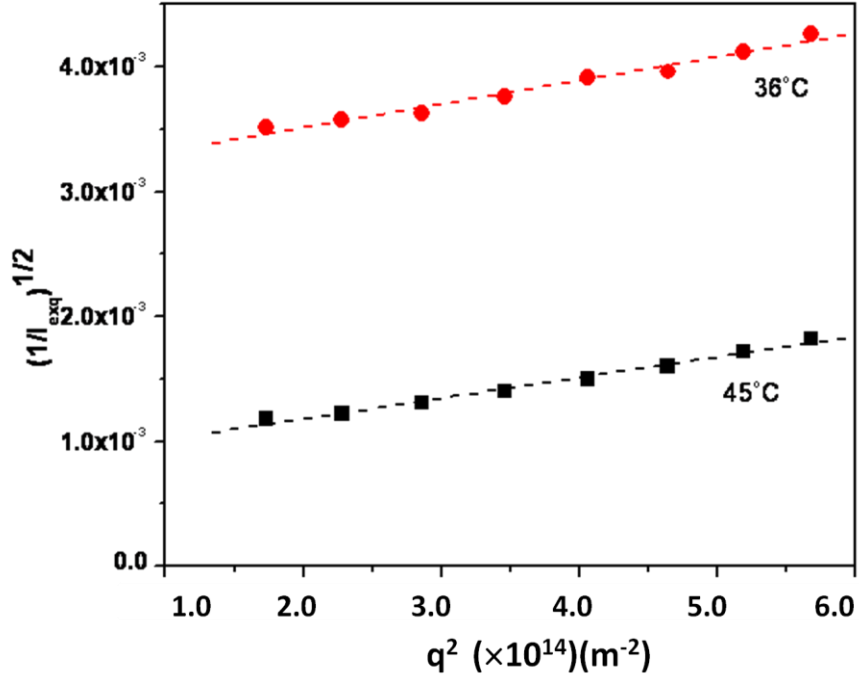


Figure 5. 10 Berry plot of (PMEO₂MA-*stat*-POEGMA₃₀₀)-*b*-PMEO₂MA in aqueous solution with concentration of 0.2 mg/ml at 36 and 45°C.

Furthermore, the change in the aggregation number, N_{agg} , of the aggregates formed from (PMEO₂MA-*stat*-POEGMA₃₀₀)-*b*-PMEO₂MA in water at different temperatures was determined from Equation 5.2.

$$N_{agg} = \frac{Mw_{micelle}}{Mw_{unimer}} \quad (5.2)$$

In this study, the M_w of micelle was obtained from the SLS measurements based on the Debye equation:

$$\frac{KC}{R(q)} = \frac{1}{M_w} \left(1 + \frac{1}{3} R_g^2 q^2 \right) + 2A_2 C \quad (5.3)$$

where K is an optical parameter $K = [4\pi^2 n_{tol}^2 (dn/dc)^2] / N_A \lambda^4$, n_{tol} is the refractive index of toluene (1.494), dn/dc is the refractive index increment of the polymer measured using

BI-DNDC and the value for the solution of (PMEO₂MA-*stat*-POEGMA₃₀₀)-*b*-PMEO₂MA is 0.152 mL/mg, N_A is Avogadro's constant, and λ is the wavelength, in this study, the wavelength is 636 nm, C is the concentration of the polymer solution, $R(q)$ is the Rayleigh ratio, q is the scattering vector, and A_2 is the second virial coefficient. The Rayleigh ratio $R(q)$, is expressed by Equation 5.4:

$$R(q) = R_{tol,90} \left(\frac{n}{n_{tol}} \right)^2 \frac{I - I_0}{I_{tol}} \sin \theta \quad (5.4)$$

where $R_{tol,90}$ is the Rayleigh ratio of toluene at scattering angle 90° with a value of $1.4 \times 10^{-5} \text{ cm}^{-1}$ at 636 nm. n is the refractive index of the solvent, I , I_0 , and I_{tol} are the scattered intensities of the solution, solvent, and toluene, respectively, and θ is the scattering angle. In our case, the concentration of the polymer solution is sufficiently low ($6 \times 10^{-4} \text{ g/mL}$), and the $2A_2C$ term in Eq. 5.3 is negligible. Therefore, the intercept of the plot of $KC/R(q)$ against q^2 yields the inverse of the apparent weight-average molar mass ($Mw_{micelle}$); consequently, the aggregation number of the micelle can be evaluated by dividing the Mw of the aggregate by the molar mass of the single polymer chain. In the present study, $KC/R(q)$ exhibited a linear relationship with q^2 at different temperatures as depicted in Figure 5.11. From the data presented in Table 5.1, we observed that the N_{agg} of the polymer aggregates increased with increasing temperature, which suggested that the aggregates reorganized due to changes in the conformation of the polymer chains.

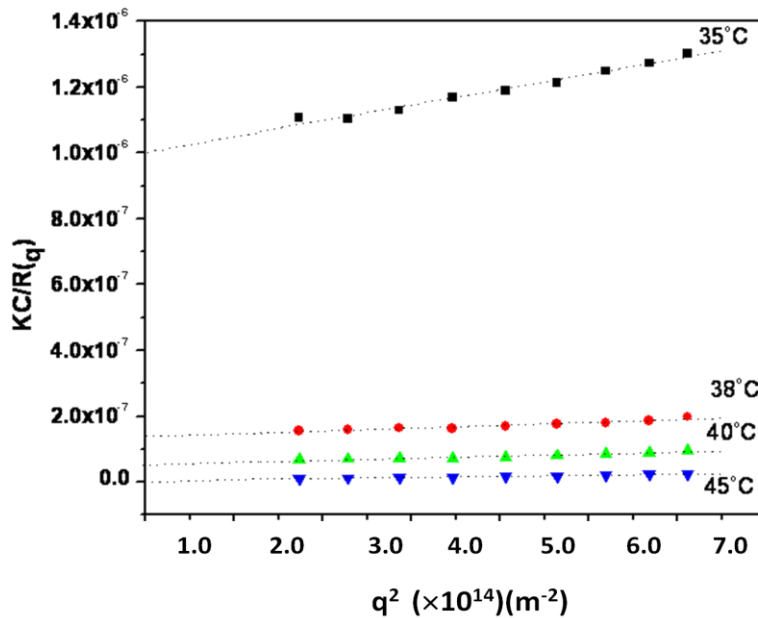


Figure 5. 11 KC/R(q) vs. the scattering vector (q^2) for 0.6 mg/ml (PMEO₂MA-*stat*-POEGMA₃₀₀)-*b*-PMEO₂MA aqueous solution at different temperatures.

5.3.4 TEM visualization of the micelles formed by (PMEO₂MA-*stat*-POEGMA₃₀₀)-*b*-PMEO₂MA

TEM images of the micelles are shown in Figure 5.12, which clearly showed that (PMEO₂MA-*stat*-POEGMA₃₀₀)-*b*-PMEO₂MA formed spherical particles in aqueous solution when the temperature exceeded the CMT. In addition, the sizes of the particles increased from

ca. 120 to ca. 220 nm when the temperature was raised from 38 to 45°C.

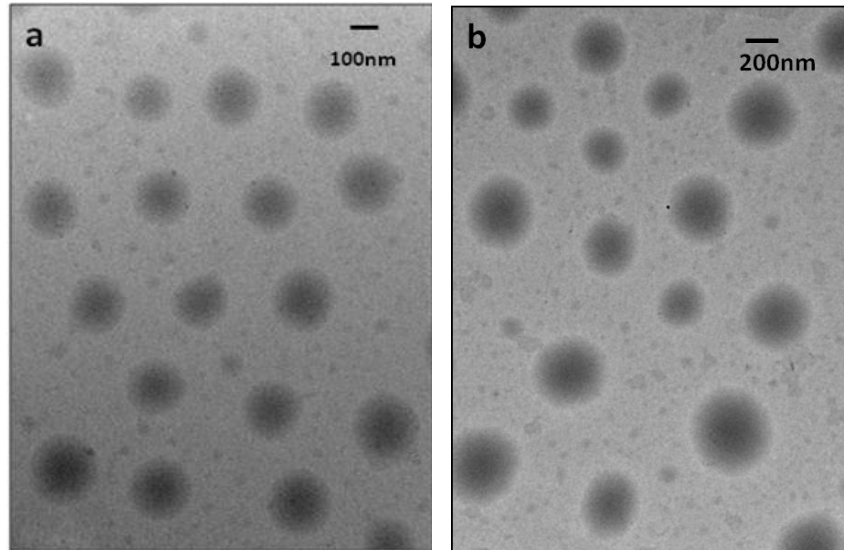


Figure 5. 12 TEM images of micelles formed by (PMEO₂MA-*stat*-POEGMA₃₀₀)-*b*-PMEO₂MA at different temperatures: (a). 38°C and (b). 45°C.

5.3.5 Proposed mechanism for the self-assembly of (PMEO₂MA-*stat*-POEGMA₃₀₀)-*b*-PMEO₂MA in aqueous solution at different temperatures

The increase in R_h , R_g , N_{agg} and R_g/R_h for (PMEO₂MA-*stat*-POEGMA₃₀₀)-*b*-PMEO₂MA in aqueous solution with increasing temperature reflects that the micelles formed above the CMT contained more polymer chains at higher temperatures. It is believed that the accumulation of the more polymer chains was driven by the increase in the hydrophobic interactions of the PMEO₂MA-*stat*-POEGMA₃₀₀ chains because these polymeric chains dehydrate at elevated temperatures. The (PMEO₂MA-*stat*-POEGMA₃₀₀)-*b*-PMEO₂MA behaves differently when compared to the temperature induced micellization of PNIPAM containing block copolymers, such as poly(sodium 2-(acrylamido)-2-methylpropanesulfonate and *N*-isopropylacrylamide) (PNaAMPS-*b*-PNIPAM), [Yusa et al. 2004] and poly (*N,N*-dimethylacrylamide-NIPAM) (PDMA-*b*-PNIPAM) [Convertine et al. 2006] In these systems, the size of the micelles

decreases when the temperature exceeds the CMT, and the loosely packed PNIPAM cores continued to shrink with increasing temperature until larger aggregates are formed at high temperature. Two possible reasons may account for the differences in the PNIPAM block copolymer and the present system. Firstly, the corona of the micelles poly(ethylene glycol) in the PNIPAM systems was not temperature sensitive, and it provides steric stabilization to the micelles, thereby retaining the morphology of the micellar structure. Secondly, the change in the hydrodynamic volume of POEGMA chains during the thermal-transition process is not as high as PNIPAM, [Hu et al. 2010] thus the hydrophobic cores formed by PMEO₂MA above the CMT does not contract as much as the PNIPAM chains.

Based on the above observations, the following physical mechanism (Figure 5.13) was proposed to describe the self-assembly of (PMEO₂MA-*stat*-POEGMA₃₀₀)-*b*-PMEO₂MA at different temperatures. Generally, three sequential steps are involved: (1) only unimers exist in the solution at temperature below the CMT; (2) core-shell micelles starts to form when the temperature is raised above the CMT; (3) larger core shell micelles are produced from the association of smaller micelles with further increase in temperatures.

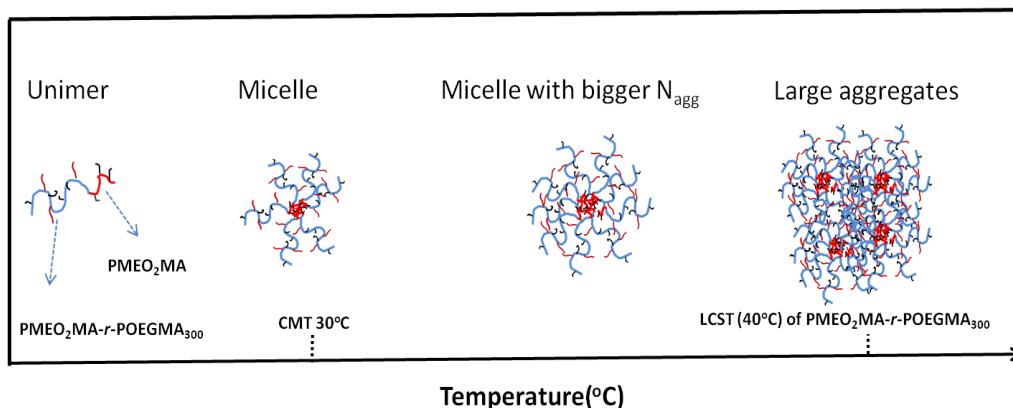


Figure 5. 13 Schematic diagram to describe the self-assembly behaviors of (PMEO₂MA-*stat*-POEGMA₃₀₀)-*b*-PMEO₂MA at different temperatures.

5.4 Conclusions

A well-defined diblock copolymer of (PMEO₂MA-*stat*-POEGMA₃₀₀)-*b*-PMEO₂MA was successfully synthesized via the atom transfer radical polymerization (ATRP). The chemical compositions and the self-assembly behavior of this copolymer in aqueous solutions was studied by NMR, GPC, DLS, SLS, UV-vis, DSC and TEM. The optical transmittance and DSC data showed that the CMT of (PMEO₂MA-*stat*-POEGMA₃₀₀)-*b*-PMEO₂MA in aqueous solution was about 30 °C. Within the temperature range from 34 to 38 °C, core-shell micelles with the size range from 40 to 60 nm were formed. Further increase in the temperature results in the formation of larger aggregates with a size of 95 nm at 45 °C. In addition, the aggregation number of the aggregates increased significantly from 76 to ~9800, and R_g/R_h ratio also increased from 0.75 to 1.13 within the temperature range of 34 to 45 °C. This indicated that the morphology of the aggregates changed from core-shell micelles to larger aggregates comprising of several collapsed preformed micelles. A mechanism was proposed to describe the self-assembly behaviors of (PMEO₂MA-*stat*-POEGMA₃₀₀)-*b*-PMEO₂MA at different temperatures. The block copolymer forms core-shell micelles with the temperature range from CMT (30°C) to the LCST of the PME₂O₂MA-*co*-POEGMA₃₀₀ (40°C) and eventually large aggregates are formed. The present study demonstrates the self-assembly of block copolymers composed of different POEGMA analogues, which is of great importance to the potential biological applications because POEGMA copolymers are biocompatible and thermal responsive.

Chapter 6 Self-assembly of thermo-responsive poly(oligo(ethylene glycol) methyl ether methacrylate)-C₆₀ in water-methanol mixtures

6. 1. Introduction

From Chapter 2, we know that various kinds of fullerene polymeric structures have been synthesized. However, most of these fullerene containing polymers are not biocompatible and they may not be suitable for biological applications due to their cytotoxicity. Therefore, after we investigated the block-copolymer of POEGMA analogues, we were eager to explore the self-assembly behaviors of POEGMA-C₆₀, which might offer more appealing properties owing to the thermal-responsive properties of POEGMA.

Since recent studies [Lutz et al. 2006a, 2006b, 2007, 2009, 2011] suggest that copolymers of OEGMA analogues prepared via atom transfer radical polymerization (ATRP) exhibited a thermal responsive behavior and the LCST of the copolymers can be tuned by varying the feed ratio of monomers. It is anticipated that amphiphilic copolymers, such as POEGMA-C₆₀ will possess interesting solution behaviors due to the thermal responsive POEGMA segments and unique properties of C₆₀. It was shown previously that the LCSTs of poly(vinyl methyl ether) in water/methanol mixtures shifted to higher temperatures as the volume fraction of methanol was increased [Schild et al. 1991], but the LCST of poly(oligoethylene oxide phosphazene) was not affected by the addition of either methanol or ethanol [Lee et al. 2000]. On the other hand, the LCST of poly(*N*-isopropylacrylamide) first decreased and then increased with the addition of methanol [Schild et al. 1991], where the LCST shifted from 32 to -7.5 °C as the volume fraction of methanol approached 0.35. A sharp increase occurred when the methanol composition increased from 0.35 to 0.45, at which point the LCST disappeared. A number of studies have

been devoted to elucidating the behavior of PNIPAM in water/methanol mixture [Tanaka et al. 2008 and 2009, Pang et al. 2010, Sun et al. 2010], however, a conclusive and definitive explanation for the unusual transition of PNIPAM in methanol/water is yet to be established. Since POEGMA possesses similar thermal responsive properties as PNIPAM, the effects of binary solvent mixtures on the LCST of POEGMA will be of significant importance for its potential applications. A recent study [Roth et al. 2011] showed that POEGMA exhibited an upper critical solution temperature (UCST) behavior in aliphatic alcohols and the UCSTs were affected by co-solvent, molecular weight, and end groups. In the present study, the LCST of POEGMA and POEGMA-C₆₀ in water/methanol solvent will be explored, and the self-assembly of POEGMA-C₆₀ in water/methanol solution at different temperatures will be elucidated. This work was published by Yao et al. [Yao et al. 2011b]

6.2 Experimental

6.2.1 Materials

The sources of C₆₀ (>99.5%) HMTETA, copper(I) chloride, methyl 2-bromopropionate (MBP), anhydrous 1,2-dichlorobenzene were the same as Chapter 3. Methanol and ethanol were purchased from Sigma-Aldrich and used as received.

6.2.2 Synthesis of PMEO₂MA-*stat*-POEGMA₃₀₀

The ATRP polymerization of PMEO₂MA-*stat*-POEGMA₃₀₀ using methyl 2-bromopropionate as initiator and HMTETA/CuCl as catalyst was performed at room temperature in ethanol. 2-(2-methoxyethoxy) ethyl methacrylate (3 g, 15.9 mmol), oligo(ethylene glycol) methyl ether methacrylate (300 g/mol) (2.05 g, 6.8 mmol), methyl 2-bromopropionate (6.43 mg, 0.38 mmol) and ethanol (4.0 mL) were added into a 25 mL flask and the mixture was bubbled

with argon for 30 mins. Then the mixture was transferred using a double tipped needle into a flask charged with CuCl (38.1 mg, 0.38 mmol) and HMTETA (178.4 mg, 0.77 mmol) equipped with a magnetic stirring bar under argon atmosphere. After stirring at room temperature for 24 h, the reaction mixture was purified by dialysis for 48 hours in a dialysis tubing with MW cutoff of 1000 Da. Finally, the oily-like product was isolated after freeze drying. The chemical structure and M_w of the polymers were characterized by ^1H NMR and GPC. A polymer with a molecular weight of 11,000 g/mol was synthesized with a polydispersity index (PDI) of 1.3.

6.2.3 Preparation of amphiphilic copolymer of (PMEO₂MA-*stat*-POEGMA₃₀₀)-C₆₀

PMEO₂MA-*stat*-POEGMA₃₀₀ (2.5 g, 0.227 mmol), C₆₀ (0.33 g, 0.454 mmol) and dichlorobenzene (10 mL) were charged into a flask filled with argon and the solution was bubbled with argon for 30 mins. Then the mixture was transferred to another argon filled flask charged with CuCl (23 mg, 0.227 mmol) and HMTETA (104 mg, 0.56 mmol) via a double tipped needle. The reaction mixture was stirred for 24 h at 90 °C. After 24 h, the reaction mixture was diluted with THF and passed through a basic alumina column twice to remove excess C₆₀. The filtrate was concentrated and dissolved in water, followed by dialysis in water for 2 days. Finally, a sticky brown product was isolated after freeze drying. The chemical structure of the polymers was characterized by ^1H NMR, ^{13}C NMR and UV-vis.

6.2.4 Sample Preparation

Light scattering measurement: Solutions of (PMEO₂MA-*stat*-POEGMA₃₀₀)-C₆₀ with concentration 0.2 mg/mL were prepared by dissolving the brown sample in water and filtered through a 0.45 μm membrane.

UV-Vis spectroscopy: Solutions of $\text{PMEO}_2\text{MA-}stat\text{-POEGMA}_{300}$ and $(\text{PMEO}_2\text{MA-}stat\text{-POEGMA}_{300})\text{-C}_{60}$ of concentration 4 mg/mL were prepared by dissolving the sample in water.

TEM analyses: A solution of $(\text{PMEO}_2\text{MA-}stat\text{-POEGMA}_{300})\text{-C}_{60}$ with concentration of 2 mg/mL in water/methanol solution was stabilized at the desired temperature for 30 mins and one drop of the solution was added to a Formvar coated copper grid. Excess amount of solution on the grid was quickly removed by a filter paper and then the grid dried at room temperature overnight.

6.2.5 Characterization

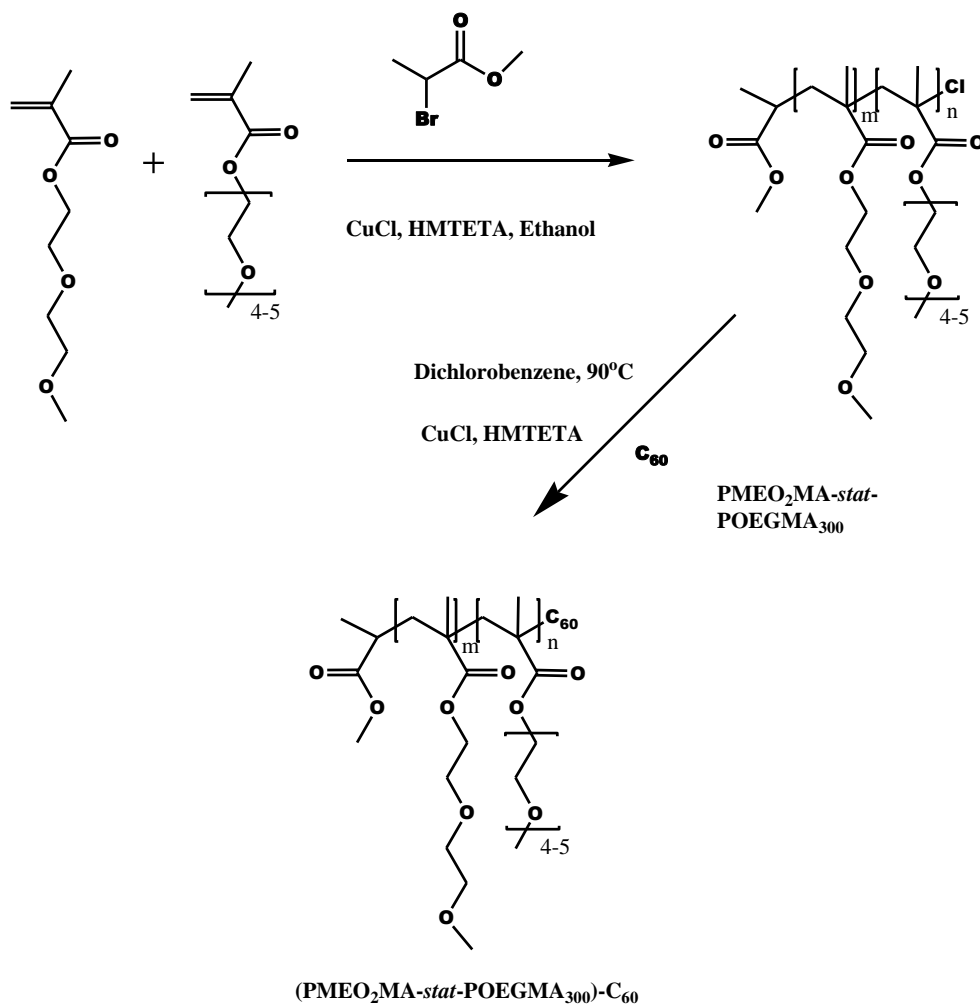
GPC, NMR, cloudy point measurements, DLS, SLS and TEM were the same as described in Chapter 5.

6.3 Results and Discussion

6.3.1 Synthesis of $(\text{PMEO}_2\text{MA-}stat\text{-POEGMA}_{300})\text{-C}_{60}$ by ATRP and ATRA

Recent studies showed that statistical copolymerization of different OEGMA analogues at various feed ratios synthesized by ATRP yielded copolymers that possessed different LCSTs. In the present study, a statistical copolymer of $\text{PMEO}_2\text{MA-}stat\text{-POEGMA}_{300}$ was synthesized and subsequently used to prepare the amphiphilic fullerene containing copolymer. A two-step reaction was adopted as shown in Scheme 6.1. First, a statistical copolymer composed of MEO_2MA and OEGMA_{300} was prepared by ATRP using HMTETA/CuCl as catalyst in ethanol at a feed composition of 7 to 3. Then, $\text{PMEO}_2\text{MA-}stat\text{-POEGMA}_{300}$ was used to synthesize the *amphiphilic* copolymer $(\text{PMEO}_2\text{MA-}stat\text{-POEGMA}_{300})\text{-C}_{60}$ in dichlorobenzene at 90 °C using ATRA reaction catalyzed by HMTETA/CuCl. The molecular weight of $\text{PMEO}_2\text{MA-}stat\text{-POEGMA}_{300}$ was about 11000 g/mol with a PDI of 1.3 as determined by GPC (Figure 6.1). It

should be noted that GPC was also attempted to measure the M_w of (PMEO₂MA-*stat*-POEGMA₃₀₀)-C₆₀ using THF or DMF as the mobile phase. However, peaks at short elution time were observed which corresponded to a molecular weight of the order 10⁶ Da. We believe this is attributed to the formation of large aggregates caused by the hydrophobic fullerene moiety. A similar phenomenon was observed in other studies [Song et al. 2003]



Scheme 6. 1 Synthetic Scheme of (PMEO₂MA-*stat*-POEGMA₃₀₀)-C₆₀.

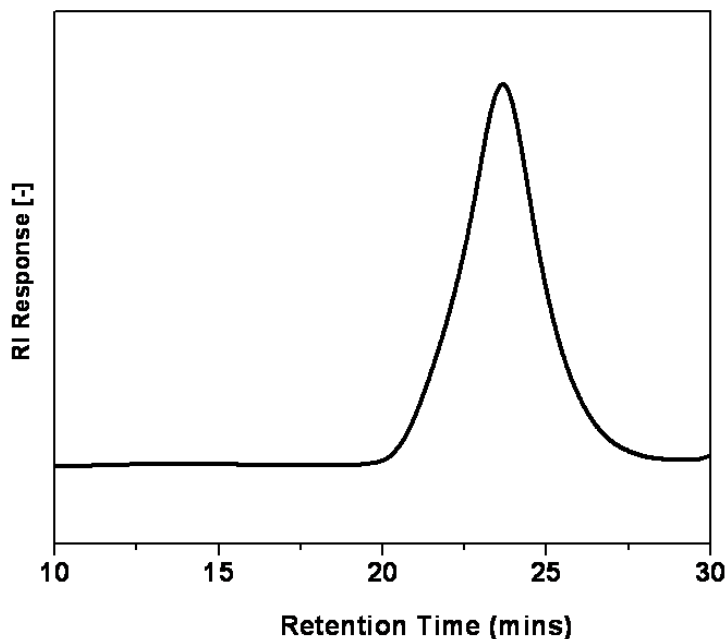
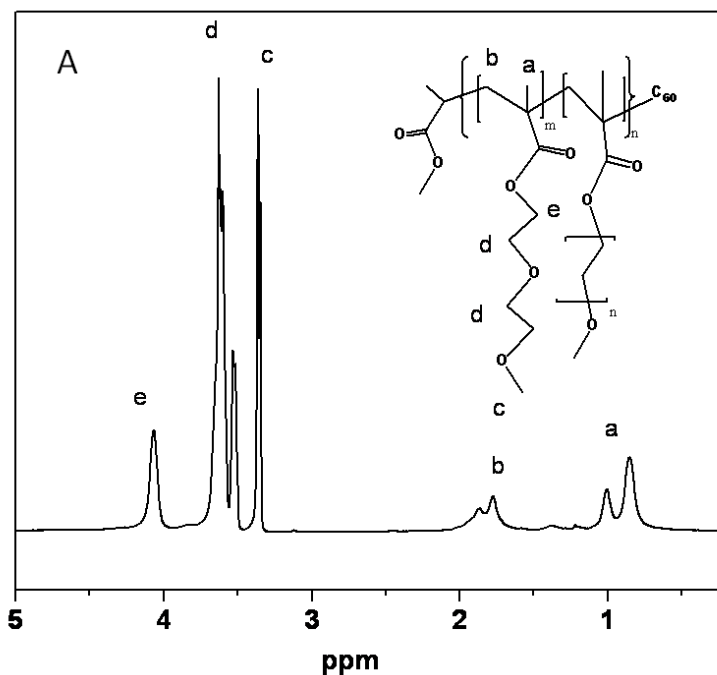


Figure 6. 1 GPC profiles of copolymer PMEO₂MA-*stat*-POEGMA₃₀₀

We believe the resulting (PMEO₂MA-*stat*-POEGMA₃₀₀)-C₆₀ is pure for the following reasons: (1) Excess amount of C₆₀ was used in the reaction to assure there was only mono C₆₀-capped product obtained and no unreacted PMEO₂MA-*stat*-POEGMA₃₀₀ remained. (2) The unreacted C₆₀ should have been removed completely by passing through an alumina column in THF solution since C₆₀ is not soluble in THF. In addition, a clear light brown solution was formed when dissolving PMEO₂MA-*stat*-POEGMA₃₀₀-C₆₀ in water, which visually indicated the formation of the covalent bond between C₆₀ and the polymer because C₆₀ will precipitate out if only physically mixing C₆₀ and PMEO₂MA-*stat*-POEGMA₃₀₀ in aqueous solution since C₆₀ is not water-soluble.

The most common characterization techniques used to confirm the successful synthesis of polymer-C₆₀ are ¹H NMR, ¹³C NMR and UV-vis. ¹H NMR of (PMEO₂MA-*stat*-POEGMA₃₀₀)-C₆₀ is shown in Figure 6.2A. All the peaks were assigned correctly to the protons of PMEO₂MA-*stat*-POEGMA₃₀₀ indicating the existence of PMEO₂MA-*stat*-POEGMA₃₀₀ in the

resulting product. In addition, ^{13}C NMR of (PMEO₂MA-*stat*-POEGMA₃₀₀)-C₆₀, shown in Figure 6.2B, confirmed the existence of C₆₀ due to the presence of the peak at 143.3 ppm, which corresponds to the aromatic carbon from C₆₀ [Johnson et al. 1990]. In UV spectrum, pristine C₆₀ has absorptions around 257 and 330 nm in water [Kato et al. 2009], whereas the covalent functionalized C₆₀ possessed an excess absorption [Chubarova et al. 2008] in the range 270-350 nm. The UV-Vis spectrum (Figure 6.3) shows a broad absorption band within the range of 250 to 500 nm for samples of (PMEO₂MA-*stat*-POEGMA₃₀₀)-C₆₀ in water. Since POEGMA does not have any absorption within this wavelength range, we concluded that the absorption of (PMEO₂MA-*stat*-POEGMA₃₀₀)-C₆₀ is from C₆₀. Therefore, a conclusion could be made that C₆₀ was covalently bonded to POEGMA from the results of proton and carbon NMR, and UV-vis.



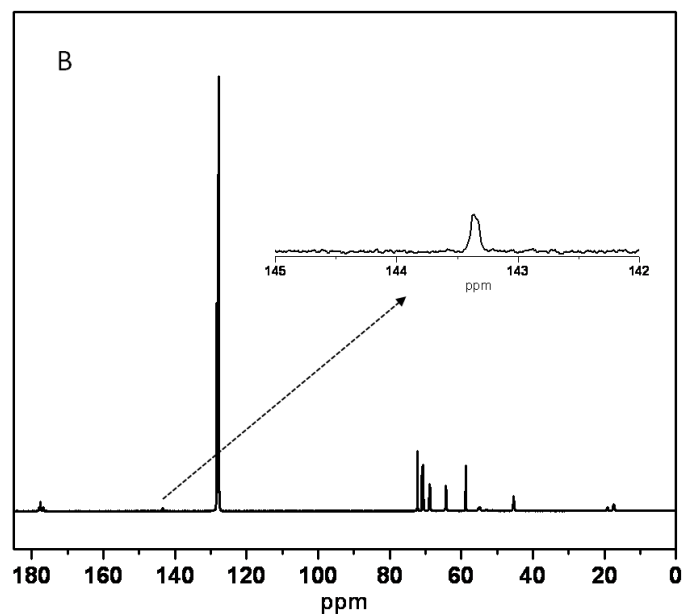


Figure 6. 2 (A). ^1H NMR spectrum recorded in CDCl_3 for $(\text{PMEO}_2\text{MA-}stat\text{-POEGMA}_{300})\text{-C}_{60}$ and (B). ^{13}C NMR spectrum recorded in C_6D_6 for $(\text{PMEO}_2\text{MA-}stat\text{-POEGMA}_{300})\text{-C}_{60}$.

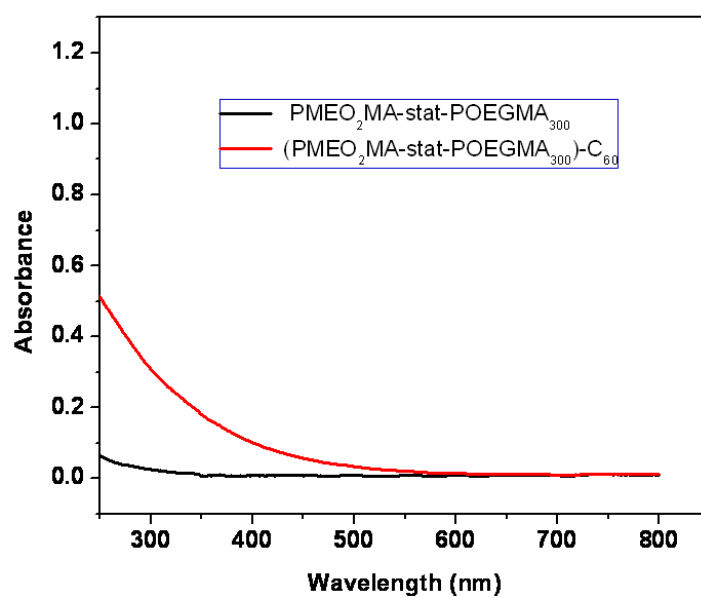


Figure 6. 3 UV-Vis spectra of $\text{PMEO}_2\text{MA-}stat\text{-POEGMA}_{300}$ and $(\text{PMEO}_2\text{MA-}stat\text{-POEGMA}_{300})\text{-C}_{60}$ in water solution.

6.3.2 Effect of methanol composition on the LCST of $\text{PMEO}_2\text{MA-}stat\text{-POEGMA}_{300}$ and $(\text{PMEO}_2\text{MA-}stat\text{-POEGMA}_{300})\text{-C}_{60}$

The LCST behavior of $\text{PMEO}_2\text{MA-}stat\text{-POEGMA}_{300}$ and $(\text{PMEO}_2\text{MA-}stat\text{-POEGMA}_{300})\text{-C}_{60}$ in water/methanol mixture was investigated using turbidity measurements by monitoring the cloud points of the solution. Figures 4a and 4b show the optical transmittance as a function of temperature (recorded at the wavelength of 500 nm at a heating rate of 1 °C/min) for a 4 mg/mL aqueous solution of $\text{PMEO}_2\text{MA-}stat\text{-POEGMA}_{300}$ and $(\text{PMEO}_2\text{MA-}stat\text{-POEGMA}_{300})\text{-C}_{60}$ respectively. $\text{PMEO}_2\text{MA-}stat\text{-POEGMA}_{300}$ solution was transparent at low temperature and the transmittance decreased sharply when a critical temperature was exceeded. Figure 6.4a shows that the LCST of $\text{PMEO}_2\text{MA-}stat\text{-POEGMA}_{300}$ shifted to a higher temperature when the volume fraction of methanol was increased. The cloud point increased from 42 to 95 °C as the volume percentage of methanol was increased from 0 to 30%. At higher methanol content, the LCST could not be measured because it exceeded the boiling point of the solution mixture. A similar increase in the LCST of $(\text{PMEO}_2\text{MA-}stat\text{-POEGMA}_{300})\text{-C}_{60}$ in methanol/water mixtures was observed (Figure 6.4b). However, the LCSTs of $(\text{PMEO}_2\text{MA-}stat\text{-POEGMA}_{300})\text{-C}_{60}$ in methanol/water mixtures were lower than $\text{PMEO}_2\text{MA-}stat\text{-POEGMA}_{300}$ (Figure 6.5). This could be attributed to the formation of micelles in $(\text{PMEO}_2\text{MA-}stat\text{-POEGMA}_{300})\text{-C}_{60}$ and the attachment of C_{60} end group to the polymer. Firstly, the formation of micelles facilitated the intermolecular interaction of polymer chains, which depressed the LCST. Secondly, the attachment of C_{60} at the end of POEGMA also lowers the LCST because it is well-known that copolymerization with hydrophobic polymers can lower the LCST. A similar phenomenon was observed for PNIPAM containing star architectures [Plummer et al. 2006].

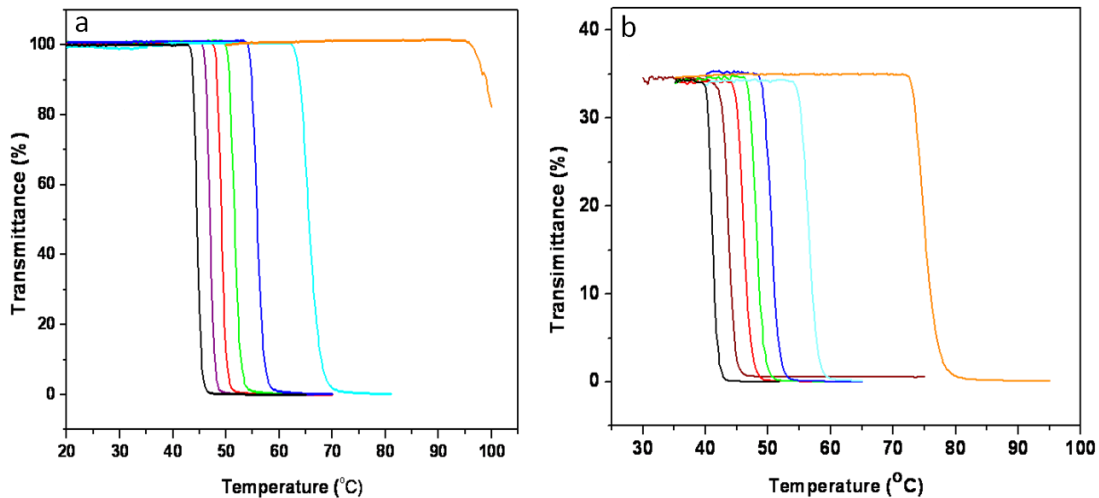


Figure 6. 4 Effects of methanol composition (from left to right: 0, 5, 10, 15, 20, 25 and 30%) on the LCST of (a). $\text{PMEO}_2\text{MA-}stat\text{-POEGMA}_{300}$ and (b). $(\text{PMEO}_2\text{MA-}stat\text{-POEGMA}_{300})\text{-C}_{60}$.

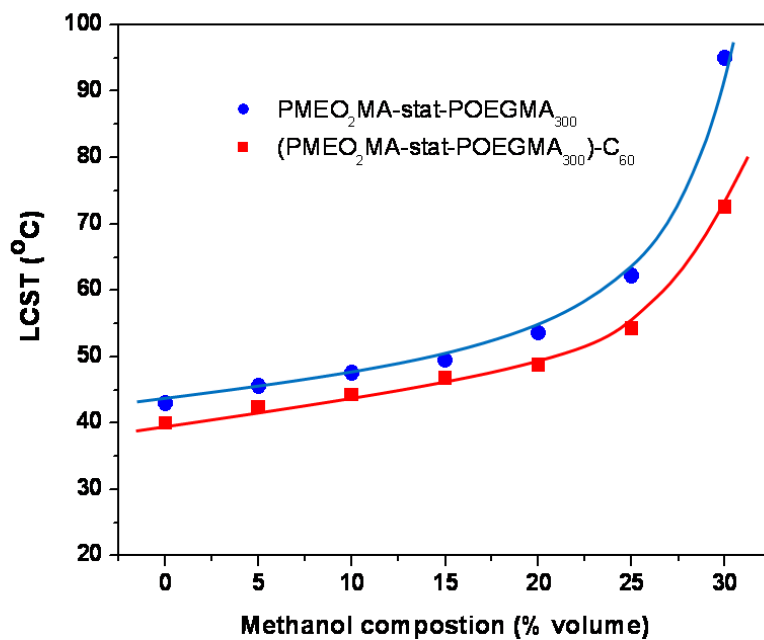


Figure 6. 5 LCSTs of $\text{PMEO}_2\text{MA-}stat\text{-POEGMA}_{300}$ and $\text{PMEO}_2\text{MA-}stat\text{-POEGMA}_{300}\text{-C}_{60}$ at various methanol contents.

6.3.3 Self-assembly behavior of (PMEO₂MA-*stat*-POEGMA₃₀₀)-C₆₀ in water/methanol at different temperatures

Dynamic light scattering (DLS) was employed to determine the critical micelle concentration (CMC) of (PMEO₂MA-*stat*-POEGMA₃₀₀)-C₆₀ in methanol/water mixtures solution at 25 °C. Figures 6.6a and b show the light scattering intensity as a function of (PMEO₂MA-*stat*-POEGMA₃₀₀)-C₆₀ concentration (mg/mL) in water and 25% methanol/water mixture respectively. The CMC of the polymer was determined to be ~7 and 11 µg/ml in water and 25% methanol/water mixture, respectively from Figure 6.6. The data in Figure 6.7 revealed that the CMC of (PMEO₂MA-*stat*-POEGMA₃₀₀)-C₆₀ increased with increasing methanol content in the binary solvent mixture. The larger CMC values at higher methanol content indicated that formation of (PMEO₂MA-*stat*-POEGMA₃₀₀)-C₆₀ unimers was favored in water over the micellization in water-methanol binary mixtures. This observation correlates with the higher solubility of PME₂MA-*stat*-POEGMA₃₀₀ in methanol than in water. An increase in the CMC with the addition of polar organic solvents had previously been reported for amphiphilic compounds [Hussain et al. 2009, Lin et al. 2002, Aguiar et al. 2002].

The hydrodynamic radius (R_h) of (PMEO₂MA-*stat*-POEGMA₃₀₀)-C₆₀ in methanol/water was measured using dynamic light scattering (DLS) and it was analyzed using the same method used in Chapter 3 and 4. Linear dependence of the decay rate (Γ) with respect to q^2 was obtained for all measurements. The R_h of (PMEO₂MA-*stat*-POEGMA₃₀₀)-C₆₀ in different water/methanol compositions and at different temperatures is shown in Figure 6.8. The size of the micelles remained unchanged for each methanol/water composition below their corresponding LCSTs. This indicated that the micellar structure is fairly stable during the heating process. When the temperature exceeded the LCST, micelles started to associate due to the dehydration of

POEGMA corona. When the temperature was increased further, DLS could not be used to measure the size of the aggregates as the solution had become cloudy. An increase in the methanol content in the binary solvent led to the formation of larger micelles when the temperatures were below their corresponding LCSTs as is evident from Figures 6.8 and Figure 6.9. It is known from CMC measurement that methanol is a better solvent for POEGMA and therefore POEGMA chains are more extended in solutions with higher methanol content. The polydispersity index ($\mu_2/\langle \Gamma \rangle^2$) obtained from DLS provides information on the deviation from monodispersity. The PDI values for all DLS measurements are less than 0.23, indicating that the micelles had a narrow size distribution.

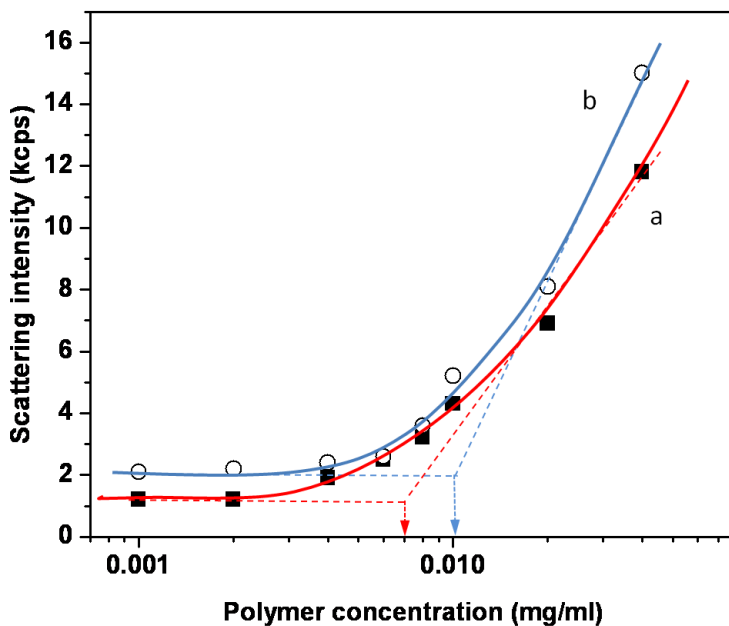


Figure 6. 6 CMC of (PMEO₂MA-*stat*-POEGMA₃₀₀)-C₆₀ in (a). water and (b). 25% methanol/water at 25°C measured by DLS.

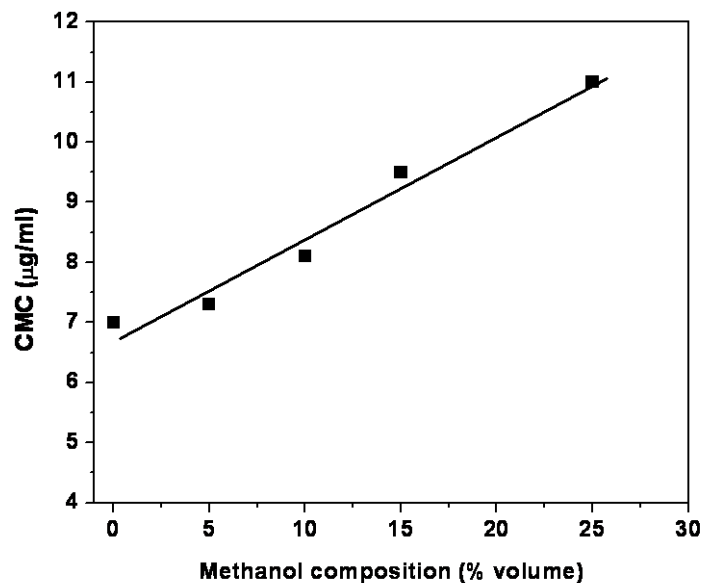


Figure 6. 7 Effect of methanol content on CMC of (PMEO₂MA-*stat*-POEGMA₃₀₀)-C₆₀ in water/methanol mixtures.

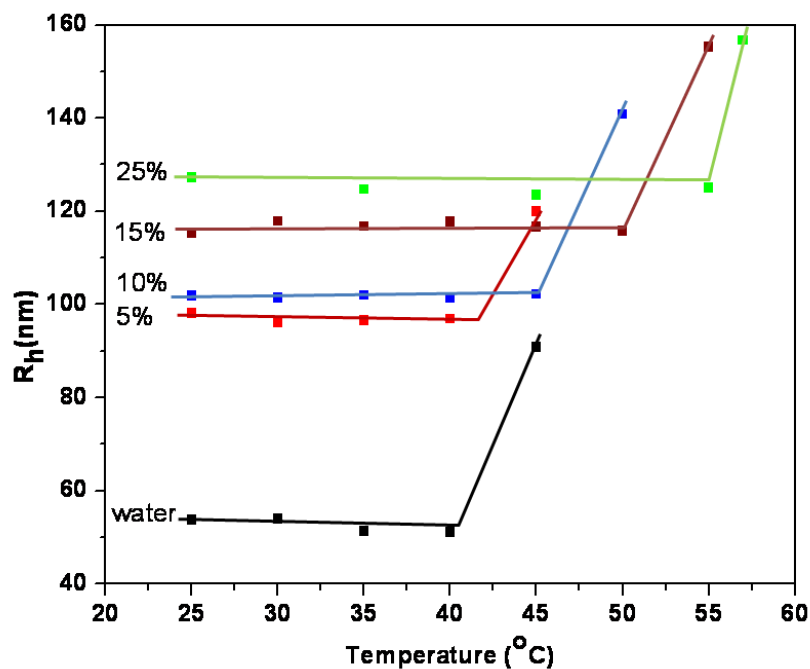


Figure 6. 8 Effect of temperature on the hydrodynamic radius (R_h) of the micelles of (PMEO₂MA-*stat*-POEGMA₃₀₀)-C₆₀ in methanol/water solution measured at 0.2 mg/ml.

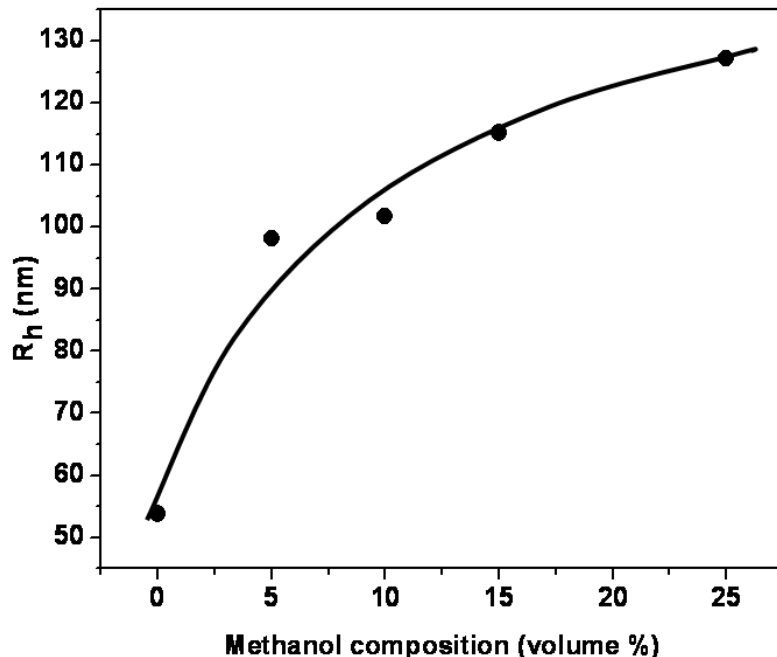


Figure 6. 9 Hydrodynamic radius (R_h) of micelles of (PMEO₂MA-*stat*-POEGMA₃₀₀)-C₆₀ in various methanol/water compositions measured at 0.2 mg/ml below the LCST.

It is known from Chapter 5 that the ratio of (R_g/R_h) is an important indicator that describes the conformation of the polymeric chains in solution. The calculated (R_g/R_h) values for the micelles of (PMEO₂MA-*stat*-POEGMA₃₀₀)-C₆₀ in various water-methanol mixtures are summarized in Table 6.1, where the R_g data were obtained from SLS measurements. At 25 °C, the (R_g/R_h) for the micelles formed from (PMEO₂MA-*stat*-POEGMA₃₀₀)-C₆₀ remained just below the value for hard-sphere micelles for all binary solvent compositions, indicating that the micelles were spherical and contained extended hydrophilic coronas. (R_g/R_h) decreased with increasing methanol content, and this is associated with a better solubility of POEGMA corona in solvent mixture containing higher methanol content. Above the LCST, (R_g/R_h) increased to ~1, suggesting that the morphology was evolving. It was known that the morphology of POEGMA chains changed from a coil to globule above LCST [Fechler et al. 2009]. Thus, core-

shell micelles became unstable and large aggregates comprising of several contracted micelles were formed.

Table 6. 1 Micelle properties of (PMEO₂MA-*stat*-POEGMA₃₀₀)-C₆₀ in water/methanol mixtures of various compositions at different temperatures

| Methanol composition (% v/v) | Below LCST | | | | Above LCST | | | |
|------------------------------|------------|----------------|----------------|--------------------------------|------------|----------------|----------------|--------------------------------|
| | 25°C | R _h | R _g | R _g /R _h | | R _h | R _g | R _g /R _h |
| 0 | 25°C | 53.8 | 41.9 | 0.78 | 45°C | 90.9 | 100.1 | 1.10 |
| 5 | 25°C | 98.2 | 76.3 | 0.77 | 45 °C | 120.0 | 113.7 | 0.94 |
| 10 | 25°C | 101.8 | 80.1 | 0.75 | 50 °C | 140.8 | 134.8 | 0.92 |
| 15 | 25°C | 115.2 | 83.1 | 0.71 | 55 °C | 155.2 | 156.9 | 1.01 |
| 25 | 25°C | 127.2 | 79 | 0.62 | 57 °C | 156.7 | 152 | 0.97 |

TEM images, shown in Figures 6.10a and b, revealed that the average size of the self-assembled structures of (PMEO₂MA-*stat*-POEGMA₃₀₀)-C₆₀ in water is smaller than that formed in 10% methanol/water at room temperature, which is consistent with the results determined from DLS measurements. Figures 6.10 c and d show the TEM images of aggregates formed in water and 10% methanol/water mixture at temperatures greater than the LCST. The spherical particles are composed of a number of dehydrated core shell micelles because hydrophobic interaction of PME₂O₂MA-*stat*-POEGMA₃₀₀ chains takes place to form larger aggregations due to the collapsed of PME₂O₂MA-*stat*-POEGMA₃₀₀ chain when the temperature exceeds the LCST. This was also consistent with the light scattering results, in which larger R_g and (R_g/R_h) were observed. One concern to use normal TEM to observe the morphology of the self-assembled

structures of (PMEO₂MA-*stat*-POEGMA₃₀₀)-C₆₀ is that the glass transition temperature (T_g) of PMEO₂MA-*stat*-POEGMA₃₀₀ is lower than room temperature, which might affect the reliability of the TEM results. The self assembly of block copolymers containing POEGMA or PEO [Holder et al. 2003, Wang et al. 2008] were observed by normal TEM and the results were consistent with other techniques. In this study, TEM results are also consistent with those obtained from light scattering technique, in which R_g/R_h value can tell us the morphology of the self-assembled structures. Therefore, we believe, the morphologies obtained from normal TEM are reliable.

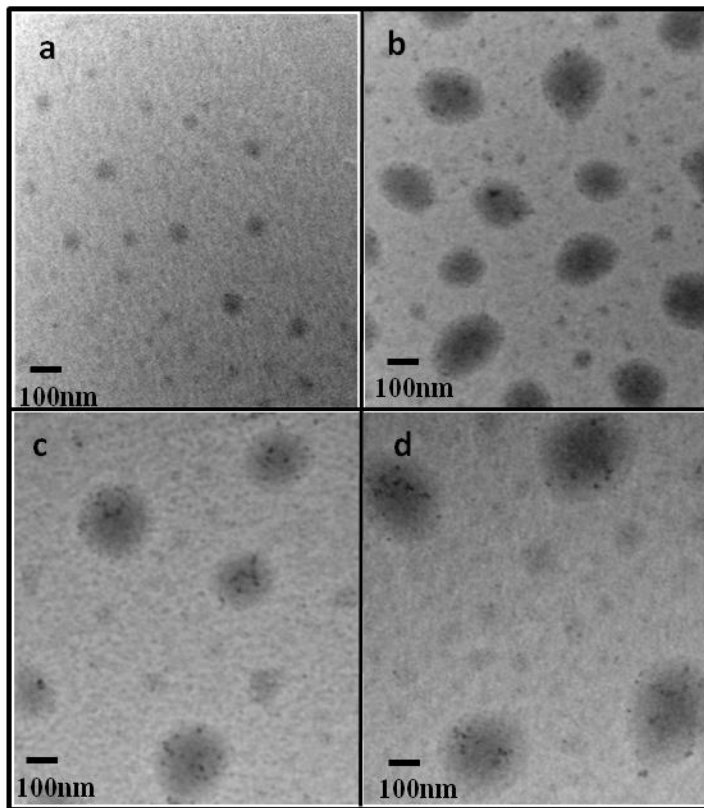


Figure 6. 10 TEM images of micelles of (PMEO₂MA-*stat*-POEGMA₃₀₀)-C₆₀ in (a) water, (b) 10 vol% methanol/water at 25 °C, (c) water at 45 °C and (d) 10 vol% methanol/water at 50 °C.

6.4 Conclusions

Amphiphilic (PMEO₂MA-*stat*-POEGMA₃₀₀)-C₆₀ copolymer synthesized via atom transfer radical polymerization (ATRP) formed spherical micelles in methanol/water mixtures of various compositions, with C₆₀ as the core and POEGMA as the corona. Cloud point measurements showed that the LCST of PMEO₂MA-*stat*-POEGMA₃₀₀ and (PMEO₂MA-*stat*-POEGMA₃₀₀)-C₆₀ increased with increasing methanol content. Lower LCSTs were observed for (PMEO₂MA-*stat*-POEGMA₃₀₀)-C₆₀ than PMEO₂MA-*stat*-POEGMA₃₀₀ in all methanol/water contents. With increasing methanol content, the CMC increased and larger micellar aggregates were formed. Above the LCST, the size of micelles increased and (R_g/R_h) increased from ~0.78 to 1.0. This is attributed to the dehydration of POEGMA shell due to the coil to globule transition at elevated temperatures. TEM images also confirmed the formation of core-shell micelles and large aggregates at temperature below and above the LCST, respectively. Based on the above observations, similar phenomena are expected for other POEGMA analogues including the homo or statistical block copolymers because they are chemically similar.

Chapter 7 Functionalization of Nanocrystal Cellulose with Fullerene Derivatives via Radical Coupling Reaction

7.1 Introduction

Nanocrystalline cellulose (NCC), discovered in 1949 by Bengt Ranby, [Ranby et al. 1949] is prepared from acid hydrolysis of naturally existing cellulose semicrystals. [Samir et al. 2005] It is abundant, renewable and biodegradable, and could contribute to the reduction of CO₂ in the atmosphere. NCC can be used as building blocks for the preparation of various functional nano-materials [Ruiz et al. 2000, Shweta et al. 2008, Eichhorn et al. 2005, Sturcova et al. 2006, Eichhorn et al. 2010] as it possesses a number of advantages, such as low density, high specific surface area, and superior mechanical properties. The utility of NCC can be explored in many diverse fields including electronics, [Mangilal et al. 2009] materials science [Sturcova et al. 2005] and biomedical science. [Wojciech et al. 2007] In order to be applied in these fields, chemical modification of NCC is necessary in reducing agglomeration, [Elisabeth et al. 2010] and imparting more versatile functions, such as fluorescence [Dong et al. 2007] temperature responsive properties. [Zoppe et al. 2010, Yi et al. 2009] Similar to the chemical nature of cellulose, the numerous hydroxyl groups on the nanocrystal surface can be used to modify NCC with small chemical molecules or polymers. For instance, NCC was labeled by fluorescent markers for bioimaging applications [Dong et al. 2007] through epoxide ring opening reaction; dual fluorescent labeled NCC was prepared for pH sensing through the thiol-ene click reaction; [Lise et al. 2010] cationic epoxypropyl trimethyl ammonium chloride (EPTMAC) [Merima et al. 2008] was attached to NCC through the epoxide ring opening reaction; nanoplatelet gel composed of NCC [Filpponen et al. 2010] and imidazolium salt functionalized NCC [Samuel et al. 2011] were prepared through the chemistry between azide and alkyne group. Polymer

functionalized NCC can be prepared by “grafting from” or “grafting to” approaches. In the “grafting from” method, the polymer chains were produced by in-situ surface initiated polymerization from immobilized initiators on the NCC surface, thus a higher grafting density is possible. However, it is very difficult to characterize the polymer without cleaving the grafted chains from NCC surface. Conversely, the “grafting to” method suffers from low theoretical polymer graftings due to steric repulsion between the grafted and reacting polymer chains. This method allows for the characterization of polymer chains prior to grafting, thus offering the possibility of controlling the properties of the resulting material. Using a grafting from approach, researchers modified NCC with poly(ϵ -caprolactone) via by ring-opening polymerization [Habibi et al. 2008a] and the mechanical performance of PCL was improved significantly when mixed with PCL-grated NCC; polystyrene modified NCC was prepared by surface initiated atom transfer radical polymerization (ATRP) [Morandi et al. 2009] and this composite demonstrated the capacity to absorb 1,2,4-trichlorobenzene and hold promise for pollutant removal applications; temperature responsive polymers, such as poly(N-isopropylacrylamide) (PNIPAM) [Zoppe et al. 2010] and poly(N,N-dimethylaminoethyl methacrylate) (PDMAEMA) [Yi et al. 2009] were grafted to NCC through ATRP and the resulted composites may have potential for use in stimuli responsive applications. Researchers used ‘grafting to’ approach to modify NCC with isothiocyanate decorated polycaprolactone [Habibi et al. 2008b] and epoxide terminated poly(ethylene oxide). [Elisabeth et al. 2010]

In the present study, we formulated a facile ‘grafting to’ method to decorate NCC with fullerene derivatives through a radical coupling reaction based on the following features: 1) hydroxyl groups on NCC surfaces can be easily converted to radicals [Roy et al. 2009] through various treatments, such as chemical initiations, irradiation with ultraviolet light or irradiation

with gamma rays; 2) C₆₀ has strong affinity to trap various kinds of radicals. In order to attach fullerene to NCC, modification of fullerene to make it water-soluble is necessary because pristine fullerene is not soluble in aqueous solvent. [Ruoff et al. 1993] In this study, two kinds of water-soluble fullerene derivatives were prepared, namely, C₆₀-(β-cyclodextrin) complex formed via a host-guest complexation [Murthy et al. 2001] and C₆₀-poly(oligo(ethylene glycol) methyl ether methacrylate) (POEGMA) prepared by atom transfer radical polymerization (ATRP). C₆₀-(β-cyclodextrin) is a non-covalent complex of C₆₀-(β-cyclodextrin), therefore the physicochemical properties of fullerene will remain intact. POEGMA was chosen to covalently modify fullerene because it possesses appealing properties, such as possible tunable thermal behavior and biocompatibility. [Lutz et al. 2006 and 2006b] To our best knowledge, this is the first reported study on the modification of NCC using fullerene derivatives via radical coupling reaction. We anticipate that the resultant NCC-fullerene systems will possess the advantages of NCC and fullerene, thereby expanding the applications of NCC to the fields of personal care, electronic, biosensors and solar cells.

7.2 Experimental

7.2.1 Materials

Nanocrystal cellulose was provide by FPIinnovations and used as received. 2-(2-methoxyethoxy) ethyl methacrylate (188 g/mol), oligo(ethylene glycol) methyl ether methacrylate (300 g/mol) were purchased from Sigma-Aldrich and they were purified by passing through a basic alumina column prior to use. 1,1,4,7,10,10-hexamethyl triethylene tetramine (HMTETA), copper(I) chloride, methyl 2-bromopropionate (MBP), sodium persulfate, methyl-β-cyclodextrin, methanol, ethanol dichlorobenzene and HPLC grade toluene were purchased from Sigma-Aldrich and used as received.

7.2.2 Preparation of NCC-C₆₀

First, an aqueous solution of C₆₀ was prepared using the solvent exchange technique. 60 mg fullerene was dissolved in 5 mL toluene and 100 mg of methyl-β-cyclodextrin was dissolved in 10 mL of water; the mixture of these two solutions was vigorously stirred at room temperature for 2 days. As a result, a yellow aqueous solution of C₆₀ stabilized by methyl-β-cyclodextrin (C₆₀-(β-cyclodextrin)) was obtained. The remaining amount of C₆₀ in toluene solution was obtained by removing toluene using a rotovap and drying in a vacuum oven, thus the amount of fullerene in the water phase was determined. Then, 26 mg (0.11 mmol) sodium persulfate and 20 mg NCC were dissolved in the C₆₀-(β-cyclodextrin) solution in a 25 mL flask. The mixture was bubbled with argon for 30 mins and stirred at 65 °C for 24 h. The final reaction mixture was purified by dialysis for 2 days in a dialysis tube with MW cutoff of 12-14 K. Finally a fluffy yellow product was isolated after freeze drying.

7.2.3 Preparation of NCC-C₆₀-POEGMA

The synthesis of NCC-C₆₀-POEGMA involved a three-step reaction. First, statistical copolymer of PMEO₂MA-*stat*-POEGMA₃₀₀ was synthesized as described below. The polymerization of PMEO₂MA- *stat*-POEGMA₃₀₀ using methyl 2-bromopropionate as initiator and HMTETA/CuCl as catalyst was performed in ethanol via ATRP at room temperature. 2-(2-methoxyethoxy) ethyl methacrylate (3g, 15.9 mmol), oligo(ethylene glycol) methyl ether methacrylate (300 g/mol) (2.05g, 6.8mmol), methyl 2-bromopropionate (6.43mg, 0.38 mmol) and ethanol (4.0 mL) were added into a 25 mL flask and the mixture was bubbled with argon for 30 mins. Then the mixture was transferred using a double tipped needle into a flask charged with CuCl (38.1 mg, 0.38 mmol) and HMTETA (178.4 mg, 0.77 mmol) equipped with a magnetic stirring bar under argon atmosphere. After stirring at room temperature for 24 h, the reaction

mixture was purified by dialysis for 48 hours in a dialysis tubing with MW cutoff of 1000 Da. Subsequently, the oil like product was isolated by freeze drying. The chemical structure and M_w of the polymers were characterized by ^1H NMR and GPC. Polymer with molecular weight of 11,000 g/mol was synthesized with a polydispersity index (PDI) of 1.3.

($\text{PMEO}_2\text{MA-}stat\text{-POEGMA}_{300}$)- C_{60} was synthesized using the following procedure. The solution of $\text{PMEO}_2\text{MA-}stat\text{-POEGMA}_{300}$ (2.5g, 0.227mmol) and C_{60} (0.33g, 0.454mmol) in dichlorobenzene was charged into a flask filled with argon and the solution was bubbled with argon for 30 mins. Then the mixture was transferred to another argon filled flask charged with CuCl (23 mg, 0.227 mmol) and HMTETA (104 mg, 0.56 mmol) via a double tipped needle. The reaction mixture was stirred for 24 h at 90 °C. After 24 h, the reaction mixture was diluted with THF and passed through a basic alumina column twice to remove excess C_{60} . The filtrate was concentrated and dissolved in water, followed by dialysis in water for 2 days. Finally, a sticky brown product was isolated after freeze drying. The chemical structure and M_w of the polymers were characterized by ^1H NMR and UV-vis.

In the last synthetic step, 52 mg (0.22 mmol) sodium persulfate and 50 mg NCC and 100 mg ($\text{PMEO}_2\text{MA-}stat\text{-POEGMA}_{300}$)- $b\text{-C}_{60}$ were dissolved in 35% methanol/water (v%) and the mixture was bubbled with argon for 30 mins, and stirred at 65 °C for 24 h. the reaction mixture was purified by dialysis for 2 days in a dialysis tubing with MW cutoff of 12-14 K. The fluffy light brown product was isolated after freeze drying and this product was further purified by washing with THF to remove the unreacted ($\text{PMEO}_2\text{MA-}stat\text{-POEGMA}_{300}$)- $b\text{-C}_{60}$. Finally, a light brown powder was isolated.

7.2.4 Characterization

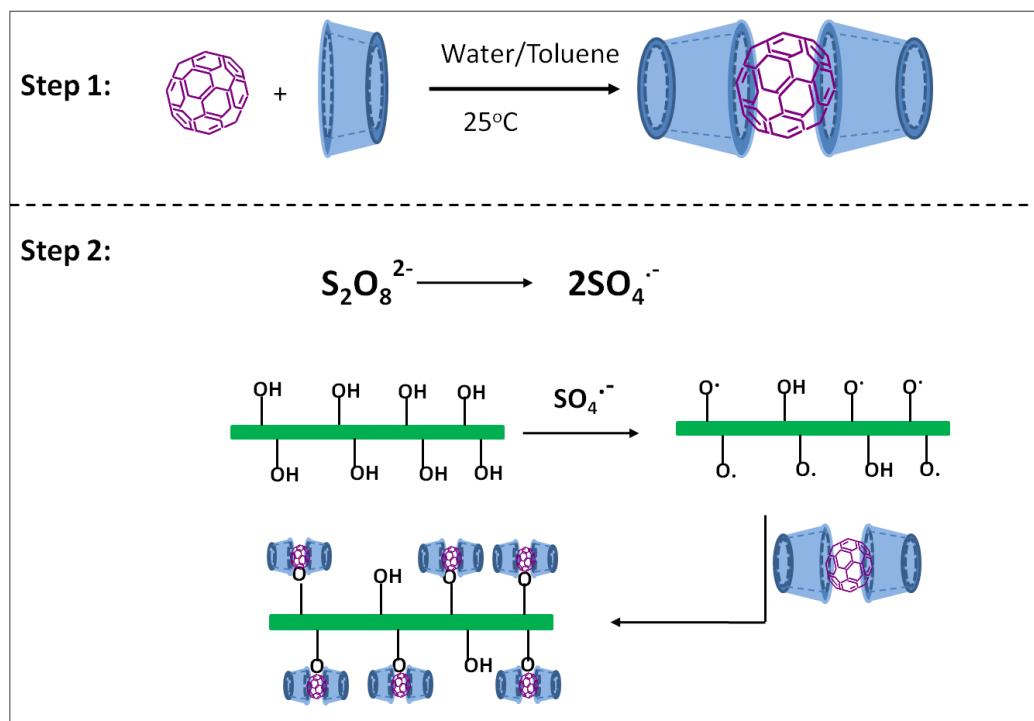
GPC, NMR, UV-vis, cloudy point measurements and TEM are the same as described in Chapter 5. TGA analyses were performed under helium flow at 20 °C/min from room temperature to 800 °C using a TA Instrument Q50 thermogravimetric analyzer (TA Instruments, USA). The antioxidant property of the prepared products was evaluated using the UV-vis, in which 3 mL of DMSO solution of DPPH with concentration of 0.05 mg/ml was prepared, into which 6 mg of the fullerene-NCC sample was added. The mixture was kept in the dark for 2 hours before the UV-Vis spectrum was recorded.

7.3 Results and Discussion

7.3.1 Synthesis and characterization of NCC-C₆₀-(β-cyclodextrin)

NCC used in this study was prepared from the acid hydrolysis of wood fibers using sulfuric acid, leaving behind a small fraction of carboxylic and sulfate ester groups on the surface of NCC. The negatively charged sulfate groups allow the NCC to disperse well in water. The dimensions of the NCC are about 10-20 nm in diameter and 200 nm in length. It has been shown that persulfate salt is efficient in converting hydroxyl groups to radicals [Roy et al. 2009] and therefore we used sodium persulfate to generate hydroxyl radicals by heating the reaction mixture to 65 °C. The poor solubility of fullerene C₆₀ in aqueous solvent requires the modification of fullerene in order to attach fullerene onto the surface of NCC in aqueous solution. A stable inclusion complex of β-cyclodextrin with C₆₀ was reported [Murthy et al. 2001] and the complex also showed radical scavenging capability. Methyl-β-cyclodextrin was used in our study to prepare the water-soluble fullerene complex because it has better water solubility than β-cyclodextrin. C₆₀ is known as being a ‘radical sponge’ and one fullerene radical

can capture up to 20 free radicals, [Yadav et al. 2008] depending on the types of radicals. There are two possible side reactions involved. Firstly, C₆₀ may capture the sulfate radical anions, and lower the generation of radicals on NCC. Second, crosslinking may occur between NCC due to dimerization. However, studies demonstrated that fullerenes did not react with sulfate radical anions, where sulfate radical anions were used for radical polymerizations in the presence of fullerene C₇₀ [Augusto et al. 2010] and single walled carbon nanotubes. [Qin et al. 2004]. Therefore we believe C₆₀ only reacts with free radicals on the surfaces of NCC. In addition, the crosslinking between NCC would not occur due to the bulky NCC structure, which prevents the dimerization process. [David et al. 1996, Morton et al. 1992] The reaction to form NCC-C₆₀-(β-cyclodextrin) involved two steps (Scheme 7.1). First, water soluble C₆₀-(β-cyclodextrin) was prepared via a solvent exchange technique by mixing fullerene/toluene solution with water. Then, the radical coupling reaction was performed by converting the hydroxyl groups on the NCC to free radicals in the presence of sodium persulfate at 65°C, and these free radicals were captured by C₆₀-(β-cyclodextrin) to form NCC-C₆₀-(β-cyclodextrin).



Scheme 7. 1 Synthetic scheme for NCC-C₆₀

The resulting product and pristine NCC in water are shown in Figures 7.1a and 7.1b respectively. It is evident that fullerene functionalized NCC dispersed readily in aqueous solution and the yellow appearance of the solution confirmed the conjugation of fullerene on NCC. Unreacted fullerene was completely removed via dialysis (MW cutoff of 12-14K) since the molecular weight of the fullerene-cyclodextrin complex was about 3344 g/mol given that one fullerene molecule complexed with two methyl- β -cyclodextrin molecules. The NCC-C₆₀ system was characterized by UV-Vis, where the peaks at 330 nm and 260 nm indicated that C₆₀ was covalently bonded to NCC because these two peaks are the signature absorption peaks of the pristine C₆₀ (Figure 7.2b). [Hare et al. 1991] The thermal degradation behaviors of NCC and NCC-C₆₀-(β -cyclodextrin) were investigated using thermogravimetric analysis (TGA) under nitrogen environment, and the results are shown in Figures 7.3a and 7.3b. The degradation profile of NCC showed two pyrolysis processes, which was explained by Wang and coworkers,

[Wang et al. 2007] The lower temperature process occurred at ~ 250 °C corresponded to the degradation facilitated by sulfate groups and the other process occurring at 300 °C was related to the slow charring process of the solid residue. After modification with C_{60} -(β -cyclodextrin), the TGA profile (Figure 7.3b) for the lower temperature process became broader compared to the pristine NCC system, which might be caused by two processes. Firstly, the insertion of fullerene onto the surface of NCC may disrupt some of the crystalline structure of NCC, which lowers the thermal decomposition temperature to ~ 200 °C. Secondly, the attachment of C_{60} to NCC might retard the pyrolysis process caused by sulfate groups, which made this process shift to higher temperature of 350 °C. TEM images of NCC- C_{60} -(β -cyclodextrin) was recorded in Figure 7.4a and the rod-like crystalline structure was observed, which suggests that the NCC structure was not damaged during the radical coupling reaction.

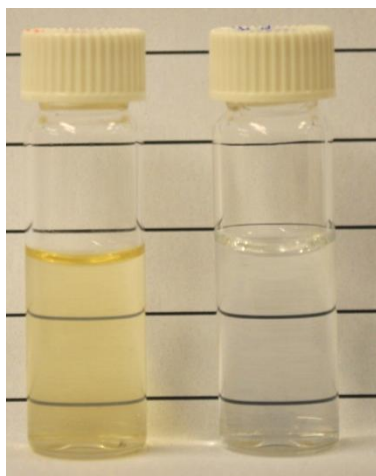


Figure 7. 1 Aqueous solutions of (a). NCC- C_{60} -(β -cyclodextrin) and (b). NCC.

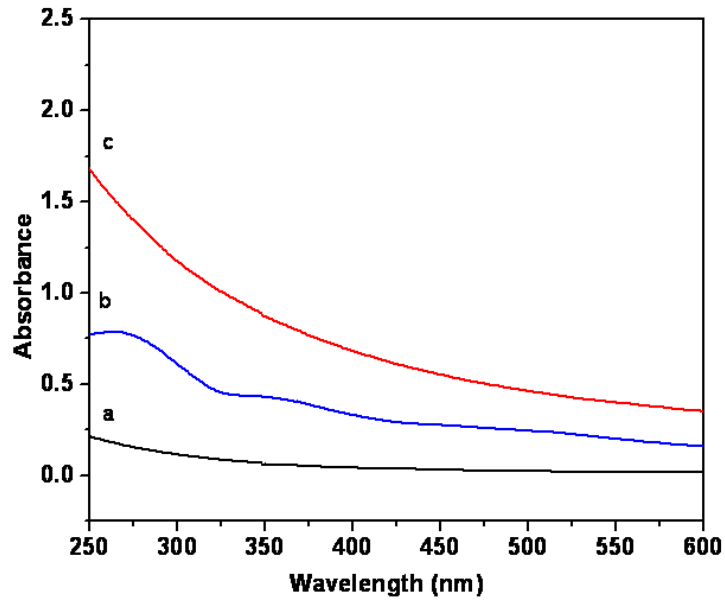


Figure 7. 2 UV-Vis spectrum of (a). NCC and (b). NCC-C₆₀-(β-cyclodextrin) and (c). NCC-C₆₀-(PMEO₂MA-*stat*-POEGMA₃₀₀) in water solution.

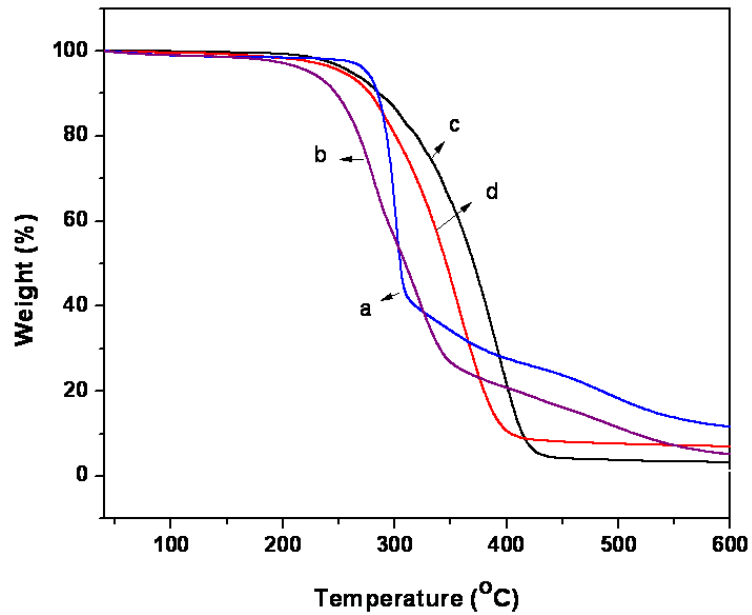


Figure 7. 3 TGA curves of (a). NCC; (b). NCC-C₆₀-(β-cyclodextrin); (c). (PMEO₂MA-*stat*-POEGMA₃₀₀)-C₆₀ and (d). NCC-C₆₀-(PMEO₂MA-*stat*-POEGMA₃₀₀).

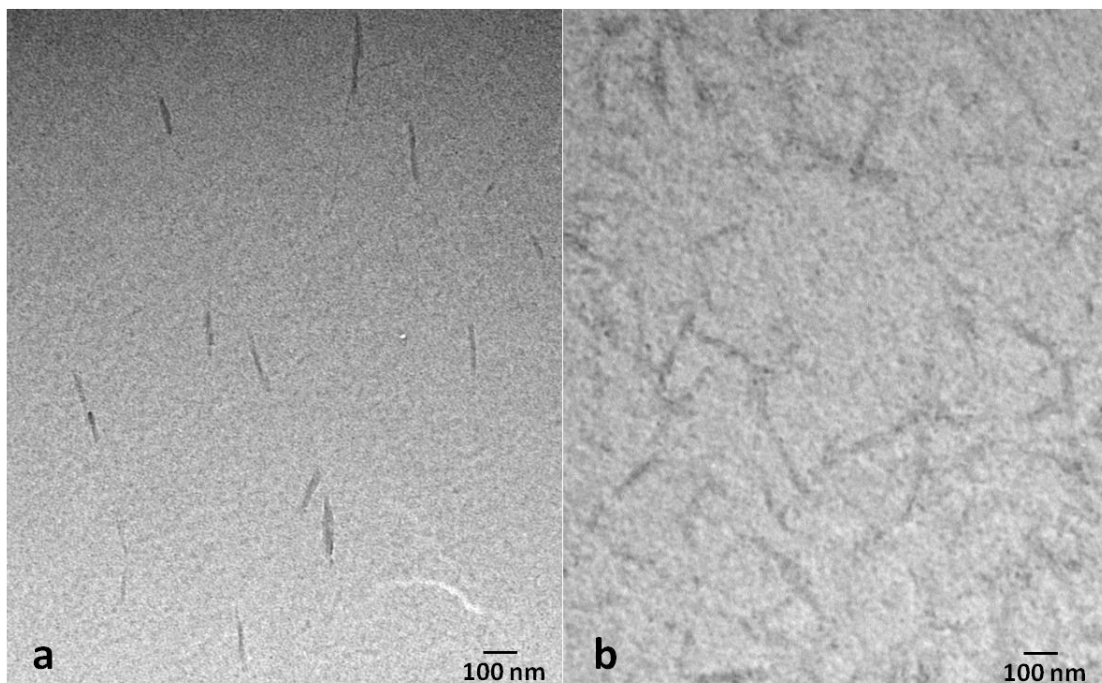


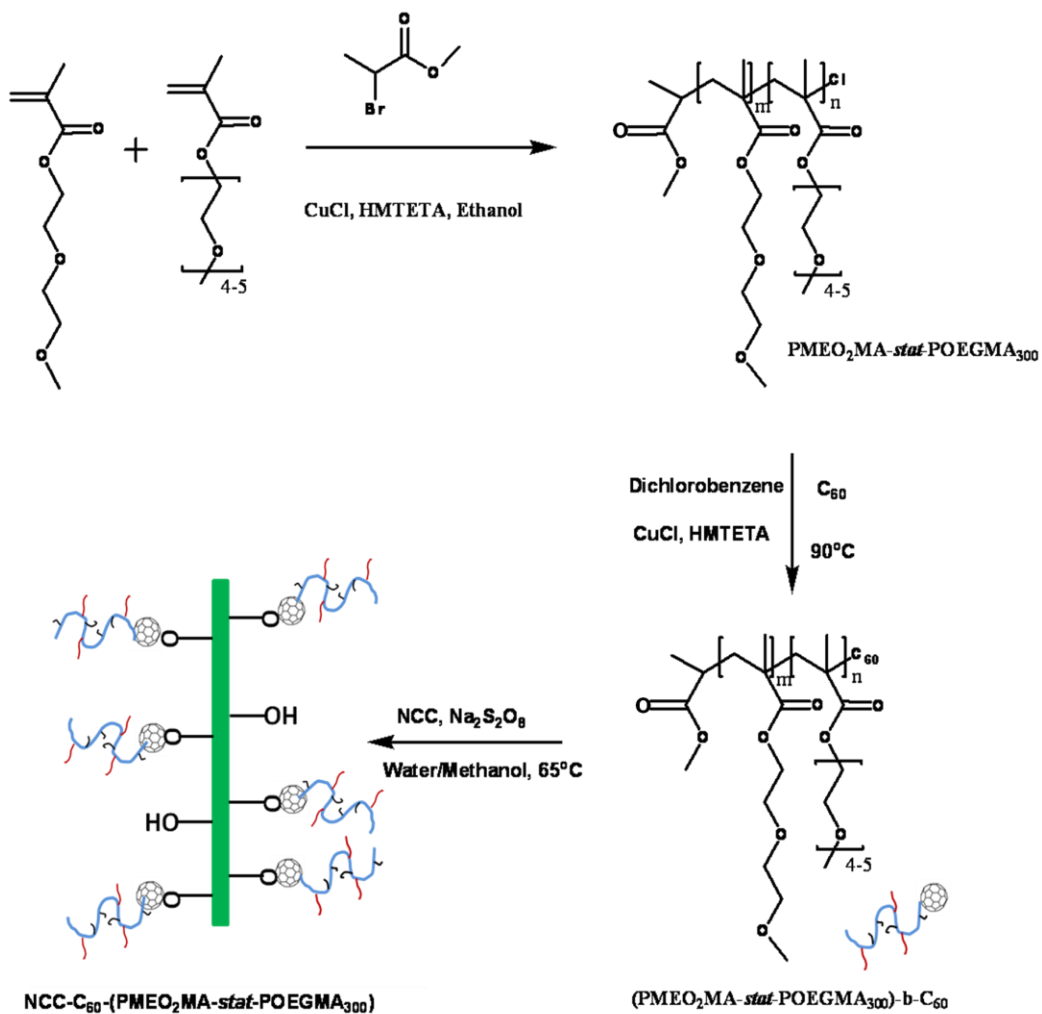
Figure 7. 4 TEM images of (a). NCC-C₆₀-(β-cyclodextrin) and (b). NCC-C₆₀-(PMEO₂MA-*stat*-POEGMA₃₀₀).

7.3.2 Synthesis and characterization of NCC-C₆₀-(PMEO₂MA-*stat*-POEGMA₃₀₀)

The successful modification of NCC by C₆₀-(β-cyclodextrin) using the radical coupling reaction prompted us to extend this grafting process to functionalize NCC with other fullerene containing derivatives. Therefore, a polymer functionalized C₆₀, i.e. (PMEO₂MA-*stat*-POEGMA₃₀₀)-*b*-C₆₀ was used to modify NCC to further explore the validity of this approach. A three-step reaction (Scheme 2) was adopted to synthesize NCC-C₆₀-(PMEO₂MA-*stat*-POEGMA₃₀₀). Firstly, a statistical copolymer consisting of MEO₂MA and OEGMA₃₀₀ units was prepared by ATRP at a feeding composition of 7 to 3 in the presence of HMTETA/CuCl as catalyst and ethanol as the solvent. PMEO₂MA-*stat*-POEGMA₃₀₀ was then capped with C₆₀ using ATRA catalyzed by HMTETA/CuCl in dichlorobenzene at 90 °C to produce (PMEO₂MA-*stat*-POEGMA₃₀₀)-*b*-C₆₀. Lastly, the radical coupling reaction was performed to prepare

(PMEO₂MA-*stat*-POEGMA₃₀₀)-*b*-C₆₀-NCC by mixing NCC, (PMEO₂MA-*stat*-POEGMA₃₀₀)-*b*-C₆₀ and sodium persulfate in 35% methanol/water (v%) under an argon atmosphere. The utilization of methanol/water instead of water as the solvent was to prevent the occurrence of precipitation caused by the thermal responsive behavior of POEGMA, since (PMEO₂MA-*stat*-POEGMA₃₀₀)-*b*-C₆₀ prepared in this study possessed a LCST of 45 °C in water, which is below the reaction temperature of 65 °C. As described in Chapter 6, the addition of methanol increases the LCST of (PMEO₂MA-*stat*-POEGMA₃₀₀)-*b*-C₆₀, thereby ensuring that the reaction mixture was homogeneous during the reaction.

Synthesis and characterization of PME₂O₂MA-*stat*-POEGMA₃₀₀ was described in Chapter 6. ¹H NMR spectra for (PMEO₂MA-*stat*-POEGMA₃₀₀)-C₆₀ and NCC-C₆₀-(PMEO₂MA-*stat*-POEGMA₃₀₀) are shown in Figure 7.5. The peaks in Figure 7.5(i) are identical with those in Figure 7.5(ii), which confirmed that (PMEO₂MA-*stat*-POEGMA₃₀₀)-*b*-C₆₀ was successfully grafted to NCC via the radical coupling reaction. The unreacted PME₂O₂MA-*stat*-POEGMA₃₀₀)-*b*-C₆₀ were removed by washing the product thoroughly with THF since PME₂O₂MA-*stat*-POEGMA₃₀₀)-*b*-C₆₀ is soluble, whereas NCC-C₆₀-(PMEO₂MA-*stat*-POEGMA₃₀₀) is not soluble in THF. The UV-Vis spectra of the aqueous solution of NCC-C₆₀-(PMEO₂MA-*stat*-POEGMA₃₀₀) (Figure 7.2c) is clearly different from NCC (Figure 7.2a). The excess absorption in the range of 260 to 350 nm is a characteristic absorption for covalently functionalized C₆₀, which implies that a covalent linkage was formed between POEGMA and C₆₀, and NCC and C₆₀. It should be noted the absorption profiles in Figure 7.2c are different from that in Figure 7.2b, which might be associated with the different functionality of C₆₀. For instance, the absorption at 330 nm was not observed for polystyrene [Chubarova et al. 2008] and PNIPAM [Zhou et al. 2007] functionalized C₆₀.



Scheme 7. 2 Synthetic scheme for $\text{NCC-C}_{60}\text{-(PMEO}_2\text{MA-}stat\text{-POEGMA}_{300})$

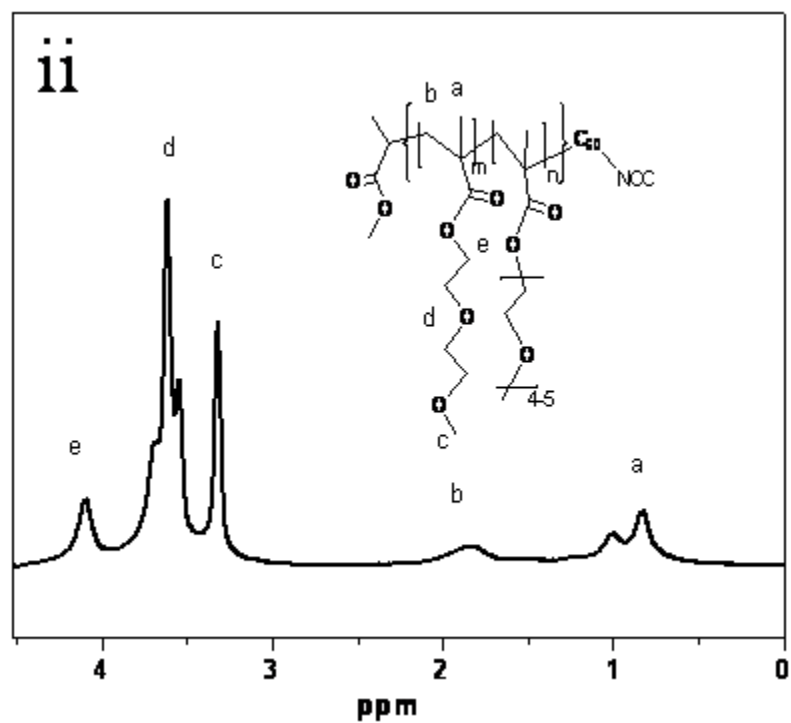
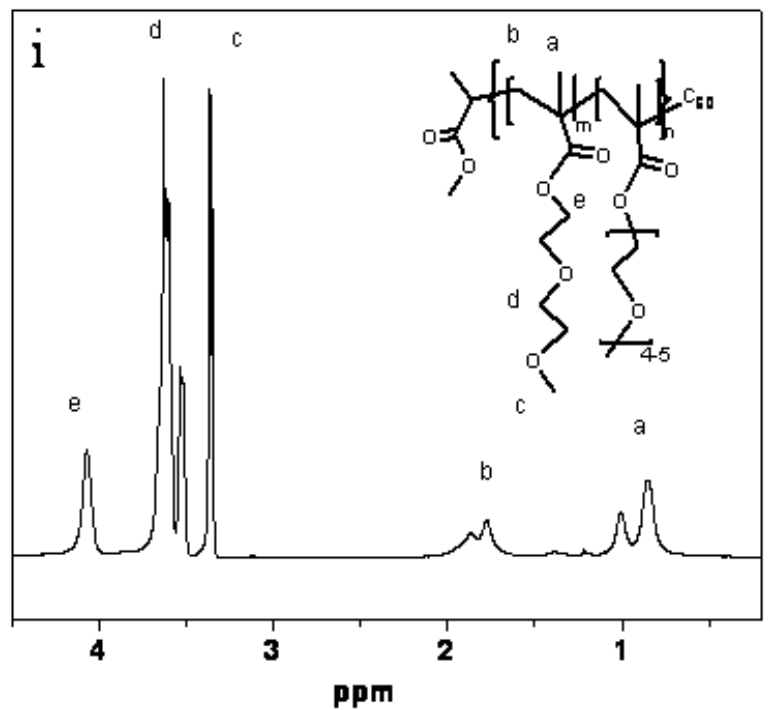


Figure 7.5 ^1H NMR spectra for (i). $(\text{PMEO}_2\text{MA-}stat\text{-POEGMA}_{300})\text{-}b\text{-C}_{60}$ (in CDCl_3) and (ii). $\text{NCC-C}_{60}\text{-(PMEO}_2\text{MA-}stat\text{-POEGMA}_{300})$ (in D_2O).

The thermal degradation behavior of NCC-C₆₀-(PMEO₂MA-*stat*-POEGMA₃₀₀) was also monitored by TGA as shown in Figure 7.3d. The degradation profile of NCC-C₆₀-(PMEO₂MA-*stat*-POEGMA₃₀₀) showed a broader temperature range compared to the degradation of NCC. The profile only revealed one pyrolysis process, which indicated that the pyrolysis associated with the sulfate groups was retarded.

The thermal responsive behavior of NCC-C₆₀-(PMEO₂MA-*stat*-POEGMA₃₀₀) was monitored by recording the cloud point of the solution using the turbidity measurements. Figure 7.6a shows the optical transmittance as a function of temperature upon heating (recorded at the wavelength of 500 nm at a heating or cooling rate of 1 °C/min) for a 4 mg/mL aqueous solution of NCC-C₆₀-(PMEO₂MA-*stat*-POEGMA₃₀₀). Upon heating, the solution became turbid when temperature exceeded the LCST of ca. 47.5 °C, which was determined from the corresponding differential curve (Figure 7.6b). Upon cooling, the solution became clear again when temperature was lower than 44 °C. A limited hysteresis was observed (difference between heating and cooling cycles) when cycling above/below the LCST of POEGMA analogues. [Lutz et al. 2006a] The hysteresis phenomenon for NCC-C₆₀-(PMEO₂MA-*stat*-POEGMA₃₀₀) may be attributed to the adsorption of POEGMA chain on fullerene molecules or NCC surfaces above the LCST. Similar observation was noticed for the system of PNIPAM and polystyrene particles. [Gao et al. 1997]

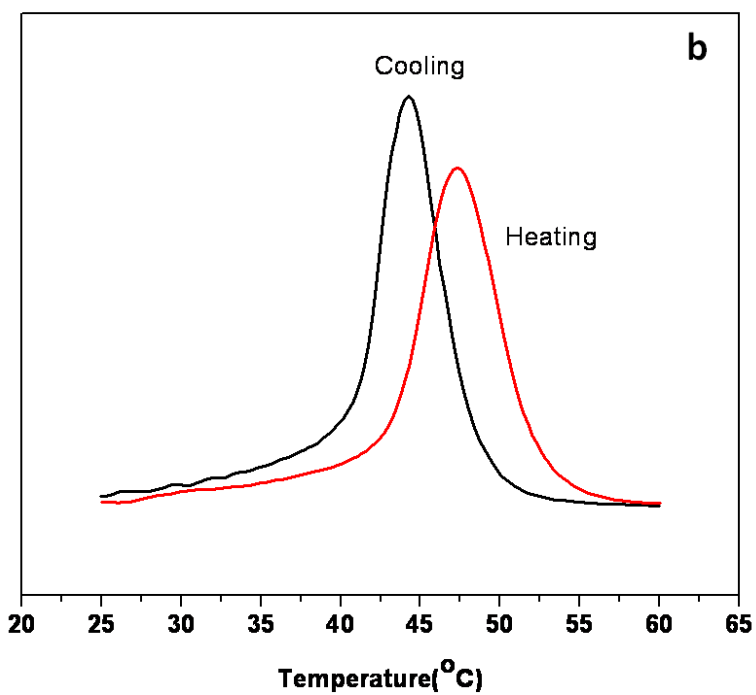
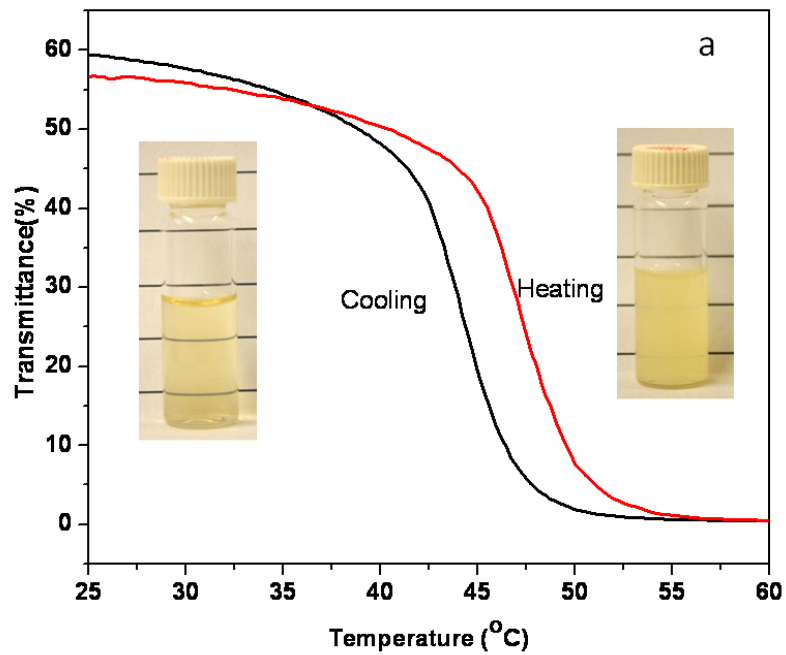


Figure 7. 6(a). UV–Vis experiment to measure the phase transitions upon heating and cooling the aqueous solution of NCC- C_{60} -(PMEO₂MA-*stat*-POEGMA₃₀₀) (4 mg/mL) and (b). Differential curves of Figure 7.6a.

7.3.3 Radical scavenging of DPPH

Finally, we evaluated the radical scavenging or antioxidant property of the prepared NCC-fullerene compounds using the stable free radical, 2,2-diphenyl-1-picrylhydrazyl (DPPH). The visual bleaching from purple to yellow color when mixing the prepared compounds with DPPH solution in dimethyl sulfoxide (DMSO) was observed. This process was also monitored by UV-Vis spectroscopy and shown in Figure 7, which showed a reduction in the peak absorbance at 520 nm when the NCC compounds were mixed with DPPH solution. We concluded these NCC-fullerene systems demonstrated a radical scavenging activity.

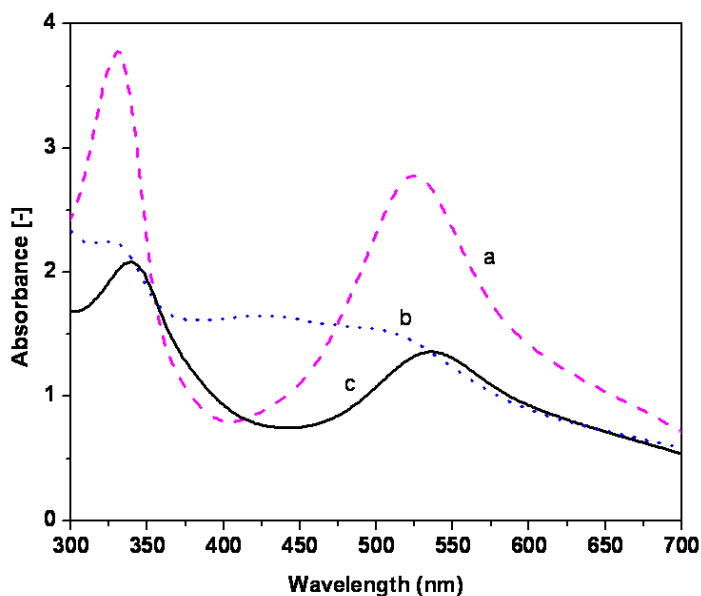


Figure 7. 7 UV-Vis to measure the DPPH radical scavenging activity: (a). DPPH in DMSO solution, (b). DPPH solution mixed with NCC-C₆₀-(β-cyclodextrin) ; (c). DPPH solution mixed with NCC-C₆₀-(PMEO₂MA-*stat*-POEGMA₃₀₀).

7.4 Conclusions

Nanocrystalline cellulose (NCC) was modified with fullerene derivatives, i.e. non-covalent complex of C₆₀-(β-cyclodextrin) and covalently functionalized (PMEO₂MA-*stat*-

POEGMA₃₀₀)-C₆₀ through a radical coupling reaction. The NCC-C₆₀ compounds synthesized by this facile reaction were characterized by UV-vis, NMR, TGA and TEM. It was observed that the NCC-C₆₀-(β -cyclodextrin) and NCC-C₆₀-(PMEO₂MA-*stat*-POEGMA₃₀₀) dispersed readily in aqueous solution. NCC-C₆₀-(β -cyclodextrin) possessed a similar thermal degradation behavior with NCC, however it exhibited a broader temperature range. The first pyrolysis process observed in pristine NCC was not evident in NCC-C₆₀-(PMEO₂MA-*stat*-POEGMA₃₀₀) system. TEM micrographs confirmed that the shape of the initial nanocrystals of cellulose remained largely unchanged for both samples. In addition, NCC-C₆₀-(PMEO₂MA-*stat*-POEGMA₃₀₀) demonstrated thermal responsive behavior in water solution and there was ~3.5 °C hysteresis associated with the heating/cooling cycle. In addition, the prepared NCC-fullerene systems demonstrated a radical scavenging activity (antioxidant) when screened with the 2,2-diphenyl-1-picrylhydrazyl (DPPH) in DMSO. We believe the method developed in this report can be extended to functionalize NCC with other chemical functionalized fullerene derivatives and the resulted NCC fullerene structures possess desirable properties that may have promising applications in the fields of biomedical, personal care, material chemistry and electronic.

Chapter 8 Conclusions and Recommendations

8.1 General Contributions

In the thesis, water-soluble fullerene containing polymers, such as PDMAEMA-C₆₀ with targeting moieties, POEGMA-C₆₀, and NCC-C₆₀ and NCC-C₆₀-POEGMA were synthesized and their solution properties were investigated. In addition, the drug loading and delivery using PDMAEMA-C₆₀ with targeting moieties was explored as well. At the same time, a thermo-responsive block copolymer composed of POEGMA analogues was synthesized and the self-assembly behavior was studied. The following conclusions can be drawn from this study.

8.1.1 PDMAEMA-C₆₀ with targeting moieties

PDMAEMA-C₆₀ with galactose functionality was successfully synthesized using the ATRP and ATRA process by removing the isopropylidene groups using TFA/water mixture. The self-assembly behaviour of PDMAEMA-C₆₀ with galactose moiety at different pH conditions were investigated by DLS. At pH 3 and 10, both polymeric micelles and unimers were present in aqueous solutions. However, smaller R_h was observed for PDMAEMA-C₆₀ samples at pH 10 than at pH 3. TEM images of the self-assembled micelles only showed the cores of the micelles due to the invisibility of PDMAEMA shells under TEM. SEM images showed the spherical particles with similar sizes to the data obtained from DLS. Chain-induced demicellization of PDMAEMA-C₆₀ aggregates by free PDMAEMA chains was observed at pH 10, and the physical mechanism for this process was elucidated. Besides pH and temperature, free PDMAEMA chains may be added to trigger and control the release of drugs.

Two model drugs, namely fluorescein and pyrene were employed to evaluate the location of drugs in the self-assembled structure of PDMAEMA-C₆₀. Results showed that these model hydrophobic drugs were encapsulated in the PDMAEMA shell, but also in the hydrophobic

fullerene core. Also, ITC results indicated that the binding energy for PDMAEMA-C₆₀ were lower than PDMAEMA for both model drugs. The drug delivery results showed that PDMAEMA-C₆₀ is an efficient drug carrier, however, it displayed cytotoxicity to the cells. The gene transfection efficacy of PDMAEMA-C₆₀ to different cell lines were investigated and results demonstrated PDMAEMA-C₆₀ possessed good gene transfection performance.

8.1.2 Block copolymer of POEGMA analogues

Well-defined diblock copolymer of (PMEO₂MA-*stat*-POEGMA₃₀₀)-*b*-PMEO₂MA was successfully synthesized via ATRP. The critical micelle temperature (CMT) of (PMEO₂MA-*stat*-POEGMA₃₀₀)-*b*-PMEO₂MA in aqueous solution was ~ 30 °C derived from the optical transmittance and DSC measurements. Core-shell micelles with R_h ranging from 40 to 60 nm were formed over a temperature range of 34 to 38 °C, whereas larger aggregates with R_h of 95 nm were formed at 45 °C. In addition, the aggregation number of aggregates increased significantly from 76 to ~9800, and R_g/R_h ratio also increased from 0.75 to 1.13 when the temperature was increased from 34 to 45 °C, which indicated that changes of morphology had occurred. It was proposed that the block copolymer forms core-shell micelles with the temperature range from CMT (30 °C) to the LCST of the PME₂O₂MA-*co*-POEGMA₃₀₀ (40 °C) and eventually large aggregates are produced.

8.1.3 Synthesis of thermal responsive POEGMA-C₆₀ and its self-assembly in solvent mixtures

Amphiphilic (PMEO₂MA-*stat*-POEGMA₃₀₀)-C₆₀ copolymer synthesized via ATRP and ATRA techniques formed spherical micelles in methanol/water mixtures of various compositions. The LCST of PME₂O₂MA-*stat*-POEGMA₃₀₀ and (PME₂O₂MA-*stat*-POEGMA₃₀₀)-C₆₀ increased with increasing methanol content. Lower LCSTs were observed for (PME₂O₂MA-

stat-POEGMA₃₀₀)-C₆₀ than PMEO₂MA-*stat*-POEGMA₃₀₀. With increasing methanol content, the CMC increased and larger micellar aggregates were formed. Core-shell micelles and large aggregates at temperature below and above the LCST were also observed by TEM.

8.1.4 Synthesis of NCC-C₆₀-(β-cyclodextrin) and NCC-C₆₀-POEGMA and their physical properties

NCC was modified with C₆₀-(β-cyclodextrin) and (PMEO₂MA-*stat*-POEGMA₃₀₀)-C₆₀ through a radical coupling reaction to produce NCC-C₆₀-(β-cyclodextrin) and NCC-C₆₀-(PMEO₂MA-*stat*-POEGMA₃₀₀). NCC-C₆₀-(β-cyclodextrin) possessed a similar thermal degradation behavior with NCC with a broader temperature range. NCC-C₆₀-(PMEO₂MA-*stat*-POEGMA₃₀₀) demonstrated thermal responsive behavior in water with a ~3.5 °C hysteresis that is associated with the heating/cooling cycle. Both NCC-fullerene systems demonstrated a radical scavenging activity when screened with 2,2-diphenyl-1-picrylhydrazyl (DPPH). We believe this radical coupling reaction can be easily applied to modify NCC with other chemical functionalized fullerene derivatives, thus the application of C₆₀ and NCC can be extended.

8.2 Recommendations for future work

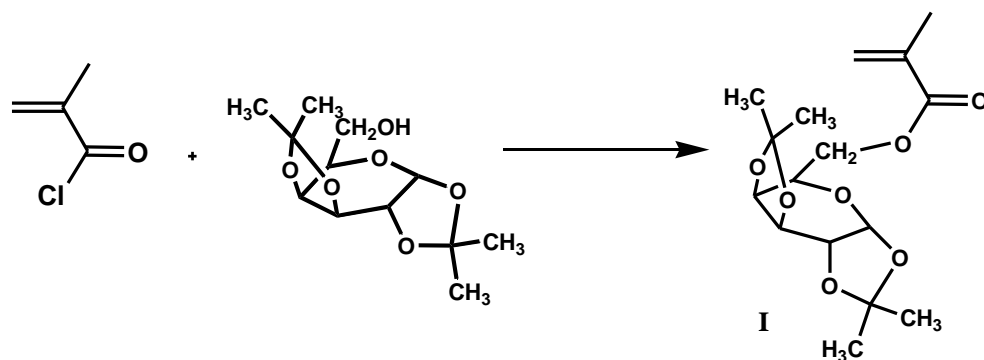
The results obtained in this thesis confirmed the followings:

- (1) the possibility of using water-soluble fullerene containing polymer as drug or gene carriers;
- (2) biocompatible responsive copolymers with and without fullerene may be beneficial to the biological field;
- (3) the radical coupling reaction to modify NCC with water-soluble C₆₀ derivatives may result in the development of a new class of novel materials with fascinating properties.

However, research is a continuous activity, hence there are many different areas that should and can be explored. Based on the results obtained so far, the following recommendations for future studies are proposed.

8.2.1 Improving the targeting efficacy of fullerene containing polymer for drug delivery applications

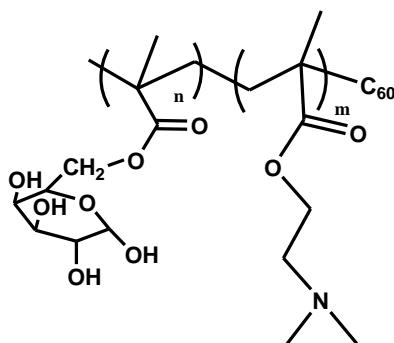
PDMAEMA-C₆₀ with galactose targeting moieties were expected to have better drug delivery efficiency to liver cells, however, we did not observe any difference in terms of the drug delivery to HepG2 and N2a cells comparing to the PDMAEMA-C₆₀ without targeting ligands. The targeting issue that needs to be addressed in the future work is increasing the galactose content so that more targeting moieties can be located at the coronas of PDMAEMA-C₆₀ micelles, therefore better targeting can be achieved. This can be accomplished by synthesizing structure I by reacting 1,2:3,4-Di-O-isopropylideneD-galactopyranose with methacryloyl chloride, then synthesize block copolymer of structure I and monomers like DMAEMA or OEGMA (here use DMAEMA as an example) using ATRP, finally end cap the copolymer with C₆₀ and removing the protecting groups. The galactose content can be varied by making different molecular weights for the block with galactose (Scheme 8.1).



1) ATRP to make block copolymer with DMAEMA

2) ATRA to add C₆₀ to the end

3) Remove isopropylidene by acid treatment



Scheme 8. 1 Synthetic scheme of PDMAEMA-C₆₀ with different galactose contents.

8.2.2 Block copolymers of POEGMA analogues with different LCSTs

The POEGMA block copolymer and POEGMA-C₆₀ systems needs to be studied in more detail. In this thesis, we only synthesized a block copolymer i.e. (PMEO₂MA-*stat*-POEGMA₃₀₀)-*b*-PMEO₂MA with LCSTs of 45 °C and 26 °C for each block. In the future work, block copolymers with LCSTs of 37°C and 26 °C, 60 °C and 26 °C should be prepared by varying the feed ratios of MEO₂MA and OEGMA₃₀₀, the thermal responsive behavior will be explored as well. Accordingly, one can make POEGMA-C₆₀ with different LCSTs in the future as well.

Drug release behavior using these block copolymers with and without C₆₀ at different temperatures can be explored. Temperature dependent release behaviors are expected for these POEGMA based systems.

8.2.3 Other methods to modify NCC using fullerene derivatives

NCC-fullerene is a new class of nanocomposite, which combines the beneficial properties of fullerene and NCC together and is expected to have significant impacts on material chemistry and biological fields. In this thesis, we developed a radical coupling method to modify NCC with fullerene derivatives and other methods to modify NCC with fullerenes need to be explored in the future. For instance, different functional groups, such as -NH₂, -N₃, and -Br or -Cl, can be attached to the surface of NCC via chemical reactions between selected chemical structures and the OH groups on NCC. Fullerene and its polymer derivatives can be used to modify these NCC bearing different functional groups through the established methods including amine addition, azido coupling, ATRA etc. The physical properties of the resultant NCC-fullerene nanocomposites should be investigated and the applications of this new class of nanomaterials should be explored in the future work.

Appendix Drug delivery and gene transfection using PDMAEMA-C₆₀

A.1 Materials

Fluorescein, HEPES buffer solution and tris acetate EDTA (TAE) were purchased from Sigma-Aldrich. Neuroblastoma cells (N2a) obtained from the American Type Culture Collection (CCL-131, ATCC, USA) were used. The cells were incubated in Dulbecco's modification of Eagle's medium (DMEM) with 10 % fetal bovine serum (FBS, Hyclone, Logan, UT) and 1 % penicillin and streptomycin under a humidified atmosphere with 5 % carbon dioxide (CO₂) at 37 °C. The plasmid DNA (pIRES-EGFP-EV71) used in this experiment expresses enhanced green fluorescent protein (eGFP).

A.2 Experimental

A.2.1 Drug delivery

0.075 mg/mL PDMAEMA-C₆₀ and 2.5 µg/mL of fluorescein were used. The fluorescein and fluorescein loaded in PDMAEMA-C₆₀ was incubated with N2a (neuronal cell line) and HepG2 (liver cell line) cells for 24 hours. Eventually, the cells were observed using a fluorescence microscope (Zeiss, Thornwood, NY, USA).

A.2.2 Gene transfection

The PDMAEMA-C₆₀/DNA complexes were prepared by adding the polymer solution to plasmid DNA solution in HEPES solution (pH 7.4) at the appropriate polymer to DNA ratio (N/P ratio). The N/P ratio was expressed via the ratio of equivalents of DMAEMA units to the number of nucleotides in DNA.

For cell transfection experiments, different cells were seeded in a 12-well plate at a density of 40 000 cells per well and incubated for 24 hr at 37 °C under a humidified atmosphere with 5 % CO₂. All materials used, except for the polymer were passed through a 0.2 µm filter to

remove dust and microorganisms. The polyplexes were prepared in a 25 mM HEPES buffered solution at N/P of 20. The polyplexes were vortexed and incubated at room temperature for 15 min, followed by 10x dilution with serum-free media and incubated for an additional 15 min. 1 mL of the diluted polyplex solution was added to the wells and incubated at 37 °C for 1 hr. The wells were then centrifuged at 280 g for 5 min. The media was removed, rinsed with phosphate buffered saline (PBS), replaced with DMEM with 10 % FBS and incubated for 24 hr at 37 °C. To view the transfection efficiency, the medium was removed, rinsed with PBS three times and viewed with PBS under a fluorescence microscope. The efficiency was compared to a positive control, a solution of the PEI/DNA polyplex at N/P ratio of 20.

A.3 Results and Discussion

A.3.1 In vitro drug delivery study

In vitro drug delivery study using PDMAEMA-C₆₀ was performed and the intracellular behaviors of the drug loaded micelles were monitored with N2a (neuronal cell line) and HepG2 (liver cell line) using a fluorescence microscope. Figures A-1a and A-1b show the micrographs of HepG2 and N2a cells. Figures A-1c and A-1d show the micrograph for cells treated with fluorescein alone, and the results indicated that fluorescein did not penetrate the cellular membrane into the cellular compartment because no fluorescence was observed. However, the drug loaded PDMAEMA-C₆₀ can readily enter the cells (Figures A-1d and A-1f). This model studies suggest that PDMAEMA-C₆₀ can be used as drug carrier to deliver hydrophobic drugs to various types of cells. However, it was observed that the viability of HepG2 and N2a cells was reduced after being incubated with drug loaded PDMAEMA-C₆₀ complex. It was suspected that PDMAEMA-C₆₀ could be cytotoxic and reduced the viability of cells. This was confirmed using trypan blue because trypan blue is able to penetrate unhealthy cells, and not live cells. After 24

hour incubation of PDMAEMA with cells, most of the cells were stained red indicating the possible penetration of trypan blue into the cells (Figure A-2). In fact, studies showed that the toxicity of polyamines in the following order: branched PEI = star-shaped PDMAEMA > linear PEI >> linear PDMAEMA = highly-branched PDMAEMA. [Schallon et al. 2010]. Since PDMAEMA-C₆₀ formed core-shell micelles, which can be considered as star-shaped PDMAEMA, the cytotoxicity is higher than linear PDMAEMA and branched PDMAEMA. In addition, targeting capability was also investigated by comparing the delivery results using PDMAEMA-C₆₀ with and without galactose targeting ligands. It was observed that the delivery efficiency to HepG2 and N2a cells were very similar for both PDMAEMA-C₆₀ with and without galactose targeting moieties, suggesting that the targeting efficacy for the carriers using PDMAEMA-C₆₀ with galactose targeting ligands was very low. This might be due the entrapment of galactose moieties within the micelles, which lowers the galactose content on the shell of the micelles, thus the targeting efficiency of the carriers was retarded.

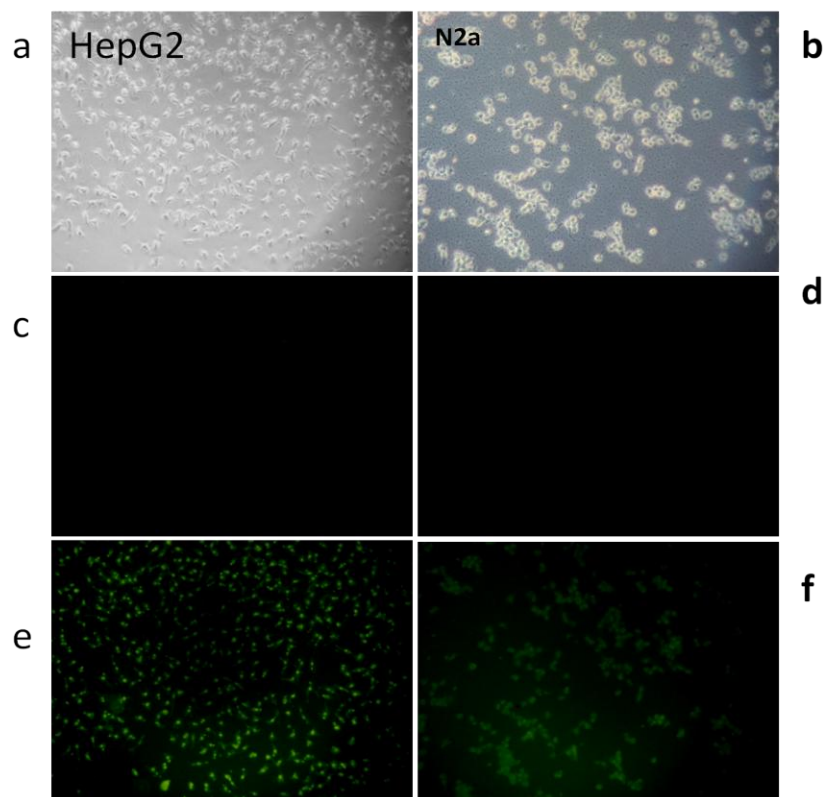


Figure A-1 Micrographs of cells (a) HepG2; (b) N2a; (c) HepG2 with fluorescein; (d) N2a with fluorescein; (e) HepG2 with fluorescein loaded PDMAEMA-C₆₀; (f) N2a with fluorescein loaded PDMAEMA-C₆₀

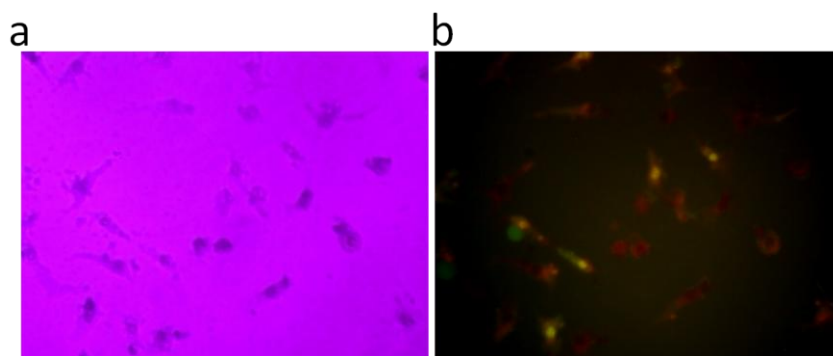


Figure A-2 Addition of trypan blue to (a). HepG2 cells; (b). HepG2 cells treated fluorescein loaded PDMAEMA-C₆₀.

A.3.2 Gene transfection using PDMAEMA-C₆₀

PDMAEMA is a water-soluble cationic polymer, which can bind to DNA via electrostatic interaction and can be used as a gene transfer agent. [Wetering et al. 1998, Verbaan et al. 2001, van Steenis et al. 2003] The transfection efficiency depended on the polymer composition. A variety of degradable hyper-branched poly(ester amine)s containing primary, secondary and tertiary amino groups were synthesized and evaluated as non-viral gene carriers, where their polymer–DNA complexes (polyplexes) were examined. [Zhong et al. 2005, Kurisawa et al. 2000] The highest transfection efficiency and low cytotoxicity rendered these hyper-branched poly(ester amine)s as safe and efficient gene-delivery vehicles. PDMAEMA facilitated cell transfection by being endocytosed, complexed with DNA, and subsequently acting as a “proton sponge” to disrupt the endosomes/lysosomes that released the DNA to the cytosol. [Jones et al. 2004] In this study, the transfection efficiency of PDMAEMA-C₆₀ and plasmid complexes was evaluated in different cell lines including HepG2, N2a and NG108 cell lines. The N/P ratio used in the study was 20. As a comparison, linear PEI was used as a control. Figure A-3 shows the transfection of pDNA using PDMAEMA-C₆₀ and the results showed that pDNA could be transfected to different cells by forming polyplex with PDMAEMA chains. Figure A-4 showed the transfection results using linear PEI. Comparing these two figures, we could observe that the transfection efficiency of PDMAEMA-C₆₀ was lower than LPEI. Also we noticed that the PDMAEMA-C₆₀ with targeting moieties possessed a lower transfection efficiency. This might be due to the partial hydrolysis of ester group of PDMAEMA.

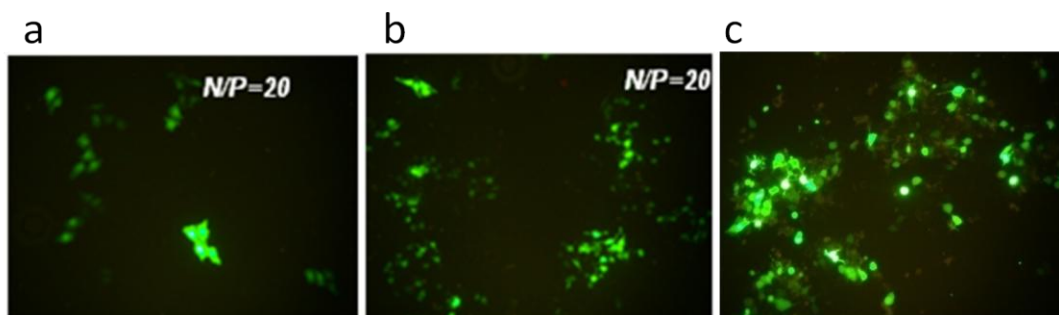


Figure A-3 Fluorescence micrographs ($\times 10$) of the gene expression using PDMAEMA- C_{60} at N/P 20 to different cells (a). HepG2; (b). N2a and (c). NG108.

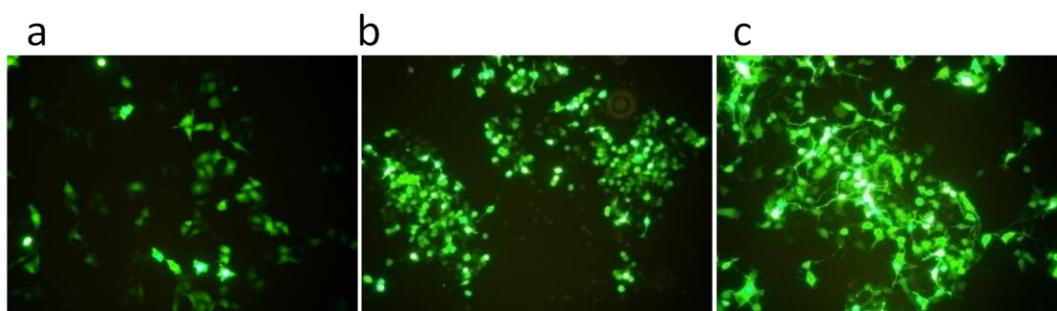


Figure A-4 Fluorescence micrographs ($\times 10$) of the gene expression using a positive control with LPEI at N/P 20 to different cells (a). HepG2; (b). N2a and (c). NG108.

A.4 Conclusions

The intracellular delivery of model drugs to different cell lines using PDMAEMA- C_{60} as drug carriers, and it was observed that PDMAEMA- C_{60} is an efficient drug carrier. However, the cell viability was reduced. In addition, PDMAEMA- C_{60} exhibited good gene transfection performance, but it was less efficient than LPEI polymer. All these preliminary results indicated that PDMAEMA- C_{60} could be an efficient drug delivery agent if the cytotoxicity can be lowered. Therefore developing other C_{60} -polymer systems with poly(ethylene-glycol) chains may reduce the toxicity of the delivery vehicles.

References

- Adams, M.L., Lavasanifar, A., Kwon G.S., Amphiphilic block copolymers for drug delivery, *J. Pharm. Sci.* 92, 1343-1355 (2003).
- Agarwal, M., Xing, Q., Shim, B.S., Kotov, N., Varahramyan, K., Lvov, Y., Conductive paper from lignocellulose wood microfibers coated with a nanocomposite of carbon nanotubes and conductive polymers, *Nanotechnology*, 20, 215602 (2009).
- Aguiar, J., Molina-Bolivar, J.A, Peula-Garcia, J.M., Ruiz C.C., Thermodynamics and micellar properties of tetradecyltrimethylammonium bromide in formamide-water mixtures, *J Colloid Interface Sci.* 255, 382-90 (2002).
- Akasaka, T., Suzuki, T., Maeda, Y., Ara, M., Wakahara, T., Kobayashi, K., Nagase, S., Kako, M., Nakadaira, Y., Fujitsuka, M., Ito, O., Photochemical Bissilylation of C₆₀ with Disilane, *J. Org. Chem.*, 64, 566-569 (1999).
- Akcasu, AZ, Han, CC., Molecular Weight and Temperature Dependence of Polymer Dimensions in Solution, *Macromolecules*, 12, 276-280 (1979).
- Aliabadi, H. M., Elhasi, S., Mahmud, A., Gulamhusein R., Mahdipoor, P., Lavasanifar, A., Encapsulation of hydrophobic drugs in polymeric micelles through co-solvent evaporation: The effect of solvent composition on micellar properties and drug loading, *Int. J. Pharmaceutics*, 329, 158-165 (2007).
- Aliabadi, H.M., Lavasanifar, A., Polymeric micelles for drug delivery, *Expert Opin Drug Deliv.*, 3, 139-62 (2006).
- Anderson, T., Nilsson, K. Sundahl, M., Westman, G., Wennerstrom, O., C₆₀ embedded in γ -cyclodextrin: a water-soluble fullerene, *Chem. Comm.*, 604-606 (1992).
- Ando, T., Kamigaito, M., Sawamoto, M., Iron (II) Chloride Complex for Living Radical Polymerization of Methyl Methacrylate, *Macromolecules*, 30, 4507-4510 (1997).

Arotcarena, M., Heise, B., Ishaya, S., Laschewsky, A., Switching the Inside and the Outside of Aggregates of WaterSoluble Block Copolymers with Double Thermoresponsivity, *J. Am. Chem.Soc.*, 124, 3787-3793 (2002).

Ashcroft, J.M., Tsyboulski, D.A., Hartman, K.B., Zakharian, T.Y., Marks, J.W., Weisman, R.B., Rosenblum, M.G., Wilson, L.J., Fullerene (C₆₀) immunoconjugates: interaction of water-soluble C₆₀ derivatives with the murine anti-gp240 melanoma antibody, *Chem. Commun.*, 3004-3006 (2006).

Ashwelland, G., Harford, J. Carbohydrate-specific receptors of the liver, *Ann. Rev. Biochem.* 51, 531-554 (1982).

Atwood, J. L., Koutsantonis, G. A., Raston, C. L., Purification of C₆₀ and C₇₀ by selective complexation with calixarenes, *Nature*, 368, 229-231 (1994).

Audouin, F., Nuffer, R., Mathis, C., Synthesis of Di- and Tetra-Adducts by Addition of Polystyrene Macroradicals onto Fullerene C₆₀, *J. Polym. Sci. Pol. Chem.*, 42, 3456-3463 (2004).

Augusto, V., Baleizao, C., Berberan-Santos, M.N., Farinha, J.S., Oxygen-proof fluorescence temperature sensing with pristine C₇₀ encapsulated in polymer nanoparticles, *J. Mater. Chem.*, 20, 1192-1197(2010).

Bader, H., Ringsdorf, H., Schmidt, B., water-soluble polymers in medicine, *Angew. Makromol. Chem.* 123, 457-485 (1984).

Bakry, R., Vallant, R.M., Najam-ul-Haq, M., Matthias, R., Szabo, Z., Huck, C.W., Bonn, G.K., Medicinal applications of fullerenes, *International Journal of Nanomedicine*, 2, 639–649 (2007).

Beers, K. L., Boo, S., Gaynor, S. G., Matyjaszewski, K., Atom Transfer Radical Polymerization of 2-Hydroxyethyl Methacrylate, *Macromolecules*, 32, 5772-5776 (1999).

Benoit, D., Harth, E., Fox, P., Waymouth, R.M., Hawker, C.J., Accurate Structural Control and Block Formation in the Living Polymerization of 1,3-Dienes by Nitroxide-Mediated Procedures, *Macromolecules*, 33, 363-370 (2000).

Bensasson, R. V., Bienvenue, F., Dellinger, S., Leach, S., Seta, P., C₆₀ in Model Biological Systems. A Visible-UV Absorption Study of Solvent-Dependent Parameters and Solute Aggregation, *J. Phys. Chem.*, 98, 3492-3500 (1994).

Bes, L., Angot, S. Limer, A. Haddleton, D.M., Sugar-Coated Amphiphilic Block Copolymer Micelles from Living Radical Polymerization: Recognition by Immobilized Lectins, *Macromolecules*, 36, 2493-2499 (2003).

Bosi S., Feruglio, L., Ros, T.D., Spalluto, G., Gregoretti, B., Terdoslavich, M., Decorti, G., Passamonti, S., Moro, S., Prato, M., Hemolytic effects of water-soluble fullerene derivatives, *J. Med. Chem.*, 47, 6711-6715(2004).

Bosi S., Ros, T. D., Spalluto, G., Prato, M., Fullerene derivatives: an attractive tool for biological applications, *Eur. J. Med. Chem.*, 38, 913-923 (2003).

Braunecker, W.A., Itami, Y., Matyjaszewski, K., Osmium-Mediated Radical Polymerization, *Macromolecules*, 38, 9402-9404 (2005).

Bronich, T. K., Keifer, P. A., Shlyakhtenko, L.S., Kabanov, A.V., Polymer micelle with cross-linked ionic core, *J. Am. Chem. Soc.* 127, 8236-8237 (2005).

Brown, P., Kamat, P.V., Quantum Dot Solar Cells. Electrophoretic Deposition of CdSe-C₆₀ Composite Films and Capture of Photogenerated Electrons with nC₆₀ Cluster Shell, *J Am Chem Soc.*, 130, 8890-8891 (2008)

Cerar, J., Skerjanc, J., Water-Soluble Fullerenes. 3. Alkali Salts of Fullerenehexamalononic AcidT_h-C₆₆(COOH)₁₂, *J. Phys. Chem. B.*, 10, 8255-8259 (2003).

Chen, Y., Huang, Z.E., Cai, R.F., Yu, B.C., Polymeric modification and functionalization of [60] fullerene, *Eur. Polym. J.*, 34, 137-151 (1998).

Chen, Y., Huang, W.S. , Huang, Z.E., Cai, R.F., Yu, H.K., Chen, S.M., Yan, X.M., Synthesis and characterization of a soluble and starlike copolymer, *Eur. Polym. J.*, 33, 823-828 (1997).

Chen, Y., Huang, Z.E., Cai, R.F., Fan, D., Hou, X., Yan, X., Chen, S., Jin, W., Pan, D., Wang, S., Photoconductivity and paramagnetism of fullerene chemically modified polymers, *J. Appl. Polym. Sci.*, 61, 2185 -2190 (1996).

Chen, Y., Wang, Y., Rassat, A., Sinay, P., Zhao, Y., Zhang, Y., Synthesis of Water-Soluble 2-Alkylcyclodextrin-C₆₀ Conjugates and Their Inclusion Complexation in Aqueous Solution, *Tetrahedron*, 62, 2045-2049 (2006).

Cheng, Z. P., Zhu, X.L., Kang, E.T., Neoh, K.G., Brush-type amphiphilic diblock copolymers from "livings"/ controlled radical polymerizations and their aggregation behavior, *Langmuir*, 21, 7180-7185 (2005).

Chiang, L.Y., Bhonsle, J.B., Wang, L. Shu, S.F., Chang, T.M., Hwu, J.R., Efficient one-flask synthesis of water-soluble [60]fullerenols, *Tetrahedron*, 52, 4963-4972 (1996).

Chiefari, J., Chong, Y.K., Ercole, F., Krstina, J., Jeffery, J., Le, T.P.T., Mayadunne, R.T.A., Meijs, G.F., Moad, C.L., Moad, G., Rizzardo, E., Thang, S.H., Living Free-Radical Polymerization by Reversible Addition-Fragmentation Chain Transfer: The RAFT Process, *Macromolecules*, 31,5559-5562 (1998).

Cho, K., Wang, X., Nie, S. Chen, Z., Shin, D.M., Therapeutic Nanoparticles for Drug Delivery in Cancer, *Clinic Cancer Research*, 14, 1310-1316 (2008).

Chochos, C. L., Kallitsis, J.K., Gregoriou, V., Rod-Coil Block Copolymers Incorporating Terfluorene Segments for Stable Blue Light Emission, *J. Phys. Chem. B*, 109, 8755-8760 (2005).

Christensen, J. E., Goodman, L., A mild method for the hydrolysis of acetal groups attached to sugars and nucleosides, *Carbohydr. Res.* 7, 510-512 (1968).

Chu, C.C., Wang, L., Ho, T.I., Synthesis of ABC-type miktoarm star polymers by “click” chemistry, ATRP and ROP, *Macromol. Rapid Commun.*, 26, 1179-1187 (2005).

Chubarova E.V., Melenevskaya, E.Y., Analysis of Interactions in fullerene-solvent-polymer system by UV-spectroscopy, *Fullerenes, Nanotubes and Carbon Nanostructures*, 16, 640-643 (2008).

Chung, J.E., Yokoyama, M., Aoyagi, T., Sakurai, Y., Okano T., Effect of molecular architecture of hydrophobically modified poly(N-isopropylacrylamide) on the formation of thermoresponsive core-shell micellar drug carriers, *J. Control. Release*, 53, 119-130 (1998).

Chung, J.E., Yokoyama, M., Okano, T., Inner core segment design for drug delivery control of thermo-responsive polymeric micelles, *J. Control. Release*, 65, 93-103 (2000).

Chung, J.E., Yokoyama, M., Suzuki, K., Aoyagi, T., Sakurai, Y., Okano, T., Reversibly thermo-responsive alkyl-terminated poly (N-isopropylacrylamide) core-shell micellar structures, *Colloids Surf. B, Biointerfaces*, 9, 37-48 (1997).

Chung, J.E., YokoyamaM., YamatoM., AoyagiT., Sakurai Y., Okano, T., Thermo-responsive drug delivery from polymeric micelles constructed using block copolymers of poly(Nisopropylacrylamide) and poly(butylmethacrylate), *J. Control. Release*, 2, 115-127 (1999).

Coca, S., Jasieczek, C. B., Beers, K. L., Matyjaszewski, K. Polymerization of acrylates by atom transfer radical polymerization. Homopolymerization of 2-hydroxyethyl acrylate, *J. Polym. Sci.: Part A: Polym. Chem.*, 36, 1417-1424 (1998).

Convertine, A.J., Lokitz, B.S., Vasileva, Y., Myrick, L.J., Scales, C.W., Lowe, A.B. McCormick, C.L., Direct Synthesis of Thermally Responsive DMA/NIPAM Diblock and DMA/NIPAM/DMA Triblock Copolymers via Aqueous, Room Temperature RAFT Polymerization, *Macromolecules*, 39, 1724-1730 (2006).

Croy, S.R., Kwon, G.S., Polymeric Micelles for drug delivery, *Curr Pharm Design*, 12, 4669-4684 (2006).

Dai, L., Advanced syntheses and microfabrications of conjugated polymers, C₆₀-containing polymers and carbon nanotubes for optoelectronic applications, *Polym. Adv. Technol.* 10, 357-420 (1999b).

Dai, L., Conjugated and fullerene-containing polymers for electronic and photonic applications: advanced syntheses and microlithographic fabrications, *J. Macromol. Sci. Rev. Macromol. Chem. Phys.* C39, 273-387 (1999a).

Dai, L., Mau, A.W.H., Controlled Synthesis and Modification of Carbon Nanotubes and C₆₀: Carbon Nanostructures for Advanced Polymeric Composite Materials, *Adv. Mater.*, 13, 899 -913 (2001).

Dai, S., Ravi, P., Leong, C.Y., Tam, K.C., Gan, L. H., Synthesis and Aggregation Behavior of Amphiphilic Block Copolymers in Aqueous Solution: Di- and Triblock Copolymers of Poly(ethylene oxide) and Poly(ethyl acrylate), *Langmuir*, 20,1597-1604 (2004a).

Dai, S., Ravi, P., Tam, K.C., Mao, B. W., Gan L.H., Novel pH-Responsive Amphiphilic Diblock Copolymers with Reversible Micellization Properties, *Langmuir*, 19, 5175-5177 (2003)

Dai, S., Ravi, P., Tan, C. H., Tam, K.C., Self-Assembly Behavior of a Stimuli-Responsive Water-Soluble [60] Fullerene-Containing Polymer, *Langmuir*, 20, 8569-8575 (2004b).

Danson, S, Ferry, D., Alakhov, V., Margison, J., Kerr, D., Jowle, D., Brampton, M., Halbert, G., Ranson, M., Phase I dose escalation and pharmacokinetic study of pluronic polymerbound doxorubicin (SP1049C) in patients with advanced cancer, *Br. J. Cancer* , 90, 2085–2091 (2004).

Dardel, B., Guillon. D., Heinrich, B., Deschenaux, R., Fullerene-containing liquid-crystalline dendrimers, *J. Mater. Chem.*, 11, 2814-2831 (2001).

David, A., Kopeckova, P., Minko, T., Rubinstein, A., Kopecek, J., Design of a multivalent galactoside ligand for selective targeting of HPMA copolymerdoxorubicin conjugates to human colon cancer cells, *Eur. J. Cancer* 40, 148-157 (2004).

Deguchi, S., Alargov, R.G., Tsuji, K., Stable dispersions of fullerenes, C₆₀ and C₇₀, in water, *Langmuir*, 17, 6013-6017 (2001).

Dhanikula, A.B., Panchagnula, R., Preparation and Characterization of Water-Soluble Prodrug, Liposomes and Micelles of Paclitaxel, *Curr. Drug Delivery*, 2, 75-91 (2005).

Discher, D.E., Eisenberg, A., Polymer vesicles, *Science*, 297, 967-972 (2002).

Dong, S., Roman, M., Fluorescently labeled cellulose nanocrystals for bioimaging applications, *J. Am. Chem. Soc.*, 129, 13810-13811(2007).

Du, J., Tang, Y., Lewis, AL., Armes, SP., pH-Sensitive Vesicles Based on a Biocompatible Zwitterionic Diblock Copolymer, *J. Am. Chem. Soc.*, 127,17982-17983 (2005).

Duan, H.W., Chen, D.Y., Jiang, M., Gan, W.J., Li, S.J., Wang, M., Gong, J., Self-assembly of Unlike Homopolymers into Hollow Spheres in Nonselective Solvent, *J. Am. Chem. Soc.*, 123, 12097-12098 (2001).

Ederle, Y., Mathis, C., Grafting of anionic polymers into C₆₀ in polar and nonpolar solvents, *Macromolecules*, 30, 2546-2555 (1997).

Eichhorn, S.J., Dufresne, A., Aranguren, M., Marcovich, N.E., Capadona, J.R., Rowan, S.J., Weder, C., Thielemans, W., Roman, M., Renneckar, S., Gindl, W., Veigel, S., Keckes, J., Yano, H., Abe, K., Nogi, M., Nakagaito, A.N., Mangalam, A., Simonsen, J., Benight, A.S., Bismarck, A., Berglund, L.A., Peijs, T., Current international research into cellulose nanofibres and nanocomposites, *J. Mater. Sci.*, 45, 1-33 (2010).

Eichhorn, S.J., Young, R.J., Davies, G.R., Modelling Crystal and Molecular Deformation in Regenerated Cellulose Fibres, *Biomacromolecules*, 6, 507-513 (2005).

Eisenburg, C., Seta, N., Appel, M., Feldmann, G., Durand, G., Feger J., Asialoglycoprotein receptor in human isolated hepatocytes from normal liver and its apparent increase in liver with histological alterations, *J Hepatol*, 13, 305-309 (1991).

Engin, K., Leeper, D.B., Cater, J.R., Thistlethwaite, A.J., Tupchong L., Mcfarlane, J.D., Extracellular pH distribution in human tumors, *Int. J. Hypertherm*, 11, 211-216 (1995).

Eyley, S., Thielemans, W., Imidazolium grafted cellulose nanocrystals for ion exchange applications, *Chem. Commun.*, 47, 4177-4179 (2011)

Farokhzad, O.C., Jon, S.Y., Khadelmhosseini, A.T., Tran, N.T., LaVan, D.A., Langer, R., Nanoparticle-aptamer bioconjugates: A new approach for targeting prostate cancer cells, *Cancer Res.*, 64, 7668-7672 (2004).

Fazeli, N., Mohammadi, N., Afshar, T.F., A relationship between hydrodynamic and static properties of star-shaped polymers, *Polymer testing*, 23, 431-435 (2004)

Fechler, N., Badi, N., Schade, K., Pfeifer, S., Lutz, J.F., Design of Thermoresponsive Materials by ATRP of Oligo(ethylene glycol)-based (Macro)monomers, *Macromolecules*, 42, 33-36 (2009).

Ferry, D.R., Seymour, L.W., Anderson, D., Hesselwood, S., Julyan, P., Boivin, C., Poyner, R., Guest, P., Doran, J., Kerr, D.J., Phase I trial of liver targeted HPMA copolymer of doxorubicin PK2, pharmacokinetics, SPECT imaging of I-123-PK2 and activity in hepatoma, *B.r J. Cancer*, 80, 413-416 (1999).

Filippone, S., Heimann, F., Rassat, A., A highly water-soluble 2:1 β -cyclodextrin–fullerene conjugate, *Chem. Commun.*, 1508-1509 (2002).

Filpponen, I., Argyropoulos, D. S., Regular linking of cellulose nanocrystals via click chemistry: Synthesis and formation of cellulose nanoplatelet gels, *Biomacromolecules*, 11, 1060-1066 (2010).

Flory, P. J., Principles of Polymer Chemistry, Cornell University Press: London, (1953).

Ford, W.T., Graham, T.D., Mourey, H.T., Incorporation of C₆₀ into Poly(methyl methacrylate) and Polystyrene by Radical Chain Polymerization Produces Branched Structures, *Macromolecules*, 30, 6422-6429 (1997)

Ford, W.T., Lary, A.L., Mourey, T.H., Addition of Polystyryl Radicals from TEMPO-Terminated Polystyrene to C₆₀, *Macromolecules*, 34, 5819-5826 (2001).

Ford, W.T., Nishioka, T., McCleskey, S.C., Mourey, T.H., Kahol, P., Structure and Radical Mechanism of Formation of Copolymers of C₆₀ with Styrene and with Methyl Methacrylate, *Macromolecules*, 33, 2413-2423 (2000b).

Ford, W.T., Nishioka, T., Qiu, F., D'Souza, F., Choi J.P., Kutner, W., Noworyta, K., Structure Determination and Electrochemistry of Products from the Radical Reaction of C₆₀ with Azo(bisisobutyronitrile), *J. Org. Chem.*, 64, 6257-6262 (1999).

Ford, W.T., Nishioka, T., Qiu, F., D'Souza, F., Choi, J.P., Dimethyl Azo(bisisobutyrate) and C₆₀ Produce 1,4- and 1,16-Di(2-carbomethoxy-2-propyl)-1,x-dihydro[60]fullerenes, *J. Org. Chem.*, 65, 5780-5784 (2000a).

Friedman, S.H., Camp, D.L.D., Sijbesma, R.P., Srdanov, G., Wudl, F., Kenyon, G.I., Inhibition of the HIV-1 Protease by Fullerene Derivatives: Model Building Studies and Experimental Verification, *J. Am. Chem. Soc.*, 115, 6506-6509 (1993).

Gan, L.B., Huang, S.H., Zhang, X., Zhang, A.X., Cheng, B.C., Cheng, H., Li, X.L., Shang, G., Fullerenes as a *tert*-Butylperoxy Radical Trap, Metal Catalyzed Reaction of *tert*-Butyl hydroperoxide with Fullerenes, and Formation of the First Fullerene Mixed Peroxides C₆₀(O)(OO^tBu)₄ and C₇₀(OO^tBu)₁₀, *J. Am. Chem. Soc.*, 124, 13384-13385 (2002).

Gan, L.H., Gan, Y.Y., Roshan Deen, G., Poly(*N*-acryloyl-*N'*-propylpiperazine): A New Stimuli-Responsive Polymer, *Macromolecules*, 33,7893-7897 (2000).

Gan, L.H., Ravi, P., Mao, B.W., Tam, K.C., Controlled/Living Polymerization of 2-(Diethylamino)ethyl Methacrylate and Its Block Copolymer with *tert*-butyl Methacrylate by Atom Transfer Radical Polymerization, *J. Polym. Sci., Part A: Polym. Chem.*, 41, 2688-2695 (2003).

Gao, J., Wu, C., The “Coil-to-Globule” Transition of Poly(N-isopropylacrylamide) on the Surface of a Surfactant-Free Polystyrene Nanoparticle, *Macromolecules*, 30, 6873-6876 (1997).

Geckeler, K. E., Hirsch, A., Polymer-bound C₆₀, *J. Am. Chem. Soc.*, 115, 3850-3851 (1993).

Geckeler, K.E., Samal, S., Syntheses and properties of macromolecular fullerenes, a review, *Polym. Int.*, 48, 743-757 (1999).

Gharbi, N., Pressac, M., Hadchouel, M., Szwarc, H., Wilson, S. R., Moussa, F., [60] Fullerene is a Powerful Antioxidant in vivo with No Acute or Subacute Toxicity, *Nano Lett.*, 5, 2578-2585 (2005).

Gohy, J. F., Creutz, S., Garcia, M., Mahltig, B., Stamm, M., Jerome, R., Aggregates Formed by Amphoteric Diblock Copolymers in Water, *Macromolecules*, 33, 6378-6387 (2000).

Gohy, J.F., Antoun, S., Jérôme, R., pH-Dependent Micellization of Poly(2-vinylpyridine)-block-poly((dimethylamino)ethyl methacrylate) Diblock Copolymers, *Macromolecules*, 34, 7435-7440 (2001).

Goldspiel, B.R., Clinical overview of the taxanes, *Pharmacotherapy*, 17, 110S-125S (1997).

Habibi, Y., Dufresne, A., Highly filled bionanocomposites from functionalized polysaccharides nanocrystals, *Biomacromolecules*, 9, 1974-1980 (2008b)

Habibi, Y., Goffin, A., Schiltz, N., Duquesne, E., Dubois, P., Dufresne, A., Bionanocomposites based on poly(ϵ -caprolactone)-grafted cellulose nanocrystals by ring-opening polymerization, *J. Mater. Chem.*, 18, 5002-5010 (2008a).

Hamaguchi, T., Matsumura, Y., Suzuki, M., Shimizu, K., Goda, R., Nakamura, I., Nakatomi, I., Yokoyama, M., Kataoka, K., Kakizoe, T.A., paclitaxel-incorporating micellar nanoparticle formulation, can extend in vivo antitumour activity and reduce the neurotoxicity of paclitaxel, *Br. J. Cancer*, 92, 1240–1246 (2005).

Han, S., Hagiwara, M, Ishizone, T., Synthesis of thermally sensitive water-soluble polymethacrylates by living anionic polymerizations of oligo(ethylene glycol) methyl ether methacrylates, *Macromolecules*, 36, 8312-8319 (2003).

Hare, J.P., Kroto, H.W., Taylor, R., Preparation and UV / visible spectra of fullerenes C₆₀ and C₇₀, *Chemical Physics Letters*, 177, 394-398 (1991).

Harsh, D.C., Gehrke, S.H.J., Controlling the swelling characteristics of temperature-sensitive cellulose ether hydrogels, *Controlled Release*, 17, 175-186 (1991).

Hasani, M., Cranston, E.D., Westmana, G., Gray, D.G., Cationic surface functionalization of cellulose nanocrystals, *Soft Matter*, 4, 2238–2244 (2008)

Hayama, A., Yamamoto, T., Yokoyama, M., Kawano, K., Hattori, Y., Maitani, Y., Polymeric micelles modified by folate-PEG-lipid for targeted drug delivery to cancer cells in vitro, *Journal of Nanoscience and Nanotechnology*, 8, 3085–3090 (2008).

Helmlinger, G., Yuan, F., Dellian, M., Jain, R.K., Interstitial pH and pO₂ gradients in solid tumors in vivo: high-resolution measurements reveal a lack of correlation, *Med.*, 3, 177-182 (1997).

Heskins, M., Guillet, J.E., Solution Properties of Poly(N-isopropylacrylamide) *J. Macromol. Sci. Chem.*, A2, 1441-1455 (1968).

Hiratsuka, T., Goto, M., Kondo, Y., Cho, C.S., Akaike, T., Copolymers for hepatocyte-specific targeting carrying galactose and hydrophobic alkyl groups, *Macromol. Biosci.* 8, 231-238 (2008).

Holder, S.J, Rossi, N.A.A., Yeoh, C.T, Durand, G.G., Boerakker, M.J, Sommerdijk, N.M., ABA triblock copolymers: from controlled synthesis to controlled function, *J Mater Chem*, 13, 2771–2778 (2003).

Hong, S.W, Kim, D.Y., Lee, J.U., Jo, W.H., Synthesis of Polymeric Temperature Sensor Based on Photophysical Property of Fullerene and Thermal Sensitivity of Poly(N-isopropylacrylamide), *Macromolecules*, 42, 2756-2761 (2009).

Horie, M., Fukuhara, A., Saito, Y., Yoshida, Y., Sato, H., Ohi, H., Obata, M., Mikata, Y., Yano, S., Niki, E., Antioxidant action of sugar-pendant C₆₀ fullerenes, *Bioorganic & Medicinal Chemistry Letters*, 19: 5902–5904 (2009).

<http://www.vc60.com>

Hu, W. H., Liu, Y.S., Lu, Z.S., Li, C.M., Poly[oligo(ethylene glycol) methacrylate- co -glycidyl methacrylate] Brush Substrate for Sensitive Surface Plasmon Resonance Imaging Protein Array, *Adv. Funct. Mater.*, 20, 3497-3503 (2010).

Hu, Z., Kimura, G., Ito, Y., Mawatari. S., Shimokawa. T., Yoshikawa. H., Yoshikawa. Y., Takada. K., Technology to obtain sustained release characteristics of drugs after delivered to the colon, *J. Drug Target*, 6, 439-448 (1999).

Hu, Z.B., Cai, T., Chi, C.L., Thermoresponsive oligo(ethylene glycol)-methacrylate- based polymers and microgels, *Soft Matter*, 6, 2115-2123 (2010).

Hua, W.K.L., Dong, T., Pan, P., Zhu, B., Inoue, Y., Fullerene End-Capped Biodegradable Poly(ϵ -caprolactone), *Macromol. Chem. Phys.* 209, 104-111 (2008).

Huang, X.D., Goh, S.H., Lee, S.Y., Miscibility of C₆₀-end-capped poly(ethylene oxide) with poly(*p*-vinylphenol), *Macromol. Chem. Phys.*, 201, 2660-2665 (2000).

Huang, Z.E., Chen, H., Cai, R.F., Rui, C.G., Zhang, F.P., Cellular Proteins That Bind to the Hepatitis B Virus Posttranscriptional Regulatory Element, *J. Appl. Polym. Sci.*, 60, 57-581 (1996).

Hussain, H., Tan, B.H., Gudipati, C.S., He, C.B., Liu, Y., Davis, T.P., Micelle Formation of Amphiphilic Polystyrene-*b*-poly(N-vinylpyrrolidone) Diblock Copolymer in Methanol and Water-Methanol Binary Mixtures, *Langmuir*, 25: 5557-5564 (2009).

Hwang, K.C., Mauzerall, D., Photoinduced electron transport across a lipid bilayer mediated by C₇₀, *Nature*, 361, 138-140 (1993).

Hwang, K.C., Mauzerall, D., Vectorial electron transfer from an interfacial photoexcited porphyrin to ground-state fullerene C₆₀ and C₇₀ and from ascorbate to triplet C₆₀ and C₇₀ in a lipid bilayer, *J. Am. Chem. Soc.*, 114, 9705-9706 (1992).

Innocenti, A., Durdagi, S., Doostdar, N., Strom, T.A., Barron, A.R., Supuran, C.T., Nanoscale enzyme inhibitors: fullerenes inhibit carbonic anhydrase by occluding the active site entrance, *Bioorganic & Medicinal Chemistry*, 18, 2822-2828 (2010).

Isobe, H., Tanaka, T., Nakanishi, W., Lemiègre, L., Nakamura, E., Regioselective Oxygenative Tetraamination of [60] Fullerene. Fullerene-mediated Reduction of Molecular Oxygen by Amine via Ground State Single Electron Transfer in Dimethyl Sulfoxide, *J. Org. Chem.*, 70, 4826-4832 (2005).

Jehoulet, C., Bard, A.J., Wudl, F., Electrochemical Reduction and Oxidation of C₆₀ Films, *J. Am. Chem. Soc.*, 113, 5456-5457 (1991).

Jeong, Y.I., Nah, J.W., Lee, H.C., Kim S.H., Cho, C.S., Adriamycin release from flower-type polymeric micelle based on star-block copolymer composed of poly (gamma-benzyl L-glutamate) as the hydrophobic part and poly(ethylene oxide) as the hydrophilic part, *Int. J. Pharm.* 188, 49-58 (1999).

Jeong, Y.I., Seo, S.J., Park, I.K., Lee, H.C., Kang, I.C., Akaike, T., Cho, C.S., Cellular recognition of paclitaxelloaded polymeric nanoparticles composed of poly(gamma-benzyl L-glutamate) and poly(ethylene glycol) diblock copolymer endcapped with galactose moiety. *Int. J. Pharm.*, 296, 151-161 (2005).

Jochum, F.D., Roth, P.J., Kessler, D., Theato, P., Double thermoresponsive block copolymers featuring a biotin end group, *Biomacromolecules*, 11, 2432-2439 (2010).

Johnson, R.D, Meijer, G., Bethune, D.S., C₆₀ Has Icosahedral Symmetry, *J. Am. Chem. Soc.*, 112, 8983-8984 (1990)

Jones, R.A., Poniris, M.H., Wilson, M.R., pDMAEMA is internalised by endocytosis but does not physically disrupt endosomes, *J. Controlled Release*, 96, 379-391 (2004).

Jule, E., Nagasaki, Y., Kataoka, K., Lactose-installed poly(ethylene glycol)-poly(D, L-lactide) block copolymer micelles exhibit fast-rate binding and high affinity toward a protein bed simulating a cell surface. A surface Plasmon resonance study, *Bioconjug. Chem.*, 14, 177-186 (2003).

Jule, E., Nagasaki, Y., Kataoka, K., Surface Plasmon resonance study on the interaction between lactose-installed poly(ethylene glycol)-poly(D,L-lactide) block copolymer micelles and lectins immobilized on a gold surface, *Langmuir*, 18, 10334-10339 (2002).

Julyan, P.J., Seymour, L.W., Ferry, D.R., Daryani, S., Boivin, C.M., Doran, J., David, M., Anderson, D., Christodoulou, C., Young, A.M., Hesslewood, S., Kerr, D.J., Preliminary clinical study of the distribution of HPMA copolymers bearing doxorubicin and galactosamine, *J. Control Release*, 57, 281-290 (1999).

Julyan, P.J., Seymour, L.W., Ferry, D.R., Daryani, S., Boivin, C.M., Doran, J., David, M., Anderson, D., Christodoulou, C., Young, A.M., Hesslewood, S., Kerr, D.J., Preliminary clinical study of the distribution of HPMA copolymers bearing doxorubicin and galactosamine, *J. Control Release*, 57, 281-290 (1999).

Kabanov, A.V., Chekhonin, V.P., Alakhov, V.Y., Batrakova, E.V., Lebedev, A.S., Meliknubarov, N.S., Arzhakov, S.A., Levashov, A.V., Morozov, G.V., Severin, E.S., Kabanov, V.A., The neuroleptic activity of haloperidol increases after its solubilization in surfactant micelles as microcontainers for drug targeting, *FEBS Lett.*, 258, 343-345 (1989).

Kalyanasundaram, K., Pyrene fluorescence as a probe of fluorocarbon micelles and their mixed micelles with hydrocarbon surfactants, *Langmuir*, 4, 942-945 (1988).

Kalyanasundaram, K., Pyrene fluorescence as a probe of fluorocarbon micelles and their mixed micelles with hydrocarbon surfactants, *Langmuir*, 4, 942-945 (1988) .

Karaulova, E.N., Bagrii, E.I., Fullerenes: functionalisation and prospects for the use of derivatives, *Rus. Chem. Rev.* 68, 889-907 (1999).

Kasermann, F., Kempf, C., Photodynamic inactivation of enveloped viruses by buckminsterfullerene, *Antiviral. Res.*, 34, 65-70 (1997).

Kataoka, K., Harada, A., Nagasaki, Y., Block copolymer micelles for drug delivery: design, characterization and biological significance, *Adv. Drug Deliv. Rev.*, 47, 113-131 (2001).

Kato, H., Nakamura, A., Takahashi, K., Kinugasa, S., Size effect on UV-Vis absorption properties of colloidal C₆₀ particles in water, *Phys Chem Chem Phys.*, 11, 4946-4948 (2009)

Kato, M., Kamigaito, M., Sawamoto, M., Higashimura, T., Polymerization of Methyl Methacrylate with the Carbon Tetrachloride/Dichlorotris- triphenylphosphine) ruthenium(II)/Methylaluminum Bis(2,6-di-tert-butylphenoxide) Initiating System: Possibility of Living Radical Polymerization, *Macromolecules*, 28, 1721-1723 (1995).

Kawauchi, T., Kumaki, J., Yashima, E., Synthesis, isolation via self-assembly, and single-molecule observation of a [60] fullerene-end-capped isotactic poly(methyl methacrylate). *J. Am. Chem. Soc.*, 127, 9950-9951 (2005).

Kim, K.H., Kim, J., Jo, W.H., Preparation of hydrogel nanoparticles by atom transfer radical polymerization of N-isopropylacrylamide in aqueous media using PEG macro-initiator, *Polymer*, 46, 2836-2840 (2005).

Kim, TY., Kim, DW., Chung, JY., Shin, SG., Kim, SC., Heo, DS., Kim, NK., Bang, YJ., Phase I and pharmacokinetic study of Genexol- PM, a cremophor-free, polymeric micelle-formulated paclitaxel, in patients with advanced malignancies, *Clin. Cancer Res.*, 10, 3708-3716 (2004).

Kitano, H., Hirabayashi, T., Gemmei-Ide, M., Kyogoku, M., Effect of Macrocycles on the Temperature-Responsiveness of Poly[(methoxy diethylene glycol methacrylate)-graft-PEG], *Macromol. Chem. Phys.*, 205, 1651-1659 (2004).

Kloser, E., Gray, D.G., Surface Grafting of Cellulose Nanocrystals with Poly(ethylene oxide) in Aqueous Media, *Langmuir*, 26, 13450–13456 (2010).

Kohori, F., Sakai, K., Aoyagi, T., Yokoyama, M., Sakurai, Y., Okano, T., Preparation and characterization of thermally responsive block copolymer micelles comprising poly(Nisopropylacrylamide- b-DL-lactide). *J. Control. Release*, 55, 87-98 (1998).

Kopacek, J., Duncan, R., Targetable polymeric prodrugs, *J. Control. Release*, 6, 315-327 (1987).

Koppe, M., Scharber, M., Brabec, C., Duffy, W., Heeney, M., McCulloch, I., Polyterthiophenes as Donors for Polymer Solar Cells, *Adv. Funct. Mater.*, 17, 1371-1376 (2007).

Kroto, H.W., Fisher, J.E., Cox, D.E., “The Fullerenes”, Pergamon Press, Oxford, UK (1993).

Kroto, H.W., Heath, J.R., O’Brien, S.C., Curl, R.F., Smalley, R.F., C₆₀: Buckminsterfullerene, *Nature*, 318, 162-163 (1985).

Krusic, P.J., Wasserman, E., Keizer, P.N., Morton, J. R., Preston, K.F., Radical Reactions of C₆₀, *Science*, 254, 1183-1185 (1991a).

Krusic, P.J., Wasserman, E., Parkinson, B.A., Malone, B., Holler, E.R., Keizer, P.N., Morton, J. R., Preston, K.F., Electron spin resonance study of the radical reactivity of C₆₀, *J. Am. Chem. Soc.*, 113, 6274 (1991b).

Kudaibergenov, S.E., Recent advances in the study of synthetic polyampholytes in solutions, *Adv. Polym. Sci.*, 144, 115-197 (1999).

Kuramoto, N., Shishido, Y., Nagai, K., Preparation of thermally responsive and electroactive poly(*N*-acryloylpyrrolidine-*co*-vinylferrocene), *Macromol. Rapid Commun.*, 15, 441-444 (1994).

Kurisawa, M., Yokoyama, M., Okano, T., Gene expression control by temperature with thermo-responsive polymeric gene carriers, *J. Controlled Release*, 69, 127–137 (2000b)

Kurisawa, M., Yokoyama, M., Okano, T., Transfection efficiency increases by incorporating hydrophobic monomer units into polymeric gene carriers, *J. Controlled Release*, 68, 1–8 (2000a).

Kwon, G., Suwa, S., Yokoyama, M., Okano, T., Sakurai, Y., Kataoka, K.J., Enhanced tumor accumulation and prolonged circulation times of micelle-forming poly(ethylene oxide-aspartate) block copolymer-adriamycin conjugates, *J. Controlled Release*, 29, 17-23 (1994).

Kwon, G.S., Law, D., Adams, M., Kostick, K.E., Schmitt, E.A., Polymeric micelle formulations of hydrophobic compounds and methods, US20040005351 (2004).

Kwon, G.S., Okano, T., Polymeric micelles as new drug carriers *Adv. Drug Deliv.Rev.*, 21, 107-116 (1996).

Kwon, G.S., Samuel, J., Lavasanifar, A., Methods and compositions for polyene antibiotics with reduced toxicity, US20056939561 (2005).

Kwon, G.S., Yokoyama, M., Okano, T., Sakurai, Y., Kataoka, K., Biodistribution of micelle-forming polymer drug conjugates, *Pharm. Res.*, 10, 970-974 (1993).

Lakowicz, J.R., Principles of Fluorescence Spectroscopy, Kluwer Academic/Plenum, New York, 2nd edn, (1999)

Lee, E.S., Na, K., Bae, Y.H., Polymeric micelle for tumor pH and folate-mediated targeting, *J. Control. Release*, 91, 103-113 (2003b).

Lee, E.S., Shin, H.J., Na, K., Bae, Y.H., Poly(L-histidine)- PEG block copolymer micelles and pH-induced destabilization, *J. Control. Release*, 90, 363-374 (2003a).

Lee, H.N., Bai, Z.F., Newell, N., Lodge, T. P., Grafting of Poly(*N*-isopropylacrylamide) with Poly(ethylene oxide) under Various Reaction Conditions, *Macromolecules*, 43, 9522-9528 (2010).

Lee, S.B., Song, S.C., Jin, J.I., Sohn, Y.S., Solvent effect on the lower critical solution temperature of biodegradable thermosensitive poly(organophosphazenes), *Polym Bull*, 45, 389-396 (2000).

Lee, S.B., Russell, A.J., Matyjaszewski, K., ATRP synthesis of amphiphilic random, gradient, and block copolymers of 2-(dimethylamino)ethyl methacrylate and *n*-butyl methacrylate in aqueous media, *Biomacromolecules*, 4, 1386-1393 (2003).

Li, C.H., Hu, J.M., Yin, J., Liu, S.Y., Click Coupling Fullerene onto Thermoresponsive Water-Soluble Diblock Copolymer and Homopolymer Chains at Defined Positions, *Macromolecules*, 42, 5007–5016 (2009a).

Li, G., Guo, L., Ma, S., Liu, J., Complex Micelles Formed from Two Diblock Copolymers for Applications in Controlled Drug Release, *Journal of Polymer Science: Part A: Polymer Chemistry*, 47, 1804-1810 (2009b).

Li, G., Song, S., Guo, L., Ma, S., Self-assembly of thermo- and pH-responsive Poly(acrylic acid)-*b*-poly(*N*-isopropylacrylamide) Micelles for Drug Delivery, *Journal of Polymer Science: Part A: Polymer Chemistry*, 46, 5028-5035 (2008).

Lin, Y.N., Alexandridis, P., Cosolvent Effects on the Micellization of an Amphiphilic Siloxane Graft Copolymer in Aqueous Solutions, *Langmuir*, 18, 4220-4231 (2002).

Liu, J., Lee, H., Allen, C., Formulation of Drugs in Block Copolymer Micelles: Drug Loading and Release, *Current Pharmaceutical Design*, 12, 4685-4701 (2006).

Liu, S., Weaver, JVM., Tang, Y., Billingham, NC., Armes, SP., Tribe, K., Synthesis of Shell Cross-Linked Micelles with pH-Responsive Cores Using ABC Triblock Copolymers, *Macromolecules*, 35, 6121-6131 (2002).

Liu, X.M., Pramoda, K.P., Yang, Y.Y., Chow, S.Y., He, C.B., Cholesteryl-grafted functional amphiphilic poly (N-isopropylacrylamide-co-N- hydroxymethylacrylamide): synthesis, temperaturesensitivity, self-assembly and encapsulation of a hydrophobic agent. *Biomaterials*, 25, 2619-2628 (2004).

Liu, X.M., Yang, Y.Y., Leong, K.W., Thermally responsive polymeric micellar nanoparticles self-assembled from cholesteryl end-capped random poly(N-isopropylacrylamide- co-N,N-dimethylacrylamide): synthesis, temperature sensitivity, and morphologies, *J. Colloid Interface Sci.* 266, 295-303 (2003).

Liu, Y., Zhao, Y.L., Chen, Y., Liang, P., Li, L., A water-soluble β -cyclodextrin derivative possessing a fullerene tether as an efficient photodriven DNA-cleavage reagent, *Tetrahedron Lett.*, 46, 2507-2511 (2005).

Liu, Y.L., Chang, Y.H., Chen, W.H., Preparation and Self-Assembled Toroids of Amphiphilic Polystyrene-C₆₀-Poly(N-isopropylacrylamide) Block Copolymers, *Macromolecules*, 41, 7857-7862 (2008).

Lowe A.B., McCormick, C.L., Synthesis and solution properties of zwitterionic polymers, *Chem. Rev.*, 102, 4177-4189 (2002).

Lowe, A.B., Billingham, N. C., Armes, S.P., Synthesis and aqueous solution properties of novel zwitterionicblock copolymers, *Chem. Commun.*, 1035-1036 (1997).

Lowe, A.B., Billingham, N.C., Armes, S.P., Synthesis and Characterization of Zwitterionic Block Copolymers, *Macromolecules*, 31, 5991-5998 (1998)

Lu, X., Zhang, L., Meng, L., Liu, Y., Synthesis of poly(N-isopropylacrylamide) by ATRP using a fluorescein-based initiator, *Polymer Bulletin*, 59, 195-206 (2007)

Lukyanov, A.N., Elbayoumi, T.A., Chakilam, A.R., Torchilin, V.P., Tumor-targeted liposomes: doxorubicin-loaded long-circulating liposomes modified with anti-cancer antibody, *Journal of Controlled Release*, 100, 135–144 (2004)

Lutz, J. F., Akdemir, O., Hoth, A., Point by Point Comparison of Two Thermosensitive Polymers Exhibiting a Similar LCST: Is the Age of Poly(NIPAM) Over? *J. Am. Chem. Soc.*, 128, 13046-13047 (2006b).

Lutz, J. F., Andrieu, J., Uzgun, S., Rudolph, C., Agarwal, S. Biocompatible, Thermoresponsive, and Biodegradable: Simple Preparation of “All-in-One” Biorelevant Polymers, *Macromolecules*, 40, 8540 (2007b).

Lutz, J. F., Polymerization of oligo(ethylene glycol) (meth)acrylates: Toward new generations of smart biocompatible materials, *J. Polym. Sci., Part A: Polym. Chem.* , 46, 3459-3470 (2008).

Lutz, J.F., Hoth, A., Preparation of Ideal PEG Analogues with a Tunable Thermosensitivity by Controlled Radical Copolymerization of 2-(2-methoxyethoxy)ethyl Methacrylate and Oligo(ethylene glycol) Methacrylate, *Macromolecules*, , 39, 893-896 (2006a).

Lutz, J.F., Hoth, A., Schade, K., Design of Oligo(ethylene glycol)-based Thermoresponsive Polymers: an Optimization Study, *Designed Monomers & Polymers*, 12, 343-353 (2009).

Lutz, J.F., Thermo-Switchable Materials Prepared Using the OEGMA-Platform , *Adv Mater* , 23, 2237–2243 (2011).

Lutz, J.F., Weichenhan, K., Akdemir, O., Hoth, A., About the Phase Transitions in Aqueous Solutions of Thermoresponsive Copolymers and Hydrogels Based on 2-(2-methoxyethoxy)ethyl Methacrylate and Oligo(ethylene glycol) Methacrylate, *Macromolecules*, 40, 2503-2508 (2007a).

Maeda, H., Wu, J., Sawa, T., Matsumura, Y., Hori, K., Tumor vascular permeability and the EPR effect in macromolecular therapeutics: a review, *J Control Release*, 65, 271-84 (2000).

Maeda, Y., Rahaman, G.M.A., Wakahara, T., Kako, M., Okamura, M., Sato, S., Akasaka, T., Kobayashi, K., Nagase, S., Synthesis and characterization of tetrakis-silylated C₆₀ isomers, *J. Org. Chem.*, 68, 6791-6794 (2003)

Mahmud, A., Xiong, X.B., Montazeri, H., Lavasanifar, A., Polymeric micelles for drug targeting, *Journal of Drug Targeting*, 15, 553-584 (2007).

Manolova, N., Rashkov, I., Damme, V. V., Begum, F., Polyether-modified fullerenes, *Polym. Bull.*, 33, 175-182 (1994).

Mao, B.W., Gan, L.H., Gan, Y.Y., Li, X.S., Ravi, P, Tam, K.C., Controlled polymerization of 2-(Dialkylamino)ethyl Methacrylates and Their Block Copolymers In Protic Solvents At Ambient Temperature via ATRP, *J Polym Sci, Part A: Polym Chem.*, 42, 5161–5169 (2004).

Mao, B.W., Gan, L.H., Gan, Y.Y., Ultra high molar mass poly[2-(dimethylamino)ethyl methacrylate] via atom transfer radical polymerization, *Polymer*, 47, 3017–3020 (2006).

Maria, S., Stoffelbach, F., Mata, J., Daran, J.C., Richard, P., Poli, R., The Radical Trap in Atom Transfer Radical Polymerization Need Not Be Thermodynamically Stable. A Study of the MoX₃(PMe₃)₃ Catalysts, *J. Am. Chem. Soc.*, 127, 5946–5956 (2005).

Martin, N., Sanchez, L., Liescas, B., Perez, I. C₆₀-Based Electroactive Organofullerenes, *Chem. Rev.*, 98, 2527 (1998).

Matsubara, Y., Tada, S. G., Nagase, S., Yoshida, Z., Intramolecular Charge Transfer Interaction in 1,3-Diphenyl-2-pyrazoline Ring-Fused C₆₀, *J. Org. Chem.*, 60, 5372-5373 (1995).

Matsumura, Y., Hamaguchi, T., Ura, T., Muro, K., Yamada, Y., Shimada, Y., Shirao, K., Okusaka, T., Ueno, H., Ikeda, M., Watanabe, N., Phase I clinical trial and pharmacokinetic evaluation of NK911, a micelle-encapsulated doxorubicin, *Br. J. Cancer*, 91, 1775–1781 (2004).

Matyjaszewski, K., Davis, T.P., Handbook of Radical Polymerization, John Wiley and Sons, Inc., Hoboken, (2002).

McCormick, C.L., Kirkland, S.E., York, A.W., Synthetic routes to stimuli-responsive micelles, vesicles, and surfaces via controlled/living radical polymerization, *J. Macromol. Sci., Polym. Rev.*, 46, 421–443 (2006).

Mertoglu, M., Garnier, S., Laschewsky, A., Skrabania, K., Storsberg, J., Stimuli responsive amphiphilic block copolymers for aqueous media synthesised via reversible addition fragmentation chain transfer polymerisation (RAFT), *Polymer*, 46, 7726-7740 (2005).

Morandi, G., Heath, L., Thielemans, W., Cellulose Nanocrystals Grafted with Polystyrene Chains through Surface-Initiated Atom Transfer Radical Polymerization (SI-ATRP), *Langmuir*, 25, 8280–8286 (2009).

Morton, J.R., Preston, K.F., Krusic, P.J., Hill, S.A. Wasserman, E., The dimerization of fullerene RC_{60} radicals [R = alkyl], *J. Am. Chem. Soc.*, 114, 5454-5455 (1992).

Murthy, C.N., Geckeler, K.E., The water-soluble β -cyclodextrin-[60]fullerene complex, *Chem. Commun.*, 1194–1195 (2001)

Mwaura, J.K., Pinto, M.R., Witker, D., Ananthakrishnan, N., Schanze, K.S., Reynolds, J.R., Photovoltaic Cells Based on Sequentially Adsorbed Multilayers of Conjugated Poly(*p*-phenylene ethynylene)s and a Water-Soluble Fullerene Derivative, *Langmuir*, 21, 10119-10126 (2005).

Na, K., Lee, E.S., Bae, Y.H., Adriamycin loaded pullulan acetate /sulfonamide conjugate nanoparticles responding to tumor pH: pH-dependent cell interaction, internalization and cytotoxicity in vitro, *J. Control. Release*, 87, 3-13 (2003).

Nagasaki, Y., Yasugi, K., Yamamoto, Y., Harada, A., Kataoka, K., Sugar-installed block copolymer micelles: their preparation and specific interaction with lectin molecules, *Biomacromolecules*, 2, 1067-1070 (2001).

Nakayama, M., Okano, T., Miyazaki, T., Kohori, F., Sakai, K., Yokoyama, M., Molecular design of biodegradable polymeric micelles for temperature-responsive drug release, *J. Control. Release*, 115, 46–56 (2006).

Nepal, D., Samal, S., Geckeler, K., EThe First Fullerene-Terminated Soluble Poly(azomethine) Rotaxane, *Macromolecules*, 36, 3800-3802 (2003).

Nielsen, L. J., Eyley, S., Thielemans, W., Aylott, J.W., Dual fluorescent labelling of cellulose nanocrystals for pH sensing, *Chem. Commun.*, 46, 8929–8931 (2010).

Nishiyama, N., Kato, Y., Sugiyama, Y. Kataoka, K., Cisplatin-loaded polymer-metal complex micelle with time-modulated decaying property as a novel drug delivery system, *Pharm. Res.*, 18, 1035–1041 (2001).

Nordmeier, E., Lechner, D., Simultaneous Frequency-Integrated and Incoherent-Elastic Light Scattering: Description of a New Photon-Correlation Spectrometer, *Polym J.*, 21, 623-632 (1989).

Oberdorster, E., Manufactured Nanomaterials (Fullerenes, C₆₀) Induce Oxidative Stress in the Brain of Juvenile Largemouth Bass, *Environ. Health Perspect*, 112, 1058–1062 (2004).

Okamura, H., Ide, N., Minoda, M., Komatsu, K., Fukuda, T., Solubility and Micellization Behavior of C₆₀ Fullerenes with Two Well-Defined Polymer Arms, *Macromolecules*, 31, 1859-1865 (1998).

Okamura, H., Terauchi, T., Minoda, M., Fukuda, T., Komatsu, K., Synthesis of 1,4-Dipolystyryldihydro[60]fullerenes by Using 2,2,6,6-Tetramethyl-1-polystyroxypiperidine as a Radical Source, *Macromolecules*, 30, 5279-5284 (1997).

Olah, G.A. , Bucsi, I., Lambert, C., Aniszfeld, R., Trivedi, N.J., Sensharma, D.K., Prakash, K.S., Polyarenefullerenes, C₆₀(H-Ar)_n, obtained by acid-catalyzed fullerenation of aromatics, *J. Am. Chem. Soc.*, 113, 9387-9388 (1991).

Pang, J., Yang, H., Ma, J., Cheng, R.J., Solvation Behaviors of N-Isopropylacrylamide in Water/Methanol Mixtures Revealed by Molecular Dynamics Simulations, *Phys Chem B*, 114, 8652-658 (2010).

Pantarotto, D., Bianco, A., Pellarini, F., Tossi, A., Giangaspero, A., Zelezetsky, I., Briand, J. P., Prato, M., Solid-Phase Synthesis of Fullerene-peptides, *J. Am. Chem. Soc.*, 124, 12543-12549 (2002).

Park, E.K., Kim, S.Y., Lee, S.B., Lee, Y.M., Folate-conjugated methoxy poly(ethylene glycol)/poly(epsilon-caprolactone) amphiphilic block copolymeric micelles for tumor-targeted drug delivery. *J. Control. Release*, 109, 158-168 (**2005a**).

Park, E.K., Lee, S.B., Lee, Y.M., Preparation and characterization of methoxy poly(ethylene glycol)/poly(epsilon-caprolactone) amphiphilic block copolymeric nanospheres for tumor-specific folate-mediated targeting of anticancer drugs, *Biomaterials*, 26, 1053-1061 (**2005b**).

Park, K., Controlled Drug Delivery: Challenges, Strategies, ACS Professional Reference Book, American Chemical Society, Washington, D.C. (**1997**).

Partha, R., Mitchell L.R., Lyon, J.L., Joshi, P.P., Conyers, J.L., buckysomes: fullerene-based nanocarriers for hydrophobic molecule delivery, *ACS Nano*, 2, 1950-1958 (**2008**).

Peltier, S., Oger, J.M., Lagarce, F., Couet, W., Benoit, J.P., Enhanced Oral Paclitaxel Bioavailability After Administration of Paclitaxel-Loaded Lipid Nanocapsules, *Pharm. Res.*, 23, 1243–1250 (**2006**).

Peng, K.J., Liu, Y.L., Preparation and toroid formation of multiblock polystyrene/C₆₀ nano hybrids, *Macromolecules*, 44, 5006-5012 (**2011**).

Plamper, F.A., Ruppel, M., Schmalz, A., Borisov, O., Ballauff, M., Müller, A.H.E., Polyethylene Crystal Orientation Induced by Block Copolymer Cylinders, *Macromolecules*, 40, 8361-8366 (**2007**).

Plummer, R., Hill, D.J.T., Whittaker, A.K., Solution Properties of Star and Linear Poly(N-isopropylacrylamide), *Macromolecules*, 39, 8379-8388 (**2006**).

Prato, M., [60] Fullerene chemistry for materials science applications, *J. Mater. Chem.*, 7, 1097-1109 (**1997**).

Qin, S., Qin, D., Ford, W.T., Herrera, J.E., Resasco, D.E., Bachilo, S.M., Weisman, R.B., Solubilization and Purification of Single-Wall Carbon Nanotubes by In Situ Radical Polymerization of Sodium 4-Styrenesulfonate, *Macromolecules*, 37, 3965-3967 (2004).

Rackaitis, M., Strawhecker, K., Manias, E., Water-Soluble Polymers with Tunable Temperature Sensitivity: Solution Behavior, *Journal of Polymer Science: Part B: Polymer Physics*, 40, 2339-2342 (2002).

Ranby, B.G., Aqueous colloidal solutions of cellulose micelles, *Acta Chem. Scand.*, 3, 649-650 (1949)

Ranga, P., Linsey, R., Mitchell, J.L.L., Pratixa, P.J., Jodie, L.C., Buckysomes: Fullerene-Based Nanocarriers for Hydrophobic Molecule Delivery, *ACS Nano*, 2, 1950-1958 (2008).

Ravi, P., Dai, S., Tam, K.C., Synthesis and Self-assembly of [60] Fullerene Containing Sulfobetaine Polymer in Aqueous Solution, *Journal of Physical Chemistry B*, 109, 22791-22798 (2005b).

Ravi, P., Dai, S., Tan, C.H., Tam, K.C., Self-Assembly of Alkali-Soluble [60] Fullerene Containing Poly (methacrylic acid) in Aqueous solutions, *Macromolecules*, 38, 933-939 (2005a).

Ravi, P., Dai, S., Wang, C., Tam, K.C., Fullerene containing polymers: a review on their synthesis and supramolecular behavior in solution, *J Nanosci Nanotechnol.*, 7, 1176-1179 (2007).

Ravi, P., Wang, C., Dai, S., Tam K.C., Self-Assembly of Well-Defined Mono and Dual End-Capped C₆₀ Containing Polyacrylic Acids in Aqueous Solution, *Langmuir*, 22, 7167-7174 (2006).

Richardson, C.F., Schuster, D.I., Wilson, S.R., Synthesis and Characterization of Water-Soluble Amino Fullerene Derivatives, *Org. Lett.*, 2, 1011-1014 (2000).

Robin, S., Guerret, O., Couturier, J.L., Gnanou, Y., Synthesis of Stars and Starlike Block Copolymers from a Trialkoxyamine Used as Initiator, *Macromolecules*, 35, 2481-2486 (2002).

Robinson, K.L., Khan, M.A., deBanez, M.V., Wang, X.S., Armes, S.P., Controlled Polymerization of 2-Hydroxyethyl Methacrylate by ATRP at Ambient Temperature, *Macromolecules*, 34, 3155-3158 (2001).

Ros, T.D., Prato, M., Medicinal chemistry with fullerenes and fullerene derivatives, *Chem. Commun.*, 663-669 (1999).

Rösler, A., Vandermeulen, G.M., Klok, H.A., Advanced drug delivery devices via self-assembly of amphiphilic block copolymers, *Adv. Drug Deliv. Rev.*, 53, 95–108 (2001).

Ross, J.F., Chaudhuri, P.K., Ratnam, M., Differential regulation of folate receptor isoforms in normal and malignant tissues in-vivo and in established cell-lines: physiological and clinical implications, *Cancer*, 73, 2432-2443 (1994).

Roth, P.J., Jochum, F.D., Theato, P., UCST-type behavior of poly[oligo(ethylene glycol) methyl ether methacrylate] (POEGMA) in aliphatic alcohols: solvent, co-solvent, molecular weight, and end group dependences, *Soft Matter*, 7, 2484-492 (2011).

Roy, D., Semsarilar, M., Guthrie, J.T., Perrier, S., Cellulose modification by polymer grafting: a review, *Chem. Soc. Rev.*, 38, 2046–2064 (2009)

Roy, I., Gupta, M.N., Smart Polymeric Materials: Emerging Biochemical Applications, *Chem. Biol.*, 10, 1161-1171 (2003).

Ruiz, M.M., Cavaille, J.Y., Dufresne, A., Gerard, J.F., Graillat, C., Processing and characterization of new thermoset nanocomposites based on cellulose whiskers, *Compos. Interfaces*, 7, 117–131 (2000).

Ruoff, R.S., Doris, S., Ripudaman, M., Donald, C. L., Solubility of fullerene (C₆₀) in a variety of solvents, *J. Phys. Chem.*, 97, 3379–3383 (1993)

Salamone, C.J., *Polymeric Material Encyclopedia*, CRC Press: Boca Raton, (1996).

Samal S., K.E. Geckeler, Cyclodextrin–fullerenes: a new class of water-soluble fullerene, *Chem. Commun.*, 1101-1102 (2000).

Samir, M.A.S.A., Alloin, F., Dufresne, A., Review of Recent Research into Cellulosic Whiskers, Their Properties and Their Application in Nanocomposite Field, *Biomacromolecules*, 6, 612–626 (2005).

Samulski, E. T., Desimone, J.M., Hunt, M.O., Menciloglu, Y.Z., Jarnagin, R.C., York, G.A., Labat, K.B., Wang, H., Flagellenes: nanophase-separated, polymer-substituted fullerenes, *Chem. Mater.*, 4, 1153-1157 (1992).

Sant, V., Leroux, J.C., pH-sensitive block copolymers for pharmaceutical compositions, US20067094810 (2006).

Sariciftci, N.S., Braun, D., Zhang, C., Srdanov, V.I., Heeger, A.J., Stucky, G., Wudl, F., Semi-conducting polymer-buckminsterfullerene heterojunctions: Diodes, photodiodes, and photovoltaic cells, *Appl. Phys. Lett.*, 62, 585-587 (1993).

Schallon, A., Jérôme, V., Walther, A., Synatschke, C.V., Müller, A.H.E., Freitag, R., Performance of three PDMAEMA-based polycation architectures as gene delivery agents in comparison to linear and branched PEI, *Reactive & Functional Polymers*, 70, 1–10 (2010).

Schild, H.G., Poly(*N*-isopropylacrylamide): experiment, theory and application, *Progress in Polymer Science*, 17, 163-249 (1992).

Schild, HG., Muthukumar, M., Tirell, DA., Cononsolvency in mixed aqueous solutions of poly(*N*-isopropylacrylamide), *Macromolecules*, 24, 948-952 (1991).

Schmaljohann, D., Thermo- and pH-responsive polymers in drug delivery, *Advanced drug delivery reviews*, 58, 1655-1670 (2006).

Shih, J.S., Chao, Y.C., Sung, M.F., Sau, G.J., Chiou, C.S., Piezoelectric crystal membrane chemical sensors based on fullerene C₆₀, *Sens. Actuators B.*, 76, 347-353 (2001).

Shin, I.G., Kim, S.Y., Lee, Y.M., Cho, C.S., Sung, Y.K., Methoxy poly(ethylene glycol)/ ϵ -caprolactone amphiphilic block copolymeric micelle containing indomethacin.: I. Preparation and characterization, *J. Control. Release*, 51, 1-11 (1998).

Sibley, S.P., Campbell, R.L., Silber, H.B., Solution and Solid State Interactions of C₆₀ with Substituted Anilines, *J. Phys. Chem.*, 99, 5274-5276 (1995).

Sinha, V. R., Kumria, R., Polysaccharides for colon specific drug delivery, *Int. J. Pharm.*, 224, 19-38 (2001).

Sjöback R., Nygren, J., Kubista, M., Absorption and fluorescence properties of fluorescein, *Spectrochim. Acta , Part A*, 51, L7-L21 (1995)

Song, T., Dai, S., Tam, K.C., Lee, S.Y., Goh, S.H., Aggregation behavior of two-arm fullerene-containing poly(ethylene oxide), *Polymer*, 44, 2529-2536 (2003b).

Song, T., Dai, S., Tam, KC., Lee, SY., Goh, SH., Aggregation Behavior of C₆₀-end-capped Poly(ethylene oxide)s, *Langmuir*, 19, 4798-4803 (2003).

Song, T., Goh, S.H., Lee, S. Y., Interpolymer Complexes through Hydrophobic Interactions: C₆₀-End-Capped Linear or Four-Arm Poly(ethylene oxide)/Poly(acrylic acid) Complexes, *Macromolecules*, 35, 4133-4137 (2002).

Soppimath, K. S., Tan, D. C. W., Yang, Y. Y., pH-triggered thermally responsive polymer core-shell nanoparticles for drug delivery, *Adv. Mater.*, 17, 318-320 (2005).

Stalmach, U., de Boer, B., Videlot, C., Van, H.P.F., Hadziioannou, G., Semiconducting Diblock Copolymers Synthesized by Means of Controlled Radical Polymerization Techniques, *J. Am. Chem. Soc.*, 122, 5464-5472 (2000).

Steenis, J.H., Van, E.M., Van, M., Verbaan. F.J., Verrijck. R., Crommelin. D.J.A., Storm. G., Hennink, W.E., Preparation and characterization of folate-targeted pEG-coated pDMAEMA-based polyplexes, *J. Controlled Release*, 87, 167-176 (2003).

Stephens, P.W., Cox, D., Lauher, J.W., Mihaly, L., Wiley, J.B., Allemande, P.M., Hirsh, A., Holczer, K., Li, Q., Thompson, J.D., Wudl, F., Lattice structure of the fullerene ferromagnet TDAE-C₆₀, *Nature*, 355, 331-332 (1992).

Stewart, D. Imrie, C.T., Role of C₆₀ in the free radical polymerisation of styrene, *Chem. Commun.*, 1383-1384 (1996).

Stockmayer, W. H., Schmidt, M., Effects of polydispersity, branching and chain stiffness on quasielastic light scattering, *Pure Appl. Chem.*, 54, 407-414 (1982).

Stockmayer, W.H., Schmidt, M., Quasi-elastic light scattering by semiflexible chains, *Macromolecules*, 17, 509-514 (1984).

Storm, G., Crommelin, D.J A., Liposomes: Liposomes: quo vadis? *Pharm. Sci. Technol. Today*, 1, 19–31 (1998).

Stuart, M.A.C., Huck, W.T.S., Genzer, J., Müller, M., Ober, C., Stamm, M., Sukhorukov, G.B., Szleifer, I., Tsukruk, V., Urban, M., Winnik, F., Zauscher, S., Luzinov, I., Minko, S., Emerging applications of stimuli-responsive polymer materials, *Nature Materials*, 9, 101-113 (2010).

Sturcova, A., Davies, G.R., Eichhorn, S.J., Elastic modulus and stress-transfer properties of tunicate cellulose whiskers, *Biomacromolecules*, 6, 1055-1061 (2005).

Sumerlin, B.S., Lowe, A.B., Thomas, D.B., McCormick, C.L., Aqueous Solution Properties of pH-Responsive AB Diblock Acrylamido Copolymers Synthesized via Aqueous RAFT, *Macromolecules*, 36, 5982-5987 (2003).

Sun, ST., Wu, P.Y., Role of Water/Methanol Clustering Dynamics on Thermosensitivity of Poly(Nisopropylacrylamide) from Spectral and Calorimetric Insights, *Macromolecules*, 43, 9501-9510 (2010).

Szwarc, M., Carbanions, Living Polymers, Electron Transfer Processes, Wiley-Interscience: New York, (1968).

Tamura, A., Uchida, K., Yajima, H., Reversible Temperature-dependent Dispersion–Aggregation Transition of Poly (N-isopropylacrylamide)–[60] Fullerene Conjugates, *Chemistry Letters*, 35, 282-283 (2006).

Tan, B.H., Hussain, H., Liu, Y., He, C.B., Davis, T.P., Synthesis And Self-Assembly of Fluorinated Brush-Type Amphiphilic Diblock Copolymers In Aqueous Solution, *Langmuir*, 26, 2361-2368 (2010).

Tan, C.H., Ravi, P., Dai, S., Tam, K.C., Polymer-Induced Fractal Patterns of [60] Fullerene Containing Poly(methacrylic acid) in Salt Solutions, *Langmuir*, 20, 9901-9904 (2004a).

Tan, CH., Ravi, P., Dai, S., Tam, K.C., Gan, L.H., Solvent Induced Large Compound Vesicles of [60] Fullerene Containing Poly(*tert*-butyl methacrylate), *Langmuir*, 20, 9882-9884 (2004 b).

Tanaka, F., Koga, T., Kojima, H., Winnik, FM., Temperature and Tension-Induced Coil-Globule Transition of Poly(*N*-isopropylacrylamide) Chains in Water and Mixed Solvent of Water/Methanol, *Macromolecules*, 42, 1321-1330 (2009).

Tanaka, F., Koga, T., Winnik, F.M., Temperature-Responsive Polymers in Mixed Solvents: Competitive Hydrogen Bonds Cause Cononsolvency, *Phys Rev Lett.* , 101, 28302-28306 (2008).

Tang, Y.Q., Liu, S.Y., Armes, S.P., Billingham, N.C., Solubilization and controlled release of a hydrophobic drug using novel micelle-forming ABC triblock copolymers, *Biomacromolecules*, 4, 1636-1645 (2003).

Taton, D., Angot, S., Gnanou, Y., Wolert, E., Setz, S. Duran, R., Synthesis and Characterization of C₆₀ End-Capped Poly (ethylene oxide) Stars, *Macromolecules*, 31, 6030 -6033(1998).

Taylor, L.D., Cerankowski L.D., Preparation of films exhibiting a balanced temperature dependence to permeation by aqueous solution: lower consolute behavior, *J. Polym. Sci. Polym. Chem. Ed.*, 13, 2551-2570 (1975).

Tegos, G.P., Demidova T.N., Arcila-Lopez, D., Lee, H., Wharton, T., Gali, H., Hamblin, MR., Cationic fullerenes are effective and selective antimicrobial photosensitizers, *Chem. Biol.*, 12, 1127-1135 (2005).

Teoh, S.K., Ravi, P., Dai, S., Tam, K.C., Self-Assembly of Stimuli-Responsive Water-Soluble [60] Fullerene End-Capped Ampholytic Block Copolymer, *Journal of Physical Chemistry B*, 109, 4431-4438 (2005).

Texier, I., Berberan-Santos, M.N., Fedorov, A., Brettreich, M., Schönberger, H., Hirsch, A., Leach, S., Bensasso, R.V., Photophysics and Photochemistry of a Water-Soluble C₆₀ Dendrimer: Fluorescence Quenching by Halides and Photoinduced Oxidation of I , *J. Phys. Chem. A*, 105, 10278-10285 (2001)

Topp, M.D.C., Dijkstra, P.J., Talsma, H., Feijen, J., Thermosensitive Micelle-Forming Block Copolymers of Poly(ethylene glycol) and Poly(*N*-isopropylacrylamide), *Macromolecules*, 30, 8518-8520 (1997).

Torchilin, V.P., Lukyanov, A.N., Gao, Z., Papahadjopoulos- Sternberg B.. Immunomicelles: targeted pharmaceutical carriers for poorly soluble drugs, *Proc. Natl. Acad. Sci. USA*. 100, 6039-6044 (2003).

Torchilin, V.P., Recent advances with liposomes as pharmaceutical carriers. *Nat. Rev. Drug Discov.* 4, 145-160 (2005).

Torchilin, V.P., Targeted polymeric micelles for delivery of poorly soluble drugs, *Cell. Mol. Life Sci.*, 6, 2549-2559 (2004).

Trail, P.A., Willner, D., Hellström, K., Research Overview: Site-directed delivery of anthracyclines for treatment of cancer, *Drug development research*, 34, 196-209 (2004).

Trubetskoy, V.S., Polymeric micelles as carriers of diagnostic agents, *Adv. Drug Deliv. Rev.*, 37, 81-88 (1999).

Tsarevsky, N.V., Matyjaszewski, K., "Green" Atom Transfer Radical Polymerization: From Process Design to Preparation of Well-Defined Environmentally Friendly Polymeric Materials, *Chem. Rev.*, *107*, 2270-2299 (2007).

Tummino, P. J., Gafni, A., Determination of the aggregation number of detergent micelles using steady-state fluorescence quenching, *Biophys J.*, *64*, 1580-1587 (1993)

Uchino, H., Matsumura, Y., Negishi, T., Koizumi, F., Hayashi, T., Honda, T., Nishiyama, N., Kataoka, K., Naito, S., Kakizoe, T., Cisplatin-incorporating polymeric micelles (NC-6004) can reduce nephrotoxicity and neurotoxicity of cisplatin in rats, *Br J Cancer*, *93*, 678-687 (2005).

Ueng, T.H., Kang, J.J., Wang, H.W., Cheng, Y.W., Chiang, L.Y., Suppression of microsomal cytochrome P450-dependent monooxygenases and mitochondrial oxidative phosphorylation by fulleranol, a polyhydroxylated fullerene C₆₀, *Toxicol. Lett.*, *93*, 29-37 (1997).

Ulbrich, K., Subr, V., Polymeric anticancer drugs with pH-controlled activation, *Advanced Drug Delivery Reviews*, *56* 1023- 1050 (2004).

Ungurenasu, C., Airinei, A., Highly Stable C₆₀ /Poly(vinylpyrrolidone) Charge-Transfer Complexes Afford New Predictions for Biological Applications of Underivatized Fullerenes, *J. Med. Chem.*, *43*, 3186-3188 (2000).

Vallant, R.M., Szabo, Z., Bachmann, S., Bakry, R., Muhammad, N.H., Rainer, M., Heigl, N., Petter, C., Huck, C.W., Bonn, G.K., Development and Application of C₆₀-Fullerene Bound Silica for Solid-Phase Extraction of Biomolecules, *Anal Chem.*, *79*, 8144-8153 (2007).

Verbaan, F.J., Oussoren, C., van Dam, I.M., Takakura, Y., Hashida, M., Crommelin, D.J.A., Hennink, W.E., Storm, G., The fate of poly(2-dimethyl amino ethyl)methacrylate-based polyplexes after intravenous administration, *Int. J. Pharm.*, *214*, 99-101 (2001)

Verónica, S.M., Limer, A.J., Haddleton, D.M., Catalina, F., Carmen, P., Biodegradable and thermoresponsive micelles of triblock copolymers based on 2-(N,N-dimethylamino)ethyl methacrylate and ε-caprolactone for controlled drug delivery *European Polymer Journal*, *44* 3853-3863 (2008).

Vinogradova, L.V., Ratnikova, O.V., Lavrenko, P.N., Structure and Hydrodynamical Properties of Heteroarm Star-Shaped C₆₀ Fullerene-containing Polymers, *Fullerenes, Nanotubes, Carbon Nanostructures*, 16, 650-653 (2008).

Virtanen, J., Arotcarena, M., Heise, B., Ishaya, S., Laschewsky, A., Tenhu, H., Dissolution and Aggregation of a Poly(NIPA-block-Sulfobetaine) Copolymer in Pure and Saline Aqueous Solution, *Langmuir*, 18, 5360-5365 (2002).

Virtanen, J., Holappa, S., Lemmetyinen, H., Tenhu, H., Aggregation in Aqueous Poly(*N*-isopropylacrylamide)-*block*-poly(ethylene oxide) Solutions Studied by Fluorescence Spectroscopy and Light Scattering, *Macromolecules*, 35, 4763-4769 (2002).

Wands, J.R., Blum, H.E., Primary hepatocellular carcinoma, *N. Engl. J. Med.* 325, 729-731 (1991).

Wang, C., Guo, Z.X., Fu, S., Wu, W., Zhu, D., Polymers containing fullerene or carbon nanotube structures, *Prog. Polym. Sci.*, 29, 1079-1141 (2004).

Wang, C., Ravi, P., Tam, K.C., Morphological Transformation of [60] Fullerene-Containing Poly (Acrylic Acid) Induced by the Binding of Surfactant, *Langmuir*, 22, 2927-2930 (2006).

Wang, C., Ravi, P., Tam, K.C., Supramolecular Complex of [60] Fullerene Grafted Polyelectrolyte and Surfactant: Mechanism and Nanostructure, *Langmuir*, 23, 8798-8805 (2007).

Wang, J.S., Matyjaszewski, K., Controlled/"Living" Radical Polymerization. Atom Transfer Radical Polymerization in the Presence of Transition Metal Complexes, *J. Am. Chem. Soc.*, 117, 5614-5615 (1995).

Wang, M., Pramoda, K.P., Goh, S.H., Reinforcing and toughening of poly(vinyl chloride) with double-C₆₀-end-capped poly(*n*-butyl methacrylate), *Macromolecules*, 39, 4932-4934 (2006).

Wang, N., Ding, E., Cheng, R., Thermal degradation behaviors of spherical cellulosenanocrystals with sulfate groups, *Polymer*, 48, 34, 86-3493 (2007).

Wang, W., Liu, R., Li, Z., Meng, C., Wu, Q., Zhu, F., Synthesis and Self-Assembly of New Double-Crystalline Amphiphilic Polyethylene-*block*-Poly[oligo(ethylene glycol) Methyl Ether Methacrylate] Coil-Brush Diblock Copolymer, *Macromol. Chem. Phys.*, 211, 1452-1459 (2010).

Wang, X.F., Zhang, Y.F., Zhu, Z.Y., Liu, S.Y., Fabrication of Fullerene-Containing Hybrid Vesicles via Supramolecular Self-Assembly of a Well-Defined Amphiphilic Block Copolymer Incorporated with a Single C₆₀ Moiety at the Diblock Junction Point, *Macromol Rapid Commun.*, 29, 340-346 (2008).

Wang, Y., Photophysical properties of fullerenes and fullerene/N,N-diethylaniline charge-transfer complexes, *J. Phys. Chem.*, 96, 764-767 (1992).

Weaver, J.V.M., Armes, S.P., Bütün, V., Synthesis and aqueous solution properties of a well-defined thermo-responsive schizophrenic diblock copolymer, *Chem. Commun.*, 18, 2122-2123 (2002).

Weis, C., Friedrich, C., Muthaupt, R., Frey, H., Fullerene-End-Capped Polystyrenes. Monosubstituted Polymeric C₆₀ Derivatives, *Macromolecules*, 28, 403-405 (1995).

Wetering, P.V., Cherng, J.Y., Talsma, H., Crommelin, D.J.A., Hennink, W.E., 2-(dimethylamino)ethyl methacrylate based (co)polymers as gene transfer agents, *J. Controlled Release*, 53, 145–153 (1998).

Wignall, G.D., Affholter, K.A., Bunick, G.J., Hunt, M.O., Menciloglu, Y.Z., Jaernagin, J.M., Desimone, J.M., Samulski, E.T., Synthesis and SANS Structural Characterization of Polymer-Substituted Fullerenes (Flagellenes), *Macromolecules*, 28, 6000-6006 (1995).

Wojciech, K. C., Young, D.J., Kawecki, M., R. Brown, M., The future prospects of microbial cellulose in biomedical applications, *Biomacromolecules*, 8, 1-12 (2007).

Wu, H.X., Cao, W.M., Cai, R.F., Song, Y.L., Zhao, L., C₆₀ end-functionalized four-armed polymers: synthesis and optical limiting properties, *J. Mater. Sci.*, 42, 6515-6523 (2007).

Wu, P.Q., Mohammad, S., Chen, H.Y., Qiang, D., Chi, W., Laser Light-Scattering Study of Poly(sulfoalkyl methacrylate)s in 0.1 M NaCl Aqueous Solution, *Macromolecules*, 29, 277-281 (1996).

Xia, Y., Burke, N.A.D., Stover, H.D.H., The End Group Effect on the Thermal Response of Narrow-Disperse Poly(N-isopropylacrylamide) Prepared by Atom Transfer Radical Polymerization, *Macromolecules*, 39, 2275-2283 (2006).

Xiao, L., Takada, H., Maeda, K., Haramoto, M., Miwa, N., Antioxidant effects of water-soluble fullerene derivatives against ultraviolet ray or peroxy lipid through their action of scavenging the reactive oxygen species in human skin keratinocytes, *Biomedicine & Pharmacotherapy*, 59, 351-358 (2005).

Yadav, B.C., Ritesh, K., Structure, properties and applications of fullerenes, *International Journal of Nanotechnology and Applications*, 2, 15-24 (2008).

Yakushiji, T., Sakai, K., Kikuchi, A., Aoyagi, T., Sakurai, Y., Okano, T., Graft Architectural Effects on Thermoresponsive Wettability Changes of Poly(N-isopropylacrylamide)-Modified Surfaces, *Langmuir*, 14, 4657-4662 (1998).

Yamamoto, S.I., Pietrasik, J., Matyjaszewski, K., ATRP Synthesis of Thermally Responsive Molecular Brushes from Oligo(ethylene oxide) methacrylates, *Macromolecules*, 40, 9348-9353 (2007).

Yamazaki, N., Kojima, S., Bovin, N. V., Andre, S., Gabius, S., Gabius, H. J., Endogenous lectins as targets for drug delivery, *Adv. Drug Delivery Rev.*, 43, 225-244 (2000).

Yan, H., Tsujii, K., Potential application of poly(N-isopropylacrylamide) gel containing polymeric micelles to drug delivery systems, *Colloids Surf., B*, 46, 142-146 (2005).

Yang, D., Li, L., Wang, C., Characterization and photoconductivity study of well-defined C₆₀ terminated Poly(*tert*-butyl acrylate-*b*-styrene), *Mater. Chem. Phys.*, 87, 114-119 (2004).

Yang, J., Li L., Wang, C., Synthesis of a Water Soluble, Monosubstituted C₆₀ Polymeric Derivative and Its Photoconductive Properties, *Macromolecules*, 36, 6060-6065 (2003).

Yang, T., Choi, M.K., Cui, F.D., Kim, J.S., Chung, S.J., Shim, C.K., Kim, D.D., Preparation and Evaluation of Paclitaxel- Loaded PEGylated Immunoliposome, *J. Control. Release*, 120, 169-177 (2007a).

Yang, T., Cui, F.D., Choi, M.K., Cho, J.W., Chung, S.J., Shim, C.K., Kim, D.D., Enhanced Solubility and Stability of PEGylated Liposomal Paclitaxel: In vitro and in vivo Evaluation, *Int. J. Pharm.*, 338, 317-326 (2007b).

Yao, Z.L., Tam, K.C., Synthesis and self-assembly of stimuli-responsive poly(2-(dimethylamino) ethyl methacrylate)-block-fullerene (PDMAEMA-b-C₆₀) and the demicellization induced by free PDMAEMA chains, *Langmuir*, 27, 6668-6673 (2011a).

Yao, Z.L., Tam, K.C., Self-assembly of thermo-responsive poly (oligo(ethylene glycol) methyl ether methacrylate)-C₆₀ in water-methanol mixtures, *Polymer*, 52, 3769-3775 (2011b).

Yasugi, K., Nakamura, T., Nagasaki, Y., Kato, M., Kataoka, K., Sugar-Installed Polymer Micelles: Synthesis and Micellization of Poly (ethylene glycol)-Poly (D,L-lactide) Block Copolymers Having Sugar Groups at the PEG Chain End, *Macromolecules*, 32, 8024-8032 (1999).

Yatvin, M.B., Kreutz, W., Horwitz, B.A., Shinitzky, M., pH-sensitive liposomes: possible clinical implications, *Science*, 210, 1253- 1255 (1980).

Yen, W., Jing, T., Alan, G. M., James, G.M., Allan, L.S., Li, D., Preparation and conductivities of fullerene-doped polyanilines, *J. Chem. Commun*, 7, 603 (1993).

Yi, J., Xu, Q., Zhang, X., Zhang, H., Temperature-induced chiral nematic phase changes of suspensions of poly(*N,N*-dimethylaminoethyl methacrylate)-grafted cellulose nanocrystals, *Cellulose*, 16:989–997(2009).

Yokoyama, M., Okano, T., Sakurai, Y., Suwa, S., Kataoka K., Introduction of cisplatin into polymeric micelle, *J. Control. Release*, 39, 351-356 (1996).

Yokoyama, M., Polymeric micelles as a new drug carrier system and their required considerations for clinical trials, *Expert Opin Drug Deliv.*, 7, 145-158 (2010).

Yoo, H.S., Lee, E.A., Park, T.G., Doxorubicin-conjugated biodegradable polymeric micelles having acid-cleavable linkages, *J. Control. Release*, 82, 17-27 (2002).

Yoo, H.S., Park, T.G., Folate receptor targeted biodegradable polymeric doxorubicin micelles, *J. Control. Release*, 96, 273-283 (2004).

Yoshida, M., Morishima, A., Morinaga, Y., Iyoda, M., Reactions of fullerols and fullerene dimer containing perfluoroalkyl groups with tributyltin hydride, *Tetrahedron Lett.*, 35, 9045-9046 (1994).

Yoshida, M., Sultana, F., Uchiyama, N., Yamada, T., Iyoda, M., Efficient synthesis of fullerene dimers containing a fluoroalkyl group, *Tetrahedron Lett.*, 40, 735-736 (1999).

You, Y.Z., Zhou, Q.H., Manickam, D. S., Wan, L., Mao, G.Z., Oupický, D., Dually responsive multiblock copolymers via RAFT polymerization: Synthesis of temperature- and redox-responsive copolymers of PNIPAM and PDMAEMA, *Macromolecules*, 40, 8617-8624 (2007).

Yu, B.G., Okano, T., Kataoka, K., Sardari, S., Kwon, G.S., In vitro dissociation of antifungal activity and toxicity for amphotericin b-loaded poly(ethylene oxide)-block-poly(β benzyl L aspartate) micelles, *J. Controlled Release*, 56, 285-291 (1998).

Yu, H., Gan, L.H., Hu, X., Gan, Y.Y., A pH-sensitive double [60] fullerene-end-capped polymers via ATRP: Synthesis and aggregation behavior, *Polymer*, 42, 2312-2321 (2007).

Yu, H., Gan, L.H., Hu, X., Venkatraman, S.S., Tam, K.C., Gan, Y.Y., A Novel Amphiphilic Double-[60] Fullerene-Capped Triblock Copolymer, *Macromolecules*, 38, 9889-9893 (2005).

Yuan, F., Dellian, M., Fukumura, D., Leunig, M., Berk, D.A., Torchilin, V.P., Jain, R.K., Vascular-permeability in a human tumor xenograft - Molecular-size dependence and cutoff size, *Cancer Res.*, 55, 3752-3756 (1995)

Yuan, W., Yuan, J., Zheng, S., Hong, X., Synthesis, characterization, and controllable drug release of dendritic star-block copolymer by ring-opening polymerization and atom transfer radical polymerization, *Polymer*, 48, 2585-2594 (2007).

Zha, L., Zhang, Y., Yang, W., Fu, S., Monodisperse temperature-sensitive microcontainers, *Adv. Mater.*, 14, 1090-1092 (2002).

Zhang, G.Z., Liu, L., Zhao, Y., Ning, F.L., Jiang, M., Wu, C., Self-Assembly of Carboxylated Poly(styrene-*b*-ethylene-co-butylene-*b*-styrene) Triblock Copolymer Chains in Water via a Microphase Inversion, *Macromolecules*, 33, 6340-6343 (2000)

Zhang, L., Eisenberg, A., Multiple Morphologies and Characteristics of "Crew-Cut" Micelle-like Aggregates of Polystyrene-*b*-poly (acrylic acid) Diblock Copolymers in Aqueous Solutions, *J. Am. Chem. Soc.*, 118, 3168-3181(1996).

Zhang, W., Shi, L., Wu, K., An, Y., Thermoresponsive Micellization of Poly(ethylene glycol)-*b*-poly(*N*-isopropylacrylamide) in Water, *Macromolecules* , 38, 5743-5747 (2005).

Zhang, X., Burt, H.M., Mangold, G., Dexter, D., Von Hoff, D., Mayer, L., Hunter, W.L., Anti-tumor efficacy and biodistribution of intravenous polymeric micellar paclitaxel, *Anticancer Drugs*, 8, 696-701 (1997).

Zhang, X., Xia, J., Matyjaszewski, K., Controlled "Living" Radical Polymerization of 2-(Dimethylamino)ethyl Methacrylate, *Macromolecules*, 31, 5167-5169 (1998).

Zheng, G., Stover, H.D.H., Formation and Morphology of Methacrylic Polymers and Block Copolymers Tethered on Polymer Microspheres, *Macromolecules*, 36, 7439-7445 (2003).

Zhong, Z., Song, Y., Engbersen, J.F.J., Lok, M.C., Hennink, W.E., Feijen, J., A versatile family of degradable non-viral gene carriers based on hyperbranched poly(ester amine)s, *J. Controlled Release*, 109, 317-329 (2005).

Zhou, G., Harruna, I.I., Zhou, W.L., Aicher, W.K., Geckeler, K.E., Nanostructured Thermosensitive Polymers with Radical Scavenging Ability, *Chem. Eur. J.*, 13, 569-573 (2007).

Zhou, P., Chen, G., Hong, H., Du, F., Li, Z., Li, F., Synthesis of C₆₀-End-Bonded Polymers with Designed Molecular Weights and Narrow Molecular Weight Distributions via Atom Transfer Radical Polymerization, *Macromolecules*, 33, 1948-1954 (2000b).

Zhou, P., Chen, G.Q., Li, C.Z., Du, F.S., Li, Z.C., Li, F.M., Synthesis of hammer-like macromolecules of C₆₀ with well-defined polystyrene chains via atom transfer radical polymerization (ATRP) using a C₆₀-monoadduct initiator, *Chem. Commun.*, 797-798 (2000a)

Zhu, S., Oberdorster, E., Haasch, M.L., Toxicity of an Engineered Nanoparticle (Fullerene, C₆₀) in Two Aquatic Species, Daphnia and Fathead Minnow, *Mar. Environ. Res.*, 62 (Suppl.), S5-9 (2006).

Zoppe, J.O., Youssefm, H., Rojas, O.J., Venditti, R.A., Johansson, L.S., Efimenko, K., Sterberg, M., Laine, J., Poly(N-isopropylacrylamide) brushes grafted from cellulose nanocrystals via surface-initiated single-electron transfer living radical polymerization, *Biomacromolecules*, 11, 2683-2691(2010).